CHARACTERIZATION OF DENDRITIC CELL AND MACROPHAGE CELL SURFACE PROTEINS

by

Ian D. Haidl

B.Sc. University of Saskatchewan, 1989

A Thesis Submitted in Partial Fulfillment of the

Requirements for the Degree of

DOCTOR OF PHILOSOPHY

in

The Faculty of Graduate Studies

DEPARTMENT OF MICROBIOLOGY AND IMMUNOLOGY

and THE BIOTECHNOLOGY LABORATORY

We accept this thesis as confirming to the required standard

THE UNIVERSITY OF BRITISH COLUMBIA

March 1996

In presenting this thesis in partial fulfilment of the requirements for an advanced degree at the University of British Columbia, I agree that the Library shall make it freely available for reference and study. I further agree that permission for extensive copying of this thesis for scholarly purposes may be granted by the head of my department or by his or her representatives. It is understood that copying or publication of this thesis for financial gain shall not be allowed without my written permission.

Department of Microbiology and Immunology

The University of British Columbia
Vancouver, Canada

Date 13 March, 1996

ABSTRACT

Dendritic cells play a critical role in the induction of the immune response and execute unique functions in comparison to other antigen presenting cells such as macrophages and B cells. The research in this thesis was directed towards characterizing molecular components of dendritic cells and macrophages. The molecules chosen for study were CD45 and an uncharacterized protein, the F4/80 molecule.

CD45 is an important receptor tyrosine phosphatase expressed as various isoforms due to highly regulated alternative splicing. Analysis of CD45 cell surface expression on purified, cultured splenic and thymic dendritic cells, and freshly isolated dendritic cells, demonstrates that dendritic cells express both the CD45R0 and CD45RB isoforms. Biochemical analysis of purified splenic dendritic cells confirms the expression of CD45R0 and CD45RB. In addition, purified splenic dendritic cell CD45 possesses intrinsic tyrosine phosphatase activity. Macrophage CD45 isoform expression is also limited largely to CD45R0 and small amounts of CD45RB or CD45RA depending on the macrophage source. CD45 from macrophages possesses comparable tyrosine phosphatase activity relative to dendritic cell CD45. The demonstration of CD45 phosphatase activity in cells lacking antigen receptors suggests a possible role for CD45 in leukocyte events such as recirculation, homing, heterophilic adhesion events, or signalling via non-antigen specific receptors.

The F4/80 molecule was first characterized over a decade ago and is known to be expressed on dendritic cells and macrophages. However, few molecular details of the F4/80 molecule had been elucidated. This study documents that the F4/80 molecule contains N-linked carbohydrates, O-linked carbohydrates, sialic acids primarily in α2-6 linkages to galactose, and chondroitin sulfate modifications. Furthermore, the extensive N-linked carbohydrate modifications contain a dominant component of repeating N-acetylglucosamine or N-

acetyllactosamine units. The protein contains extensive intramolecular disulfide bonds, has a slow rate of intracellular transport ($T_{½}$=60 minutes), and has a basic pI of 7.5 for the entire molecule in spite of the negative post-translational modifications. The modifications of the F4/80 molecule described may also account for certain functional properties. For example, chondroitin sulfate can mediate interactions with CD44 and fibronectin, whereas α2-6 linked sialic acids are involved in the binding to CD22. Thus, a substantial description of the biochemical nature of the F4/80 molecule is provided, which leads to direct inferences for potential functions of the molecule.

In characterizing CD45 and the F4/80 molecule, this work provides a better understanding of two proteins of dendritic cells and macrophages. This information should assist both the basic understanding of dendritic cell and macrophage biology and in developing experimental and clinical targets for functional modulation of dendritic cells and macrophages.

TABLE OF CONTENTS

LIST OF TABLES

LIST OF FIGURES

ACKNOWLEDGMENTS and DEDICATION

The work represented in this thesis is only a part of the learning experience that has occurred in the time of my Ph.D. thesis work. I thank Dr. Wilfred Jefferies for his enthusiasm and supervision of my research and for providing an atmosphere in which I learned about the many aspects involved in scientific endeavors. I also wish to acknowledge the contribution of Dr. Reinhard Gabathuler, whose daily presence and technical expertise were invaluable.

The positive research environment has also been contributed to by the Department of Microbiology and Immunology and the Biotechnology Laboratory at UBC. In particular, my committee members, Dr. Rob McMaster, Dr. Fumio Takei, and Dr. Ross Petty, have provided supportive and critical opinions of my judgments whenever required. Other individuals, too numerous to mention, have made UBC an enjoyable and educational research community. I am grateful to The MRC of Canada for support that was instrumental in my time at UBC.

Many individuals deserve credit for assisting with my research. Prior to starting my Ph.D. studies, the enthusiasm of Dr. Peter Bretscher in teaching immunology initiated my curiosity in the immune system. Dr. Pauline Johnson was instrumental in all aspects of the CD45 research and writing. David Ng assisted with the tyrosine phosphatase assays. Dr. Ruedi Aebersold and Hamish Morrison provided invaluable advice and assistance at the outset of the F4/80 molecule purification. Pearl Hui and Shannon Awrey completed many of the experiments to assess the CD45 sedimentation coefficient. Dr. Rick Stokes provided the BCG activated macrophages and innumerable conversations about macrophages. Drs. Frank Tufaro and Bruce Banfield were always willing to talk about glycosaminoglycans. Dr. Jacob Hodgson was also invaluable for his advice, enthusiasm, and encouragement. I had the good fortune to be supervised by or collaborate directly with three individuals who received a portion of their scientific training in Dr. Alan Williams' lab. This has given me an appreciation of the magnitude of both his contribution to science and of the sadness of his loss.

The individuals with whom I worked daily deserve a special acknowledgment. Sylvia, Jonas, Malcolm, and Cachou have reinforced the human and scientific value of dedicated, knowledgeable, and pleasant scientists. Daphne and Nancy have each contributed daily support in their unique roles. To my fellow students, Gregor, Roger, Forest, Cyp, Joseph, Mike, Kathy, Hagen, Heather, Carol-Ann, Renee, Edmond, Judie, Greg, Alex, Jacqueline, and Brandie, and others again too numerous to mention, I give a thanks for everything shared in and out of the lab. Special thanks to Roger, Forest and Gregor, and sometimes others for enthusiasm, hard work, and being partners in 'It's a Miracle Inc.'

Finally, I wish to acknowledge those closest to me, my parents, my brothers Mark, Kent and Kevin, and my love, Annette. For encouragement, love, support, and teaching me the value of independence and thought (and hockey), I will be forever grateful to my parents. To my brothers, especially Kevin who shared the low points of my thesis work, I am indebted for much more than the toughness and love acquired from being one of four boys in a family. Annette has brought happiness and perspective to my life from her loving, caring, and thoughtful essence. Through her presence I have experienced the richness of life, as two people share both joy and sadness. Her support, guidance, and love have become an essential, incalculably valuable component of my life.

Dedication *To Annette and my parents.*

1. GENERAL INTRODUCTION

The discovery of new insights and systems in science is the product of the prior research which developed a context for current hypotheses and of the ingenuity of the individual researcher and his or her colleagues. The work described in this thesis is no exception as it extends and clarifies concepts that are the products of many researchers' work. The beginning of this thesis is therefore a short historical account which highlights some of the significant advances in immunology prior to the application of modern techniques to the study of the immune system. Following this, a more focused introduction of the nature of antigen presenting cells and post-translational protein modifications will describe the more specific nature of the research in this thesis. Finally, the introduction to each chapter will describe the proteins of antigen presenting cells that were studied, CD45 and the F4/80 molecule.

1.1 The immune system

1.1.1 A brief historical perspective

The survival of higher organisms including human beings is intrinsically linked to the ability to survive insults from pathogenic organisms. The requirement for the maturation of each generation has necessitated the evolutionarily driven development of a survival mechanism which adapts to protect the population from infectious agents and other foreign molecules which cause the death of individuals in the population. Any such system would require the individual to respond quickly to any pathogenic organism and to be able to adapt to the ever changing milieu

of pathogenic organisms which are also driven by evolution to evade elimination by the prospective host.

One of the first historical accounts of the concept of immunity is conveyed by Thucydides as he observed and survived the plague in ca. 450 BC : "Yet still the ones who felt most pity for the sick and the dying were those who had had the plague themselves and had recovered from it. They knew what it was like and at the same time felt themselves to be safe, for no one caught the disease twice, or, if he did, the second attack was never fatal" (1). Although the understanding of the mechanisms of disease and immunity was still within the realm of demonology and mystical spirituality, the practical consequences of immunity (survival) were apparent to all.

Seminal advances in the study of the immune system were perhaps initiated with the observation by Edward Jenner, that immunity to the smallpox virus was present in groups of farm workers that daily encountered the related cowpox virus (2,3). This observation and his subsequent vaccination study accentuates several key elements of an immune response (IR): the specificity of the response, the 'memory' of the body to respond against subsequent challenges of the same or closely related pathogen, and that an IR can be induced to specific agents by the immunization with that agent, or in the case of cowpox, a related agent. Other cultures had also utilized vaccination to prevent various afflictions, including the Chinese who, for over 20 centuries before Jenner, used dried exudate from smallpox lesions to infect individuals and induce protection against smallpox. However, Jenner's observations occurred at the time of the intellectual renaissance in European culture, amidst a wealth of other scientific advances. In the 1670's and 80's, Anton van Leeuwenhoek had developed a microscope that allowed him to visualize bacteria (4). These curious observations were largely ignored until the 1800's when

industrial revolution advanced the quality and availability of instruments including the microscope. With intellectual freedom and the technological advances, the application of scientific method to biological problems began in earnest. Louis Pasteur and Robert Koch are only two of many scientists that were involved in the explosion of knowledge that occurred before the end of the 19th century. Many major bacterial pathogens were identified including the causative agents for Anthrax (*Bacillus anthracis*), Syphilis (*Treponema pallidum*), and Diphtheria (*Corynebacterium diptheriae*). Koch's postulates also defined the concept that a single, specific organism would cause a specific disease. The vaccination protocol which Jenner had applied to smallpox, was now utilized by Pasteur and others to attempt protection against infectious agents in humans and animals.

At the level of the individual, the mechanism of immunity is now known to depend upon the proper functioning of a complex immune system. Phagocytic activities of cells in response to microbial infection were documented in 1887 by Metchnikoff (5) as was the presence of protective proteins in the serum of infected individuals. The specificity of these proteins in serum was clearly demonstrated by the ability of immune serum to precipitate the antigen to which the individual was immune, but not unrelated antigens (6). These proteins were identified as the γ-globulins according to their electrophoretic pattern (7) and termed as immunoglobulin (Ig) due to their induction during the IR. The springboard for studies into modern immunology was provided by the systematic, genetic analysis of transplantation rejection carried out in the 1940's and 1950's by George Snell. Although transplantation is not an event which is involved in evolutionary development, the rejection of tissue from an unrelated individual is similar to the clearing of pathogenic organisms. A single locus was identified as the primary controlling region for the acceptance or rejection of transplants. This locus was termed the major

histocompatibility complex (MHC). Inbred strains of mice, disparate at only the MHC locus, would accept transplants from mice with the same MHC (syngeneic), but reject transplants from mice with differences in the MHC locus (allogeneic) (8,9). The MHC locus has now been characterized and consists of three loci, classes I, II and III. The genes in these loci encode proteins that serve as the targets for the IR against foreign proteins (MHC class I and II proteins), several genes involved in 'processing' the antigens (see Sections 1.2.1 and 1.2.2), and other proteins with immune related functions such as tumor necrosis factor-α (TNF-α) and complement C4. Proteins unrelated to the IR such as the enzyme 21-hydroxylase are also encoded by the MHC locus(10). The ultimate sequencing of the MHC class I and II protein genes, revealed an unprecedented degree of gene polymorphism (10). The three class I MHC genes have up to 100 alleles each in humans. Since each individual has 6 class I MHC alleles (3 from each parent), there are 6 different MHC class I proteins present to be involved in the IR. The extensive allelic polymorphism ensures that the population as a whole will survive any given pathogen even if a number of individuals in that population perish.

Even prior to the deoxyribonucleic acid (DNA) cloning of the MHC region, the resolution of the functional nature of the MHC class I or class II protein was further clarified in the early 1970's with the description of MHC restriction: the requirement of T cells that developed in the context of one MHC type to recognize a foreign protein in the context of the same MHC in order to recognize that same foreign protein (11). This description propelled immunology forward and prepared immunologists to utilize the huge technical advances that monoclonal antibody (mAb) generation, x-ray crystallography, protein biochemistry, and recombinant DNA techniques provided. We now have an understanding of the IR down to the level of molecular structure for certain aspects of the immune system.

1.1.2 The specific immune response

The ability of the immune system to produce a specific response against seemingly any antigen, posed an intriguing and puzzling question for immunologists: how does the immune system generate such diversity and specificity? The ability of individuals to produce specific Ig against a seemingly limitless repertoire of foreign molecules provided the first focus for studying the generation of specificity. The production of Abs in soluble form and in large amounts facilitated their characterization. The generation of diversity was ultimately explained by the clonal selection of lymphocytes which each have a unique antigen receptor created by gene rearrangement ((12), reviewed in (5,13)). When the antigen receptor encounters antigen, the cell undergoes activation and expansion, producing many clones from the original selected cell. The presence of about 10^9 cells with different specificity at any one time in the body, ensures that a given antigen will likely be recognized by at least one cell which will undergo clonal expansion to induce an IR. To prevent generating an IR to self-molecules, other mechanisms eliminate or inactivate cells which rearrange the antigen receptor genes to produce an anti-self receptor (14).

The cells possessing antigen-specific receptors are B and T lymphocytes. The B cell antigen receptor is a membrane-bound form of Ig produced by alternative splicing. The binding of the antigen to the surface Ig (sIg) will induce the cell to become activated and divide. For most monomeric antigens, the B cell response also depends on helper T cells to produce cytokines such as interleukin-2 (IL-2) which serve as a necessary second signal to trigger B cell proliferation. Upon activation, a B cell will produce a soluble Ab which will bind to the antigen. As is expected for a secreted protein, Abs recognize the intact conformation of molecules, both conformational and linear epitopes, as they exist in the extracellular environment. By binding to

proteins or organisms, Ab will inactivate them directly or identify these foreign entities for clearance by other immune mechanisms.

In contrast to Ig, T cells possess a specific T cell receptor (TcR) which is exclusively expressed as a membrane protein and recognizes denatured peptides of proteins which form a complex with MHC class I or II proteins (15). As described above, the MHC region was originally identified by the genetic analysis of transplantation rejection. The nature of the foreign protein that was recognized by the T cell was the subject of much debate. The analysis of macrophage (mϕ) and B cell stimulation of T cells began to elucidate the requirement for proteolytic processing of foreign proteins (reviewed in (16)). Upon providing soluble protein or bacteria to the antigen presenting cells (APCs), a 30-60 minute period was required before T cell stimulation could occur. This 'processing' step was inhibitable by agents such as chloroquine and leupeptin that interfere with lysosomal protease function (17,18). Furthermore, fixation of cells before the processing step was completed, prevented T cell activation, whereas fixation after the processing step did not (17). Another key observation was that presentation of digested forms of the antigen were not inhibited by the chloroquine or fixation processes (19,20). This research culminated with the mapping of the Ia (mouse MHC class II) restricted presentation of a lysozyme peptide to a 16 amino acid fragment of lysozyme.

The recognition of class I MHC restricted T cells was also demonstrated to be dependent on only small peptides of the antigenic proteins which associate with the MHC class I in order to be recognized by T cells (21). The class I MHC antigen processing pathway appeared to be distinct from the class II since chloroquine did not interfere with MHC class I presentation, but protein synthesis inhibitors did. Therefore, the general paradigm evolved that MHC class I proteins presented peptides from proteins synthesized inside the cell while MHC class II

pathway appeared to present proteins acquired by endocytosis. This general model does have certain exceptions (see (22,23) for examples), but is still a constructive generalization. Antigen processing will be more fully explained in Sections 1.2.1 and 1.2.2.

Once at the cell surface, MHC class I or II are recognized by TcRs which recognize the MHC-peptide complex. Additional molecules are also involved in the interactions between the T cell and APC such as the adhesion molecule pairs LFA-1 and ICAM-1 and CD2 and LFA-3 (24). CD4 and CD8 on T cells participate in the TcR-MHC complexes with MHC class II and I respectively (25). Because of these co-receptor functions, $CD4^+$ T cells typically recognize MHC class II and $CD8^+$ cells MHC class I. CD28 is a T cell molecule which upon binding to the B7-1 or B7-2 molecule of APCs, produces a second signal required for TcR-mediated T cell activation (26).

MHC class I is expressed on most nucleated cells of the body with a few exceptions (27). Therefore, all cells can potentially be recognized by $CD8^+$ T cells with a TcR specific for MHC class I. This allows the $CD8^+$ T cells, which are typically cytotoxic T lymphocytes (CTLs), to continuously monitor all cells of the body for infection or 'abnormal' self-protein synthesis. Intracellular pathogens such as viruses will synthesize proteins that are degraded and presented on the infected cell's MHC class I. Tumor cells can synthesize altered self-proteins which are also targets for CTL killing (28,29). Therefore, it is important that MHC class I is expressed on most cells to permit the detection of their infection or transformation.

MHC class II is primarily expressed on specialized cells of the immune system including dendritic cells (DCs), activated mϕs, and activated B cells (30). MHC class II is also inducible on certain other cell types including epithelial cells and activated T cells in some systems (31,32). This expression pattern suggests that MHC class II has a more specialized role in

controlling the immune system. The $CD4^+$ cells that recognize MHC class II influence the IR by the secretion of specific cytokines to induce the activation of B cells, the switching of Ig isotype, activation of mϕs, enhancement of CTL development, and numerous other functions (33). Since these cells were identified as helping other cells, the $CD4^+$ T cells are referred to as helper T (T_h) cells. In addition to a signal transduced by the binding of the B cell surface Ig to the antigen, B cell division and maturation into antibody secreting cells depends on cytokines such as IL-2 and IL-4 from helper cells to provide a second stimulus. IL-2 will also help CTL activation which makes T helper cells important in CTL development.

Since the presence of a strong $CD4^+$ T_h response is important to the entire IR, T cell activation by the specialized APCs is critical. It is therefore of interest to understand each phase of APC function, from antigen uptake and processing, to the activation of T cells and other immune system functions that these cells may control. In addition, a definition of the roles that B cells, mϕ, and DCs occupy would also assist in developing mechanisms to modulate the IR.

1.2 Antigen presentation and antigen presenting cells

The mechanisms involved in processing of antigens are clearly important in understanding the role of APCs in the IR. Therefore, a brief outline of the MHC class I and II processing pathways will proceed a description of the APC activity of mϕs and B cells. This discussion should set the context for a more detailed introduction to the nature of the DC, the cell type which directed the research focus of this thesis.

1.2.1 Class I MHC

The nature of the MHC class I-antigenic peptide complex was resolved in 1987 with the solving of the crystal structure for HLA-A2, a human MHC class I protein (34). The structure revealed a binding cleft formed by the α-helical sides and β-pleated sheet floor dictated by the α1 and α2 domains of the MHC encoded heavy chain. MHC class I also associates with a non-MHC encoded protein β_2-microglobulin (β_2m) (Figure 1A) which stabilizes the structure after peptide binding for transport to the cell surface for recognition by T cells. The crystal structure also revealed an electron dense material in the binding cleft which represented the array of peptides able to bind HLA-A2. The crystal structure of MHC class I molecules after loading with a single peptide permitted the delineation of the crystal structure of the peptide and MHC class I regions interacting with the peptide (35). These results confirmed other studies which had predicted specific anchor residues in the peptides which bind into pockets, designated A to F, formed by the MHC class I protein (36). For example, the mouse H-2 K^b molecule binds 8 amino acid peptides with a Phe or Tyr residue in position 5 and a Leu at position 8 due to the specificity of the MHC pockets (36,37). The peptide's N-terminal amino acid is anchored by pocket A whereas pocket F has affinity for the C-terminal amino acid. The remaining amino acids can be variable to some degree and will specify minor interactions with the MHC pockets or interactions with the TcR. Figure 1B shows a view of the MHC-peptide complex that a T cell would view as it approaches in attempting to bind (34).

The pathway that results in the MHC class I-peptide expression at the cell surface begins with the cytoplasmic synthesis of a foreign organism or self-protein (schematically represented in Figure 2). The degradation of the protein is carried out by the proteasome (40). The multisubunit proteasome complex (41) consists of a barrel-like structure created by two rings at

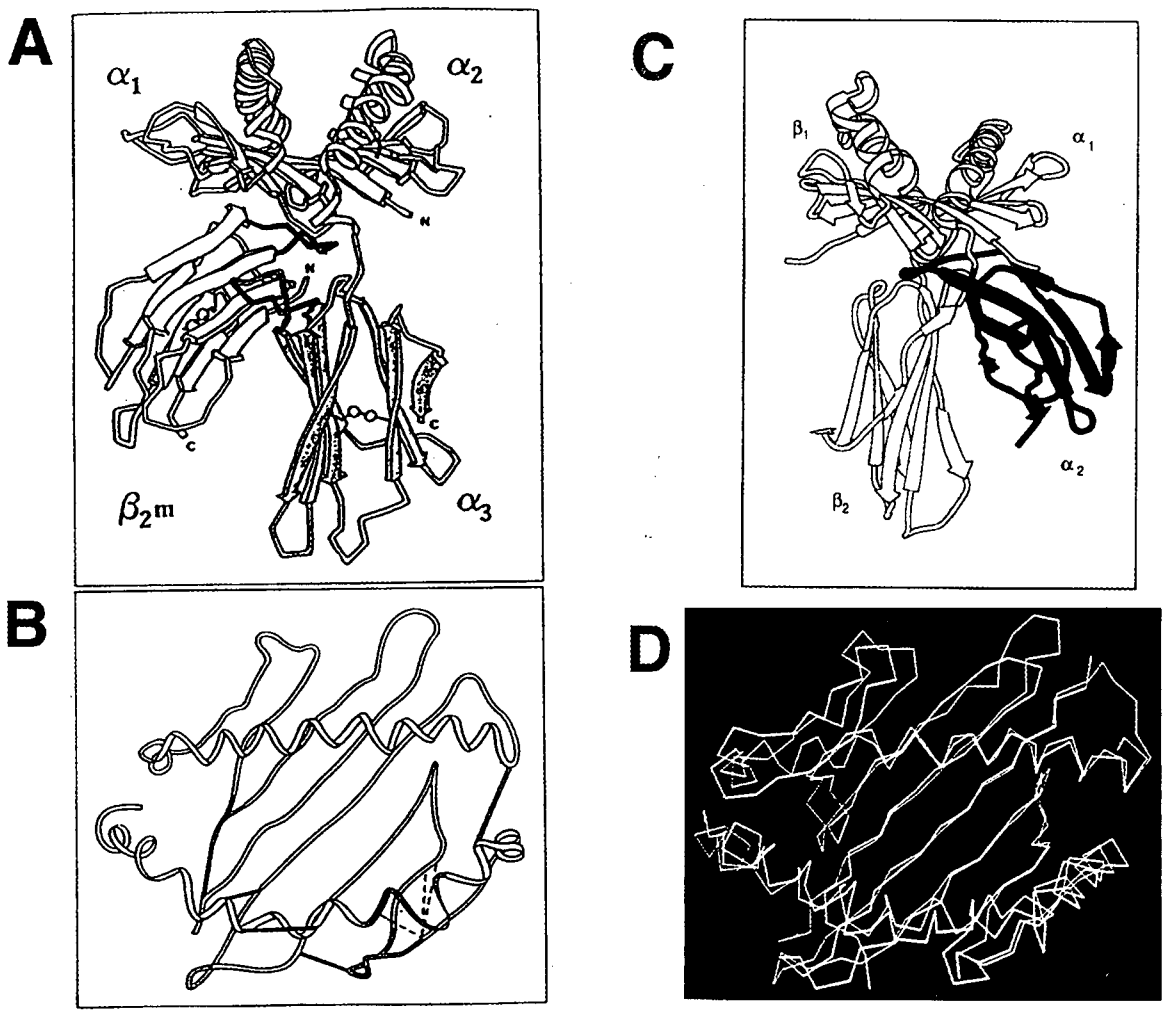

Figure 1: 3-Dimensional Structure of MHC class I and II

A) The 3-dimensional structure of the human class I protein, HLA-A2, is shown from the side and B) from the perspective of the TcR looking down into the peptide binding cleft. The depictions are derived from (34).

C) The 3-dimensional structure of the human class II protein, HLA-DR1. D) The peptide binding clefts of MHC class I and MHC class II as seen from above, are drawn to indicate their similarity. The depictions are derived from (38) and (39).

each end of the barrel composed of seven α subunits each and two rings for the middle of the barrel created by seven β subunits each. Interestingly, two of the optional low molecular weight proteins (LMP) of the proteasome, LMP-2 and LMP-7, are encoded in the MHC (40). The proteasome degrades proteins into peptides of 8 to 10 amino acids due to the molecular spacing of the catalytic β subunits. Perhaps not coincidentally, MHC class I preferentially binds peptides of 8 to 10 amino acids.

The peptides from the proteasome are transported into the endoplasmic reticulum (ER) by TAP-1 and TAP-2 (**T**ransporter associated with **A**ntigen **P**resentation) (30). These proteins are members of the adenosine triphosphate (ATP) binding cassette family of transporter proteins. The two proteins are encoded in the MHC class II locus and exist as polymorphic alleles which may complement the MHC polymorphism. The nature of the complex is commonly proposed to be a heterodimer of TAP-1 and TAP-2, but functional transport of at least some peptides can occur in the presence of only one of the TAP molecules (42). Furthermore, TAP molecules are physically associated with the MHC class I heavy chain in the ER, which should serve to increase the local concentration of peptide for MHC class I binding.

The assembly of the final complex of MHC class I heavy chain, peptide , and β_2m is generally dependent on the presence of all three components. The MHC class I heavy chain is retained in the ER by the chaperone calnexin which is displaced upon peptide binding (43). The binding of β_2m to the complex, stabilizes the peptide binding and completes conformational changes in the complex which permit the egress of the complex from the ER, through the Golgi to the cell surface (Figure 1 and Figure 2). The dependence of this process on peptide and β_2m, is emphasized by cell lines and knockout mice lacking a TAP-1 molecule (and therefore lacking

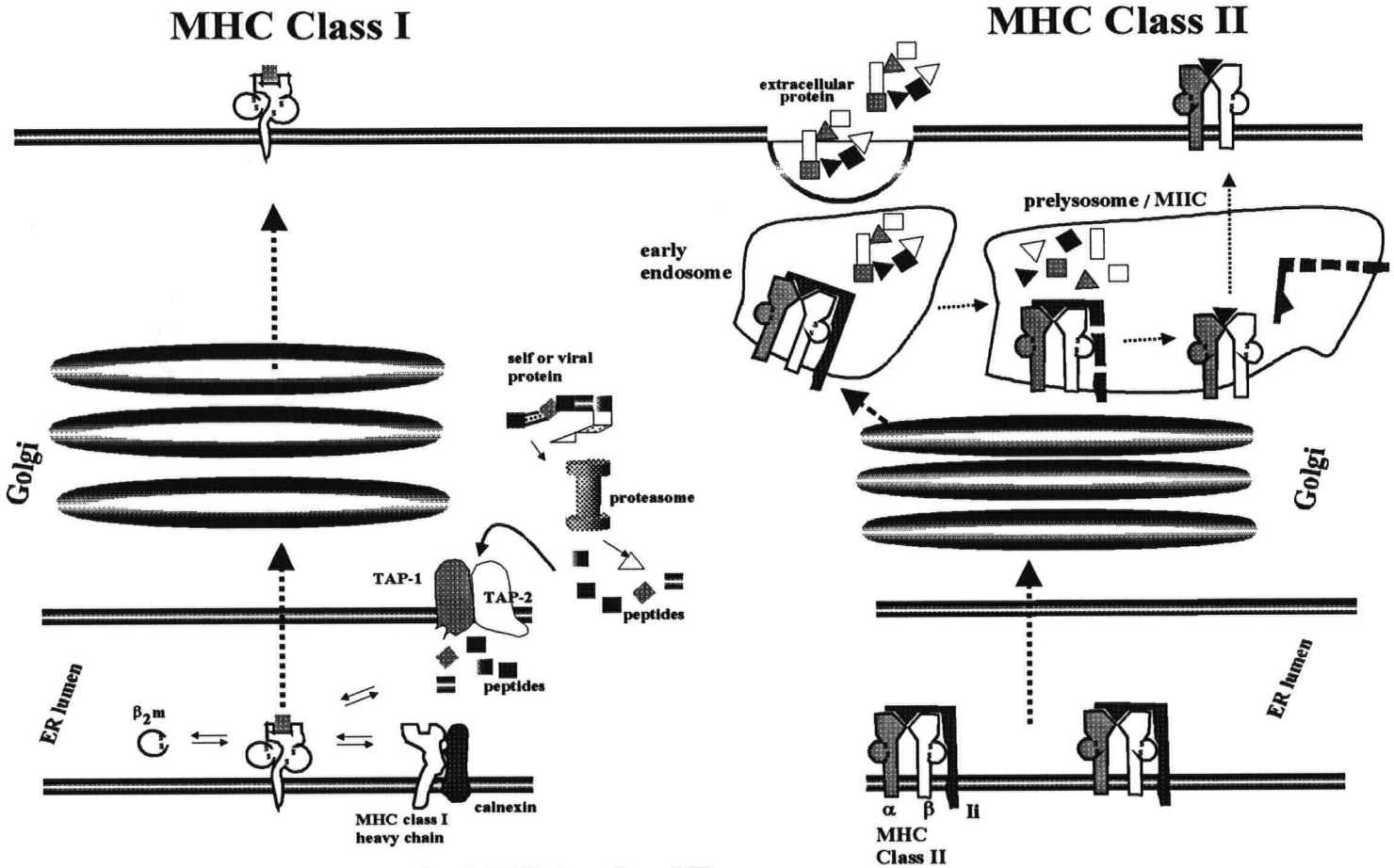

Figure 2: Classical antigen processing pathways for MHC class I and II

The MHC Class I pathway begins with the intracellular synthesis of a viral or self antigen. The protein is digested by the proteasome into peptides which are transported into the ER by TAP-1 and 2. The peptides bind to the MHC class I heavy chain which together form a stable complex with β_2m. This complex is then transported through the Golgi apparatus to the cell surface.

The MHC class II antigen processing pathway involves endocytosis of extracellular proteins and degradation in lysosomes or pre-lysosomes. The MHC class II heterodimer is assembled in the ER with the Invarinant chain (Ii) and transported through the Golgi to the endosomal network. Proteolysis of the Ii frees the MHC class II peptide binding cleft to permit the binding of peptides. The MHC class II-peptide complex is then transported to the cell surface. See text for more details.

the majority of peptides in the ER) or β_2m which express significantly less MHC class I on the cell surface (44,45).

The exquisite levels of control for the surface expression of class I MHC likely reflect the important consequences of aberrant expression, recognition and cell killing by CTLs. Ultimately, the immune system wishes to retain the ability to present peptides from infected or tumorogenic cells while ensuring that normal cells are not indiscriminately attacked by CTLs.

1.2.2 Class II MHC

As briefly outlined in Section 1.1.2, MHC class II primarily presents peptide antigens derived from proteins acquired from the extracellular environment. The processing of endocytosed protein had been assumed to occur in an endosomal compartment, although the precise compartment proposed varied in different cell types and in work from different laboratories (30,46). The MHC class II processing pathway is represented in Figure 2. Lysosomes do appear to be the most efficient compartment for producing peptides, but proteolysis can also occur in early endosomes and in a newly characterized compartment, the MHC class II containing compartment (MIIC) (47,48). The synthesis of the MHC class II proteins and their assembly and transport to the peptide binding compartment is well characterized (reviewed in (48)). The MHC class II α and β chains assemble in the ER with the invariant chain (Ii) into a nonamer ($\alpha_3\beta_3Ii_3$) (49). The Ii serves two primary purposes. The first is to block the peptide binding cleft to prevent ER peptides from binding to class II, and the second is to route the MHC class II proteins to the endocytic pathway (50,51). The Ii is cleaved in the MIIC leaving only the Ii fragment in the binding cleft. This CLIP (class II Ii peptide)

peptide is likely removed by the MHC class II related DM molecule which also localizes to the MIIC (52). The empty class II molecule is then free to bind peptides which have accumulated in the MIIC before transport to the cell surface.

The crystal structure of the MHC class II molecule did not produce many surprises (38) (Figure 1C and D). The overall structure is similar to MHC class I with α helices and β pleated sheets forming a peptide binding cleft contributed to by the α and β chains. The cleft ends are relatively open compared to MHC class I, providing no anchoring via the N-and C-terminal residues. Instead, the MHC class II peptide is anchored via the pockets within the cleft. This allows the peptides to extend from the end of the groove as long as the anchor residues are aligned in the cleft. This explains the heterogeneity in the size of peptides associated with MHC class II (53). The structural combination of peptide and MHC that the T cells will recognize is relatively similar to that of MHC class I (Figure 1D).

1.2.3 Antigen presenting cells

1.2.3.1 Macrophages and B cells

Mϕs, B cells, and DCs are the cell types considered as professional APCs. The focus of the research in this thesis has been on describing protein molecules in DCs which could contribute to the unique DC functions. Therefore, DC function and phenotype will more be thoroughly discussed in Section 1.2.3.2. The antigen presentation and other functions of B cells and mϕs are interesting on their own and are relevant as comparative systems for DCs.

B cells, primary function is to produce and secrete Abs against specific molecules in an IR. As outlined in Section 1.1.2, the B cells are clonally selected by their antigen specificity,

clonally expanded in response to antigen and cytokines in the ensuing IR, and ultimately secrete Abs. The expression of MHC class II in activated B cells, also endows B cells with the ability to stimulate T helper cells. The B cell is in a desirable situation to influence the class II MHC restricted IR since the B cell surface Ig preferentially concentrates the antigen recognized by the sIg. The sIg-antigen complex can be endocytosed and delivered to compartments where peptides from the antigen will dominate the repertoire of peptides which will be bound by MHC class II (54). The entire IR is thus skewed towards producing T_h cells with specificity for proteins that are recognized at a higher affinity by the B cell sIg, and therefore concentrated more efficiently. The subsequent secretion of cytokines from the activated T_h cells will ensure that the B cell will continue to divide, perhaps undergo class switching, and continue to secrete antibody.

Experiments comparing the antigen presenting capability of DCs with B cells have found that even activated B cells stimulate a primary T cell response four-fold less efficiently than DCs (55-57). The B cell as an APC is more important in a secondary response where B cells preferentially activate T_h cells with specificity for the antigen bound by the sIg.

Mϕs are considered a Jack-of-all-trades since they fulfill many functions in the immune system. The phagocytic activity of mϕs is utilized for several purposes including the removal of dead cells from the bone marrow and thymus, the removal of bacteria, and the uptake of foreign proteins. Mϕ surface receptors play a key role in these mϕ functions. Fc receptors of several types are present on most mϕs and function to bind Ab-antigen complexes(58). The Ab may have bound to a soluble protein which will be endocytosed and digested with the Ab-FcR complex. The Ab may also bind to an intact organism or virus which will normally be phagocytosed and destroyed. Ab can also recognize foreign proteins expressed on infected cells which can lead to the cell's elimination by antibody dependent cellular cytotoxicity (ADCC).

Mϕs also remove bacteria via receptors for the complement C3b molecule which opsonizes pathogens. The Man-Fuc receptor is one well characterized receptor involved in binding and uptake of glycoproteins (59). The scavenger receptor is notable for its involvement in the uptake of lipopolysaccharide (LPS), lipoteichoic acid, and oxidized lipoprotein. Several receptors are also involved in the uptake of low density lipoproteins (LDLs) from the circulation (60).

The activation of mϕs by cytokines such as Interferon-γ (IFN-γ), functions to eliminate intracellular pathogens. The induction of nitric oxide production and the oxygen burst which produces oxygen radicals, act in concert with mϕ proteases to eliminate most intracellular pathogens such as *Listeria monocytogenes*, salmonellae, mycobacteria, and leishmaniae which can otherwise replicate inside the cell (61-63). Mϕ activation also induces MHC class II expression. Mϕs were initially considered the primary APC due to their obvious systems for protein uptake and degradation (16). Mϕs are clearly capable of stimulating T cells, but most systems utilized secondary responses or T cell lines and clones to assess T cell activation. The general failure of mϕs to function in the initial, primary IR is now clear (64). However, mϕs likely retain an important role in subsequent IRs since antigen can be concentrated via Fc receptor binding of Ab-antigen complexes and since the requirements for T cell activation in a secondary response are satisfied by mϕs.

1.2.3.2 Dendritic cells

1.2.3.2.1 Identification, classification, and development

DCs are a trace population of cells within the immune system, representing only 0.5 to 1.0 percent of leukocytes. The phenotype of DCs, with their dendritic processes, amorphous nucleus, motile

nature, and apparent lack of classical endocytosis (65) separates DCs from mϕs. This original morphological and histochemical description of DCs was soon supported with distinct tissue distribution and functional data for DCs relative to mϕs (66-68). In particular, the DC was recognized as a potent stimulator of T cell responses (68). Despite the limited number of DCs, these cells perform unique and essential roles in initiating several key immunological phenomena including primary, secondary, and memory T cell stimulation, transplant rejection, and the maintenance of self-tolerance (reviewed in (69)). DCs form an interactive network of cells between lymphoid organs (spleen, lymph nodes, Peyer's patches, etc.), lymphatics, blood, skin (Langerhans Cells (LCs)), and various organs (heart, liver, and lung). The location of DCs at all of these locations creates an antigen sampling system to monitor the entire body for foreign molecules, infection, or tumor development (69-71).

DCs have been known to be bone marrow derived, but a more precise description of their developmental lineage has only recently been completed. The key observation has been the dependence of DC development on granulocyte-macrophage colony stimulating factor (GM-CSF). The addition of GM-CSF to bone marrow cultures (72) or blood mononuclear cells (73), preferentially expands DCs from a proliferating precursor. Non-proliferating DCs are released from clusters of cells which contain the proliferating precursor. This precursor is, not surprisingly, from the myeloid lineage since granulocytes and mϕs can be derived from the same precursor cultures (74). GM-CSF effects are augmented by TNFα (75) and IL-1 (76) which likely serve to upregulate the number of GM-CSF receptors (75,77). GM-CSF responsive DC precursors are also present in the blood and may serve as an extra source of DCs to replenish DCs throughout the body (73). Development of thymic DCs from precursors common to thymocytes and thymic DCs has been documented as an alternative to myeloid development and may be relevant for the function of DCs in thymocyte tolerance induction (78).

1.2.3.2.2 Function and Phenotype

DCs are unique in their ability to stimulate a primary T cell response, including the primary mixed lymphocyte reaction (MLR) (68), response to superantigen (79), and primary CTL response to hapten (80) and viral antigen (81). As few as 1 DC per 100 responder T cells will still produce maximal proliferation in primary MLRs (68). B cells and mϕs do not efficiently stimulate primary T cells (57,68,81), although all three APC types can stimulate secondary T cell responses (56). Antibody production against soluble antigen is also thought to depend largely on DCs in a primary response (64,82) since antigen specific B cells can be isolated from DC-T cell clusters during the initiation of the IR. DCs are also implicated in thymic T cell tolerance since cell activation of a thymocyte leads to deletion rather than activation (83,84). Bone marrow chimera experiments have suggested the presence of a bone marrow derived cell type involved in thymic deletion of T cells (85), although thymic epithelium is also clearly involved in the tolerizing process. Further experiments (86-88) have shown that DCs are capable of inducing self tolerance in the thymus, although cell types such as B cells and thymic epithelia are also involved.

In order for DCs to be able to efficiently present antigen to T cells, the DC must first acquire the antigen, process the antigen into immunogenic peptides, and present the MHC-peptide complex to T cells. For MHC class I presentation, the DC can be infected by the intracellular pathogen, the proteasome digests the endogenously made protein, the peptides are translocated into the ER by the TAP proteins, and MHC class I assembles before it is transported to the surface as discussed in Section 1.2.1. The acquisition of proteins for the MHC class II presentation pathway has been more difficult to explain. The original, and still valid, description of DCs described the apparent lack of an active endocytic pathway and lysosomal system for uptake and degradation of exogenous protein

(65,66,89,90). Instead 'vacuoles' were observed which did not fit the expectations of a lysosomal degradative pathway (65-67). DCs do not acquire peptides regurgitated from mϕs. A T cell clone will not be stimulated by DCs of the restricting MHC if mixed with MHC mismatched mϕs (64,91). More careful analysis of the DC endocytic pathway has now explained the apparent mystery of DC class II antigen processing. Analysis of isolated LCs demonstrated the presence of acidic endosomes which were absent following *in vitro* culture (92). The functional correlate of these two LC populations is that freshly isolated LCs (fLCs) are capable of processing and presenting whole antigen, but cultured LCs (cLCs) cannot (93). Similar observations apply to fresh splenic DCs which can process exogenous antigen whereas overnight cultured splenic DCs cannot (94,95). The ability of DCs and LCs to endocytose antigen *in vivo* was also demonstrated in several systems (64,96,97). For example, antigen is detectable in DCs as soon as two hours after intraperitoneal injection (64). Mϕs are still not functional six hours post-injection even in stimulating a secondary response (64). Fluid phase uptake in DCs has now been shown to be greater than in other cell types (98-100), but proceeds via macropinocytosis rather than pinocytosis. The uptake of large vesicles permits the uptake of one cell volume of fluid per hour by one DC (99). The macropinocytotic vesicles are transported inside the cell where at least a portion of their contents fuse with the class II rich vesicles (99,101).

DCs also possess receptor-mediated mechanisms for antigen uptake which, although not antigen specific like B cell surface Ig, serve to concentrate antigens inside the DCs. DCs utilize FcRγ, the DEC-205 protein, and the Man-Fuc receptor (99,102,103) for protein internalization. The internalized proteins are then processed and efficiently presented by DCs. Interestingly, DEC-205 contains 10 C-type lectin domains and therefore also exhibits the general specificity for carbohydrates like the Man-Fuc receptor (103). Since the degradation pathway is underdeveloped in DCs, these receptors are more actively recycled, allowing the repetitive uptake of proteins (99).

The antigen processing capacity of DCs is also controlled by their rate of MHC class II synthesis (104,105). fLCs synthesize both MHC class II α and β chains as well as Ii very rapidly, whereas *in vitro* cultured LCs have very low rates of MHC class II α and β synthesis and Ii synthesis with a concomitant increase in MHC class II molecule stability at the cell surface. The LC MHC class II shows no decrease in expression after 32 hours, whereas MHC class II on mϕs is reduced by 55% after 20 hours (105). Therefore, the antigens acquired from the skin will be efficiently processed and displayed with MHC class II and not displaced by the continued processing of new MHC class II. This ensures that the antigens acquired by LCs as they surveyed the skin for foreign agents, are presented to T cells in the draining lymph nodes.

As the LC migrates to the lymph node, one can conceptually envision the LC changing its physiology from antigen uptake and processing to enhanced T cell stimulatory capabilities. This expectation has been shown to be true. For example, if peptide antigen is provided, the cLC can stimulate T cells 10-fold more efficiently than fLC (93). The change between fLC and cLC is thought to mimic the alterations which occur as an LC acquires antigen and migrates to the local lymph node. The control of this DC 'maturation' is mediated by cytokines and other factors produced by the innate, non-specific IR or factors commonly associated with inflammation. The immature state is likely maintained by GM-CSF produced by keratinocytes and IL-4 (99). TNF-α is produced in dermal tissue following antigen encounter and likely induces DCs to begin migration to the local lymph node (106). IL-1, which has long been known to augment DC T cell stimulatory properties (107,108), is also commonly produced by mϕs as an early inflammatory response. LPS is another common immune regulator found at the site of bacterial infection. All three of TNF-α, IL-1, and LPS initiate the down-regulation of antigen processing functions of DCs including macropinocytosis which is otherwise utilized constitutively by DCs (99). The phenotypic, stepwise alteration from the antigen

acquisition and processing stage to the T cell stimulatory phase is now considered a hallmark characteristic of DCs.

The phenotypic change between the two stages of DC maturation, also encompasses cell surface molecules. The DC cell surface expresses several molecules which are important for function including those molecules involved in DC adhesion mechanisms, MHC molecules for interaction with the TcR, DC costimulatory molecules, and receptors which serve to modulate DC function. As DCs begin the maturation phase, molecules including the FcRγI and Ii are downregulated and other molecules such as MHC class II, ICAM-1, LFA-1, B7-1, and B7-2 are upregulated (57,94,95,109) The adhesion molecules of DCs include ICAM-1, ICAM-3, LFA-1, heat stable antigen, and LFA-3 (57,110,111). These molecules are important for DC adhesion to T cells since antibodies which disrupt the LFA-1 binding interfere with the primary MLR and affect DC-T cell cluster stability (112). However, this effect is proceeded by an antigen independent, LFA-1 independent, clustering of DCs with T cells (112,113) which is also crucial for DCs' potency in stimulating the primary IRs (82,113). This clustering allows TcR specific interactions to occur after which the other adhesion molecules strengthen the DC-T cell binding. Since T cell recognition of antigen is determined by TcR interaction with MHC class I or II molecules and associated antigen peptides (15), it is not surprising that DCs constitutively express very high levels of MHC class I and II proteins which are further upregulated as DCs prepare to encounter T cells.

The activation of T cells is generally considered to require two signals, one via the TcR and one via costimulatory molecules (26,32). DCs express high levels of receptors for CD28, B7-1 (CD80) and B7-2 (CD86), which are both expressed at high levels on DCs and are upregulated following maturation (57,100,114-117). Interference with the binding of DCs to CD28 reduces T

cell stimulation by 3-fold in one system (57) and 90% in another system (117), but not to background levels, which indicates other costimulatory mechanisms may also be present on DCs.

As described above, the modulation of DC function and phenotype is controlled by cytokines and inflammatory factors. The presence of receptors for GM-CSF and IL-1 has been clearly shown (76) as has a low level of CD14 for binding LPS (100). IL-4 and TNF-α receptors are also present. The presence of CD40 on DCs (118) also has functional implications for DC maturation. The CD40-CD40 ligand (CD40-L) interaction was first shown to be important for T cell dependent B cell activation (119) where B cell CD40 engagement induces a proliferative rather than apoptotic response to surface Ig signaling. CD40 crosslinking on DCs increases DC viability likely also by prevention of apoptosis (120,121). In addition, CD40 ligation upregulates LFA-3, B7-1, B7-2, CD25, and class II MHC (120). The production of TNF-α, IL-8, and macrophage inflammatory protein-1α by DCs is also induced. Therefore, upon encountering CD40-L on T cells in the lymph node, DC maturation is further driven to optimize T cell stimulation and DC viability is increased. A representation of some of the molecules involved in the DC-T cell interaction is shown in Figure 3.

In addition to the antigen presentation functions of DCs, DCs have also become implicated in allergic responses mediated by IgE. DCs express CD23, the low affinity IgE receptor, and FcRεI, the high affinity receptor for IgE (122-124). DCs have been shown to bind IgE in allergic responses (124,125) and crosslinking of FcεRI has been shown to evoke a calcium flux in DCs (126,127). DCs could be presenting the IgE-bound allergen to T cells, thus potentiating the anti-allergen T cell response. Alternatively, the DCs may produce cytokines or other effector molecules triggered by the Ca^{++} flux. The precise role of DCs in controlling of the IgE-mediated IR remains to be determined.

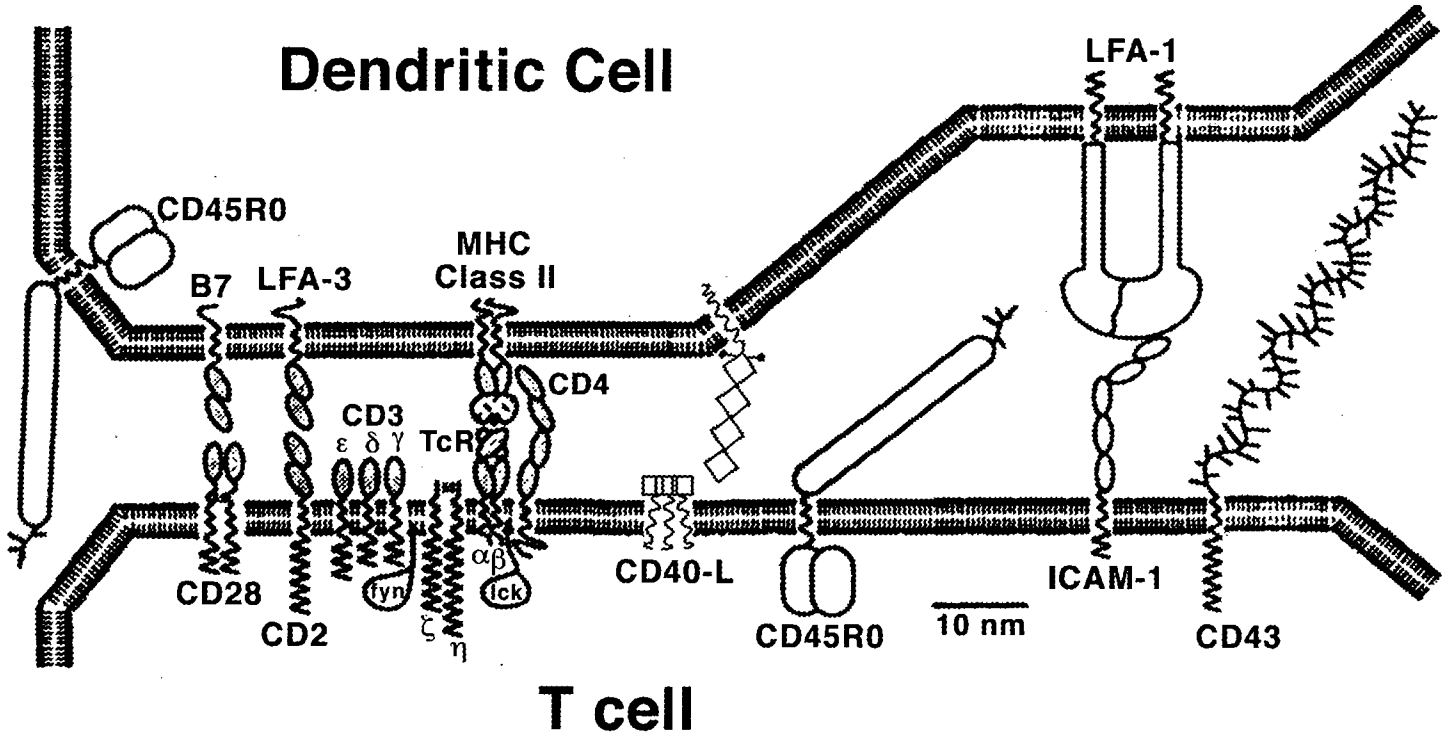

Figure 3: DC-T cell molecular interactions

The molecules involved in a DC-T cell interaction are represented. See text for a description of the individual components. This figure has been adapted from (129) with the authors' permission. The molecules are all represented to scale except for CD40 and CD40-L.

The specialized functions of DCs places them in a unique position for controlling the IR. A desirable IR could be augmented by increasing DC function whereas an unwanted IR such as autoimmunity or transplant rejection could potential be prevented by interfering with DC function.

The use of DCs as nature's adjuvant (128) has been proposed and utilized in vaccination protocols for the induction of antibody and CTL responses. Antigen provided extracellularly will be endocytosed and presented via the class II MHC pathway to stimulate a $CD4^+$ helper T cell response as shown with numerous soluble proteins (reviewed in (69)) and for organisms such as mycobacteria (97). Although a primary CTL response has been induced by *in vitro* infection of DCs (81), a more practical delivery approach may be using soluble proteins delivered in pH-sensitive liposomes (130). A CTL response to soluble ovalbumin was efficiently elicited by DCs if pulsed *in vitro* or *in vivo* with antigen in pH sensitive liposomes. The ease and efficiency of this system may prove useful in designing vaccines to promote CTL based immunity.

DCs are also notably unique in their ability to overcome antigen presentation deficiencies. In the mutant bm13 and bm14 mouse strains, the $H\text{-}2D^b$ presentation of the H-Y antigen is defective due to mutations in the bm13 or 14 molecules' peptide binding clefts. However, purified $H\text{-}2D^{bm13}$ or $H\text{-}2D^{bm14}$ DCs can stimulate $H\text{-}2D^b$, H-Y specific T cells (131). The unique ability of DCs to mediate T cell stimulation under certain conditions is readily applicable to cancer treatment (70). Studies have reported the successful induction of anti-tumor immunity utilizing DCs pulsed with tumor cell membranes *in vivo* before injecting the DCs into the animal (132,133). Reports of clinical trials involving the generation of DCs from blood precursors (134) and pulsing with isolated tumor cells prior to infusion into the patient are not likely far off.

The ability of DCs to produce antigen specific primary CTL *in vitro* is also relevant to immune based treatment of tumors. Viral models have demonstrated the outgrowth of virus specific

CTL from naive populations when DC stimulators were infected with virus or incubated with a specific viral peptide (81,135). The ability to expand tumor specific CTL *in vitro* utilizing the patient's T cells, DCs, and a tumor sample has yet to be explored.

The strong stimulatory capacity of DCs and high MHC expression also support hypotheses which implicate DCs in autoimmune disease (136-138) and as the passenger leukocytes responsible for graft rejection (139). Studies tracing DC migration following heart transplantation revealed that donor DCs leave the graft and home to the recipient spleen where recipient T cell stimulation occurs resulting in graft rejection (140). This situation also likely occurs in transplants of skin and kidney where DCs are also present (141,142). *In vitro* pretreatment of thyroid gland allografts with a mAb and complement, showed near 100 percent acceptance of grafts pretreated with MHC class II mAb or the DC-specific mAb 33D1 (143). Similarly, allografts of dissociated islets of Langerhans are also accepted if pretreated with anti-MHC class II or the 33D1 mAb (144). The successful adaptation of protocols to remove DCs from solid tissue transplants may also reduce the rejection rate in these procedures.

The importance of DCs in HIV infection is also worth noting. While the majority of research in the HIV field is concerned with T cell infection, infection of mϕs, DCs, and follicular dendritic cells is likely of equal importance (145,146). DCs isolated from HIV^+ patients contain infectious virus (147) and purified DCs from uninfected patients can be productively infected with HIV (148). Therefore, it is likely that DCs serve as a reservoir for HIV prior to disease onset and provide a mechanism for subsequent infection of $CD4^+$ T cells (149). Furthermore, DCs have also been implicated in mechanisms for killing of uninfected T cells by rare HIV^+ T cells (150).

1.3 Post-translational modifications of plasma membrane antigens

The previous section has highlighted the presence of several cell surface molecules that are important for DC function. The functions of these molecules range from the establishment of cell-cell interactions to providers of T cell costimulatory signals to growth factor receptors to the ultra-specialized MHC class I and II molecules. By understanding the functional role of each molecule, the composite picture of DC function has become clearer. In undertaking the characterization of DCs, many of the mechanisms described in Section 1.2.3.2 were not understood and many questions of DC function still remain now to be answered. We had hypothesized that DC cell surface molecules would be central to DC function and therefore concentrated on characterizing DC cell surface proteins. The following sections, therefore, introduce general qualities of cell surface proteins. Key among these, and a central theme of the research, are the post-translational modifications which proteins undergo. These modifications perform key structural and functional roles for proteins as will be described in Section 1.3.

Proteins of the plasma membrane are initially synthesized by ribosomes and directed to the ER by the signal peptide-signal recognition protein interaction (151). The signal sequence is cleaved, the protein translation is completed, and the protein remains associated with the ER membrane via one or more transmembrane sequences. Typically the protein's N-terminus is in the ER lumen and the C-terminus in the cytoplasm. Proteins showing this orientation are referred to as a Type I membrane proteins whereas Type II proteins utilize an internal signal sequence and are in the inverse orientation relative to Type I proteins. Type III proteins do not fall under either of the Type I or II categories. One of the first modifications to the protein occurs co-translationally by the addition of an oligosaccharide to certain Asn residues. This process will described further in Section 1.3.1. The translated protein is often bound by

chaperone molecules such as the heat shock protein family members, BIP, or calnexin. The formation of disulfide bonds, catalyzed by protein disulfide isomerase, is an early event in the folding of many proteins (152). Following proper folding, proteins destined for the plasma membrane leave the ER and pass through the cis, medial, and trans-Golgi apparatus which are the sites of many of the processes described in the following sections. Most proteins are then delivered to the plasma membrane, although some including MHC class II (described in Section 1.2.2), are routed through the trans-Golgi network and other post-Golgi vesicular compartments prior to arriving at the cell surface or remaining in intracellular compartments.

1.3.1 N- and O-linked glycosylation

1.3.1.1 Synthesis

Several reviews describing the mechanism and control of N-linked glycosylation exist (153,154) so mechanistic detail will not be delved into here. Instead, the processes that occur will be related to the effect of structural alterations or to the demonstrated or proposed function of the particular carbohydrate structure. N-linked glycosylation can occur on Asn residues in the sequence Asn-X-Ser/Thr where X is not Pro or Gly. The initial core oligosaccharide is transferred to the Asn from a dolichol-phosphate lipid carrier in the ER. The core oligosaccharide has the structure shown in Figure 4.

The oligosaccharide processing is initiated immediately in the ER by the removal of the terminal Glc residue and subsequent removal of the other two Glc residues. The removal of zero, one, or two core Man residues is also possible at this stage to produce a $Man_{9,8,or7}GlcNAc_2$

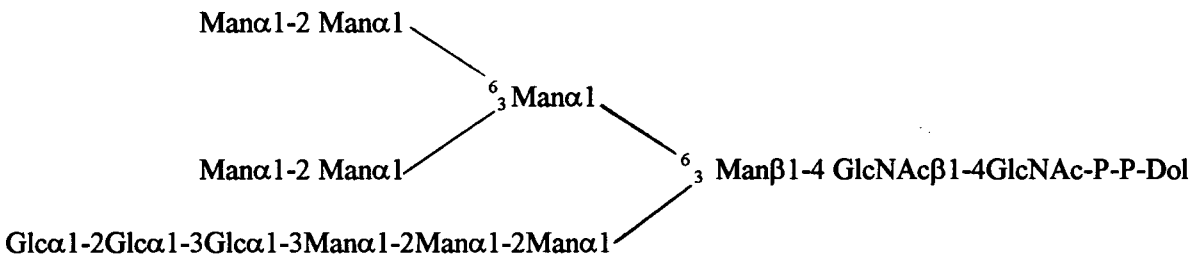

Figure 4: Structure of the core N-linked oligosaccharide

The structure of the N-linked oligosaccharide transferred from the dolichol phosphate carrier is represented. The abbreviations for the respective monosaccharides are identical to those described in Figure 5.

structure. This structure is then reglucosylated and immediately deglucosylated again which has functional implications as described in the next section.

Upon exiting the ER and entering the cis-Golgi, the N-linked glycan is further modified by the removal of two Mans, one from the α1-3Manα1-6Manβ1-4GlcNAc branch and one from the α1-3Manβ1-4GlcNAc branch, to form a $Man_5GlcNAc_2$. Proteins destined for lysosomal expression do not lose these two Man groups, but are instead phosphorylated on specific Man residues. This phosphorylation ultimately targets the glycoprotein to the lysosome via binding to the Man 6-phosphate receptor (155,156). For non-lysosomal glycoproteins, the $Man_5GlcNAc_2$ form is transported to the cis-Golgi where processing continues by the addition of GlcNAc to the terminus of the α1-3Manβ1-4GlcNAc branch. An important technical note is that the enzyme endoglycosidase H (Endo H) will recognize the $Man_{5,7,8,or\ 9}\ GlcNAc_2$ structure and cleave the oligosaccharide between the core GlcNAcβ1-4GlcNAc bond. Since Endo H does not recognize the glycan after further trimming of Man residues and GlcNAc addition to the α1-6Man branch in the medial-Golgi, only the glycans in the ER, cis-Golgi, and early medial-Golgi

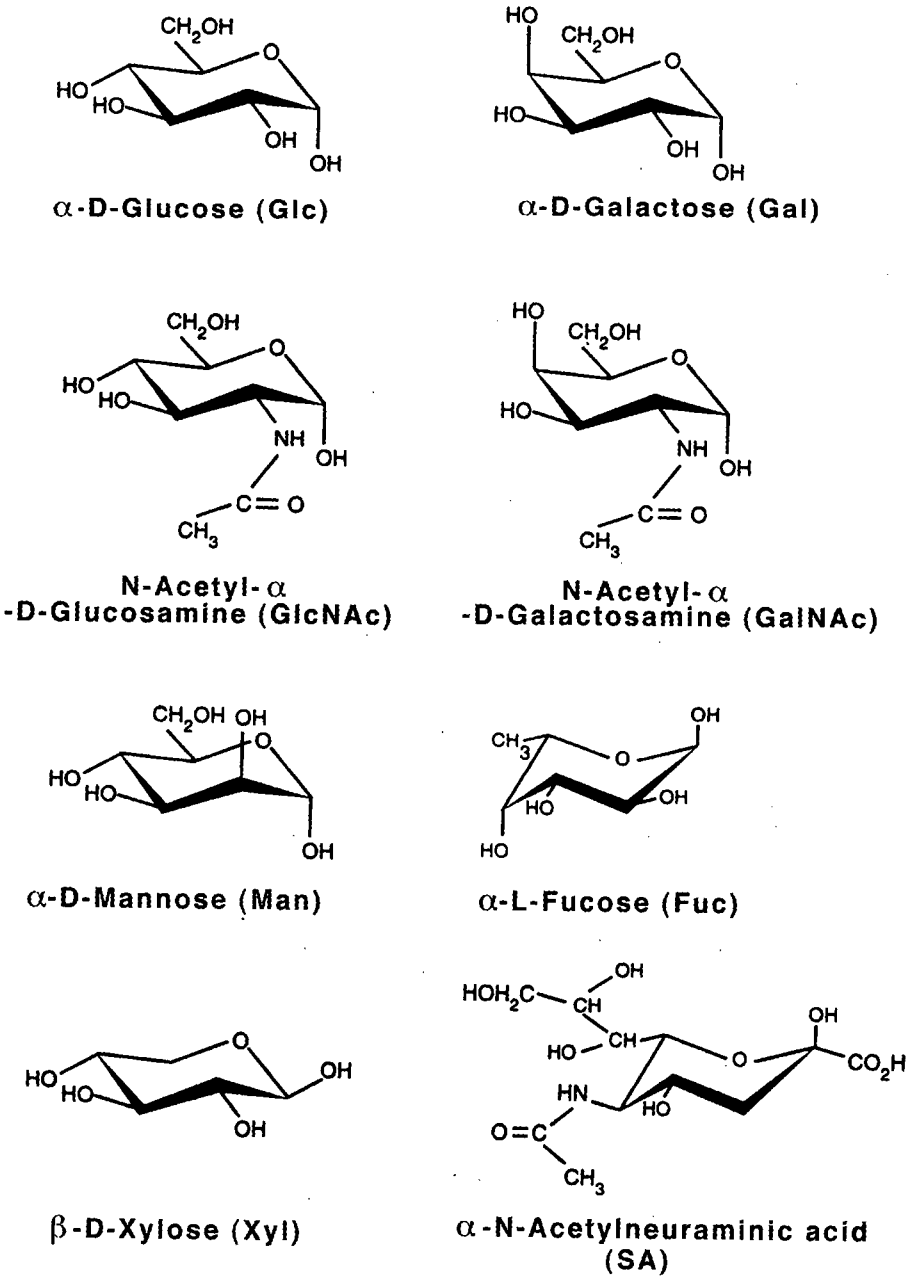

Figure 5: Structures of monosaccharides most commonly found in glycoproteins

The structures of the monosaccharides that commonly occur in glycoproteins are shown. The abbreviations utilized throughout the body of this thesis are indicated for each monosaccharide. The variations in different forms of sialic acids are not indicated and are collectively referred to as sialic acids throughout the text.

are sensitive to Endo H. Glycan structures in the late medial-Golgi and trans-Golgi are resistant to Endo H cleavage. The kinetics of protein transport from the ER to the medial-Golgi can therefore be monitored by the conversion from an Endo H sensitive to Endo H resistant form.

The removal of two more Man residues from the α1-3Manα1-6Manβ1-4GlcNAc branch is the final trimming of the oligosaccharide. Nucleotide monosaccharides act as donors to feed the enzymatic addition of the terminal glycan residues in the medial and trans-Golgi. The sugars added at this point include the GlcNAc residues in the medial-Golgi to which more GlcNAc, or Gal, Fuc, and SA can be added as the glycoprotein passes through the trans-Golgi and trans-Golgi network to the plasma membrane.

The sequence of events is subject to many levels of control at each step of carbohydrate processing. For example, only 30-40% of potential Asn-X-Ser/Thr sequences are glycosylated (153). The processing of the core oligosaccharide is also extremely variable and can result in carbohydrate structures classified into high Man, hybrid, and complex carbohydrates forms. The general structures of these forms and some variations in the final structures of complex N-linked carbohydrates are shown in Figure 6. Even the same protein from one cell type is often glycosylated differently, as was shown most clearly with rat Thy-1 (157). There are 8 different glycoforms of the thymocyte Thy-1 which differ in the usage of the 3 N-linked glycosylation sites and in the specific structures at each site. Thy-1 expressed in brain tissue has four glycoforms, none of which is shared with the thymocyte glycoforms. Differences of glycosylation patterns for various proteins in different species have also been demonstrated (158). The example of Thy-1 is only one example of many, but should inform the reader that the control of N-linked glycosylation is a complex process that is still not entirely understood.

N-linked Carbohydrates

1) high Man

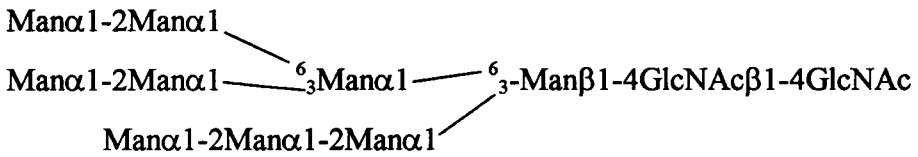

2) hybrid

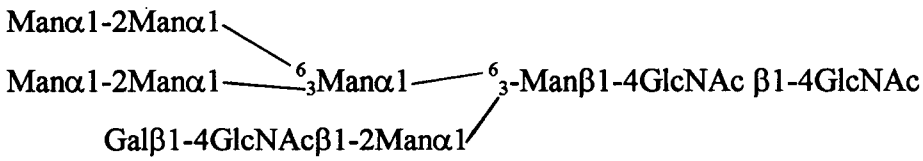

3) complex

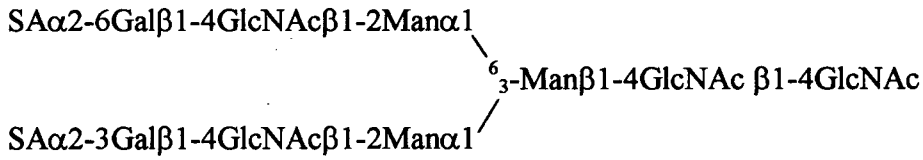

O-linked carbohydrates

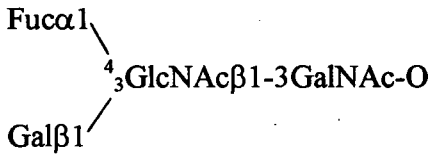

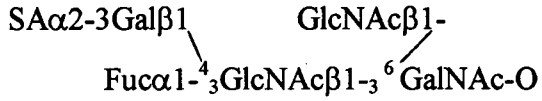

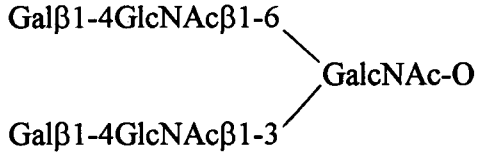

Figure 6: Potential structures of some N- and O-linked carbohydrates.

O-linked glycosylation is not initiated until the protein reaches the Golgi apparatus where polypeptide-N-GalNAc transferase adds a GalNAc to a Ser or Thr residue. Elongation of the glycan occurs entirely by the stepwise addition of monosaccharides from activated sugars (reviewed in (159)). The core structures of O-linked carbohydrates are generally grouped into 5 classes with the terminal structures built onto these core glycans. Although the O-linked structures are not as large nor as branched as N-linked structures, extensive variation is still possible. The structures in Figure 6 indicate only a few of the potential termini of O-linked glycans. The O-linked carbohydrates also have diverse functions as discussed in the next section.

1.3.1.2 Function

The largest advances in glycobiology in the past few years have been in the identification of functional roles for carbohydrates. One function for carbohydrates is their participation in the folding and transport of glycoproteins. The reglucosylation of $Man_7GlcNAc_2$ in the ER is catalyzed by the enzyme UDP-Glc:glycoprotein glucosyltransferase (160). This protein recognizes the N-linked carbohydrate via the GlcNAc residue attached to Asn, and also recognizes denatured peptide regions of glycoproteins (161). Since calnexin has affinity for monoglucosylated carbohydrate (162), calnexin and UDP-Glc:glycoprotein glucosyltransferase likely form a mechanism to retain incorrectly folded proteins in the ER (163). Once the protein is correctly folded, the N-linked glycans can also influence the protein's ultimate cellular localization. The role of the Man-6 phosphate in lysosomal targeting was explained above. N-linked glycosylation also apparently directs the apical localization of proteins. Unglycosylated mutants of growth hormone preferentially localize to the basolateral surface, whereas glycosylated growth hormone regains apical localization (164).

N-linked glycans are also important for stabilizing the structure of several proteins. For example, the hinge region carbohydrates of IgG interact to strengthen the interaction of the two heavy chains (165). Interestingly, the same glycosylation site of the two IgG heavy chains have distinct glycan structures, which emphasizes the fine regulation of carbohydrate processing. Carbohydrates have also been demonstrated to directly participate in the stabilization of the protein backbones, including the example of human CD2 (166). The single high Man N-linked glycan of human CD2 apparently stabilizes a cluster of 5 Lys residues which otherwise destabilize the CD2 structure and disrupt the CD58 binding site. Rat CD2 has a Glu residue among the Lys cluster which obviates the need for the N-linked glycan (167).

O-linked carbohydrates can also affect the local glycoprotein structure. Regions with a high local concentration of O-glycans in one domain often form extended structures such as in CD45 (168) or the mucin-like CD43 (169). This effect is likely due to a combination of the amino acid sequence in these domains which is generally high in Pro residues and the O-linked glycans. The functional result of the extended structure is to lift the remainder of the protein away from the membrane and most other membrane proteins to permit molecular interactions to occur (169).

Carbohydrates are now also recognized as participants in specific molecular interactions. The progressive characterization of mammalian lectins has resulted in the identification of families of lectins including C-type lectins (Ca^{++} dependent carbohydrate binding) and galectins (soluble β-Gal binding lectins) (170). In addition, Ig superfamily members such as CD22 and sialoadhesin have carbohydrate binding activity (171,172). The characterization of these carbohydrate binding proteins has also focused much research into identifying ligands for these proteins

Selectins are a family of proteins with the shared structural elements of several extracellular short consensus repeat domains similar to domains found in complement-regulatory proteins, a single

epidermal growth factor (EGF) domain, and an N-terminal C-type lectin domain (173-175). The three selectins E, P, and L are selectively expressed on activated endothelium (E and P), platelets following activation (P), and leukocytes (L). The interaction between leukocyte and endothelial selectins and their respective ligands mediates initial cell-cell adhesion events in response to inflammation. IL-1, LPS, and TNF-α upregulate endothelial E- and P-selectin surface expression (176,177), permitting the interaction of P-selectin with the leukocyte ligand PSGL-1 to initiate leukocyte rolling on the endothelium (178-180). The subsequent tight binding and leukocyte extravasation into tissues is mediated by leukocyte integrin interactions (174,178). L-selectin binds to lymph node and Peyer's patch high endothelial venule (HEV) selectin ligands, MadCAM-1, CD34, and GlyCAM-1 (181). This specificity explains the functional characterization of L-selectin as the lymphocyte homing receptor (182).

Selectin ligands are extremely variable although most contain SA, sulfate and/or Fuc residues in the recognition sequence (173) (Figure 7). Consequently, the removal of SA, sulfate, or Fuc from selectin ligands can destroy selectin binding (173). These carbohydrate sequences can be found on N- and O-linked carbohydrates, but the selectin ligands characterized to date appear to primarily be mucin-like molecules with high levels of O-linked carbohydrates (173). In addition to the carbohydrate recognition specificity, sulfation of Tyr residues in the P-selectin ligand, PSGL-1, is also critical to P-selectin binding (183,184). The general roles of sulfation will be described in Section 1.3.2.

Other members of the C-type lectin family include the asialoglycoprotein receptor, the mϕ Gal receptor, CD23, collectins, soluble Man binding proteins, the mϕ Man receptor, and the DEC-205 protein. CD23 is the low affinity IgE receptor, FcεRII, but the lectin domain appears not to be necessary for IgE binding (185). Instead, CD21 carbohydrates appear to mediate CD21-CD23

A

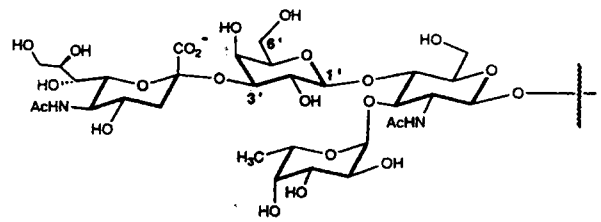

sialyl Lewis x
[SAα2-3Galβ1-4(Fucα1-3)GlcNAcβ1-]

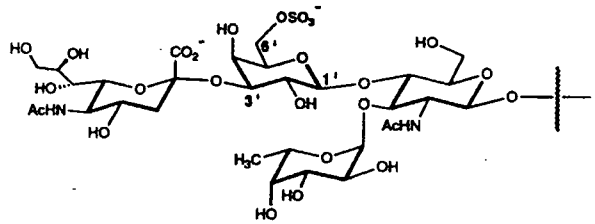

6-sulfate sialyl Lewis x
[SAα2-3(SO -6)Galβ1-4(Fucα1-3)GlcNAcβ1-]

B

SAα2-6GalNAcα1-
SAα2-3Galβ1-4GlcNAcβ1-
SAα2-3Galβ1-4GlcNAcβ1-3Galβ1-4(Fucα1-3)GlcNAcβ1-
SO_4-3Galβ1-4GlcNAcβ1-
SO_4-3Galβ1-4(Fucα1-3)GlcNAcβ1-

Figure 7: Selectin ligand structure

A) The structure of sialyl Lewis x and a sulfated derivative. B) Additional carbohydrate structures representative of other selectin ligands.

interaction which potentiates the IgE IR (186,187). The asialoglycoprotein receptor has specificities for Gal and GalNAc and is expressed primarily in liver hepatocytes where it serves to remove desialylated proteins from the blood (188). Collectins are soluble C-type lectins with collagen-like domains found in the liver and serum which appear to preferentially bind carbohydrates of pathogens to initiate immune recognition (189). Man binding proteins are also soluble proteins which have specificity for Man, Fuc, and GlcNAc residues. These proteins can be upregulated in the acute IR and serve to opsonize cells for complement mediated killing or phagocytosis (190-192). In contrast, the Man receptor and DEC-205 proteins are membrane-bound and contain multiple C-type lectin domains in a single polypeptide (59,103). The carbohydrate specificity of DEC-205 has not been investigated, but the Man receptor will bind to terminal Man, Fuc, or GlcNAc. Since these termini are more commonly found on bacteria than pathogens, the Man receptor will preferentially induce the phagocytosis of foreign organisms (190). The DEC-205 protein likely serves to enhance antigen acquisition by DCs and thymic epithelial cells (103) (see also Section 1.2.3.2).

The S-type lectins have now been unified under the classification of galectins, a family of molecules with specificity for N-acetyllactosamine, lactose, and Gal residues(193). The galectins are secreted, soluble molecules, but display distinct tissue localization. For example, thymic epithelial cells express galectin-1, but not galectin-2 (194). Galectin-1 on thymic epithelia appears to mediate binding of thymocytes to thymic epithelium via carbohydrates of CD45 and CD43, indicating a role for galectins in thymocyte development. Galectin-1 does appear to mediate T cell apoptosis by binding to CD45 (195). Galectin-3 is produced by numerous cell types including keratinocytes, activated mϕs, epithelial cells, and colon carcinomas. Galectin-3 has been implicated many functional processes including in FcεRI signaling in mast cells and DCs (196,197), IL-1 production in monocytes (198), cell-cell adhesion (126), and binding to ECM components (199). Galectin-3

monomers have the intriguing ability to dimerize via a Pro/Gly rich N-terminal domain. This dimerization will increase the affinity of Galectin-3 carbohydrate and permit crosslinking of recognition structures via the C-terminal lectin domain. Other galectins such as 1 and 2 can be naturally found as dimers (200).

Other proteins with requirements for carbohydrate in their recognition structures are CD22 and sialoadhesin which bind to ligands containing SA. CD22 is a member of the Ig superfamily which possess specificity for α2-6 linked SA residues in its terminal 2 Ig domains (171). The binding to α2-6 linked SA is also dependent on the context of the surrounding protein, not merely on the SA (171). Ligands for CD22 have included all isoforms of CD45 (201). The CD22-CD45 interaction likely plays a role in T cell-B cell binding which is important in B cell antigen presentation to and activation of T cells. Sialoadhesin is also an Ig superfamily member, with 17 Ig domains that is primarily expressed on mϕ populations (172). Sialoadhesin has specificity for α2,3 linked SA not α2,6 linked SA (202) which is likely involved in mϕ adhesion events (202).

Studies of CD44 have also demonstrated an additional role for carbohydrates and glycosaminoglycans (GAGs) on glycoproteins. CD44 exists in three activation states with respect to its hyaluronic acid (HA) binding: inactive, inducible, or constitutively active (203). Removal of the N-linked carbohydrates, SA, or removal of the chondroitin sulfate (described in detail in the next section) moieties could each convert CD44 from a non-binding state to a constitutively active HA binding phenotype (204,205).

1.3.2 Sulfation

The trans-Golgi and trans-Golgi network appear to be the location of most sulfation reactions, where the sulfation reactions appear to be individually controlled by the expression of specific enzymes. Sulfate can be incorporated into several modifications of proteins including N- and O-linked carbohydrates, GAGs, and Tyr residues. These components appear to have a wide variety of functions, although the sulfate residues are most often involved in creating recognition structures that are ligands for specific receptors.

Proteins which contain sulfated N-linked carbohydrates include certain glycoprotein hormones. Studies of the pituitary hormone lutropin, identified the sulfated sequence SO_4-4GalNAcβ1-4GlcNAcβ1-2Manα (206) which is specified by a sequence Pro-X-Arg-Lys 6-9 amino acids from the N-linked attachment site (207). The sulfated sequence is bound by a receptor on both liver endothelial and Kupffer cells, which removes lutropin from the circulation (208). Sulfated N-and O-linked glycans are also implicated in selectin-mediated binding as described in Section 1.3.1.2. and shown in Figure 7.

Tyr sulfation is also a biologically relevant protein modification (209). The consensus site for Tyr sulfation includes an Asp or Glu preceding the Tyr, which signals the trans-Golgi network enzyme tyrosylprotein sulfotransferase to sulfate the Tyr (210). As described in Section 1.3.1.2, Tyr sulfation of the P-selectin ligand, PSGL-1, is critical for P-selectin binding (183,184). These groups, therefore concluded that P-selectin binding to PSGL-1 is dependent on the O-linked sialyl Lewis x and the sulfated Tyr residues which colocalize to the molecule's amino terminus. Tyr sulfation is also implicated in increasing the binding von Willebrand factor to Factor VIII (211) and hirudin to thrombin (212). In addition, Tyr sulfation increases the rate of proteolytic activation of progastrin to gastrin (213).

Another important class of sulfated proteins is the proteoglycans. Proteoglycans are modified by GAGs, repeating disaccharide units which are added to Ser residues and sulfated in the trans-Golgi (reviewed in (214)). HA is also a GAG, but is not attached to proteins or sulfated since it is synthesized on the plasma membrane and directly exported in free form. The initial carbohydrate addition typically consists of a glucuronic acid β1-3Galβ1-3 Galβ1-4Xylβ-Ser core where Ser-Gly-X-Gly is a common acceptor sequence. The nature of the disaccharide repeat differs between the different classes as shown in Figure 8. The sulfation of GAGs occurs after disaccharide chain synthesis and is intricately linked to the deacetylation of GlcNAc residues (215). O-sulfation can also occur at carbon C-6 and occasionally C-3. The GAGs are amongst the most negatively charged molecules in nature, with heparin possessing up to 3 negative charges per disaccharide (214).

Proteoglycans are likely to play an important role in the structure of the extracellular matrix (ECM). Heparan sulfate (HS) proteoglycans will mediate interactions with laminin and fibronectin, thus anchoring the proteoglycan to the ECM. HA forms a net-like structure in the ECM and can be specifically bound by CD44 to mediate cell migration. CD44 also has affinity for chondroitin sulfate (CS) GAGs which can mediate cell adhesion and cell migration (216,217). The binding of GAGs by CD44 is likely important in leukocyte migration by binding to HEVs (218), thus complementing the role of L-selectin. Anchoring of cells to the ECM by CD44 may conversely serve to retain the leukocytes once they have reached the site of inflammation. Splice variants of CD44 have also been correlated with metastatic phenotype of certain tumors (219).

GAGs heparin and CS also modulate blood clotting via the actions of heparin on anti-thrombin and CS on heparin cofactor II (214). Thrombomodulin is a cell surface protein on

A

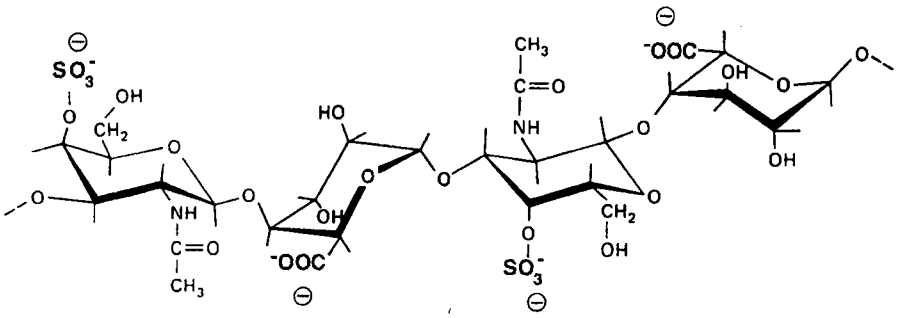

B

GAG	Disaccharide
Hyaluronic acid	D-glucuronic acid—GlcNAc
Chondroitin Sulfate A	D-glucuronic acid—GalNAc-4-sulfate
Chondroitin Sulfate B	D-glucuronic acid or L-iduronic acid—GalNAc
Chondroitin Sulfate C	D-glucuronic acid—GalNAc-6-sulfate
Heparan sulfate	D-glucuronic acid or L-iduronic acid—GlcNAc
Heparin	D-glucuronic acid or L-iduronic acid—GlcNAc
Keratan sulfate	D-Gal—GlcNAc

Figure 8: Classes of GAGs and their disaccharide repeat structure

A) The structure of the disaccharide of chondroitin sulfate B is shown. The high degree of negative charge for each disaccharide is also indicated. B) The other classes of GAGs and their disaccharide repeats are listed. The sulfate linkages have only been indicated for chondroitin sulfate A and B since this differentiates the two classes. Only HA is not naturally sulfated.

endothelial cells which inhibits blood clotting. A CS chain on thrombomodulin inhibits the action of thrombin bound to EGF repeats of thrombomodulin (214).

GAGs are also involved in the binding of growth factors to their specific receptors. Basic fibroblast growth factor (bFGF) binds to specific cell surface receptors, but is dependent on the cell surface expression of HS (220). In the case of bFGF, the GAGs appear to bind to the bFGF and facilitate bFGF dimer formation (221). The dimers then interact with the bFGF receptors which likely also dimerize to induce signal transduction. For other growth factor receptors, GAG binding to the growth factors has been suggested as a mechanism to increase the cell surface concentration of growth factor prior to high affinity binding by the specific receptors (179,222).

1.3.3 Phosphorylation

Phosphorylation of proteins is one of the most studied post-translational modifications. Phosphorylation of Tyr or Ser and Thr residues is involved in numerous cell processes including transmembrane signaling, cytoplasmic signal transduction, nuclear localization, transcription factor activity, and cell cycle control. The recent characterization of phosphatases has also emphasized that dephosphorylation and phosphorylation control many cellular events. As such, a complete review of these processes is beyond the scope of this thesis. Instead, a few pertinent examples should serve to indicate the general functional implications, mechanisms, and control of protein phosphorylation.

Tyr kinases are generally divided into receptor-like transmembrane and cytoplasmic Tyr kinases. The EGF receptor is a prototype of the receptor Tyr kinases which, upon binding EGF, dimerizes and undergoes autophosphorylation (223). Receptor dimerization in the activation of

kinase activity and downstream signal transduction, is a common theme for the activation of many receptor families (224). The autophosphorylation initiates downstream signaling by recruiting and activating other signal transduction components including the Ser/Thr kinases MAP kinase (mitogen activated protein kinase) and RAF-1 (225-228).

Although several kinases are localized to the cytoplasm, these kinases are often intimately involved in plasma membrane signal transduction (229,230). The functional role and control of cytoplasmic Tyr kinases is exemplified by the T cell protein $p56^{lck}$ (231). None of the components of the TcR have intrinsic Tyr kinase activity, but TcR signaling is nonetheless initiated by Tyr phosphorylation. The phosphorylation is probably due to the cytoplasmic kinases associated with the TcR, ZAP-70 and the 2 src family kinases $p59^{fyn}$ and $p56^{lck}$ (231,232). Cell lines without $p56^{lck}$ are unable to properly respond to TcR engagement as seen by a lack of Tyr phosphorylation and subsequent downstream signaling events (233). $p56^{lck}$ will localize to the plasma membrane via N-terminal myristylation, a unique interaction with the cytoplasmic domain of CD4 or CD8, via its SH2 domain, via a unique interaction with the IL-2 receptor, or via a recently described interaction with CD45 (234-237). These alternatives likely serve to ensure that sufficient amounts of $p56^{lck}$ are localized to the membrane during T cell activation. $p56^{lck}$ will presumably phosphorylate the Tyr residues on **I**mmunoreceptor family **T**yrosine-based **A**ctivation **M**otifs (ITAMs) which have the sequence [D/E-X_7-D/E-X_2-Y-X_2-L/I-X_7-Y-X_2-I/L] (238). ITAMs are present on CD3 ε,γ, and δ and the ζ chain which, upon phosphorylation, recruit SH2 containing proteins including phosphatidyl inositol 3-kinase and ZAP-70 to the TcR complex. This results in the generation of diacylglycerol, inositol-3-phosphate, subsequent Ca^{++} flux, and protein kinase C (PKC) activation and leads to IL-2 gene transcription and T cell activation (239).

Phosphatases do not simply counteract the action of kinases, but initiate positive responses in cells. T cell activation again provides an instructive example of this role of phosphatases. The role of the receptor protein Tyr phosphatase (PTP) CD45 is likely to dephosphorylate the negative regulatory Y-505 site of $p56^{lck}$, which activates $p56^{lck}$ to phosphorylate the ITAM motifs on the TcR proteins. The Y-505 of $p56^{lck}$ is thought to serve as a site for the intramolecular binding of its N-terminal SH2 domain to the C-terminal Y-505. In this form, the Tyr kinase is thought to be inactive, whereas dephosphorylation of Y-505 releases $p56^{lck}$ into an enzymatically active form (240). The TcR signal transduction complex thus illustrates how phosphorylation is involved in creating structures for molecular interactions and in regulating enzymatic activity. The coordinate regulation of kinases and phosphatases in TcR mediated signal transduction is a useful paradigm for the importance of both kinases and phosphatases.

Ser and Thr phosphorylation is also important in numerous physiological responses. Among the important Ser/Thr kinases are PKC, PKA, MAP kinases and Raf kinases. The Raf kinases and MAP kinases are involved in downstream signaling from membrane events of which the TcR is once again a relevant example. As mentioned above, the many isoforms of PKC can be activated by the production of diacylglycerol. PKA is activated by cAMP increases and is involved in numerous physiological processes. Raf-1 was originally characterized as a proto-oncogene (241). Following TcR triggering, Raf-1 is activated by a PKC dependent process (242). Raf-1 is able to phosphorylate and thereby activate the MAP kinase kinases, which then phosphorylate MAP kinases resulting in MAP kinase activation (226-228). MAP kinase provides a link to the cell cycle control due to its phosphorylation of FAR1 (243). Phosphorylated FAR1 binds to and inactivates the cdc28 kinase-cyclin1, 2, or 3 complex. This block in cdc28 activity

induces cell cycle arrest. MAP kinase can also regulate transcription factor activity by phosphorylating proteins such as c-jun. (244).

As a final note, phosphorylation of His residues also appears to be relevant to eukaryotic systems. Phosphorylation of His in the P-selectin cytoplasmic domain following platelet activation was demonstrated (245). This phosphorylation was proposed to be important for translocation of P-selectin from intracellular granules and may be relevant for other membrane signal transduction events.

This discussion of protein phosphorylation should indicate the importance of this post-translational modification for a number of proteins. Protein phosphorylation can affect enzyme activity, subcellular localization, and protein-protein interactions. The identification of phosphorylation of a protein is often central to determining the role it occupies in a specific signal transduction pathway and in the cell as a whole.

1.3.4 Other modifications

Proteins are also subject to numerous other modifications which are briefly outlined here. Cytoplasmic proteins can also be modified by the attachment of a lipid moieties such as myristic acid. The lipid addition is specified by sequences in the N-terminus of proteins and serves to localize the protein to the plasma membrane (reviewed in (246)). This addition is often critical as demonstrated by the transforming activity of ras which is dependent on the palmitylation attachment (247).

Amino acids can be modified following translation to produce, for example, hydroxyproline from Pro and 2-amino-3-oxopropionic acid from Cys. The role of hydroxyproline in hydrogen bonding of the collagen triple helical structure is well known. The

function of 2-amino-3-oxopropionic acid (modified Cys) is not as well known, but is critical to the catalytic activity of sulfatases (248). Individuals with a genetic defect in the ability to modify the Cys residue, have a general deficiency in sulfatase activity. These individuals have a clinical phenotype of leukodystrophy and mucopolysaccharidosis since sulfated molecules cannot be metabolized (249).

Ubiquitin modification is a common, well characterized protein modification which tags a protein for degradation by the cytoplasmic proteasome (reviewed in (250)).

The addition of a glycosylphosphatidylinositol (GPI) membrane anchor, rather than the standard hydrophobic transmembrane protein domain, is an important post-translational modification described on increasingly more proteins (reviewed in (251,252)). Following translation, the putative transmembrane segment is cleaved at a consensus recognition site, and the GPI is added (253). The GPI tail endows the molecule with interesting properties such as increased mobility in the membrane, the ability to be released from the cell surface by specific phospholipases, and internalization via a clathrin independent endocytosis system (254-256). If the protein is released by a phospholipase, the glycan moiety of the GPI tail remains on the protein to contribute to the released molecule's glycosylation.

1.4 Objectives and approaches

The focus of this research was designed to address the molecular basis of DC function. Several molecular aspects of DC function still remain uncharacterized. For example, do DCs produce novel cytokines? What factors are responsible for *in vivo* DC differentiation? Which molecules are required for DC migration? Which molecules process antigens in DCs? Which molecules mediate antigen independent clustering with T cells?

In deciding upon strategies to address these unsolved questions, we considered that many answers would lie in the characterization of DC cell surface molecules. The unique functions of DCs appear to be due to the expression of largely DC-specific molecules such as DEC-205 and the combined expression of other molecules which can also be found on other cells such as B7-1, CD40, ICAM-1, and LFA-1. Therefore, we wanted to characterize both proteins that appeared novel to DCs as well as DC proteins expressed by other cells, but with potentially important functions on DCs.

Monoclonal antibodies specific for human DCs have still not been produced despite much effort (257). The characterization of mouse DC-specific proteins is provided by a limited number of mAbs, including 33D1 (258), N418 (259), MIDC-8 (260), and NLDC-145 (261). Due to the availability of these specific mAbs, the research project focused on mouse DCs. Molecular characterization of the antigens recognized by the anti-DC mAbs was minimal at the outset of the project. The NLDC-145 mAb recognizes the DEC-205 protein with its 10 C-type lectin domains (103), which is expressed on DCs, thymic epithelial cells, and a limited number of leukocytes as described in Section 1.2.3.2 (261,262). The N418 mAb is specific for murine $CD11_c$ which is largely DC-specific and labels all DCs (94,259), but does react with certain B cell and mϕ subsets (Ian Haidl and Richard Stokes, UBC, unpublished observations). This distribution of $CD11_c$ in the mouse is far more restricted than humans where $CD11_c$ is expressed on macrophages and neutrophils and therefore not useful as a human DC marker. The N418 mAb does not appear to alter T cell stimulating or clustering ability of DCs so its function is not presently known. The 33D1 mAb is specific for the major subset (90%) of spleen and Peyer's patch DCs and many tissue DCs, but does not label DCs in other locations, although this observation has been challenged (110). The molecule recognized by 33D1 is still uncharacterized. The MIDC-8 mAb recognizes a primarily intracellular antigen of unknown identity and function. The NLDC-145 and MIDC-8 mAbs appear to bind to a

separate subset of DCs from 33D1 which comprise 10 % of splenic DCs and almost all non-spleen lymphoid DCs (263).

Another mAb which labels DCs is the F4/80 mAb which was originally characterized by its reactivity to subsets of mϕs (264). The expression pattern of the F4/80 molecule is intriguing since expression in mϕs and DCs is modulated relative to body site location and state of cellular activation. The F4/80 molecule is expressed on most lymphoid DCs, but is lost after one day of culture (94,95). Fresh LCs express higher levels of F4/80 (89,265), but this expression is also lost upon antigen stimulation or *in vitro* culture (89,93) as DCs progress from the antigen acquisition and processing phase to the T cell activation phase (see Section 1.2.3.2). Given this differential expression, the F4/80 molecule may regulate antigen processing, cell-cell adhesion, or cell migration. The characterization of the F4/80 molecule will be the subject of Chapter 4 of this thesis.

Among the other non-DC-specific proteins that we found of interest was CD45. CD45 has been extensively studied in lymphocytes due to the exquisitely controlled expression of multiple isoforms and more recently due to the role of CD45 in lymphocyte antigen receptor mediated signal transduction (266). The isoform expression of CD45 and CD45's functional role in non-lymphocyte hematopoietic cells, has received relatively little attention. In the context of DCs, CD45 could fulfill functions via its large extracellular domain in mediating cell-cell interactions, cell migration, or by mediating protein-protein interactions in the cell membrane. Alternatively, CD45 could be involved in DC functions requiring intracellular signaling such as DC maturation, DC cytokine responsiveness, and the potentiation of DC APC function during the IR. These possibilities will be more thoroughly introduced and considered in Chapter 3 where the characterization of DC and mϕ CD45 is described.

2. MATERIALS AND METHODS

2.1 Cellular Methods

2.1.1 Tissue culture

The cell lines utilized for the research described in this thesis are listed in Table 1. Several cell lines were obtained through the generosity of the individuals indicated below: J774.2 (Dr. Matthew Sharpe), P388D_1-mϕ (Dr. Robert Hancock), L cells (Thymidine kinase$^-$, L-M tk$^-$) (Dr. Frank Tufaro). L106A6 and L36B3 are L cells transfected with the cDNAs for CD45RABC or CD45R0 isoforms respectively and were obtained from Dr. Pauline Johnson and Arpita Maita. The remaining cell lines were obtained from the American Type Culture Collection (ATCC). All cell lines were grown in RPMI or DMEM supplemented with 10% fetal bovine serum (FBS), 2 mM L-glutamine and 5 x 10^{-5}M 2-mercaptoethanol (2-ME) (complete tissue culture media). Alternatively, hybridomas were cultured in a protein free medium (PFHM, Gibco) supplemented with 2 mM L-Gln, and 5 x 10^{-5}M 2-ME. Antibiotic use was avoided, but when antibiotics were required, 100 units/ml penicillin and 100 μg/ml streptomycin were used.

Adherent cells were propagated by allowing the cells to grow to 85-90% confluence, detaching the cells by treatment with 0.05% trypsin in phosphate buffered saline (PBS) + 1 mM ethylenediaminetetraacetic acid (EDTA) at 37°C, diluting the cells into fresh complete culture media, and plating the cells in fresh tissue culture treated dishes (Nunc). Non-adherent cells were propagated by allowing the cells to grow to $5x10^5$ to $1x10^6$ cells/ml and diluting the cells to $1x10^5$ cells/ml in fresh complete tissue culture media.

Cell Line	*Description*	*Source*
RAW309 Cr.1	Mouse mϕ	ATCC TIB 69
J774A.1	Mouse mϕ	ATCC TIB 67
J774.2	Mouse mϕ	M.Sharffe (NY,NY)
P388D$_1$-mϕ	Mouse mϕ	B.Hancock (UBC)
P388D$_1$-leukemia	Mouse leukemia	ATCC CCL 46
WEHI-274	Mouse mϕ	ATCC CRL 1679
L cells	Mouse embryonic fibroblast	F.Tufaro (UBC)
L10A6	L cells transfected with the cDNA for murine CD45RABC.	P.Johnson (UBC)
L36B3	L cells transfected with the cDNA for murine CD45R0	P.Johnson (UBC)
F4/80	Hybridoma producing a mAb specific for a mouse mϕ 160 kDa protein.	ATCC HB 198
SFR8-B6	Hybridoma producing a mAb specific for HLA-Bw6.	ATCC HB 152
33D1	Hybridoma producing a mAb specific for mouse DCs.	ATCC TIB 227
N418	Hybridoma producing a mAb specific for mouse CD11c, primarily expressed on DCs.	ATCC HB 224
M1/9	Hybridoma producing a mAb specific for all isoforms of murine CD45.	ATCC TIB 122
14.8	Hybridoma producing a mAb specific for isoforms of murine CD45 with exon A.	ATCC TIB 164
I3/2	Hybridoma producing a mAb specific for all isoforms of murine CD45	Ian Trowbridge (San Diego, Ca)

Table 1: Cell lines used in this thesis

Large scale cultures of RAW 309 Cr.1 cells were grown in 3 litre spinner flasks (Belco) which had been siliconized to prevent cell attachment. The cells were grown in normal tissue culture medium (complete RPMI) with the flasks sealed and placed into a non-CO_2 37°C incubator. The cell spinners were set at 60-70 rpm to maintain the cells in suspension. The cells were maintained between $1x10^5$ and $1x10^6$ cells per ml and typically grew to a maximum cell density of $1x10^6$ to $2x10^6$ cells per ml.

2.1.2 Animals

All animals were maintained in accordance with the Canadian Council on Animal Care guidelines. Animals were housed at the UBC animal care facilities located at South Campus or at the Department of Microbiology and Immunology animal facility. Food and water was provided *ad libitum*. Animals were maintained under normal conditions, not specific pathogen free conditions. Mice of the BALB/c strain and C57Bl/6 inbred strains were used for most studies. Both sexes of mice between the ages of 5 and 20 weeks old were used with similar results for all purposes described in this thesis. Animals were humanely sacrificed by CO_2 euthanasia.

2.1.3 Dendritic cell purification

Splenic and thymic DCs were purified essentially by the methods described by Steinman et al (263). BALB/c and C57Bl/6 male and female mice aged 6-16 weeks were used with similar results. Organs were removed from humanely sacrificed animals and subjected to collagenase digestion. Each spleen and thymus was injected with 0.5 ml of 100 units per ml of collagenase (Sigma Type III) in Hank's Balanced Salt Solution without carbonate. Following incubation at 37° for 45 minutes, spleens were passed through wire screens to create a single cell suspension. The original thymus perfusate was discarded and collagenase was added at 400 U/ml to cover disrupted thymi. Thymi were incubated for an additional 30 minutes at 37° before passing through wire mesh to create a single cell

suspension. Splenic and thymic cells were resuspended to 5 x 10^7 cells/ml in dense bovine serum albumin (BSA) (density=1.080 g/ml), added to 15 or 30 ml Corex tubes, and overlaid with RPMI. The tubes were then centrifuged at 10,000 g for 45 minutes at 4°C. Interface cells were harvested, washed, and plated at 2 x 10^7 cells per 60 mm dish. After incubation at 37° for 60 to 120 minutes, the non-adherent cells were removed with several washes of warm complete tissue culture media. After a further incubation of 30 minutes at 37°C, non-adherent cells were again removed before continuing the incubation overnight in RPMI+10 % FBS. Sixteen to 20 hours after the initial plating, the non-adherent cells were collected and replated in fresh dishes for 30 to 60 minutes to allow contaminating mϕs to adhere. The remaining non-adherent cells were harvested and used as purified DCs. The purity of the splenic DC populations was 85 to <95 % as assessed by specific mAb labeling and morphology of the purified populations. The major contaminating populations were mϕs and B cells which generally constituted 10 % and less than 5 % respectively of the purified populations.

2.1.4 Peritoneal macrophage preparation

Resident peritoneal mϕs (RPMs) were harvested from BALB/c mice aged 5-16 weeks by peritoneal lavage with 7 mls PBS + 30 mM citric acid. Peritoneal exudate cells (PECs) were harvested 4 days after intraperitoneal injection of 2 mls of 4% Brewer's Thioglycollate Broth (Difco). PECs were harvested by peritoneal lavage as for RPMs. The harvested cells were washed with supplemented RPMI and plated into tissue culture treated petri dishes. Two hours after initial culture, the non-adherent cells were removed and the remaining adherent cells were used for overnight radioactive labeling or were cultured overnight in complete RPMI before cell surface labeling or pulse-chase radioactive labeling.

Mϕs from Bacille Calmette Guérin (BCG) infected mice were produced and harvested as described (267). BALB/c mice were injected i.v. with 10^6 BCG (strain Pasteur, TMC #1011). Crude BCG extract (250 μg) was injected into each mouse 21 days after BCG infection. After 3 days, the peritoneal cells were harvested and treated as described above.

2.1.5 Fluorescence activated cell sorter (FACS) analysis

Cell lines grown as described above or mouse cell populations purified as described above were harvested and washed once in 1.5 ml of FACS buffer (DMEM, 2.0% calf serum, 20 mM 4-(2-hydroxyethyl)-1-piperazineethanesulfonic acid (HEPES), 20 mM azide) prior to staining. Adherent tissue culture cells were removed by treatment with versene (137 mM NaCl, 2.7 mM KCl, 0.5 mM EDTA, 8.1 mM Na_2HPO_4, 1.5 mM KH_2PO_4, 1.1 mM glucose) at 37°C for 5 minutes. Mϕs isolated from mice (section 2.1.4) were removed from plates by treatment with versene for 30 minutes at 4°C and gentle scraping of the plates. For primary antibody staining, 200 μl of each mAb were added per sample as either purified antibody diluted to 10μg/ml in FACS buffer or as tissue culture supernatants + 20 mM NaN_3. Following incubation for 45 minutes on ice, the samples were washed twice with 1.5 ml of FACS buffer. Detection of the primary mAb was achieved by addition of 100 μl of the secondary antibody at 10μg/ml in FACS buffer. Goat-anti-mouse IgG fluorescein isothiocyanate (FITC) (Jackson 115-095-062), a goat-anti-hamster IgG FITC (107-095-142), or a Donkey-anti-rat IgG FITC (Jackson 712-095-153) were used depending on the nature of the primary mAb and cell population being labeled. Following a 45 minute incubation on ice, the cells were washed once in FACS buffer and once in PBS and fixed in 1.5% paraformaldehyde in PBS. Cells were analyzed on a Becton Dickinson FACScan. Dead cells were gated out using forward scatter and side scatter

parameters. Fluorescent compensations were determined by analyzing control single labeled and double labeled populations. Five thousand events were collected for each sample.

The double staining protocol for DC CD45 isoform analysis (Chapter 3) was initiated with the anti-CD45 mAb for 45 minutes on ice, followed by 100 µl of a highly specific donkey anti-rat IgG FITC (Jackson 712-095-138) at 10 µg/ml for 45 minutes on ice. To block free anti-rat IgG sites, cells were incubated with 50 µl of 40 % rat serum in FACS buffer for 15 minutes on ice. N418 supernatant (100 µl) was then immediately added to each sample and incubated for a further 45 minutes on ice followed by 100 µl of a highly specific biotinylated goat anti-hamster (Jackson 107-065-142) at 10 µg/ml in FACS buffer plus 10% normal rat serum. 100 µl of a 1:100 dilution of Streptavidin-PE (Jackson 016-110-084) was added for 30 minutes on ice to complete staining. Cells were then washed and fixed with 1.5% paraformaldehyde in PBS. 33D1 was directly coupled to biotin and detected with streptavidin-PE. Use of biotinylated goat anti-hamster increased the fluorescent signal obtained and produced lower background than biotinylated N418 preparations. As a control for the non-specific binding of the hamster IgG N418, normal hamster serum or the hamster mAb 145-2C11 specific for mouse CD3 was used since purified splenic DCs typically contain less than one percent T cells (data not shown). Notably, no non-specific staining occurs when double staining with either the negative control rat IgG SFR8-B6 or the positive control I3/2. Cells were analyzed on a Becton Dickinson FACScan. Dead cells were gated out using forward scatter and side scatter parameters. Fluorescent compensations were determined by analyzing control single labeled and double labeled populations. Three to ten-thousand events were acquired for each sample. For histogram analysis N418 positive cells were selected to determine the reactivity of the control or CD45 antibodies with DCs.

2.2 Protein Techniques

2.2.1 Antibodies

The mAbs used for the research described in this thesis are described in Table 2. Nomenclature for CD45 isoforms is defined throughout this thesis with reference to their particular use of exons A, B, and C. For example, CD45RA contains only exon A, while CD45RAB contains exons A and B. The CD45R0 isoform lacks exons A, B, and C. CD45RABC, is most commonly referred to as B220 since it is the major isoform present in B cells and has an apparent M_r of 220 kilodaltons (kDa). All anti-CD45 mAbs were utilized as tissue culture supernatants. SFR8-B6 is a rat IgG_{2b} mAb used as an control since it does not react with mouse cells (268). Both IgG_{2a} and IgG_{2b} isotypes displayed a similar level of background staining in FACS analysis. A rabbit antiserum recognizing a common CD45 epitope was used for immunoblotting (provided by Dr. J. Marth, UBC, Vancouver, Canada) (269). As described in Table 2, T24/31 and IM7.8.1 were generous gifts of Bob Hyman, and YN1/1 and YE1/9.9.1 were kind gifts from Fumio Takei.

2.2.2 Cell surface biotinylation

Cells were collected by centrifugation and washed twice with 25 ml of biotin labeling buffer (Hank's Balanced Salt Solution minus phosphates, 10 mM glucose, plus 10mM $NaHCO_3$, pH 7.4) at 4°C. Cells were finally resuspended to 1 - 2 x 10^7 cells/ml in labeling buffer. Alternatively, adherent cells were left adhered to petri dishes for the washing and labeling procedure. A stock solution of sulfo-N-hydroxy succinimide biotin (sNHS-biotin, Pierce) was prepared at 10 mg/ml in labeling buffer immediately prior to use. While gently vortexing the cells, 80 µl of biotin stock solution was

mAb	*Specificity**	*Isotype***	*Source*
M1/70	C3Bi receptor	IgG_{2b}	ATCC TIB 128
N418	CD11c; DC-specific in the murine system	Hamster IgG	ATCC HB 224
GK1.5	CD4	IgG_{2b}	ATCC TIB 207
IM7.8.1	CD44	IgG_{2b}	Dr. Robert Hyman
I3/2	CD45, all isoforms	IgG_{2b}	Dr. Ian Trowbridge
M1/9	CD45, all isoforms	IgG_{2b}	ATCC TIB 122
RA3-6B2	CD45, B220 (exon A)	IgG_{2a}	Dr.Robert Coffman
14.8	CD45, exon A	IgG_{2b}	ATCC TIB 164
16A	CD45, exon B	IgG_{2a}	Dr. Kim Bottomly
MB23G2	CD45, exon B	IgG_{2a}	Dr. Ellen Puré
MB4B4	CD45, exon B	IgG_{2b}	Dr. Ellen Puré
DNL1.9	CD45, exon C	IgG_{2a}	Pharmingen
Rabbit 132	CD45-specific antisera against all CD45	Rabbit serum	Dr. Jamie Marth
53-6.72	CD8	IgG_{2b}	ATCC TIB 105
33D1	DC cell-surface antigen	IgG_{2b}	ATCC TIB 227
34-5-8S	D^d	mouse IgG_{2a}	ATCC HB 102
2.4G2	FcRγII	IgG_{2b}	ATCC HB 197
SFR8-B6	HLA-Bw6, human	IgG_{2b}	ATCC HB 152
B21-2	$I\text{-}A^{b,d}$	IgG_{2b}	ATCC TIB 229
MK-D6	$I\text{-}A^d$	mouse IgG_{2a}	ATCC HB 3
YN1/1	ICAM-1	IgG_{2b}	Dr. Fumio Takei
PC61	IL-2 receptor	IgG_{2b}	ATCC TIB 222
F4/80	mϕ/DC glycoprotein	IgG_{2b}	ATCC HB 198
YE1/9.9.1	transferrin receptor (TfR)	IgG_{2b}	Dr. Fumio Takei
T24/31	Thy-1	IgG_{2b}	Dr. Robert Hyman

* All specificities are against murine molecules unless noted.

** All mAbs are rat unless otherwise noted.

Table 2: Description of antibodies

added per $2x10^7$ cells. For adherent cells, 1.0 ml of an 800 μg/ml sNHS-biotin solution in labeling buffer was added to each 100 mm petri dish. The cells were incubated 15 minutes on ice with occasional shaking before washing extensively with tissue culture medium to remove and neutralize free sNHS-biotin. Following labeling, cells were lysed in lysis buffer (1.0% NP-40, 120 mM NaCl, 4 mM $MgCl_2$, 20 mM Tris(hydroxymethyl)aminomethane (Tris) pH 7.5, and 4 μg/ml phenylmethylsulfonylfluoride (PMSF)). 50 mM L-Lys was also included in the lysis buffer to ensure quenching of any remaining sNHS-biotin. Five mM IAA was also included in the lysis buffer where indicated.

2.2.3 Biotin-hydrazide labeling

PECs (day 1 after isolation) or RAW 309 Cr.1 cells were left adhered to 100 mm tissue culture dishes and washed twice with 10 mls PBS. $NaIO_4$, 1 mM in PBS, was added to the cells for 15 minutes on ice. The $NaIO_4$ was removed and 10 mls of 20 mM Na_2SO_4 in PBS was added to the cells for 5 minutes at room temperature. The Na_2SO_4 was removed and the cells were washed 3 times with 10 mls of PBS at room temperature. Biotin hydrazide, 1 mM in PBS, was added to the cells for 30 minutes at room temperature. The biotin hydrazide was removed, the cells were washed 3 times with 10 mls of PBS, and the cells were lysed in lysis buffer (1.0% NP-40, 120 mM NaCl, 4 mM $MgCl_2$, 20 mM Tris pH 7.5, and 4 μg/ml PMSF).

2.2.4 Metabolic labeling

2.2.4.1 $^{[35]}$S-methionine-cysteine

Metabolic labeling of cell lines and PECs was done with 150 μCi/ml [^{35}S]-Met-Cys PRO-MIX (Amersham) in DMEM minus Met and Cys (Gibco). For pulse chase analysis of protein

transport, the cells were cultured in medium without Met and Cys for one hour before adding 150 μCi/ml [^{35}S]-Met-Cys for a 15 minute pulse. The radioactivity was replaced with complete tissue culture medium for the duration of the chase time. Five percent dialyzed calf serum (GIBCO) was added for overnight (18 hour) labeling. Following labeling cells were lysed with lysis buffer (1.0 % NP-40, 140 mM NaCl, 10 mM Tris, 2 mM EDTA, pH 7.4, 40 μg/ml PMSF).

2.2.4.2 ^{35}S Na_2SO_4

Sulfate labeling was accomplished by incubating the PECs or cell lines with ^{35}S Na_2SO_4 (ICN) at 0.5 mCi/ml in RPMI without sulfate (Gibco) supplemented with 2 mM L-glutamine. For pulse chase analysis, the cells were cultured in the sulfate deficient medium for one hour before adding Na_2SO_4 at 0.5 mCi/ml for a 15 minute pulse. The radioactivity was replaced with complete tissue culture medium for the duration of the chase time. Five percent dialyzed calf serum (GIBCO) was added for overnight (18 hour) labeling. Following labeling cells were lysed with lysis buffer (1.0 % NP-40, 140 mM NaCl, 10 mM Tris, 2 mM EDTA, pH 7.4, 40 μg/ml PMSF).

2.2.5 Tunicamycin treatment of cells

Tunicamycin treatment was used to interfere with N-linked glycosylation prior to pulse chase analysis with [^{35}S]-Met-Cys. Cells were pretreated with or without 7 μg/ml tunicamycin in complete tissue culture medium for 1 hour. The control cells without tunicamycin were treated with 0.0014% dimethyl sulfoxide (DMSO) wherever tunicamycin was added to the treated cells. The medium was then removed and medium minus Met and Cys was added to the cells with or without tunicamycin for 1 hour. PECs were next pulsed for 15 minutes with 150 μCi/ml [^{35}S]-Met-Cys with or without tunicamycin and chased with complete medium with or without tunicamycin for the times indicated before the cells were lysed in lysis buffer (1.0 % NP-40, 140 mM NaCl, 10 mM Tris, 2 mM EDTA,

pH 7.4, 40 μg/ml PMSF). The lysates were utilized for immunoprecipitations as described in Section 2.2.7.

2.2.6 Cell surface crosslinking

Cells were harvested or cultured as described in Sections 2.1.1 and 2.1.4. Cells were labeled with [^{35}S]-Met-Cys for 18 hours as described in Section 2.2.4.1. Prior to crosslinking the cells were washed 3 times with 10 mls PBS. [3.3'-Dithiobis(succinimidylpropionate)] (DTSSP) was added to the cells at 100 μg/ml/10^7 cells and incubated for one hour on ice with mixing every 15 minutes. The cells were washed 3 times with 10 mls of unsupplemented DMEM to remove and inactivate the DTSSP. The cells were lysed in 1.0% v/v NP-40, 120 mM NaCl, 50 mM Tris, 2 mM $MgCl_2$, 10 mM IAA, 40 μg/ml PMSF, pH 7.5 and utilized for subsequent procedures.

2.2.7 Immunoprecipitation

All procedures were performed at 4°C or on ice. Cell lysates were first clarified by centrifuging 20 minutes at 10,500g at 4°C. The resulting supernatants were precleared by incubating 15 minutes with 2 μl rabbit anti-rat IgG serum and 5 μg of purified SFR8-B6, followed by two successive one hour incubations with 50 μl of a 1:1 slurry of protein A Sepharose (Pharmacia) and centrifugation for 5 minutes at 10,500 g at 4°C. CD45 was immunoprecipitated by adding 100 μl total volume of I3/2 and M1/9 supernatants for 30 minutes at 4°C, followed by 60 minutes incubation with 45 μl of a 1:1 protein A Sepharose slurry which had been coated with rabbit anti-rat IgG (Jackson 312-005-003). To preclear lysates of the B exon containing isoforms of CD45, lysates were immunoprecipitated with 100 μl of an equal mix of mAbs MB23G2, and MB4B4 followed by protein A Sepharose coated with rabbit anti-rat IgG. The procedure was repeated before one final incubation

with protein A Sepharose coated with rabbit anti-rat to ensure removal of all antibody before precipitating the remaining CD45 with I3/2 and M1/9. Alternatively, immunoprecipitations with the mAbs F4/80, I3/2, and M1/9 were performed with the mAb coupled at 2-4 mg/ml of beads to CNBr activated Sepharose according to the manufacturer's instructions (Pharmacia). The appropriate beads, 15 µl per tube, were added for 60 minutes at 4°C. All beads were washed twice in one ml of low salt buffer (0.2% v/v NP-40, 2 mM EDTA, 10 mM Tris pH 7.5, 150 mM NaCl), once in one ml of high salt buffer (0.2% v/v NP-40, 2 mM EDTA, 10 mM Tris pH 7.5, 500 mM NaCl), and once in one ml 10 mM Tris pH 7.5. Proteins were eluted from beads by boiling in 3% SDS with 30 mM dithioithreitol (DTT), followed by the addition of IAA to 80 mM, and resolved on 5-10% or 5-15% gradient polyacrylamide SDS-PAGE gels or 7.5% polyacrylamide minigels. DTT was replaced by distilled water in the preparation of non-reduced samples. Where samples were subjected to further processing such as glycosidase digestion (Section 2.2.8) before SDS-PAGE, the proteins were eluted from the mAb-Sepharose columns with 50 mM diethylamine (DEA), 0.5% w/v octylglucoside (C_8Glc), pH 11.5.

2.2.8 Glycosidase digestions

All endoglycosidases and neuraminidases were purchased from Boehringer Mannheim. *Vibrio cholera* neuraminidase digestion was performed in 50 mM NaAc, 4 mM $CaCl_2$ pH 5.5 using 1 mU of enzyme for 2 hours at 37°C. After neuraminidase digestion, digestion was initiated in 20 mM Na Cacodylate, 20 mM NaH_2PO_4 pH 6.5 at 37°C for 12 hours with 1.0 mU of enzyme. Newcastle's Disease Virus (NDV) neuraminidase digestion utilized the manufacturer's buffer with 1 mU enzyme for 2 hours at 37° C. Endo H digestion was performed for 20 hours at 37° C in 70 mM NaCitrate pH 5.5 with 2.5 mU of enzyme for the first 12 hours, followed by a fresh 2.5 mU for the remaining 8 hours. For peptide-N-glycosidase F (PNGase F) digestion, the proteins were first denatured in 0.2%

SDS, 20 mM EDTA, 50 mM Na_2HPO_4, pH 7.8. C_8Glc was added to give a final percentage of 1.0% w/v C_8Glc and 0.1% w/v SDS and 0.5 mU of enzyme was added per sample. Digestion proceeded at 37°C for 12 hours. PNGase F and a PNGase/Endo F mixture produced comparable results.

GAGs were analyzed by digestion of immunoprecipitated proteins with Chondroitinase ABC and Heparinase III (Sigma). 10 mU of Chondroitinase ABC in 60 mM NaAc, 60 mM Tris, pH 8.0 and 0.5 U of Heparinase III in 0.1 M NaAc, 1 mM CaAc, pH 7.0 were utilized. The samples were incubated for 12 hours at 40°C.

2.2.9 SDS-PAGE, autoradiography, and isoelectric focusing

Sodium dodecyl sulfate-polyacrylamide gel electrophoresis (SDS-PAGE) was performed essentially according to the method of Laemmli (270). Large gels (25 cm x 30 cm) were used for 5-15% or 5-10% polyacrylamide gradient gels. Minigels (10 x 7 cm) were poured and run with the BioRad MiniProtean system.

Isoelectric focusing (IEF) analysis was performed as previously described (271) utilizing a 3:1 ratio of pH 5-7 ampholytes:pH 3.5-10 ampholytes (Pharmacia) before second dimension separation on 5-10 % gradient SDS-PAGE (25 cm x 30 cm).

Gels with radioactive protein samples were fixed in 30% v/v methanol, 10% acetic acid for 45 minutes at room temperature. A 45 minute incubation in Amplify (Amersham) or in 1M NaSalicylate in 30% v/v methanol completed the treatment of the gel prior to drying and exposure of the dried gel to film (Kodak XAR) at -80°C.

2.2.10 Silver staining

Silver staining of protein gels was initiated by fixation in 12% w/v trichloroacetic acid (TCA), 50% v/v methanol for 30 minutes. All steps of the silver staining protocol were performed at room

temperature with shaking. Following fixation, the gel was transferred to 10% v/v ethanol, 5% v/v acetic acid for 20 minutes. The gel was transferred to 0.06% w/v $KMnO_4$, 0.02% w/v $CuSO_4$, for 8 minutes and immediately transferred to 7.5% v/v ethanol for 3 consecutive 1 minutes washes, one 8 minute wash, and one 40 minute wash. The gel was transferred to ddH_2O for 20 minutes before placing in 0.1% w/v $AgNO_4$ for one hour. The silver staining was developed by rinsing the gel briefly in ddH_2O and incubating in 2% w/v K_2CO_3, 0.04% v/v formaldehyde until the protein staining reached the desired level. The silver staining reaction was terminated by a 4 minute incubation in 1.0% v/v acetic acid.

2.2.11 Western blotting

Following SDS-PAGE, proteins were transferred to Immobilon-P polyvinylidene difluoride (PVDF) membrane (Millipore) using the Tris-Gly-methanol transfer system (272). To detect cell surface biotinylated proteins, the membranes were immediately placed in blocking buffer (2% BSA, 0.05% Tween-20, 250 mM thimerosal, in PBS) for one to two hours at room temperature. Alternatively, the PVDF membranes were thoroughly dried and used for the remaining staining protocol without rewetting in methanol. Membranes were washed three times for five minutes in wash buffer (0.1% BSA, 0.05% Tween-20, 250 mM thimerosal in PBS) before adding streptavidin-horseradish peroxidase (SA-HRPO) (Jackson, 016-030-084) diluted 1:10,000 in wash buffer. After incubating 30 minutes at room temperature, membranes were washed in three five minute incubations of wash buffer and one five minute wash of PBS. Finally, membranes were developed according to the manufacturer's instructions for enhanced chemiluminescence (ECL) detection (Amersham) and exposed to x-ray film (Kodak XRP or XAR).

To Western blot total CD45, the membranes were completely dried after transfer before incubating with a 1:1000 dilution of anti-CD45 antisera in wash buffer for one hour at room

temperature. Following three five minute washes in wash buffer, protein A HRPO (1:10,000 in wash buffer, BioRad) was added to the blot for one hour at room temperature. The membranes were washed again and detection was completed using ECL as above.

Biotinylated lectins used for blotting were from Vector Research (provided by Dr. Peter Lansdorp, UBC, Vancouver, Canada) and were used at 0.5 μg/ml in wash buffer. The lectins used and are as follows: *Datura stramonium* lectin (DS), *Phaseolus vulgaris* erythroagglutinin (PHA-E), *Phaseolus vulgaris* leukoagglutinin (PHA-L), *Bandeirea simplificifolia* lectin I, *Pisum sativum* lectin, *Lens culinaris* lectin, *Dolichus biflorus* agglutinin, *Vicia villosa* lectin, *Ricin communis* agglutinin (RCA), *Ulex europaeus* agglutinin I. Incubations, washing, and detection with SA-HRPO and ECL were performed as described above. For certain experiments the Miniblotter-16 (Immunetics) was used to analyze multiple lectins on a single blot.

2.2.12 Tyrosine phosphatase assay

The PTP activity of DC CD45 was assayed essentially as previously described (273). DCs, mϕs, and cell lines were prepared as described (Sections 2.1.1, 2.1.3, and 2.1.4) and lysed on ice for 10 minutes in 0.5% Triton-X100, 20 mM Tris pH 7.5, 150 mM NaCl, 2 mM EDTA, 0.2 mM PMSF, 1.0 μg/ml pepstatin, 1.0 μg/ml leupeptin, and 1.0 μg/ml aprotinin. The lysates were centrifuged at 16,000 g for 20 minutes at 4°C after which all cell lysates were adjusted to $2x10^6$ cells/ml in lysis buffer. CD45 was immunoprecipitated with 5 μl of I3/2-Sepharose CL-4B beads (Pharmacia, 4 mg/ml packed beads) per ml of lysate. SFR8-B6 conjugated Sepharose beads (10 μl at 2 mg/ml) were used to assess non-specifically immunoprecipitated proteins. Following end over end incubation at 4°C for two hours, the immunoprecipitates were washed twice with one ml of lysis buffer and twice with protein PTP buffer (50 mM Imidazole-Cl pH 7.2, 1.0 mM EDTA, 0.1% w/v2-ME, 0.05% w/v

Brij 96). The immunoprecipitates were finally resuspended in 100 µl PTP buffer such that every 10 µl of the suspension contained CD45 immunoprecipitated from 2 x 10^5 cells. 10 µl of each bead suspension was added per well to 100 µl microtitre plate wells (Costar) and equilibrated to 30°C. The reaction was initiated with the addition of 10 µl of the Tyr phosphorylated peptide, fyn 525-537 p531 (TATEPQpYQPGENL), to a final concentration of 6 mM in PTP buffer. The plate was agitated at 120 rpm during the assay. The reaction was stopped by the addition of 80 µl malachite green reagent (1 part 0.135% malachite green-oxalate in distilled water, 1 part 4.2% molybdate in 4 M HCl, 2 parts distilled water, and Tween-20 to a final concentration of 0.01%). The release of inorganic phosphate was measured by determining the absorbance at 650 nm and converted to nmol phosphate released utilizing KH_2PO_4 to establish a standard curve.

2.2.13 Membrane preparation

Total cellular membranes were prepared according to the Tween-40 methodology as described by Williams and Barclay (274). RAW 309 CR.1 cells were harvested by centrifugation and washed twice in 50 mls of PBS. The cells were resuspended to 5 x 10^8/ml in PBS and proteolytic inhibitors were added to the following concentrations: IAA 5 mM, 4 mM EDTA, 10 µg/ml pepstatin, 40 µg/ml PMSF, and 5 µg/ml leupeptin. An equal volume of 5% w/v Tween-50 in 10 mM Tris, 140 mM NaCl, pH 7.4, 0.02% w/v NaN_3 was added to the cell suspension. The cells were mixed at 4°C for 60 minutes and Dounce homogenized on ice. The homogenate was centrifuged at 650 g for 5 minutes and 4°C to remove nuclei and unhomogenized cell components. The supernatant was removed and placed on ice. The pellet was re-extracted in $1/6^{th}$ of the original volume of 2.5% w/v Tween-40 to which protease inhibitors had been added at half of the concentration described above. Following homogenization, the homogenate was

centrifuged as above. The pellet was re-extracted and homogenized until the intact cell number was less than 5% of the starting cell number.

The supernatants from the 650 g centrifugations were placed into SW28 centrifugation ultraclear tubes (344058, Beckman) and centrifuged at 100,000 g at 4°C for one hour in a Beckman SW28 rotor. The supernatant (cytosolic fraction) was removed and the remaining pellet was used as a crude membrane fraction. This pellet was solublized in 1.0% v/v NP-40, 10 mM Tris, 150 mM NaCl, and protease inhibitors as described for the 2.5% Tween-40 solutions. The resulting lysate was homogenized on ice, placed into SW28 tubes, and centrifuged at 100,000 g in an SW28 rotor at 4°C for one hour. The supernatant was removed and place on ice. The lysate pellet was resuspended in $1/6^{th}$ the original volume of NP-40 lysis buffer, homogenized, and centrifuged as above. The resulting supernatant was pooled with the initial lysate supernatant and utilized for mAb affinity chromatography. Samples of the homogenates and centrifugation supernatants and pellets were retained for analysis of the F4/80 molecule content. All material was stored at -80°C until further use.

2.2.14 Monitoring of F4/80 molecule purification

Monitoring of a molecule's purification can be performed by SDS-PAGE analysis of purified fractions. Although monitoring for the molecule's antigenic epitope provides a more rapid and quantitative assay of the desired molecule's purification (274), this assay could not be successfully used for antigen inhibition of the F4/80 mAb binding to fixed cells. Therefore, the F4/80 molecule purification was monitored by silver staining (section 2.2.10) of fractions eluted from an F4/80 mAb column (section 2.2.15.1).

The purification for the F4/80 molecule was also monitored by DS lectin blotting after the reactivity of the DS lectin with the F4/80 molecule was characterized (section 4.2.2.6.1).

This analysis involved NP-40 solublization of samples removed from each stage of the purification. The NP-40 lysates were immunoprecipitated with F4/80-Sepharose beads and the samples were separated by SDS-PAGE, blotted to PVDF, and probed with biotinylated DS (see sections 2.2.7, 2.2.9, and 2.2.11). The intensity of the signal for each sample was determined be densitometric analysis. The amount of F4/80 molecule at each stage of purification was represented by the number of cell equivalents recovered relative to the value for intact cells (taken as 100% recovery). The protein quantity present at each stage of the F4/80 molecule purification was determined by the BioRad Coomassie Blue assay or by OD_{280} for the final column elutions since the protein concentration in the fractions was low. The F4/80 molecule content and the total protein at each stage were used to determine the purification factor for the F4/80 molecule.

2.2.15 Chromatography

2.2.15.1 Monoclonal antibody affinity chromatography

Affinity chromatography was performed essentially as described by Williams and Barclay (274). Lysates of RAW 309 Cr.1 cells or lysates derived from membrane enriched fractions of these cells (Section 2.2.13) were utilized for affinity chromatography on a F4/80-Sepharose column. The F4/80 and SFR8-B6 mAbs were purified from tissue culture supernatants of cells grown in 10% FBS (screened for reduced bovine IgG content) or in PFHM medium plus 0.1% FBS utilizing a protein G column according to the manufacture's instructions (Pharmacia). Bovine IgG was purified from calf serum for use as a non-specific Ab. The purified Abs were switched into 0.5 M NaCl, 0.1 M $NaHCO_3$, pH 8.3 by gel filtration chromatography with Sephadex G-50 (Pharmacia). The Abs were coupled to CNBr-activated Sepharose CL-4B

(Pharmacia) according to the manufacturer's instructions. Five milligrams of Ab were coupled per ml of final gel volume.

All chromatography procedures were performed at 4°C. The SFR8-B6 and F4/80-Sepharose columns were treated with elution buffer (0.1M DEA, 0.5% w/v C_8Glc, pH 11.5) prior to testing of the column with radioactive cell lysates to determine if the F4/80 mAb was still recognizing the F4/80 molecule. After the elution was completed, the column was re-equilibrated with 0.2% v/v NP-40, 20 mM Tris, 150 mM NaCl, 1 mM EDTA, pH 7.5 plus 20 mM NaN_3. The NP-40 lysate prepared in section 2.2.13 was first passed through a 40 ml packed volume of bovine IgG-Sepharose in a 2.5 cm diameter column (BioRad). A column flow rate of 10-15 ml/hour was maintained by recycling lysate through the column via a peristaltic pump for 18 hours. The lysate from the bovine IgG-Sepharose column was applied to a 5 ml SFR8-B6-Sepharose column. The lysate was passed through this precolumn at 10-15 ml/hour until three volumes of the lysate had passed through the column. The precleared lysate was applied to a 5 ml F4/80-Sepharose column in a BioRad Dispocolumn. A column flow rate of 10-15 ml/hour was maintained by recycling lysate through the column via a peristaltic pump for 18 hours.

The column was first washed with 6 column volumes of 0.2% v/v NP-40, 20 mM Tris, 150 mM NaCl, 1.0 mM EDTA, pH 7.5 plus 40 μg/ml PMSF at 15-20 ml/hour. Washing was continued with 6 column volumes of 0.2% v/v, 20 mM Tris, 1.0 mM EDTA, 0.75M NaCl, pH 7.5 plus 40 μg/ml PMSF at 15-20 ml/hour. The next washes were with 4 column volumes of 20 mM Tris pH 7.5, followed by 2 column volumes of 0.5% w/v C_8Glc, 20 mM Tris pH 8.0, both at 15-20 ml/hour. Elution of the column was performed with 0.5% w/v C_8Glc, 50 mM DEA, pH 11.5 at 15-20 ml/hour. Eluted fractions of 1.0 ml were immediately neutralized with 50 μl of 1.0 M NaH_2PO_4 and PMSF was added to 40 μg/ml. The OD_{280} and ^{35}S content of each fraction

were determined. Fractions with ^{35}S were analyzed by silver staining to determine the presence of the F4/80 molecule. Purifications which were done after the development of DS lectin blotting, also used DS lectin blotting to determine presence of the F4/80 molecule.

2.2.15.2 *Datura stramonium* lectin affinity chromatography

DS lectin (Sigma) was coupled to CNBr-activated Sepharose at 2-4 mg/ml of final Sepharose gel volume according to the manufacturer's instructions (Pharmacia). The DS-Sepharose column was eluted with 0.5% w/v C_8Glc, 50 mM DEA, pH 11.5 prior to further use and stored in 0.2% v/v NP-40, 20 mM Tris, 150 mM NaCl, 1.0 mM EDTA, pH 7.5 plus 20 mM NaN_3. The DS-Sepharose was utilized following prior use of a mAb-Sepharose column to purify the protein of interest. For small scale analytical samples, NaCl was added to the eluate from the mAb column to 0.15 M. The DS-Sepharose was processed exactly as described for the immunoprecipitation protocol described in Section 2.2.7. For large scale purifications of the F4/80 molecule, the eluted fractions from the F4/80-Sepharose column which were positive for ^{35}S counts were pooled, NaCl was added to 0.15 M, and the eluate was added to 1 ml of the DS-Sepharose. The batch incubation was for 6 hours to permit binding of the F4/80 molecule to the DS lectin. The DS-Sepharose was transferred to a 12 ml BioRad dispocolumn and washed as described above for the F4/80 mAb column (Section 2.2.15.1). Proteins were eluted from the DS-Sepharose with 0.5% w/v C_8Glc, 50 mM DEA, pH 11.5 at 15-20 ml/hour. The OD_{280} and ^{35}S content of each fraction were determined. Fractions with ^{35}S were analyzed by silver staining to determine the presence of the F4/80 molecule. Purifications which were done after the development of DS lectin blotting, also used DS lectin blotting to determine presence of the F4/80 molecule.

2.2.15.3 Anion exchange chromatography

Anion exchange chromatography was performed on an FPLC system (Pharmacia). A Mono Q resin was used with a column height of 5 cm and a column diameter of 0.5 cm (HR5/5 column, Pharmacia). The ^{35}S Met-Cys labeled samples were prepared as in section 2.2.4.1, but were lysed in 1.0% v/v NP-40, 0.5% w/v CHAPS, 50 mM Tris, pH 9.0. The column was pre-equilibrated with lysis buffer plus 1.0M NaCl before a final equilibration in lysis buffer. The sample was loaded onto the Mono Q column in lysis buffer at 1.0 ml/min. The flow rate was maintained at 1.0 ml/minute throughout the column elution. Column loading proceeded for 2 minutes, followed by a further 4 minutes of washing with wash buffer. Column elution was achieved by an increase to 0.2 M NaCl over the next four minutes and a subsequent increase of the NaCl concentration to 0.5 M over 30 minutes. The NaCl concentration was then increased sharply to 1.0 M over 5 minutes and maintained at 1.0 M for a further 5 minutes. 1.0 ml fractions were collected and samples were removed for the determination of the radioactivity in each fraction. Even numbered fractions were analyzed by immunoprecipitation with F4/80-Sepharose beads as described in section 2.2.7.

2.2.16 Protease and CNBr digestion

The purified F4/80 molecule eluted from the affinity columns, was first denatured with 30 mM DTT and 6M urea at 80°C for 10 minutes. IAA was added to 80 mM and incubated at room temperature for 30 minutes in the dark. The samples were desalted with a Sephadex G25 column (Pharmacia) and further desalted and concentrated with a centricon-30 (Amicon). The sample was subjected to cleavage by CNBr, Lys-C, or Glu-C digestion.

CNBr digestion was accomplished in 70% trifluoroacetic acid (TFA) and 0.3 mg/ml of CNBr. The protein was incubated in an oxygen free atmosphere for 24 hours at room

temperature in the dark. The reaction mix was next lyophilized, resuspended in 100 µl ddH_2O, and lyophilized again.

Lys-C digestion to cleave the protein at Lys residues utilized a digestion buffer of 100 mM Na_2HPO_4, 1 M urea, pH 8.2. The protein was kept in a 30 µl reaction volume to which 0.2 µg of Lys-C (Promega) was added. Incubation was for 18-24 hours at 37°C. A further 0.2 µg of Lys-C was added after 12-14 hours of incubation.

Glu-C digestion utilized 50 mM NH_4Ac, 1 M urea, pH 4.0 for cleavage at Glu residues only, or 50 mM NaH_2PO_4, 1 M urea, pH 7.8 for cleavage at Glu and Asp residues. The reaction volumes were again 30 µl to which 0.2 µg of Glu-C (Promega) was initially added and 0.2 µg was added after 12-14 hours of incubation at 37°C. The incubation was continued for 18-24 hours.

The lyophilized protein from CNBr digests or the solution following enzyme digests was resuspended in SDS-PAGE loading buffer for analysis by 10-17.5% SDS-PAGE

2.2.17 Amino acid analysis and peptide sequencing

Amino acid analysis and peptide sequencing were performed by Ms. Sandy Kielland of the Protein Microchemistry Centre at the Department of Biochemistry and Microbiology, University of Victoria, Victoria, BC, Canada. Proteins were blotted to PVDF membrane, extensively rinsed in ddH_2O, and hydrolyzed in 6N HCl for 16-24 hours prior to amino acid analysis with an Applied Biosystem 420A derivatizer-analyzer system. N-terminal or CNBr peptides were sequenced from proteins blotted to PVDF membrane also using standard sequencing techniques. Phenylisothiocyanate (PITC) chemistry was employed for amino acid

derivatization. The sequencing was performed with an Applied Biosystem 470A gas phase sequencer.

2.2.18 Sucrose density centrifugation

Density gradient ultracentrifugation was performed similarly to the procedures described by Martin and Ames (275) and Cresswell (49). PEC cell lysates were prepared as described in section 2.1.4 and 2.2.4.1 with the following modifications. PECs were cultured 48 hours after initial isolation in supplemented RPMI in the presence or absence of 200 U/ml murine IFN-γ (Genzyme). The PECs were labeled with [^{35}S] Met-Cys for 1 hour followed to allow transport of CD45 to the cell surface (Figure 22). The cells were lysed in 1.0% w/v C_8Glc rather than NP-40 lysis buffer. The cell lysates were **not** centrifuged at 10,800 g for 20 minutes before use. Gradients of sucrose from 5-20% in 50 mM phosphate buffer, pH 7.5, plus 0.5% C_8Glc, were poured with a 0.2 ml cushion of 20% w/v sucrose at the bottom of the tube and 11 ml of the sucrose gradient. Gradients were prepared with a gradient maker into SW41 (344059, Beckman) tubes. Detergent lysates from equivalent numbers of cells were overlaid onto the sucrose gradients and centrifuged in an SW41 rotor at 4°C and 148,000g (36,800 rpm) for 24 hours for CD45 analysis and 184,000g (38,600 rpm) for 29 hours for I-A^d. Following centrifugation, the lysate was removed as the first fraction. Fractions 2 through 12 of 1.0 ml were manually collected from the top of the gradient. The collected fractions were immunoprecipitated with the anti-CD45 mAbs M1/9, F4/80, or B21-2 (see Table 2) as described in Section 2.2.7 and analyzed by SDS-PAGE and fluorography as described in Sections 2.2.9. and 2.2.7.

2.2.19 Densitometry

Quantitation of radioactive proteins separated by SDS-PAGE and exposed to x-ray film was performed where necessary with a Molecular Dynamics laser densitometer.

2.3 Nucleic Acid Techniques

2.3.1 Description of plasmids

The three variably spliced exons of mouse CD45 are each inserted into the pGEM3 polycloning site at the SmaI site (Promega) as described (276). The exon 4, 5 and 6 inserts contain the nucleotides 206-349, 350-497, and 498-628 respectively of the mouse CD45 cDNA sequence. The plasmids are referred to as p6pGEM3 for the plasmid with the exon 4 insert, p4pGEM3 for the plasmid with the exon 5 insert, and pCpGEM3 for the plasmid with the exon 6 insert.

2.3.2 Description of oligonucleotides

In order to determine the expression of CD45 isoforms by reverse transcriptase-polymerse chain reaction (RT-PCR), 2 oligonucleotides were used for the PCR and one additional oligonucleotide for blotting of the CD45R0 isoform. The sequences of the oligonucleotides for PCR have been previously described (276) and are as shown below.

IHCD45-1 5' ACCATGGGTTTGTGGCTCAAACT 3'

(nucleotides 128-150 sense)

IHCD45-2 5' GCTATGGTTGTGCTTGGAGGGTC 3'

(nucleotides 689-711 antisense)

The oligonucleotide used to detect the amplified CD45R0 PCR product was designed with 11 nucleotides from exon 3 (underlined below) and 12 nucleotides from exon 7. The T_m of the entire 23-mer is 75.4°C in 2M NaCl whereas the T_m for the individual exon 3 11-mer and

exon 7 12-mer portions are 48.1°C and 57.6°C respectively. Therefore, hybridization at 65°C in 2M NaCl resulted in the detection of the exon 3/exon 7 boundary present in CD45R0, but no detection of other CD45 isoforms.

IHCD45-3 5' TGAGGCTGGCACGATCACTGGGT 3'

(nucleotides 639-650/210-220 antisense)

2.3.3 RNA purification

Total ribonucleic acid (RNA) was purified from cells by the guanidinium isothiocyanate (GITC) protocol (277). Briefly, cells were washed in PBS and pelleted by centrifugation. The cell pellet was lysed in 6 mls of 4M GITC, 25 mM NaCitrate pH 7.0, 0.8% v/v 2-ME. The cell lysate was passed through a 23 gauge needle 6 to 10 times in order to shear DNA. The cell lysate was next layered onto a 4 ml CsCl cushion (5.7 M CsCl, 25 mM NaAc pH 5.0, 0.1 mM EDTA) in SW41 tubes (344059, Beckman). The tubes were centrifuged at 32,000 rpm at 23°C for 16 hours in the SW41.1 rotor. The RNA pellet was resuspended in 200 µl ddH_2O with 0.2 U/ml RNAsin and 1.07 mM DTT. The RNA was ethanol precipitated, centrifuged and resuspended in ddH_2O plus RNAsin and DTT. The resulting RNA was quantitated by the OD_{260} and stored at -80°C before use.

2.3.4 First strand cDNA synthesis

First strand cDNA synthesis was performed using standard molecular biology techniques (277). Total RNA (1.0 µg) was added to the reaction mixture which contained the following components at the final concentration listed: 2.5 mM MeHgOH, 10 mM DTT, 0.6 U/ml RNAsin, 1X reverse transcriptase reaction buffer (25 mM Tris-HCl, 37.5 mM KCl , pH 8.3), 1

mM dNTPs, and 12.5 μg/ml oligo dT_{12-18} (Pharmacia). The mixture was made up to a volume of 19 μl with ddH_2O and heated to 42°C for 2 minutes. 1.0 μl of reverse transcriptase (4 Units, Superscript, BRL) was added and the reaction was continued at 42°C for 1 hour. The reaction mix was incubated at 75°C for 5 minutes before placing the tubes at 4°C until use in the PCR reaction.

2.3.5 Polymerase Chain Reaction

The first strand cDNA was used for a template in the PCR reaction. One μl of the first strand product was diluted with ddH_2O, denatured at 95°C for 5 minutes, and placed on ice. PCR reaction buffer (Boehringer) was added to 1X strength (10 mM Tris-HCl, 1.5 mM $MgCl_2$, 50 mM KCl, pH 8.3) and dNTPs added to the final reaction concentration of 1.0 mM. For the primers IHCD45-1 and IHCD45-2, 125 pmol of each was added per reaction. Finally, 0.5 U Taq polymerase was added. Following an initial 5 minute 95°C incubation, the samples were cycled with a denaturation step of 45 seconds at 95°C, an annealing step of 30 seconds at 65°C, and an extension time of 60 seconds temperature at 72°C. The PCR reaction was performed with a Perkin Elmer GeneAmp 9600. After 29 cycles, a final extension step at 72°C for 10 minutes was performed before cooling the samples to 4°C. Typically 12.5 μl of a 25 μl reaction volume for each sample was analyzed by 2.0% w/v agarose gel electrophoresis. The representation of the PCR reaction procedure and the expected products for the different isoforms are described in Figure 9.

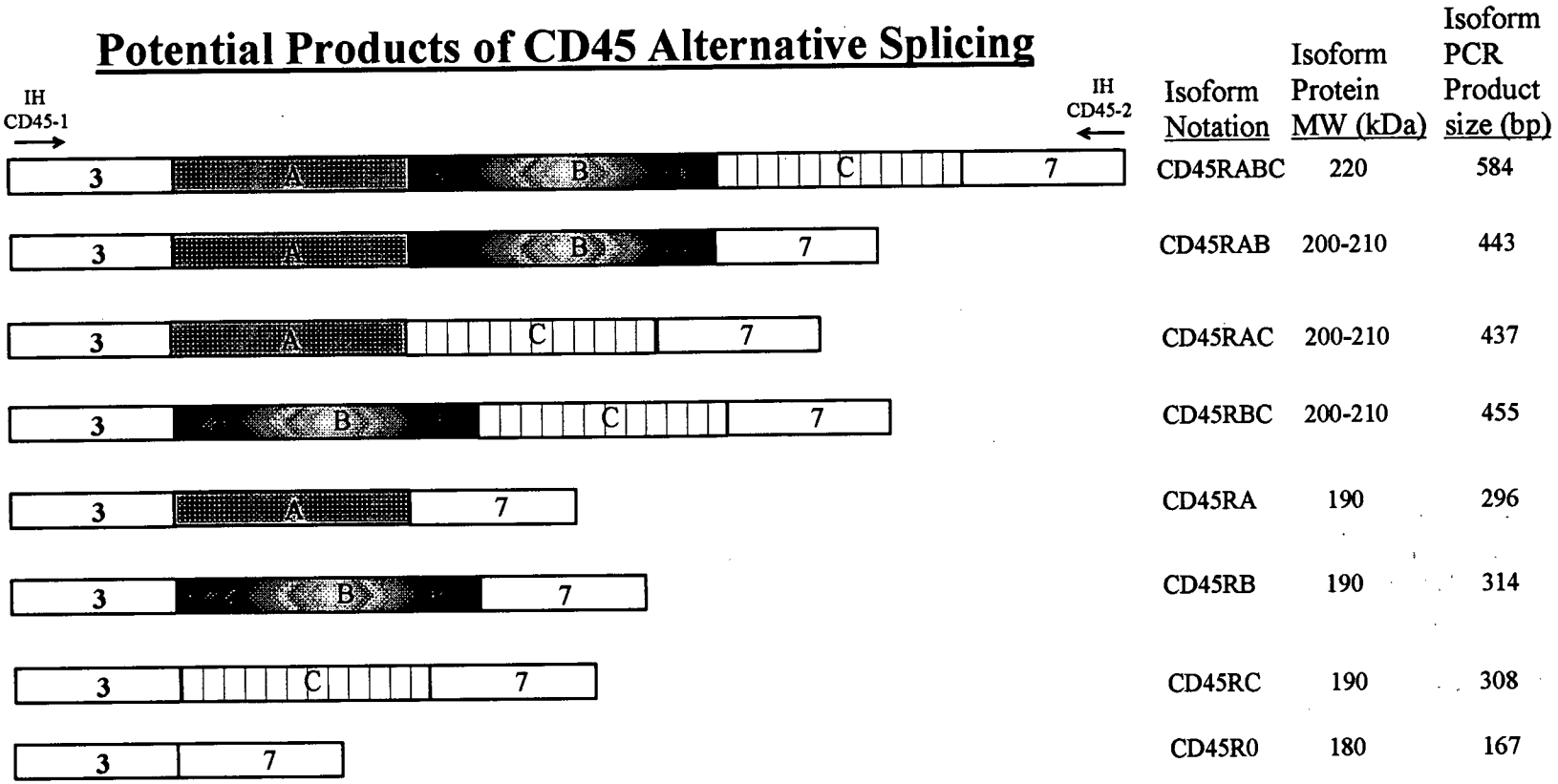

Figure 9: Isoforms of CD45 are generated by alternative splicing

The products of alternative splicing events involving exons 4,5, and 6 (or exons A, B, and C) of the CD45 mRNA are represented. These three exons will contribute to the N-terminal, O-linked glycosylation region, resulting in a change in the size, shape, and charge of the molecule (see Figure 10). The expected molecular weight of the various isoforms in SDS-PAGE analysis is indicated. The sites of binding for the oligonucleotides IHCD45-1 and IHCD45-2 are also shown. The sizes of the PCR product in base pairs (bp) for each isoform following RT-PCR analysis are listed.

2.3.6 Agarose gel electrophoresis and blotting

Agarose gel electrophoresis was performed essentially as described by Sambrook *et al* (277). Typically, 0.5X Tris-Borate-EDTA was used as the buffering system for 1% to 2% w/v agarose gels. Gels included a final concentration of 0.1 μg/ml ethidium bromide.

DNA separated by agarose gel electrophoresis was blotted to Hybond-N (Amersham) by capillary blotting as described (277). The agarose gel was incubated in denaturation solution (1.5M NaCl, 0.5M NaOH) for 30 minutes at room temperature, rinsed briefly in ddH_2O, incubated in neutralization solution (1.5 M NaCl, 0.5 M Tris, 1 mM EDTA, pH 7.2) for 15 minutes at room temperature, and rinsed briefly in ddH_2O before capillary blotting. Following capillary blotting, the DNA was crosslinked to the Hybond-N filter by exposure to UV light (254 nm wavelength) for 4 minutes.

2.3.7 ^{32}P labeling of probes and hybridization

The exon specific probes were generated by random priming of the pGEM3 constructs described in section 2.3.1. The random priming reaction contained 50 ng of the plasmid DNA, 50 μCi [$\alpha^{32}P$] deoxycytidine triphosphate (dCTP), 10 U Klenow fragment, 40 μg/ml BSA, 0.2 M HEPES, 50 mM Tris-HCl pH 8.0, 5 mM $MgCl_2$, 1 mM 2-ME, 0.4 mM of each dNTP, 200 μg/ml random hexamers (Boehringer), and ddH_2O added to 50 μl final volume. Prior to the addition of the Klenow fragment, the reaction mixture was incubated at 95°C for 5 minutes and placed on ice. After addition of the Klenow fragment, the reaction mixture was incubated at 22°C for 12 hours.

The oligonucleotide IHCD45-3 was used to detect the CD45R0 isoform PCR product which uniquely possesses the exon 3/exon 7 boundary (Figure 9). IHCD45-3 was labeled by 3' tailing with terminal deoxynucleotide transferase (TdT). The reaction contained 50 ng IHCD45-

3, 50 μCi [α^{32}P]dCTP, 25 U TdT, 0.75 mM $CoCl_2$, reaction buffer to 1X concentration (0.1 M potassium cacodylate, 12.5 mM Tris, 125 μg/ml BSA, pH 6.6) and ddH_2O to a volume of 50 μl. The labeling mixture was incubated at 37°C for 4 to 6 hours.

Unincorporated ^{32}P was removed from random primed plasmids or TdT tailed oligos by nick-spin chromatography with Sephadex G-50 spin columns (Pharmacia).

The random primed probes were denatured at 95°C for 5 minutes and placed on ice before use. Filters were prehybridized in 12X SSC, 5X Denhardt's, 0.5% SDS, and 100 μg/ml sheared herring sperm DNA for 1 hour at 65°C. The denatured random primed probes or labeled IHCD45-3 were added to the filters in 12X SSC, 5X Denhardt's, and 0.5% SDS. Random primed probes were incubated 12 to 18 hours at 65°C with the filter before washing once at room temperature with 2X SSC, 0.5% SDS and typically three times in 0.1X SSC, 0.5% SDS at 68°C. IHCD45-3 was incubated with the filters for 2 to 6 hours at 65°C before washing once at room temperature in 12X SSC, 0.5% SDS and twice for one minute in 2X SSC, 0.5% SDS at 65°C. The filters were exposed to Kodak XAR film at -70°C.

3. CHARACTERIZATION OF CD45 IN DENDRITIC CELLS AND MACROPHAGES

3.1 Introduction

The characterization of DCs has primarily concentrated on their unique functional capabilities. However, the molecular mechanisms responsible for these unique abilities had remained largely unaddressed at the time of initiation of this research project. Thus, a characterization of DC proteins could provide important information to explain DC biology and provide targets for experimental manipulation of the IR by targeting DC function. The comparison of DCs to mϕs is also important in defining the contribution of DCs and macrophages to IRs and in defining the biology of mϕs themselves. The beginning of this chapter describes testing of a sensitive labeling and detection system for cell surface proteins for use with DCs. The characterization of CD45 on DCs was of significant interest (as described in the next sections) which directed the research towards the characterization of DC and mϕ CD45.

3.1.1 The general characteristics of the CD45 protein.

CD45 is expressed at the cell surface of all lineages of hematopoietically derived cells with the exception of mature erythroid cells (reviewed in (266,278)). CD45 is among the most abundant lymphocyte glycoproteins which led to its characterization by several mAbs against human, mouse, and rat CD45. CD45 can be divided into structural domains consisting of an extracellular N-terminal region which is heavily O-glycosylated, a Cys rich membrane proximal extracellular region which contains primarily N-linked glycosylation, a transmembrane segment, and a cytoplasmic region which consists of two PTP domains (Figure 10A). As described in the following section (Section 3.1.1.1), alternative splicing generates distinct protein isoforms with isoform specific protein backbones and the differential inclusion of O-glycosylation sites. The tendency of O-glycosylated regions to form

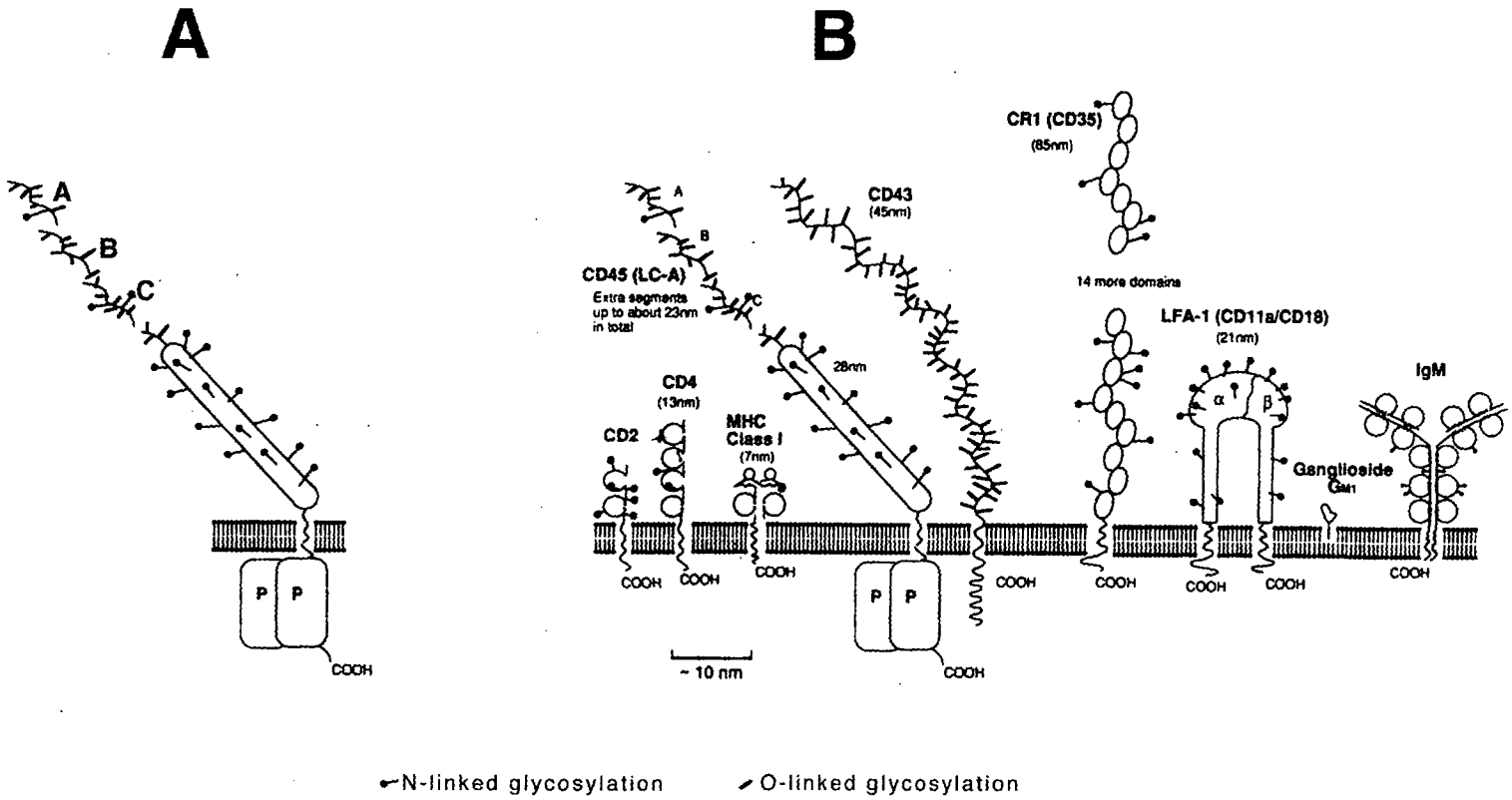

Figure 10: CD45 protein structure and comparison with other membrane glycoproteins

A) The structure of the CD45 molecule is shown. The two cytoplasmic Tyr phosphatase domains, the transmembrane domain, the extracellular membrane proximal Cys rich region, and a portion of the O-glycosylation rich N-terminal region are present in all CD45 isoforms. The alternatively spliced regions encoded by exons A, B, and C are shown as they would occur if included in the protein. The O-linked glycosylation rich regions form extended structures that cause CD45 to reach up to 51 nm out from the membrane. B) CD45 is represented to scale in relation to other membrane proteins involved in antigen recognition or cell-cell interactions. This figure was adapted from (129) with the authors' permission.

extended structures, could cause the CD45 protein to extend further from the membrane than most typical transmembrane proteins, 51 nm from the membrane for the CD45 isoform containing all of the alternatively spliced exons (Figure 10B).

3.1.1.1 Alternative splicing of the CD45 gene

The alternative splicing of exons 4, 5, and/or 6 (also called exons A, B, and C, respectively) increases the molecular complexity of CD45 expression by the generation of different protein isoforms (279-283). The eight potential products of the alternative splicing events are outlined in Figure 9. Alternative splicing events involving exon 7 have been detected at the mRNA level although a protein product from this mRNA has not been detected (284).

The alternative splicing events appear to be tightly regulated as evident from the cell type specific isoform expression. B cells primarily express the CD45RABC isoform which is also referred to as B220 due to its 220 kDa apparent molecular mass in SDS-PAGE. In contrast thymocytes primarily express the CD45R0 isoform. CD45R0 lacks all of the alternatively spliced exons and demonstrates an apparent molecular mass of 180 kDa. Peripheral T cells also demonstrate regulation of isoform expression with naive T cells expressing isoforms with alternatively spliced exons (285,286). Activated and memory T cells return their expression to primarily CD45R0 (287). The regulation of CD45 isoform expression can be further delineated among the TH_1 and TH_2 cell lines (276). TH_1 cells express primarily CD45R0 whereas TH_2 clones appear to express several isoforms with one or two alternatively spliced exons. The patterns of CD45 isoform expression outlined here are not absolute and may represent the dominant occurrence in a given cell population. Finer analyses can detect further variations among thymocyte, naive, and activated T cell populations. For example, activated T cells can regain expression of alternatively spliced exons in the CD45 isoforms following

an initial change to CD45R0 (288-291). More detailed reviews of CD45 isoform expression can be found in (278) and (266). The regulation of CD45 isoform expression and the effort which the cell must expend to exert this control, suggest that the CD45 isoforms likely have different functional properties.

The control of CD45 alternative splicing is still not fully understood, but has been postulated to involve specific factors which either positively (292) or negatively (293) regulate splicing events. The transfection of a minigene construct including only exons 3 to 7 into B cells, T cells, and L cells demonstrated that alternative splicing of the minigene mirrored the endogenous splicing pattern (292). In L cells, which do not normally express CD45, only the splicing form between exons 3 and 7 was seen. This result was interpreted to support the requirement for trans-acting factors in the inclusion of exons 4, 5, and 6. Further support for this idea was provided from the fusion of B cells, which primarily express the CD45RABC isoform, and T cells, which predominantly express the CD45R0 isoform. The hybrid cells demonstrate a B cell splicing pattern with the inclusion of CD45 alternatively spliced exons. Other studies have demonstrated that signals flanking or within the alternatively spliced exons are important for directing correct alternative splicing (294). Therefore, trans-acting factors which interact with the sequences surrounding or in the alternatively spliced exons likely mediate specific splicing events, whereas the production of CD45R0 would be the default product in the absence of the proposed trans-acting factors.

3.1.1.2 Tyrosine phosphatase activity of CD45

The identification of the placental phosphatase PTP1B (295) and its homology with the two CD45 cytoplasmic domains, led to the demonstration of CD45's phosphatase activity (296). Other studies with mutant T cell (297,298) and B cell lines (299) which lack CD45 pointed to the

requirement for CD45 in signal transduction following antigen receptor stimulation. Tyr phosphorylation, inositol triphosphate production, and an increase in Ca^{++} flux which normally take place following CD3/TcR engagement are absent in CD45 negative T cell lines (298,300). Not surprisingly, normal TcR signaling is dependent on the CD45 PTP activity (301) which may serve to dephosphorylate negative regulatory sites on $p56^{lck}$ and $p59^{fyn}$ (302,303). CD45 may function similarly in B cells where $p56^{lyn}$ and/or $p56^{blk}$ may be the target for CD45 PTP activity (304,305). The src family kinases subsequently phosphorylate ITAM motifs on proteins in the antigen receptor complexes including CD3 γ, δ, ε, the TcR ζ chain, Igα, and Igβ. The phosphorylated ITAM motifs likely serve as a scaffold upon which proteins with SH2 domains, such as PI-3-kinase and ZAP-70, bind and initiate further downstream signaling events (238). Studies of CD45 knockout mice have confirmed the importance of CD45 in T cells (306). Mice without CD45 have a dramatic defect in T cell development in addition to producing B cells and mast cells that are defective in their signaling capacities through specific surface receptors (307).

More specific functional and structural analysis has provided detailed knowledge of the CD45 phosphatase domains. Of the two phosphatase domains, only the membrane proximal domain possesses phosphatase activity (308), although mutations in the membrane distal phosphatase domain will affect the membrane proximal domain's phosphatase activity (309,310). The interaction between the two domains may also negatively regulate the membrane distal domain's activity since the expression of the distal phosphatase domain independently of the membrane proximal domain results in PTP activity (311). The phosphorylation of CD45 on Ser, Thr, and Tyr residues has also been implicated in the regulation of CD45 function. Ser/Thr phosphorylation correlated with inhibition of CD45 PTP activity (312), but the significance of Tyr phosphorylation (313)is not yet clear. These

findings resulted from non-physiological or *in vitro* analysis so further investigation will be required to clarify the *in vivo* role of CD45 phosphorylation on CD45 phosphatase activity.

3.1.1.3 Isoform specific functions

As described in Section 3.1.1.1, functional differences for each isoform have been inferred from the tight regulation of isoform expression in different cell types. This control is most evident in T cells where naive T cells express higher molecular weight isoforms that include the alternatively spliced exons, whereas activated and memory T cells primarily express the low molecular weight isoform, CD45R0, or the single exon isoforms (285,286). Functional differences for the CD45 isoforms have been described in lymphocytes (269,314-316). Each isoform expressed on memory, but not naive, T cells appears capable of associating with a unique co-receptor or co-stimulatory molecule such as CD2, LFA-1, or CD4/CD8 in the T cell membrane (314,315). Likewise, in human peripheral T cells, CD45R0 is associated with CD2, CD45RA is associated with LFA-1, and CD45RC is associated with CD4 or CD8 (315). In mouse memory T cells, CD45 appears to be associated with CD4 or CD8 and the TcR/CD3 complex (314). These altered membrane dynamics could explain why memory and naive T cells have differential sensitivity and response kinetics to T cell activation signals (25,317).

The expression of individual isoforms in antigen specific T cell lines and in transgenic mice indicates that specific isoforms can differentially affect T cell proliferation in response to antigen or TcR stimulation (269,316). In thymocytes CD45R0 is typically the dominant isoform expressed. Chui *et al* found that the transgenic expression of CD45RABC in thymocytes increased thymocyte proliferation in an MLR or in response to TcR crosslinking (269). CD45RABC enhanced thymocyte Tyr phosphorylation and Ca^{++} flux following TcR engagement. The transgenic overexpression of

CD45R0 in thymocytes had little effect, but did potentiate TcR signaling if phorbyl myristic acid was added as an additional stimulus. In these transgenics, CD45RABC was able to interfere with the anti-CD4 mediated inhibition of TcR signaling, whereas CD45R0 had no effect. The transfection of specific CD45 isoforms into a $CD45^-$ T cell clone also differentially rescued TcR signaling capabilities (316). In this case, the transfection of CD45RABC caused a poor response to antigen, whereas CD45R0 or CD45RC transfected cells possessed a good response to antigen. In all cases the expression level and the PTP activity of CD45 was similar, indicating that the domains from alternatively spliced exons were modulating the T cell response.

Despite the prediction that different isoforms may alter the binding of CD45 to different ligands in cell-cell interactions, the search for a CD45 ligand is still in progress. The binding of CD45 to CD22 has been clearly demonstrated, but this interaction is mediated by the specificity of CD22 for α2-6 sialic acid residues on CD45 (201,318). The interaction is not specific for CD45 and occurs between CD22 and all CD45 isoforms (171). Galectin-1 has also been proposed as a CD45 ligand via binding of the Galectin-1 lectin domain to the carbohydrates of CD45 (194). The existence of specific receptors for CD45 isoforms remains to be demonstrated.

3.1.2 Rationale for characterizing CD45 on dendritic cells and macrophages

CD45 is not only expressed on lymphocytes, but also on other hematopoietic cells including mϕs and DCs. Whereas CD45 appears to be implicated in lymphocyte antigen receptor signal transduction, the function of CD45 on other hematopoietic cell lineages which lack antigen receptor complexes may extend to other physiological functions. The extracellular region of CD45 could be functionally relevant as a receptor for other proteins involved in cell-cell adhesion with DCs and mϕs

or in interactions between molecules within the cell membrane (314,315). In this respect, the characterization of the isoforms expressed by DCs and mϕs is of interest since isoform specific functions described for lymphocytes may also be relevant to non-lymphocyte membrane protein interactions.

Some attempts have been made to address the function and isoform expression of CD45 in DCs, but the results are largely inconclusive. mAbs to human CD45 have been shown to disrupt primary MLRs and T cell-DC clustering (319). The majority of the effect appears to be mediated through T cell CD45 as judged by preincubation of separate populations with anti-CD45 mAbs prior to the MLR. However, blocking of CD45 expressed on DCs did result in a significant inhibition of the MLR. Analysis of human LCs have shown results varying from expression of low quantities of known isoform epitopes despite high expression of total CD45 (320) to expression of CD45R0 and CD45RB (127). FACS analysis and staining of cytospin preparations of human blood DCs showed expression of CD45RA, RB, and R0 epitopes (122). Mϕ CD45 isoform expression has not been extensively characterized. Human monocytes have been reported to express the CD45R0 and CD45RA isoforms (321).

The PTP activity of CD45 could also be involved in DC and mϕ antigen presenting function, tissue localization, and/or differentiation. Signal transduction events in DCs and mϕs including responsiveness to cytokines, Tyr phosphorylation, and calcium fluxes have been described. In studies of DC signal transduction, the responsiveness of DCs to specific cytokines has been the only indication of active signal transduction pathways in DCs. GM-CSF has been implicated in enhancing the T cell stimulatory functions of DCs, supporting the *in vitro* viability of purified DCs, and in the stimulation of DC production from DC precursors in the blood and bone marrow. TNF-α and IL-1

have also been well characterized for their effect on DCs (see Section 1.2.3.2). Thus, signal transduction pathways must be present and active in DCs, potentially involving CD45.

The presence of CD16(FcRγIII), CD32(FcRγII), and CD64(FcRγI) on mϕs and CD32(FcRγII) on DCs indicated the presence of signaling pathway involving Tyr phosphorylation and calcium fluxes (322). Tyr phosphorylation of mϕs in response to stimulating agents such as LPS (323,324) also indicated further responses in which CD45 could be involved. The characterization of mϕ src family kinases such as hck (325) indicated potential targets of CD45 PTP activity, analogous to CD45's activation of T cell $p56^{lck}$ by dephosphorylation of the negative regulatory Tyr 505. Therefore, it was reasonable to speculate that CD45 and its PTP activity could be involved in signal transduction in cells lacking classical antigen receptors.

The demonstration of FcRεI on DCs (122) also indicated the potential involvement of CD45 in DC response to IgE. The FcRεI complex consists of an α chain which binds IgE, a non-covalently associated β chain, and a disulfide linked γ chain homodimer. The γ chain is also used in the CD16(FcRγIII), CD32(FcRγII), and CD64(FcRγI) complexes (326) and is related to the ζ chain which forms a homodimer in the TcR/CD3 complex (327). The cytoplasmic ζ chain domain is capable of mediating T cell activation following crosslinking even if ζ is expressed independently of the TcR/CD3 complex (328,329). The phosphorylation of ITAM motifs in the ζ cytoplasmic domain by T cell kinases $p56^{lck}$ or $p56^{fyn}$ likely recruits other proteins with SH2 domains to the signaling complex to initiate downstream events (238). The presence of ITAM motifs in the FcRεI γ and β chains indicates that CD45 may be involved in the regulation of DC kinases which phosphorylate these ITAM motifs.

3.1.3 Objectives

The characterization of the CD45 isoforms expressed by DCs and the comparison to mϕ and lymphocyte isoform expression patterns was the initial goal of these studies. This initial characterization led to interest in characterizing the potential for CD45 to exist as multimers at the cell surface. The characterization of DC and mϕ CD45 phosphatase activity was pursued to support the possibility of CD45 being involved in the activity, migration, and differentiation of DCs and mϕs before investigations of specific signaling pathways were undertaken. CD45 PTP activity also required further definition since the existence of multimers can negatively influence the PTP activity of CD45 (330). Finally, a demonstration of DC CD45 PTP activity would be the first identification of an enzymatically active, isolated component of signal transduction in DCs.

3.1.4 Approach

The study of DC proteins had been severely hampered by the difficulty in isolating sufficient quantities of DCs and the previous absence of DC culture methods or DC cell lines. Therefore, the determination of isoform expression of DCs required the use of methods which allow the detection of protein or mRNA from small numbers of cells. Three approaches were used to provide complementary and corroborative information about CD45 isoform expression. The first method was FACS analysis. FACS analysis is suited to the analysis of limited cell numbers since staining and detection can involve 50,000 cells per sample. The study of murine DCs rather than human DCs was also preferable for several reasons including the existence of DC-specific mAbs and improved purification methods for murine DCs which permit phenotypic and biochemical characterization of murine DCs. Therefore, the analysis of isoform expression on different murine cell types was initiated

by single staining of homogeneous populations (i.e. mϕs) with a panel of mAbs with anti-CD45 exon dependent mAbs (Table 2) or double labeling of mixed populations (i.e. DCs) using the anti-CD45 mAb panel and a DC-specific mAb. Since an anti-CD45R0 mAb is not available in the murine system, a second method to analyze CD45R0 was required.

The biochemical characterization of CD45 affords a method to help delineate specific isoforms. By developing a sensitive cell labeling system, biochemical analysis of DC CD45 was made easier, although still challenging. The exon dependent mAbs can be used to immunoprecipitate all higher molecular weight isoforms of CD45. If this precleared lysate is subjected to immunoprecipitation with mAbs to common CD45 epitopes, CD45R0 should be clearly detected as the predominant isoform remaining. This biochemical analysis would also provide the opportunity to assess if the protein isoforms of DCs and mϕs exhibit similar migration in SDS-PAGE relative to lymphocyte CD45. Differences in the apparent molecular weight could imply altered glycosylation of CD45 in DCs and mϕs which has been reported in the comparison of CD45 between lymphocytes before and after activation (331,332).

The third method to assess CD45 isoform expression was RT-PCR which determines which CD45 isoform transcripts are expressed in a particular cell population (276). This method is dependent on pure populations of cells and on the assumption that the cell type of interest is still expressing the mRNA for CD45.

CD45 PTP activity from different cells was directly assessed by immunoprecipitating CD45 and quantitating the amount of PTP activity and the amount of CD45 present. This allows a comparison of the PTP activity from different cells relative to the amount of CD45 present (273).

In attempting to demonstrate CD45 multimers, three approaches were utilized. Co-immunoprecipitation provided the first impetus to study the phenomenon, but provided inconsistent

results. Therefore, the existence of multimers was assayed after chemical cross-linking of cell surface molecules and by ultracentrifugation through sucrose gradients. These two approaches should detect molecular complexes via the covalent crosslinking of associated molecules or the migration characteristics of detergent solublized CD45, respectively.

3.2 Results

3.2.1 Testing of a sensitive cell surface protein labeling and detection system for the characterization of DC surface proteins

3.2.1.1 Development of a biotin labeling system

The largest problem in the analysis of DC proteins was the limited number of DCs which could be isolated from mice. Therefore, the development of a system which would permit the detection of proteins from small numbers of DCs was required. For the cell surface labeling of cells, the most common methods are iodination of Tyr residues of proteins with ^{125}I or labeling of glycoproteins with ^{3}H following sodium periodate treatment.

An alternative to radioactive labeling of cell surface proteins, is to label with activated biotin derivatives such as sNHS-biotin. The detailed protocol for cell surface biotinylation with sNHS-biotin is described in section 2.2.2. A titration of the sNHS-biotin reagent, indicated that 100 to 1600 μg/ml/2x10^7 cells produced significant biotinylation of the cell surface molecules (Table 3). The decreased labeling for 3200 μg/ml sNHS-biotin is indicative of the detrimental effect of the high final concentration of DMSO on the cells. The concentration of DMSO was

kept below 1.0 % to avoid internal protein labeling. Therefore, 800 μg/ml/2x10^7 cells of sNHS-biotin was routinely utilized for cell surface biotinylation. The results obtained in representative labeling experiments are described in the following section (3.2.1.2).

sNHS-biotin concentration (μg/ml)	*mean linear fluorescence units*
0	0
100	102.4
200	143.7
400	276.6
800	427.2
1600	565.2
3200	27.0

Table 3: Titration of sNHS-biotin for cell surface biotinylation

P388D_1-leukemia cells were cell surface biotinylated with the concentrations of sNHS-biotin indicated (see Section 2.2.2). Following cell surface biotinylation, the cells were analyzed by FACS analysis with SA-FITC. The mean linear fluorescence (MLF) was derived by subtraction of the MLF of unlabeled cells from the MLF of each sample.

3.2.1.2 Determination of the sensitivity of the labeling system

Prior to utilizing the cell surface biotinylation protocol for DC protein analysis, the protocol was first tested on cell lines to determine the efficacy of the system. The P338D_1-leukemia cell line was utilized as a test cell line since initial analysis indicated it expressed DC

Figure 11: Determination of the sensitivity of the cell surface biotinylation system

A) $P388D_1$-leukemia cells were analyzed by FACS analysis with the following mAbs with specificity for the molecules indicated in each panel: i) SFR8-B6, ii) T24/31, iii) 2.4G2 iv) YE1/9.9.1 v) IM7.8.1, vi) YN1/1. The mean linear fluorescence values (MLF) for each mAb following subtraction of the control mAb MLF, are shown for each mAb. B) $P388D_1$-leukemia cells were collected by centrifugation and washed with biotin labeling buffer to initiate the biotin labeling protocol (Section 2.2.2). Following labeling, the cells were lysed in NP-40 lysis buffer. Lysate corresponding to the number of cells indicated in the figure, was utilized for immunoprecipitation of the TfR with the mAb γE1/9.9.1. When the initial volume of lysate was less than 200 µl, lysis buffer was added to make the final volume 200 µl prior to the addition of the mAb. The immunoprecipitated proteins were analyzed by 5-15% gradient SDS-PAGE and transferred to PVDF membrane. The location of biotinylated proteins was completed by blotting with SA-HRPO, reacting the membrane with ECL reagents, and exposing the membrane to film. The exposure shown is a 60 second exposure to Kodak-XRP film.

A

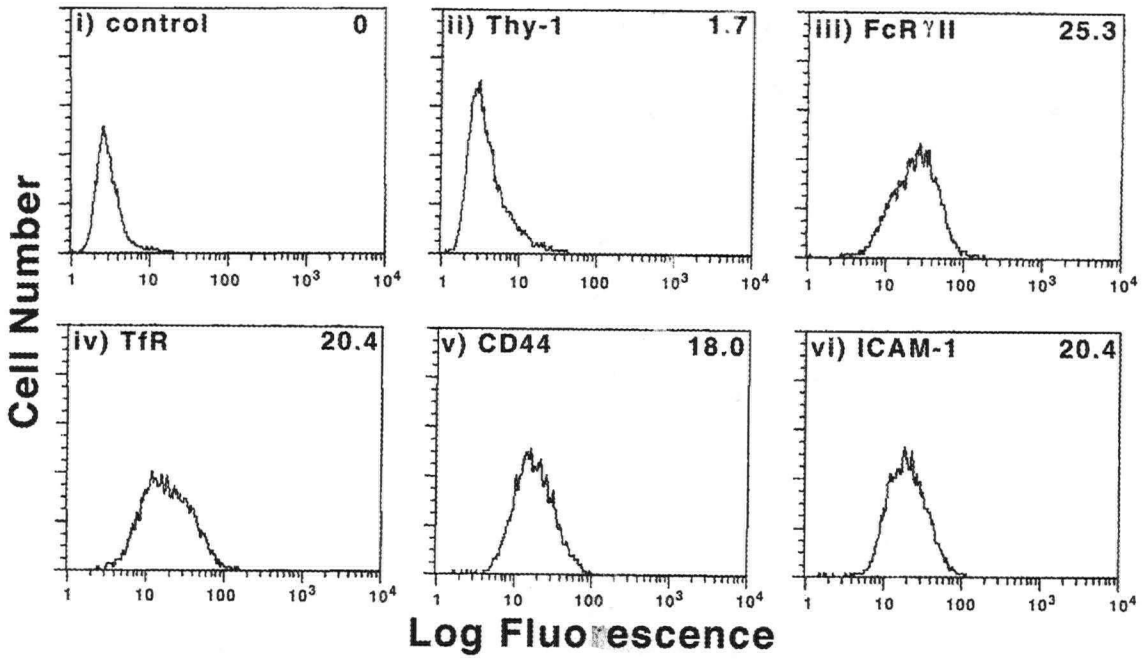
i) control 0
ii) Thy-1 1.7
iii) FcRγII 25.3
iv) TfR 20.4
v) CD44 18.0
vi) ICAM-1 20.4
Cell Number
Log Fluorescence
1
10
100
10³
10⁴

B

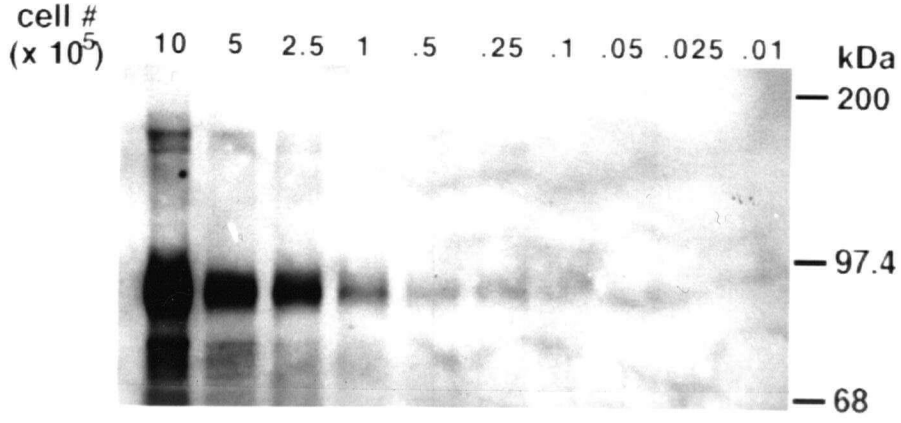
cell #
(x 10⁵)
10 5 2.5 1 .5 .25 .1 .05 .025 .01
kDa
200
97.4
68

and mϕ antigens. A FACS analysis of the $P388D_1$-leukemia cells shows the expression of several leukocyte antigens. Among these proteins, the TfR was expressed at comparable levels to most other proteins (Figure 11A) and was selected as a test molecule to evaluate the biotinylation and detection system. The immunoprecipitation of TfR from lysates of cell surface biotinylated $P388D_1$-leukemia cells, is shown in Figure 11B. The number of cells in the initial lysate was varied from $1x10^6$ to $1x10^3$. The exposure time required to detect TfR from $1x10^6$ cells was only 5 seconds. To detect TfR from $1x10^4$ cells, an exposure time of 60 seconds was required. Proteins present in grossly different amounts, as in Figure 11B, can still be clearly detected by utilizing different exposure times with ECL detection which is not possible with insoluble enzyme products. The ability to detect proteins from as few as 10000 mammalian cells suggested that the cell surface biotinylation and ECL detection system would be optimal for analyzing DC cell surface proteins.

3.2.2 CD45 isoform expression on murine DCs determined by FACS analysis

3.2.2.1 Purified Murine Splenic DCs

In order to investigate the expression of CD45 isoforms on mouse DCs, purified splenic DCs, purified thymic DCs, and 'fresh' splenic DCs were analyzed. These populations were chosen since phenotypic and functional differences have been described between DCs from different anatomic locations and after *in vitro* culture used in purification protocols (93,94,263). For example, thymic DCs are $N418^+$, NLDC-145^+, $J11d^+$, and $33D1^-$ while most splenic DCs are $N418^+$, NLDC-145^-, $J11d^-$, and $33D1^+$. Splenic and thymic DCs purified by BSA density centrifugation and differential adherence were analyzed using rat anti-mouse CD45 mAbs (listed in Table 2) and the hamster mAb

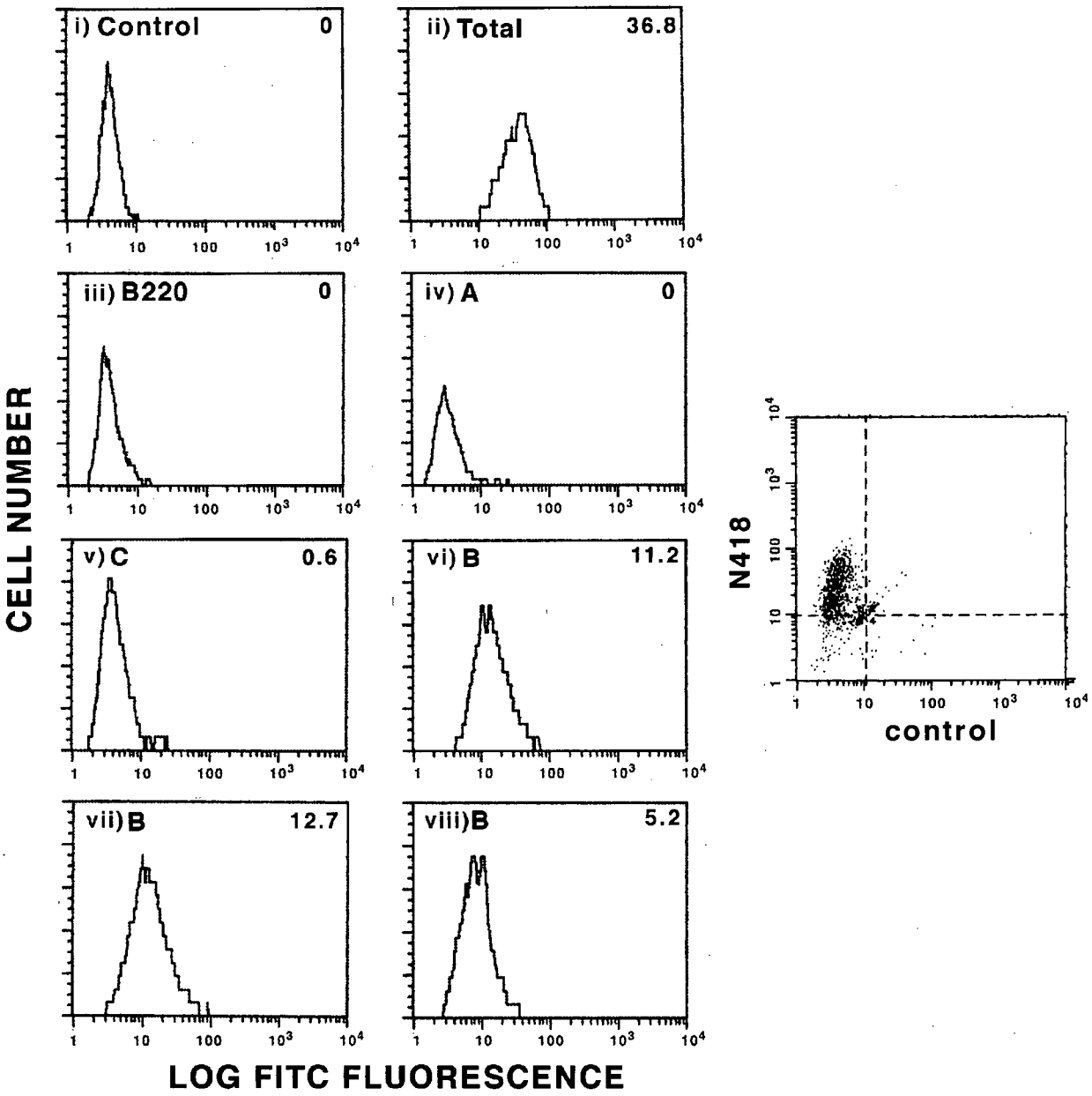

Figure 12: CD45 isoform expression by purified murine splenic DCs

Murine splenic DCs purified after overnight culture were analyzed by two-color FACS analysis. $N418^+$ cells were analyzed to determine the reactivity of the following antibodies with DCs: i) SFR8-B6 ii) I3/2, iii) RA3-6B2, iv) 14.8, v) DNL1.9, vi) MB4B4, vii) 16A, and viii) MB23G2. The exon or isoform specificity of the mAbs are indicated in the different panels. The MLF obtained with each mAb are indicated in each panel. The dot plot shown indicates the results of single staining with N418 to confirm that the cells analyzed are DCs and indicates the FL2 gate used to selectively analyze $N418^+$ cells.

N418 which is primarily specific for DCs. Staining of purified splenic DCs with exon dependent antibodies demonstrated that only the B exon dependent antibodies, 16A, MB23G2, and MB4B4 are reactive with DCs (Figure 12). Splenic DCs did not express the RA3-6B2 epitope which is thought to be specific for the CD45RABC isoform present on B cells. In addition, neither the exon A specific mAb 14.8 nor the C exon specific mAb DNL1.9 reacted with DCs. The results obtained in experiments with N418 were reproduced in experiments where the DC-specific 33D1 mAb was used instead of the N418 antibody (not shown). Therefore, among isoforms containing the A, B, and C exons, only the isoform containing the B exon is expressed on purified splenic DCs. However, the labeling of DCs with the pan-specific CD45 mAb was consistently higher than the labeling with the B exon dependent mAbs which suggested that the CD45R0 isoform which lacks all of the alternatively spliced exons may also be expressed on splenic DCs.

3.2.2.2 Purified Murine Thymic DCs

DCs from different tissues exhibit heterogeneity in both their function and in cell surface phenotype (89,263). In order to assess possible differences in CD45 isoform expression between thymic and splenic DCs, thymic DCs were purified and analyzed by two-color FACS analysis with N418 and the anti-CD45 mAb panel. The results indicated that thymic DCs have the same CD45 expression pattern as purified splenic DCs (Figure 13). Thymic DCs showed expression of the B isoform, but no expression of the A and C exons or the B220 B cell epitope. Once again the labeling with B exon dependent mAbs was lower than the labeling with the pan-specific CD45 mAb, apparently even lower than for splenic DCs, which indicated that the CD45R0 isoform may constitute the remaining CD45 expressed by thymic DCs.

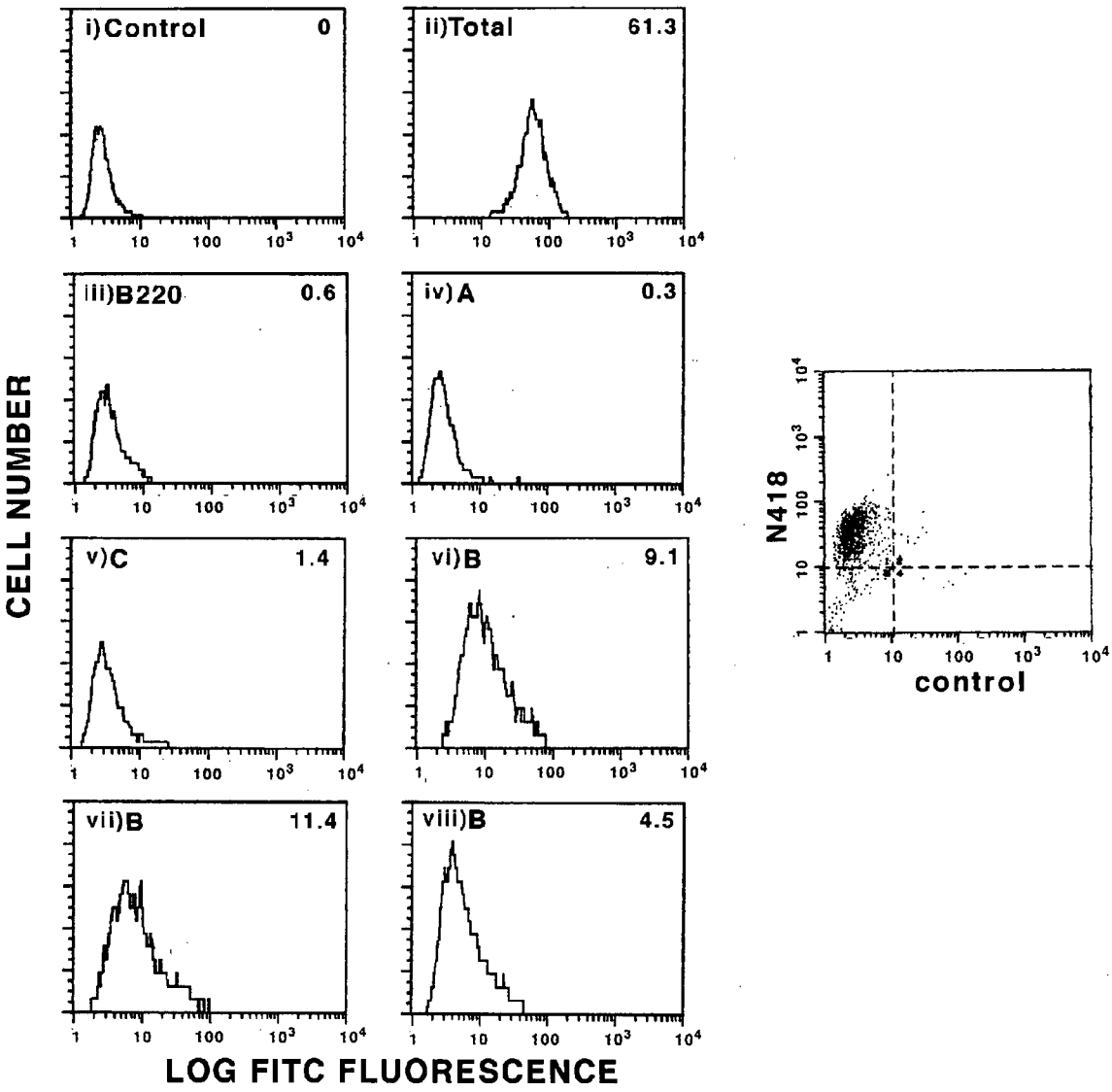

Figure 13: CD45 isoform expression by purified murine thymic DCs

Murine thymic DCs purified after overnight culture were analyzed by one or two-color FACS analysis. $N418^+$ cells were analyzed to determine the reactivity of the following antibodies with DCs: i) SFR8-B6 ii) I3/2, iii) RA3-6B2, iv) 14.8, v) DNL1.9, vi) MB4B4, vii) 16A, and viii) MB23G2. The exon or isoform specificities of the mAbs are indicated in the different panels. The MLF obtained with each mAb are indicated in each panel. The dot plot shown indicates the results of single staining with N418 to confirm that the cells analyzed are DCs and indicates the FL2 gate used to selectively analyze $N418^+$ cells.

3.2.2.3 Fresh Murine Splenic DCs

It has been previously established that the phenotype of isolated DCs changes in some respects when an overnight culture step is used in the purification procedure (93,94). In order to determine if the CD45 isoform expression is similar for freshly isolated and cultured DC isolates, fresh splenic cells enriched for DCs were derived from the BSA interface following centrifugation. This population was subjected to FACS analysis as described for the purified DC populations. The majority of fresh splenic DCs exhibit clear reactivity with the B exon specific antibodies 16A, MB23G2, and MB4B4 (Figure 14). The reactivity of fresh splenic DCs with the B exon specific antibodies is again lower than for the pan-specific mAbs. This observation is similar to the results for cultured DCs implying that fresh DCs also express a large amount of CD45R0. The CD45RB expression is similar on the fresh splenic DCs (30% of total CD45 MLF) relative to cultured splenic (25%), whereas cultured thymic DCs have a lower expression of CD45RB (11% of total CD45). Notably, fresh splenic DCs express nearly three-fold more CD45 than cultured DCs. However, the decrease in CD45 expression is likely a non-specific down-regulation since the expression level of N418 also decreases approximately two-fold after overnight culture (data not shown). Furthermore, decreased expression of CD45 in purified DC populations has been previously described (333,334). These DCs are not reactive with the mAbs RA3-6B2, 14.8, or DNL1.9 which recognize the B220 isoform, A exon, and C exon respectively. However, a small subpopulation (15%) of fresh $N418^+$ cells express A, B, and C exons plus the RA3-6B2 epitope. Further analysis of these cells indicates that all $B220^+$ cells are also surface Ig^+, suggesting that this small percentage of $N418^+$ cells are B cells, not DCs (Figure 14). Therefore, fresh splenic DCs exhibit the same phenotype of CD45 isoform expression as purified, cultured splenic DCs.

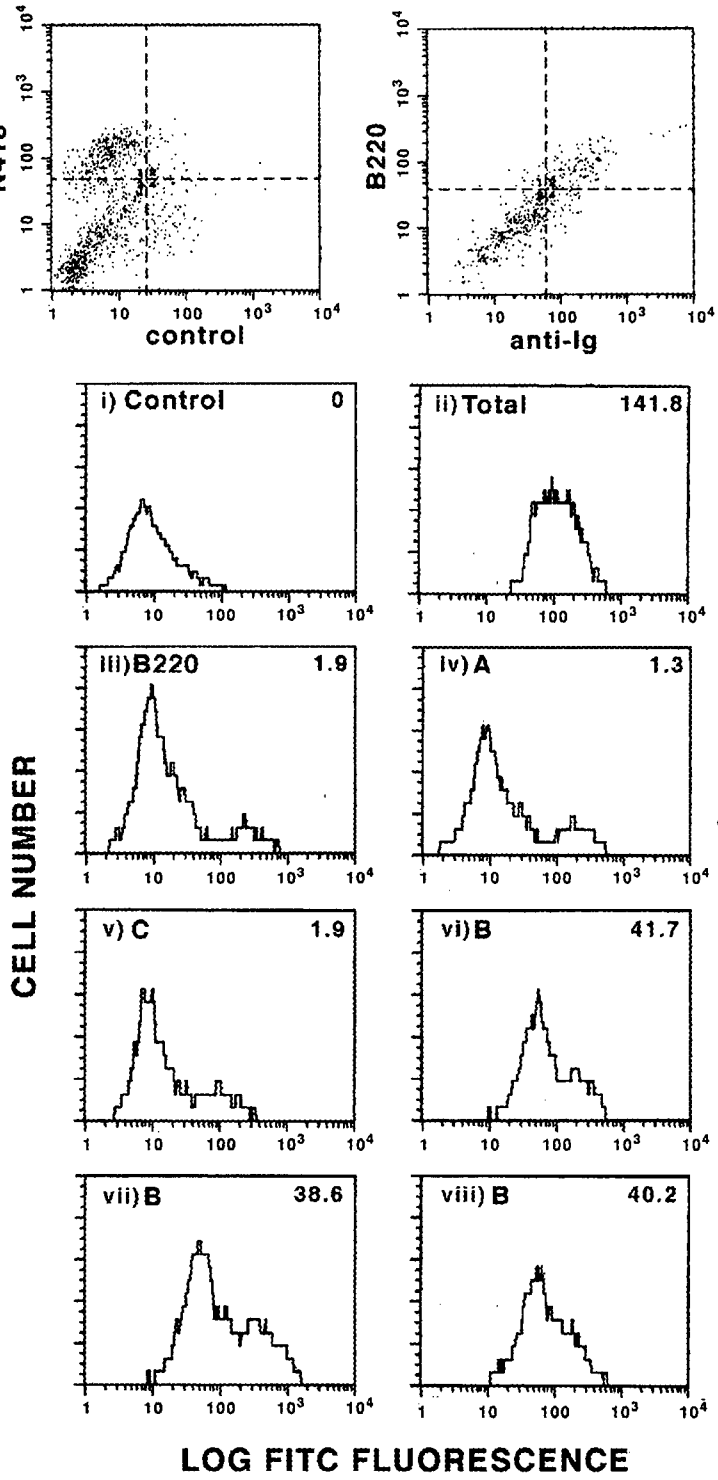

Figure 14: CD45 isoform expression by fresh murine splenic DCs

a) Freshly isolated murine splenocytes were enriched for DCs by density centrifugation before two color FACS analysis. $N418^+$ cells were analyzed to determine the reactivity of the following antibodies with DCs: i) SFR8-B6 ii) I3/2, iii) RA3-6B2, iv) 14.8, v) DNL1.9, vi) MB4B4, vii) 16A, and viii) MB23G2. The MLF obtained with each mAb are indicated in each panel. The cells expressing high levels of the alternatively spliced exons were eliminated from analysis of individual mAb reactivity of the DC population (see dot plot of anti-IgM versus B220 and text for details). The dot plot shown indicates the results of single staining with N418 to confirm that the cells analyzed are DCs and indicates the FL2 gate used to selectively analyze $N418^+$ cells. The staining of cells from the BSA interface with N418 and anti-IgM is shown to demonstrate the absence of $N418^+$ IgM^- cells.

3.2.3 Biochemical characterization of CD45 on purified murine splenic DCs

3.2.3.1 Total CD45, B exon positive, and B exon negative CD45 isoforms

To address further the identity of DC CD45 isoforms, the biochemical nature of DC CD45 was characterized. Since overnight cultured splenic DCs can be prepared in large enough quantities for protein labeling and biochemical analysis, this DC population was characterized further. FACS analysis of purified splenic and thymic DCs suggested that the quantity of the CD45RB isoform detected only contributes a subset of the total CD45 expression as determined by the panspecific CD45 mAb I3/2. Since neither the A nor C exon specific antibodies showed any reactivity with cultured DCs, the expression of CD45R0, for which a specific antibody is not available in the mouse system, was predicted to constitute the remaining CD45 on DCs. The immunoprecipitations clearly showed that the majority of CD45 present on DCs was a 180 kDa form (Figure 15). A 190 kDa isoform was also apparent, although the abundance of the 180 kDa isoform caused a merging of the 180 kDa signal with the 190 kDa signal. The predominant CD45 form on thymocytes was the 180 kDa CD45R0 form (335) which comigrated with the major DC CD45 protein. Bulk splenocyte lysate contained the entire molecular weight range of CD45 isoforms from 180 kDa to 220 kDa. To confirm the identity of the 190 kDa protein as CD45RB and to ensure that the DC 180 kDa protein was not a differentially glycosylated CD45RB isoform, lysates were subjected to sequential immunoprecipitations. By first immunoprecipitating with B exon specific mAbs, most high molecular weight CD45 isoforms were effectively precleared from bulk thymus, bulk spleen, and splenic DC lysates. The B exon specific immunoprecipitations from DC lysates contained only the 190 kDa form. The subsequent precipitation of total CD45 from lysates of all three populations demonstrated that the 180 kDa isoform (CD45R0) was the predominant isoform remaining. Since splenic DC lysates

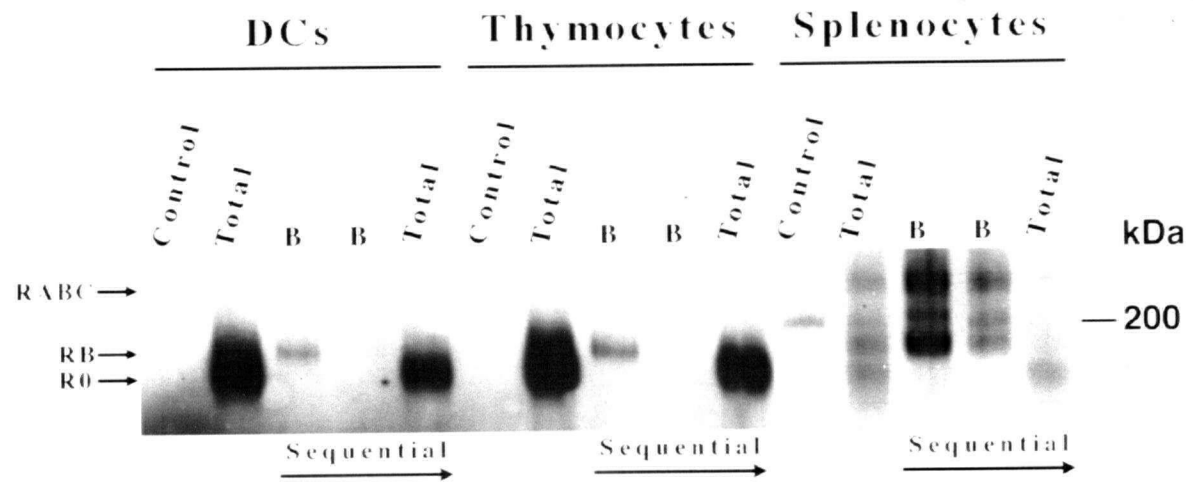

Figure 15: Immunoprecipitation of total cell surface CD45, B exon positive, and B exon negative CD45 isoforms from purified murine splenic DCs

Total CD45 was immunoprecipitated from total thymocytes, total splenocytes, and splenic DCs purified by overnight culture that were labeled with biotin. Lysates of each population were immunoprecipitated with mAbs which recognize all CD45 isoforms. In addition to immunoprecipitating total CD45, a sequential immunoprecipitation was performed where the B exon reactive isoforms were immunoprecipitated first before immunoprecipitating the remaining CD45 molecules. 8.5×10^5 DCs and 1.0×10^6 thymocytes and splenocytes were used for each immunoprecipitation.

precleared of B exon reactive CD45 molecules contained only the 180 kDa form, the absence of CD45RA or CD45RC molecules on splenic DCs was further confirmed. The CD45RB isoform from DCs comigrated with the bulk thymocyte CD45RB, which indicated that possible differential glycosylation in DCs was not affecting the SDS-PAGE migration of the CD45 isoforms. Furthermore, Western blotting of total DC CD45 with B exon specific antibodies detected only the 190 kDa protein whereas an antisera which recognizes all CD45 isoforms detected both the 180 and 190 kDa CD45 isoforms (Figure 16). Therefore, both the FACS analysis and cell surface labeling experiments demonstrate that the CD45 isoform expression on cultured murine splenic DCs is limited to the co-expression of CD45R0 and CD45RB.

3.2.3.2 Co-immunoprecipitation of CD45R0 with CD45RB

In attempting to replicate the sequential immunoprecipitation of the DC CD45RB and R0 isoforms, the following intriguing, but anomalous[1] result was obtained (Figure 16). The B exon specific mAbs effectively precleared most high molecular weight CD45 isoforms from bulk thymus cell lysates. Although the expected 190 kDa CD45RB isoform was the major protein immunoprecipitated from splenic DC lysates with the B exon-specific mAbs, a 180 kDa isoform was also precipitated (Figure 16A). Western blot analysis with the B exon specific MB4B4 mAb demonstrated that the 180 kDa protein did not contain the B exon, but was recognized by an antisera specific for all CD45 isoforms (Figure 16B). This implied that the 180 kDa CD45R0 isoform may be co-precipitating with CD45RB. The 190 kDa protein was recognized by both MB4B4 and the antisera which once again confirmed the expression of the CD45RB isoform on splenic DCs. The co-immunoprecipitation was not always apparent in splenic DC CD45RB immunoprecipitations indicating that dissociation may occur under non-optimal conditions. In addition, the 180 kDa protein was apparent in some CD45RB immunoprecipitations from thymocytes, which indicated that the observed phenomenon is not DC-specific. The subsequent precipitation of total CD45 from lysates of DCs and thymocytes demonstrated that the 180 kDa isoform (CD45R0) was the predominant isoform remaining.

---

[1] This result was obtained in one of four experiments with DC CD45. Similar results were also obtained in 2 of 7 experiments performed with thymocyte CD45.

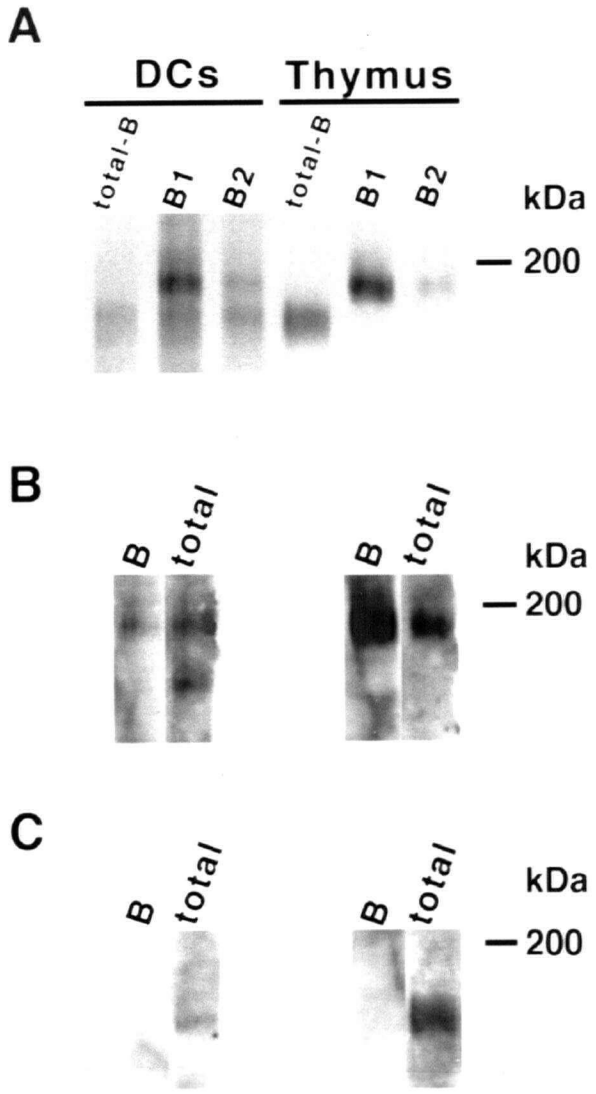

Figure 16: CD45R0 can be co-immunoprecipitated with CD45RB in purified murine splenic DCs

A) Lysates from cell surface biotinylated splenic DCs and bulk thymocytes were utilized for CD45 immunoprecipitations as follows: First, CD45 isoforms containing the B exon were immunoprecipitated with a mixture of the exon B specific antibodies MB4B4 and MB23G2 (B1). This step was repeated to ensure that all isoforms containing the B exon were depleted from the original lysates (B2). Total CD45 was then immunoprecipitated from the B exon depleted lysates using M1/9 which recognizes all CD45 isoforms (total-B). Lysates corresponding to 3 x 10^5 DCs and 2 x 10^6 thymocytes were used as starting material for the sequential immunoprecipitations. The immunoprecipitated proteins were separated by 5-10% SDS-PAGE, transferred to PVDF membrane, and detected with SA-HRPO and ECL. B) The B1 lanes from A, were Western blotted with the mAb MB4B4 against the B exon (B exon) or a rabbit antisera which recognizes all isoforms (total). C) The Total-B lanes from A were Western blotted with either the anti-exon B specific antibody MB4B4 (B exon) or a rabbit antisera specific for all CD45 isoforms (total).

3.2.4 Tyrosine phosphatase activity of CD45 from purified murine splenic DCs

In addition to the possible functional importance of specific isoform expression by certain cell types, the PTP activity of CD45 is also required for CD45 functions including TcR mediated signaling events (303). In addition, CD45 PTP activity can apparently be inhibited by dimerization (330). Since PTP activity could be important in DC CD45 function, we sought to determine if DC CD45 is functional as a PTP. We assessed this question by immunoprecipitating CD45 from purified cultured splenic DCs and assaying the CD45 PTP activity (273). DC CD45 demonstrated significant PTP activity (Figure 17A). Controls for non-specific immunoprecipitation of PTP activity from DCs and immunoprecipitations from the CD45 negative L cell line contained no PTP activity. Western blotting of the immunoprecipitated material used in the PTP assay clearly showed that CD45 was present in the DC lysate immunoprecipitate with I3/2, but absent in the control immunoprecipitations (Figure 17B). The inability to detect the B220 isoform by blotting showed that B cell CD45 was not present in significant amounts in the DC lysate. Mϕs, which comprise only 5-10% of a splenic DC preparation, exhibited up to 1.2 fold of CD45 activity per cell and a similar PTP activity per amount of CD45 present (Figure 20 and Table 4). Therefore, the majority of CD45 activity isolated from purified splenic DCs was due to DC CD45. This suggested that DC CD45 would be fully capable of mediating signaling events in DCs via its PTP activity.

Figure 17: Tyrosine phosphatase activity of purified murine splenic DCs

A) Splenic DCs were purified by overnight culture and lysed. Following immunoprecipitation of total CD45 or immunoprecipitation with an isotype control, the PTP activity of the immunoprecipitates was assayed. 2×10^5 cell equivalents were used for each time point. B) The immunoprecipitates assayed for phosphatase activity were analyzed by 7.5% minigel SDS-PAGE and Western blotting to detect CD45. 7×10^5 cell equivalents were loaded in each lane shown.

A

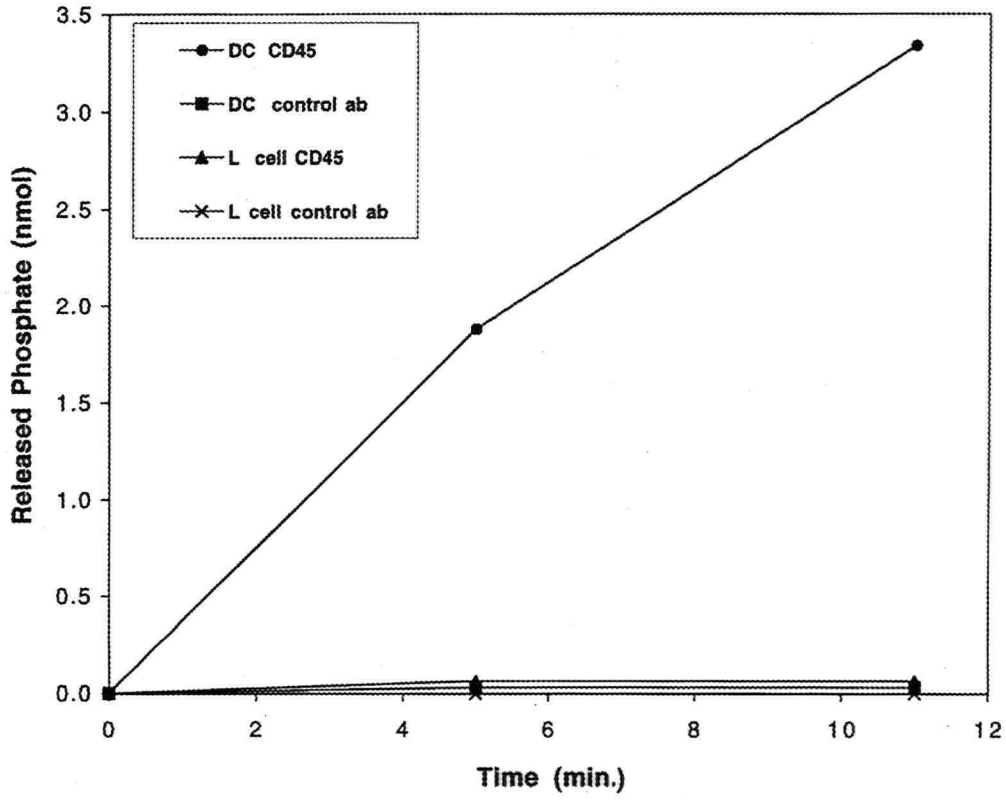
DC CD45
DC control ab
L cell CD45
L cell control ab
Released Phosphate (nmol)
3.5
3.0
2.5
2.0
1.5
1.0
0.5
0.0
0
2
4
6
8
10
12
Time (min.)

B

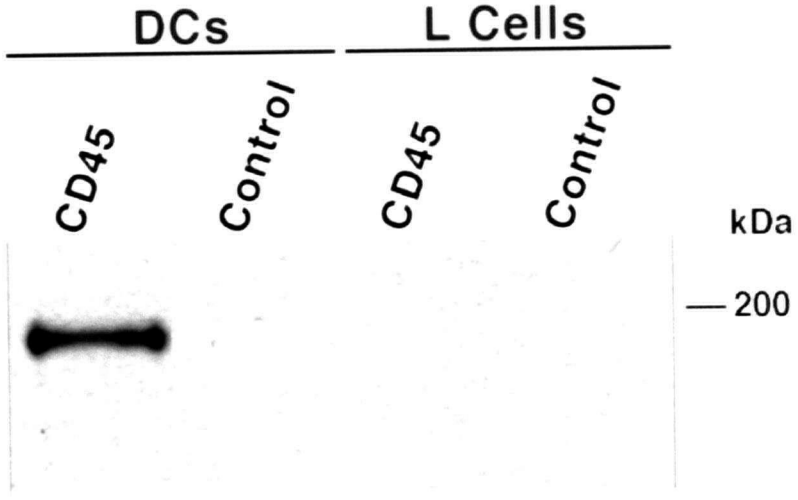
DCs
L Cells
CD45
Control
CD45
Control
kDa
200

3.2.5 CD45 isoform expression on macrophages

3.2.5.1 FACS analysis of CD45 isoforms on macrophages

The restricted isoform expression of CD45 in DCs, including the inclusion of the alternatively spliced B exon, suggested that isoform expression may be directly regulated in DCs. The close lineage relationship of DCs and mϕs and their shared expression of certain cell surface molecules, suggested that the isoform expression of murine macrophages should be examined. A common pattern of isoform expression could imply that DC CD45 isoform expression is merely a retention of the CD45 expression pattern from earlier stages of DC differentiation. However, a different pattern of isoform expression would suggest that DCs specifically alter the CD45 isoform expression in their terminally differentiated state. The isoform expression of mϕs themselves was also of interest. Expression of the alternatively spliced exons would indicate the retention of factors responsible for alternative splicing of exons A, B, and C. Furthermore, if different isoforms are utilized in mϕs versus DCs, one could infer that CD45 isoforms may have different functions in mϕs and DCs as has been suggested for T cell CD45 isoforms.

Mϕ CD45 isoform expression was therefore examined in PECs and two mϕ cell lines, J774.2 and RAW 309 Cr.1 by assessing the reactivity of exon dependent mAbs (as described in Table 2). The results of this analysis demonstrated that the expression of total CD45 is higher than the expression of isoforms containing the alternatively spliced exons (Figure 18). This result was similar to that obtained for DCs (Figure 12, Figure 13, and Figure 14), which suggested that mϕs also express a large amount of CD45R0. The three macrophage populations exhibited slight differences in their reactivity with exon dependent mAbs. All mϕ populations were negative for

reactivity with the anti-exon C mAb DNL1.9. Similarly, the expression of the B220 reactive mAb was not detected on all mϕ populations. The RAW 309 Cr.1 cells exhibited reactivity with the exon A and exon B specific mAbs whereas J774.2 cells were reactive only with the exon A mAb. The PEC population analyzed displayed a low overall reactivity with the exon B mAb, although the majority of cells (97%) were negative for expression of the B exon. The remaining 3% of cells that were positive for expression of exon B could be a mϕ subset or another contaminating cell type. The expression of exon A on PECs was small, but occurred on all cells analyzed (the median of the cells analyzed is the same as the mean for exon A shown in (Figure 18)). Therefore, among all three populations of cells, only exon A is expressed on all cell types. The RAW 309 Cr.1 cell line also expresses the B exon. Since the expression of total CD45 is higher than the expression of isoforms containing the alternatively spliced exons, CD45R0 is likely the major isoform expressed on all mϕ populations.

3.2.5.2 RT-PCR analysis of CD45 isoform expression of the J774.2 cell line

To analyze the mϕ cell populations for the expression of CD45R0, RT-PCR was utilized. RT-PCR identifies the presence of the CD45R0 transcript which can be determined by the size of the PCR product and the blotting of the PCR product with a probe specific for the exon3/exon7 boundary. The J774.2 cell line was chosen for this analysis since it is a homogeneous population and had the clearest pattern of CD45 isoform expression by FACS analysis (Figure 18). The FACS analysis results predicted that only the CD45R0 and CD45RA isoforms should be expressed on J774.2 cells.

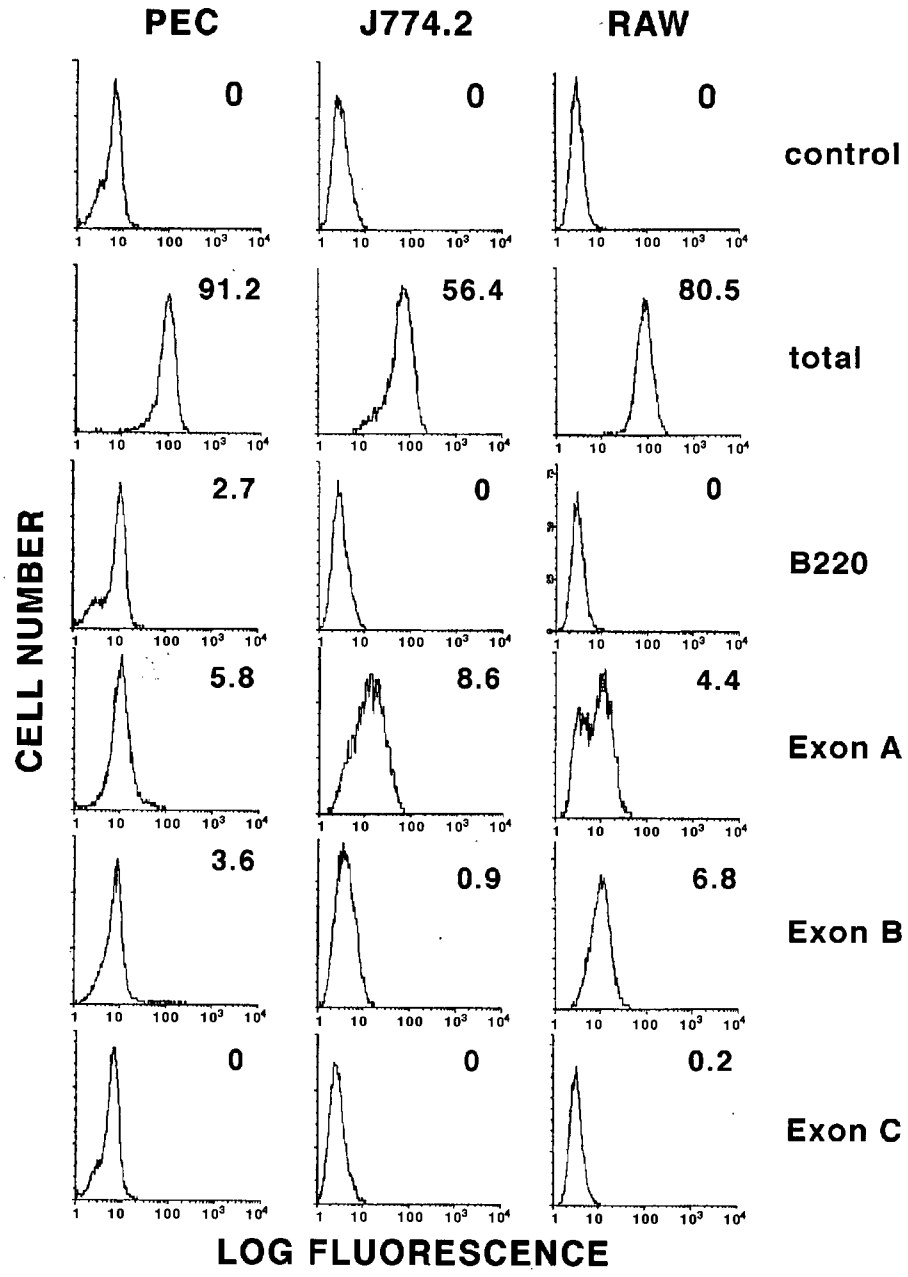

Figure 18: CD45 isoform expression of murine macrophages by FACS

PECs were thioglycollate elicited and analyzed after one day of *in vitro* culture. The cell populations were detached with versene and all cell populations were prepared for FACS analysis as described in Section 2.1.5. The mAbs utilized for each sample were as follows: control, SFR8-B6; total, I3/2; B220, RA3-6B2; Exon A, 14.8; Exon B, MB23G2; Exon C, DNL1.9. The values shown for each panel are the MLF values following subtraction of the negative control mAb MLF. The log fluorescence axes each range from 1 to 10,000 fluorescence units.

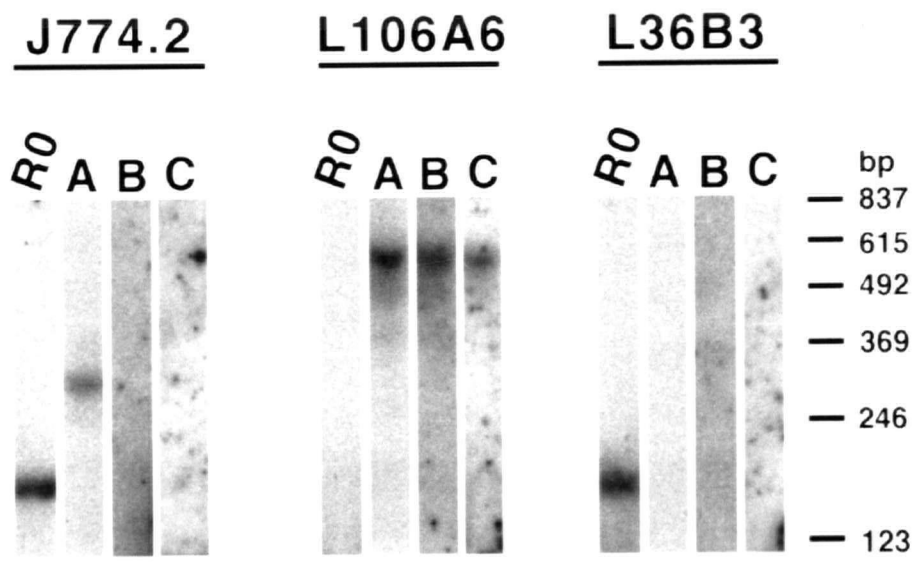

Figure 19: CD45 isoform expression by the J774.2 murine macrophage cell line as determined by RT-PCR

mRNA from J774.2 cells, L106A6 cells, and L36B3 cells was isolated, reverse transcribed, and subjected to PCR with primers to CD45. The PCR products were separated by 2% agarose gel electrophoresis, blotted to Hybond-N, and probed with probes for CD45R0, exon A, exon B, or exon C. The blots were exposed to Kodak-XAR film at -80°C for the following times: CD45R0 3 hours; Exon A, 3 hours; Exon B, 7 hours; and Exon C, 5 hours.

Total RNA was prepared from J774.2 cells, reverse transcribed, and subjected to PCR with primers to CD45 (see all of Section 2.3 for details). The PCR products were separated by agarose gel electrophoresis, blotted to Hybond-N, and probed with probes for CD45R0, exon A, exon B, or exon C. The protocol was also performed with L cell transfectants of CD45RABC, L106A6, and CD45R0, L36B3 as positive controls. The results of this analysis clearly demonstrated that the CD45 isoform mRNA expression of J774.2 cells consists of CD45R0 and CD45RA (Figure 19). This result agrees with the CD45 isoform surface expression of J774.2 cells by FACS analysis.

3.2.6 Tyrosine phosphatase activity of CD45 from macrophages

The implication of CD45 PTP activity in mϕ signal transduction events, provided the impetus to directly assess mϕ CD45 PTP activity. In addition, the characterization of mϕ CD45 was desired as a comparison to the DC CD45 PTP activity described in Section 3.2.4.

PECs and the RAW 309 Cr.1 cells were both analyzed in relation to splenic DCs for the relative CD45 PTP activity. In addition to these three cell populations, L cells were used as a CD45 negative cell source. An anti-CD45 or control mAb was used in immunoprecipitations from lysates of all cell lines. For each sample, $2x10^5$ cell equivalents were utilized for each PTP assessment (Figure 20A). Immunoprecipitates were also analyzed by Western blotting to detect all CD45 in the samples (Figure 20B). The result of the phosphatase assay clearly showed that both PECs and RAW 309 Cr.1 cells had significant PTP activity associated with CD45. The amounts of CD45 present from the three cell populations primarily agreed with FACS analysis (Figure 12 and Figure 18). One exception was that the RAW 309 Cr.1 cells showed equivalent CD45 expression relative to PECs by FACS whereas the Western blot showed RAW 309 Cr.1 cells to have less CD45 than even splenic DCs. Up to two-fold variation in the CD45 expression of RAW 309 Cr.1 and PECs in culture, was observed by FACS analysis. Densitometry of the Western blot revealed that the CD45 activity from PECs and RAW 309 Cr.1 cells, correlated well with the amount of CD45 present (Table 4) . The slightly higher PTP activity of RAW 309 Cr.1 CD45 may be related to the cell line's transformed status, although further experiments would be required to address this issue.

Figure 20: Tyrosine phosphatase activity of murine macrophages

A) Thioglycollate elicited PECs were analyzed after 1 day of *in vitro* culture. Splenic DCs were purified by overnight culture and lysed. RAW 309 Cr.1 cells were harvested from tissue culture. Following immunoprecipitation of total CD45 or immunoprecipitation with an isotype control, the PTP activity of the immunoprecipitates was assayed. The nmols of phosphate released per $2x10^5$ cell equivalents of each cell type are shown for each time point. B) The immunoprecipitates assayed for phosphatase activity were analyzed by 7.5% minigel SDS-PAGE and Western blotting to detect CD45. 7×10^5 cell equivalents were loaded in each lane shown.

A

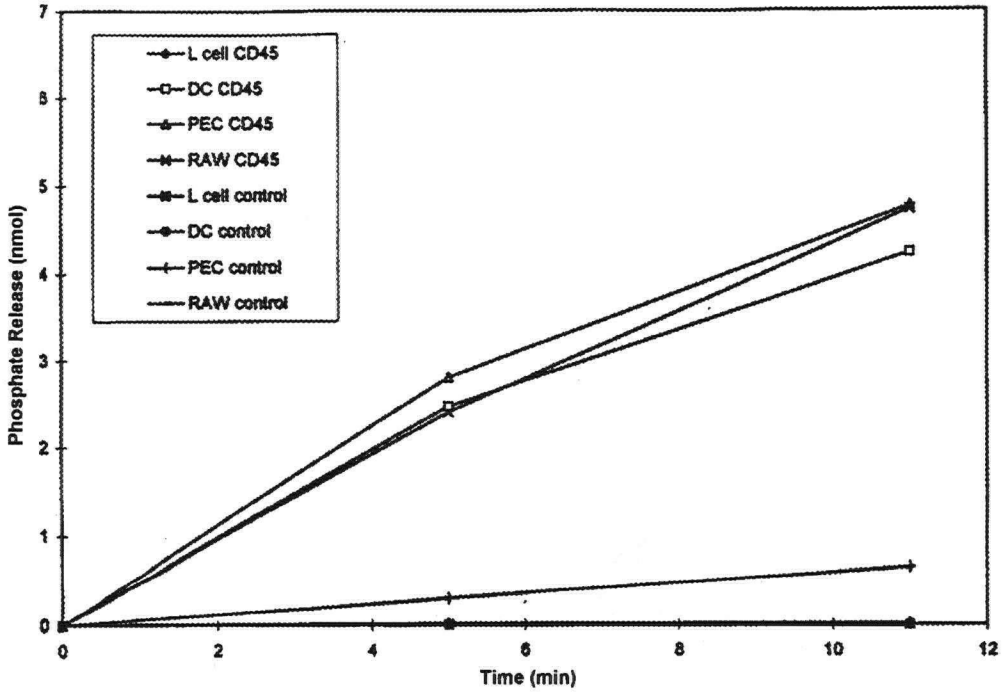
L cell CD45
DC CD45
PEC CD45
RAW CD45
L cell control
DC control
PEC control
RAW control
Phosphate Release (nmol)
Time (min)
0
1
2
3
4
5
6
7
8
10
12

B

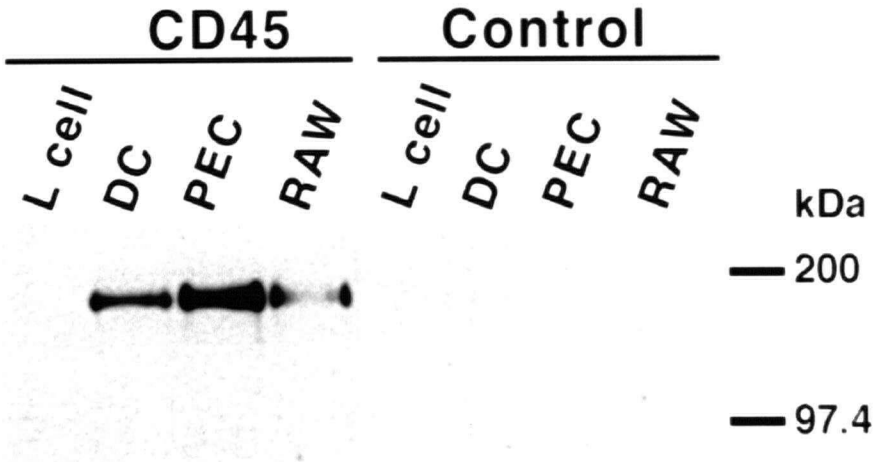
CD45
Control
L cell
DC
PEC
RAW
L cell
DC
PEC
RAW
kDa
200
97.4

Cell Type	*PTP activity per $2x10^5$ cells (nmol/min)*	*Relative CD45 amounts (Relative Densitometer Units)*	*PTP activity per equivalent amount of CD45 (nmol/min/ relative densitometer Units)*
PECs	0.50	1.0	0.50
RAW309 Cr.1	0.46	0.63	0.73
Splenic DCs	0.44	0.74	0.59

Table 4: Tyrosine phosphatase activity of macrophage and DC CD45

The PTP activity per $2x10^5$ cells was calculated from the data in Figure 20A. The relative amount of CD45 was determined by densitometry analysis of Figure 20B.

3.2.7 Assessment of physical association of CD45 on macrophages

The co-immunoprecipitation of CD45R0 with CD45RB in Figure 16 suggested the alluring prospect that CD45 could be associating in multimer complexes on DCs. Since co-immunoprecipitation proved to be an inconsistent method for detecting CD45 multimers, we attempted to address the physical nature of cell surface CD45 by other methods. The inability to obtain large numbers of DCs and their poor labeling with [^{35}S]-Met precluded the use of DCs for analysis of the physical nature of CD45 on mϕs and DCs. Therefore, PECs were studied to determine if the presence of CD45 multimeric complexes could be demonstrated.

3.2.7.1 Sucrose Density Centrifugation

The technique of sucrose density centrifugation provides a method to differentiate between the molecular mass of protein complexes (275). If the Stokes' radius of the complex is also known or determined, then the molecular mass of the protein complex can be calculated based on the migration of the complex through a sucrose gradient during ultracentrifugation. The characterization of MHC class II and Ii complexes is one particularly clear example of the utilization of sucrose density centrifugation to determine the size of a protein complex (49). This study demonstrated that the Ii/MHC class II complex is a 260 kDa complex which consists of nine subunits, three each of Ii, the MHC class II α, and MHC class II β chains. Conversely, the α and β chains assemble into simple dimers with a molecular mass of 63 kDa in the absence of Ii. Since the results with the MHC class II/Ii complex were well defined, we[2] sought to establish the technique of sucrose density centrifugation utilizing MHC class II as a standard. The behavior of CD45 in a sucrose gradient could then be assayed to determine if the migration of CD45 is consistent with multimeric complexes.

3.2.7.1.1 Class II MHC

PECs were treated with IFN-γ for 48 hours prior to a one hour labeling with [^{35}S]-Met-Cys. During this labeling period most of the MHC class II complexes were expected to consist of MHC class II α and β complexed with Ii (30,336). Following lysis of the cells in C_8Glc, the lysate was layered over a 5-20% sucrose gradient with C_8Glc and centrifuged as described

---

[2] The work described in sections 3.2.7.1, 3.2.7.1.1, and 3.2.7.1.2 was performed to a large degree by Ms. Pearl Hui with initial contributions by Ms. Shannon Awrey. Dr. Wilfred A. Jefferies and I supervised this work.

(Section 2.2.18). The fractions were harvested and I-A^d was immunoprecipitated from the fractions. The MHC class II is clearly recovered in fractions 8, 9, and 10. The values obtained from Figure 21 indicated that the I-A^d complex migrated to a radius of 129.7 mm after starting from an initial radius (measured to the meniscus of the overlaid lysate) of 72.4 mm prior to centrifugation. The angular velocity was calculated automatically by the centrifuge during the centrifugation run to be 3.85 x 10^3 radians/sec. The density and viscosity of the sucrose at a given migration distance and at 4°C was calculated from refractometry of the fractions to create a standard curve for the 5-20% sucrose gradient and known values for sucrose (337). The Stokes' radius of the αβIi complex, 72 Å, was taken from (49) and v, the assumed partial specific volume of the C_8Glc -protein complex, was assumed as 0.77 cm^3/g (49,275).

The values for class II MHC obtained for $S_{20,w}$ and M_r were in agreement with the values obtained by Roche *et al* (49). Our $S_{20,w}$ value was 12.3 S compared to 11.1 S from Roche *et al.* Our calculated M_r of the (I-A)^d-Ii-detergent complex was 433 kDa, similar to the 390 kDa reported by Roche *et al* for the protein-detergent complex. By assuming that each gram of protein binds to 0.5 g of detergent (49,275), our value for the αβIi complex was 289 kDa, which is in close agreement with the result of 260 kDa obtained by Roche *et al.* These results indicated that sucrose sedimentation could be utilized to assess the nature of CD45.

Calculations of sedimentation coefficient and molecular mass of I-A^d.

1. $S_{T,m}=\ln(r_2/r_1)\div\omega^2 t$

$S_{t,m}$= sedimentation coefficient at temperature T in medium m.

r_1= radius to the initial sample position.

r_2= radius to the measured migration of the sample.

ω= angular velocity during centrifugation.

t=time of centrifugation

2. $S_{20,w}=S_{t,m}[\eta_{r,m}(\rho_p-\rho_{20\text{-}w})/\ \eta_{20,w}(\rho_p-\rho_{t,m})]$

$S_{20,m}$= sedimentation coefficient at 20°C in water.

η=viscosity of medium

ρ_p =density of the particle analyzed. This value is 1/v (1.30 g/ml)

$\rho_{20,w}$=density of water at 20°C (0.9988 g/ml).

3. $(M_r)(1-v\rho_{20,w})=6\pi N_A S_{20,w} R_e$

v=0.77 cm^3/g (the partial specific volume of a protein-detergent complex)

M_r= molecular mass of the complex

N_A= Avagadro's number, 6.022 x 10^{23} molecules/mole

R_e= Stokes' radius

Figure 21: Sucrose density centrifugation analysis of murine PEC class II MHC

PECs were pulsed with [^{35}S]-Met-Cys for one hour and lysed in 1.0 % C_8Glc. Lysate from $4x10^6$ cells was overlaid onto a 5-20% sucrose gradient containing 1.0% C_8Glc. The gradients were centrifuged at 184,000 g for 29 hours at 4°C in a Beckman SW41Ti rotor. The original cell lysate was collected as the first fraction, after which 1.0 ml fractions were manually collected from the tube. Each fraction was immunoprecipitated with B21-2 and Rabbit anti-rat coated Protein-A Sepharose beads. The samples were analyzed by 5-15% SDS-PAGE and autoradiography. The exposure shown is a 22 day exposure to Kodak-XAR film.

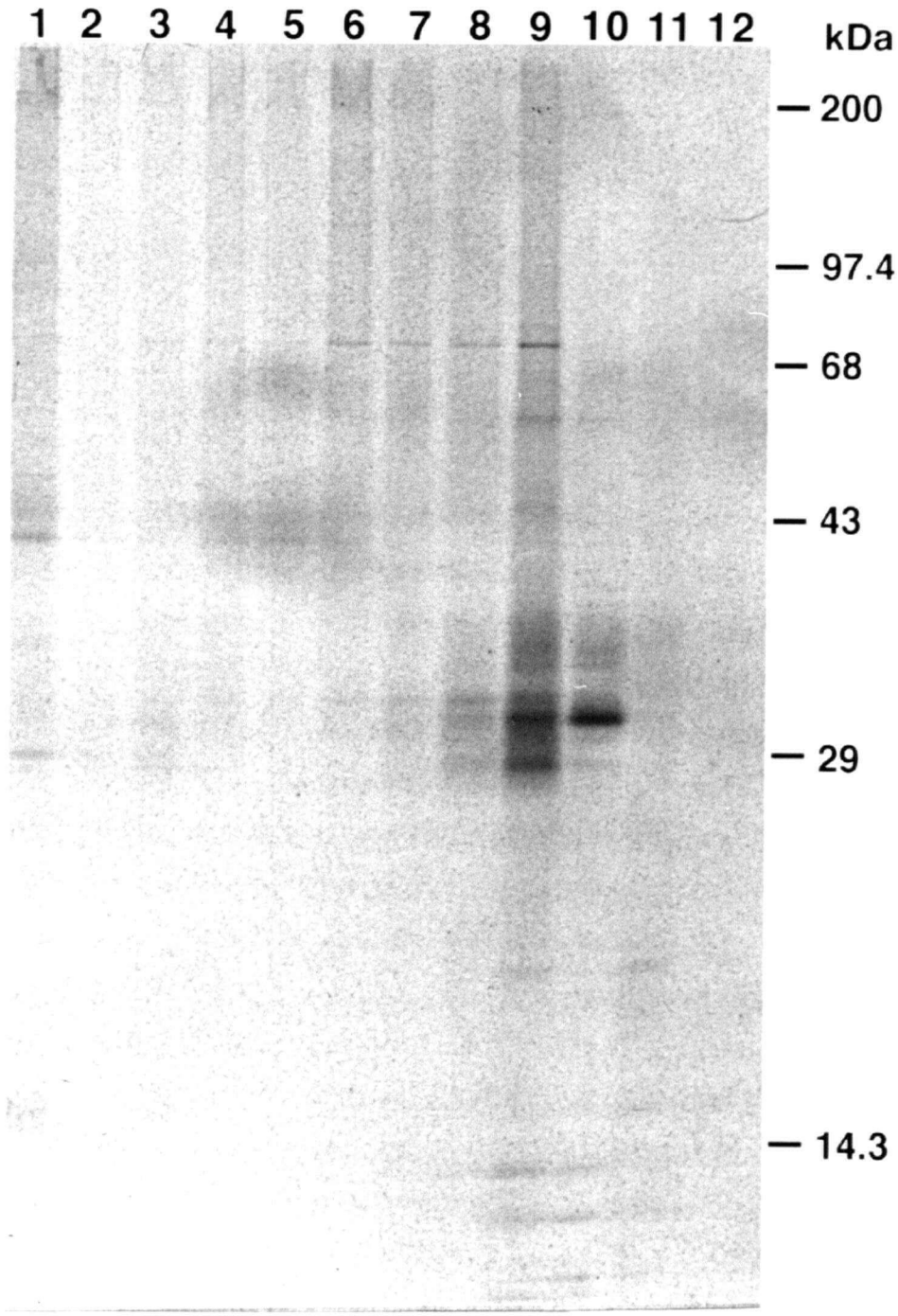
1 2 3 4 5 6 7 8 9 10 11 12
kDa
200
97.4
68
43
29
14.3

3.2.7.1.2 CD45

In order to study the sedimentation coefficient of cell surface CD45, it was important to establish that the labeled protein would reach the cell surface. Just as the MHC class II complex is dependent on its state of processing, CD45 could behave differently in the ER and Golgi apparatus than in the plasma membrane. An analysis of the transport kinetics of mϕ CD45 demonstrated that CD45 was quickly transported from the ER and through the Golgi (Figure 22). The $T_{½}$ for transport to an Endo H resistant form was only 15 minutes, which indicated that the protein was transported to the surface during the one hour of [^{35}S] Met-Cys labeling.

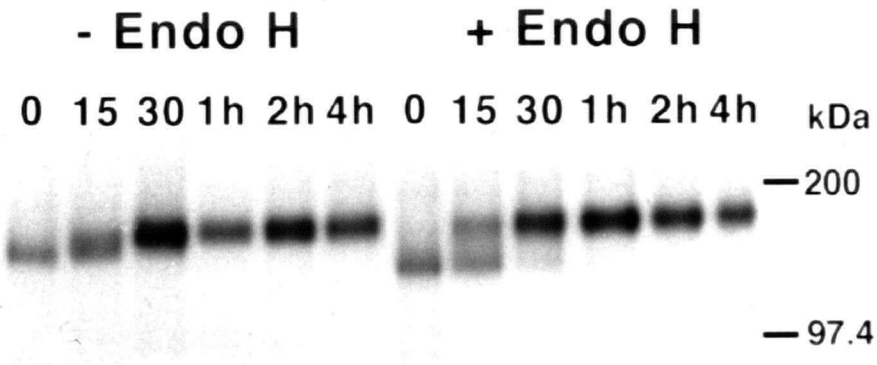

Figure 22: Transport of CD45 in PECs

PECs were pulsed for 15 minutes with [^{35}S]-Met-Cys and chased with cold, complete medium for the times indicated before the cells were lysed. CD45 was immunoprecipitated from detergent lysates of 3 x 10^6 cells at each time point. The immunoprecipitated proteins were next incubated for 20 hours in the presence or absence of Endo H. The proteins were separated by 5-10% SDS-PAGE and the gel was prepared for fluorography. The gel was exposed for 24 hours to Kodak-XAR film.

CD45 was immunoprecipitated from the fractions of a 5-20% sucrose gradient following ultracentrifugation of PEC, C_8Glc lysate. Similar results were obtained for PECs grown in the presence or absence of IFN-γ, so only the results for untreated PECs are shown in Figure 23. The distribution of CD45 throughout the gradient is not as defined as for I-A^d, with CD45 isolated from fractions 5 to 12 (fraction 12 is the bottom of the tube). Due to the wide distribution of CD45 in the sucrose gradient, each fraction was analyzed separately for the CD45 sedimentation coefficient and its molecular mass. The data and results of the calculation for $S_{20,w}$ and M_r for each fraction are shown in Table 5.

Fraction	*Migration R_2 (mm)*	*$S_{t,m}$ (Sv)*	*$S_{20,w}$ (Sv)*	*M_r (kDa) protein-detergent*	*M_r (kDa) protein*	*% of Total CD45*
5	99.1	2.45	6.23	229	152	8.70
6	106.8	3.04	8.29	305	203	33.8
7	114.4	3.57	10.6	389	259	13.6
8	122.4	4.08	13.1	482	321	12.5
9	129.7	4.55	15.9	584	389	8.60
10	137.3	5.0	19.0	699	465	8.11
11	145	5.42	22.6	829	552	4.35
12*						8.94

* The sedimentation coefficient was not calculated for fraction 12 since this fraction includes proteins which may have sedimented to the bottom of the tube prior to the end of centrifugation.

Table 5: Physical properties of CD45 calculated from ultracentrifugation analysis

Figure 23: Sucrose density centrifugation analysis of PEC CD45

PECs were pulsed with [^{35}S]-Met-Cys for one hour and lysed in 1.0 % C_8Glc. Lysate from $4x10^6$ cells was overlaid onto a 5-20% sucrose gradient containing 1.0% C_8Glc. The gradients were centrifuged at 148,000 g for 24 hours at 4°C in a Beckman SW41Ti rotor. The original cell lysate was collected as the first fraction, after which 1.0 ml fractions were manually collected from the tube. Each fraction was immunoprecipitated with M1/9-Sepharose beads and the samples were analyzed by 5-10% SDS-PAGE and autoradiography. The exposure shown is a 43 day exposure to Kodak-XAR film.

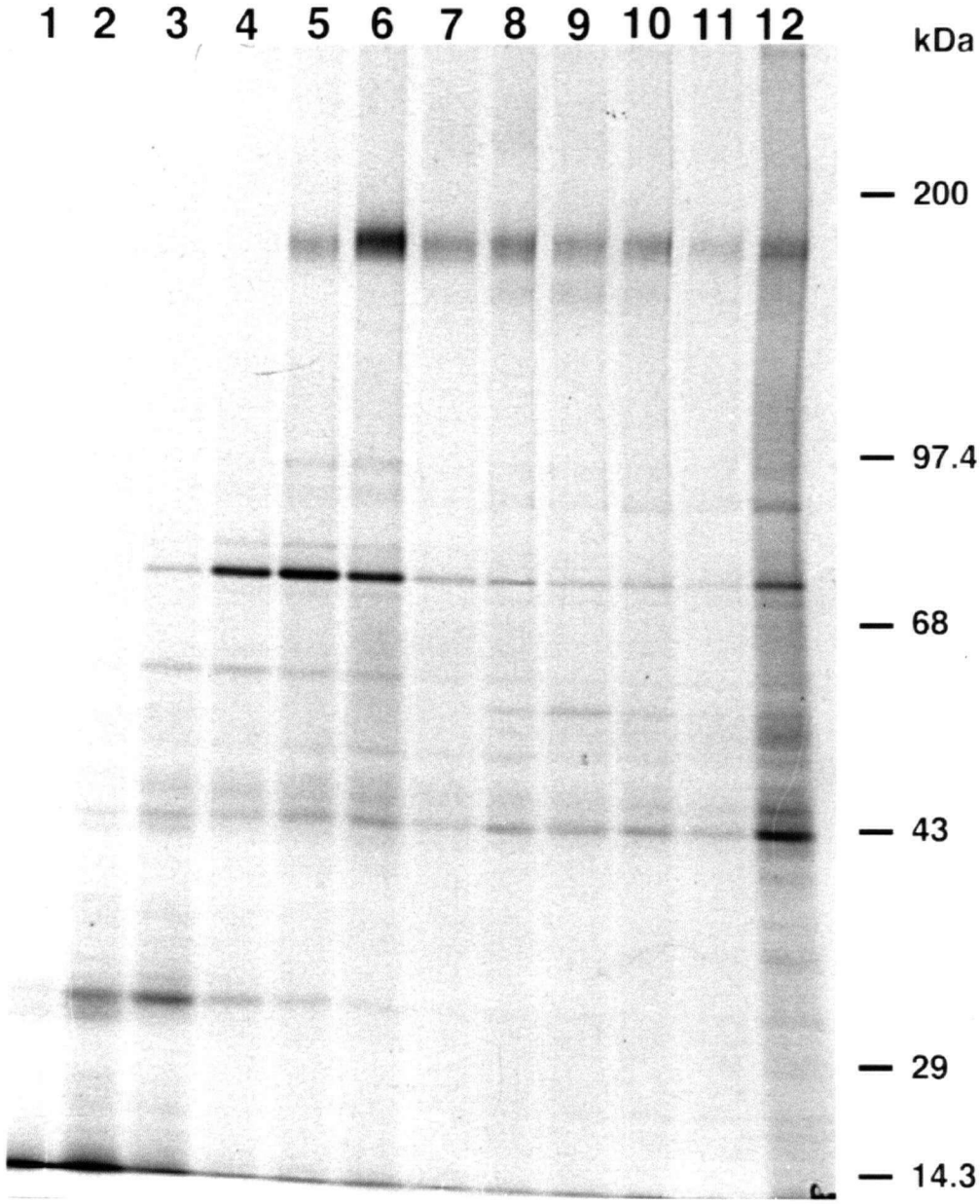
1 2 3 4 5 6 7 8 9 10 11 12
kDa
200
97.4
68
43
29
14.3

The wide distribution of CD45 in the sucrose gradient indicates the participation of CD45 in multiple molecular complexes, with different sedimentation coefficients and molecular masses. However, the identity of the participants in those complexes cannot be unambiguously determined. Although CD45 may be associating as a dimer or multimer in the fractions with higher $S_{20,w}$ values, the association of CD45 with other proteins (338,339) could equally well explain the observed sedimentation coefficients. However, the higher Mr complexes do not appear to have additional proteins specifically associated with CD45 (Figure 23). This suggests that CD45 homomultimerization may account for the different Mr complexes detected by sucrose density centrifugation. These possibilities are more thoroughly discussed in Section 3.3.4.

3.2.7.2 Cell surface cross-linking

The desire to demonstrate a direct association of CD45 prompted us to attempt cell surface crosslinking of CD45 prior to cell lysis and CD45 immunoprecipitation. CD45 crosslinking experiments have been utilized to demonstrate CD45 dimers (339) and other CD45 protein complexes (340). These studies have produced conflicting results with the prevalent concern that the crosslinked proteins are not necessarily specifically associated with CD45. Crosslinking would be the result of the abundant nature of CD45 on the cell surface (reviewed in (335)). Therefore, in attempting to detect CD45 dimers on PECs, the concentration of crosslinker was reduced to 164 μM in an attempt to minimize non-specific crosslinking. The crosslinking reagent, DTSSP, contains a disulfide bond in the center of the 12Å spacer between the two crosslinking sNHS groups. The sNHS groups should crosslink adjacent CD45 molecules since a sNHS-biotin molecule efficiently labels CD45 (Figure 37).

To evaluate the degree of crosslinking, class I MHC was used as a positive control. The 12 kDa β_2m interacts non-covalently with the 43 kDa MHC class I heavy chain. This interaction normally dissociates in conditions utilized for SDS-PAGE analysis. By crosslinking cell surface proteins, the interaction between β_2m is made covalent resulting in a 60 kDa complex of β_2m and the class I MHC heavy chain (Figure 24). The samples in Figure 24 were all run in non-reducing conditions to maintain intact complexes. Under reducing SDS-PAGE conditions, the complex is separated into the individual β_2-m and heavy chain proteins (data not shown). The MHC class I, β_2m complex represented only a portion of the total class I MHC and β_2m protein since the concentration of crosslinker was low. When the same conditions were utilized for cell surface crosslinking and CD45 immunoprecipitation, a 360 kDa complex was not detected. Although the amount of the 180 kDa form of CD45 appeared to be decreased when the samples were run non-reduced to keep the complexes intact, a defined high molecular mass complex unique to the CD45 immunoprecipitation (Figure 24) that would be indicative of a CD45 multimer was not detected.

Figure 24: Analysis of PEC CD45 following cell surface crosslinking

Thioglycollate elicited PECs were harvested and cultured overnight (18 hours) in 150 μCi/ml [^{35}S]-Met-Cys. The cells were crosslinked with 100 μg/ml of DTSSP + 10 mM IAA for one hour on ice (see Section 2.2.6 for details). Lysates from crosslinked and untreated cells were immunoprecipitated with a control mAb (SFR8-B6), anti-D^d (34-5-8S), anti-CD45 (M1/9), and anti-F4/80 molecule (F4/80). The samples were not reduced in order to maintain intact protein complexes. The samples were analyzed by 5-15% SDS-PAGE. The gels were analyzed by autoradiography by exposure to Kodak XAR film. An 84 hour exposure is shown.

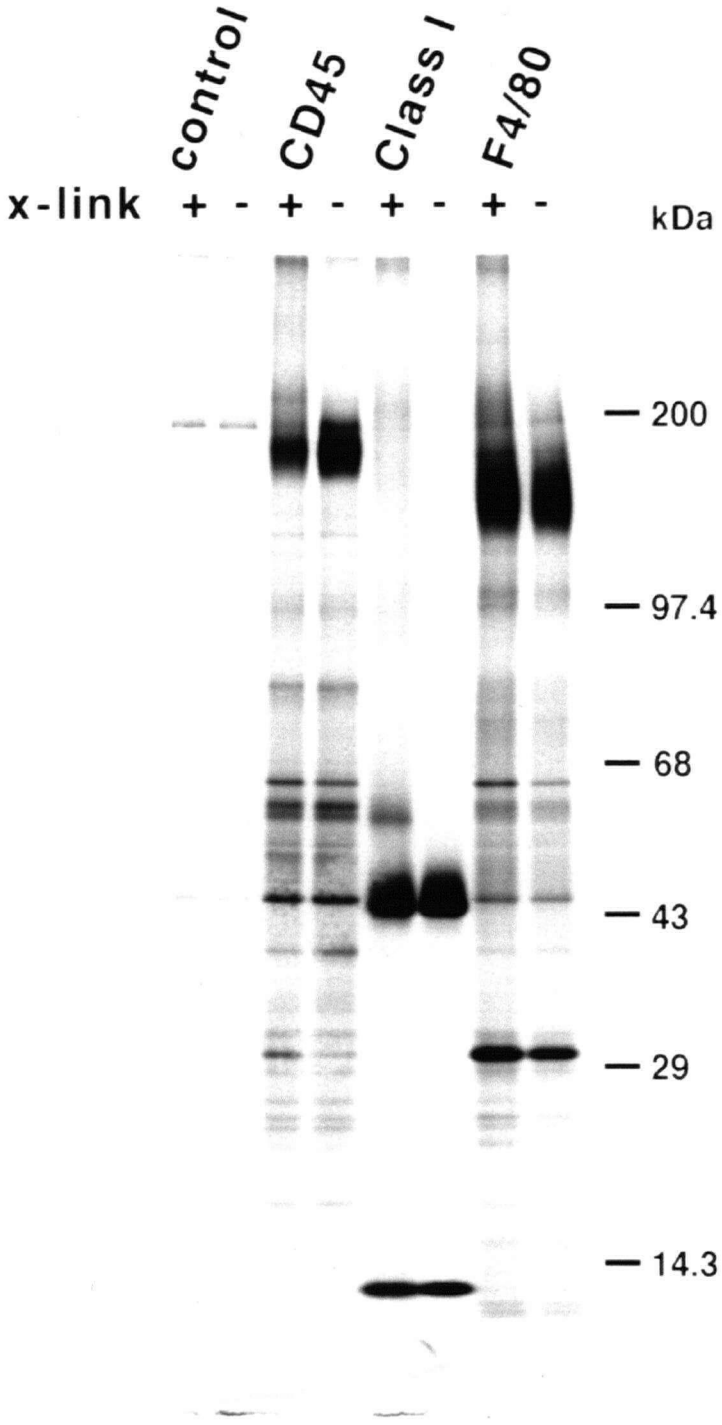
control
CD45
Class I
F4/80
x-link + - + - + - + -
kDa
200
97.4
68
43
29
14.3

3.3 Discussion

3.3.1 CD45 isoform expression in DCs and macrophages

Although CD45 isoform expression in lymphocytes has received extensive study, the isoform expression in DCs and mϕs has received little attention. The emergence of isoform specific functions (269,316) the implication of CD45 in myeloid development (341), and the potential for CD45 involvement in DC/mϕ signal transduction events (127,322), have all suggested that CD45 may be important in non-lymphocytes.

The predominant expression of CD45R0 on all populations of DCs, indicates that alteration of isoform expression is not a mechanism utilized by DCs to alter their function. For example, freshly isolated splenic DCs are more efficient at acquiring antigen relative to cultured DCs, but less efficient at stimulating T cells (94,95). Although the CD45 isoform does not change, the 3-fold decrease in total CD45 upon *in vitro* culture could alter DC function, although this possibility is difficult to address.

The CD45 isoform expression of mϕs also showed the predominant expression of CD45R0. The utilization of alternatively spliced exons was not as restricted as with DCs, with all three populations expressing the A exon, and RAW 309 Cr.1 cells also utilizing the B exon. The common usage of exon A may indicate that exon A is preferentially utilized in mϕ CD45. Human monocytes also limit their expression of CD45 isoforms to CD45R0 and CD45RA (342). The isoform expression by RT-PCR was successfully determined in mϕ cell lines (Section 3.2.5.2), but not in DCs. RT-PCR from DC populations has still not been reported except for human

LCs (127), which are at a more metabolically active stage of differentiation and can be purified to near 100% homogeneity due to the paucity of hematopoeitic cells in the skin.

The differential utilization of alternatively spliced exons between mϕs and DCs, could imply a functional role for the CD45RB isoform on DCs and the CD45RA isoform on mϕs. At least DCs specifically retain mechanisms for the expression of CD45RB. CD45R0 is the major isoform expressed by DCs and is likely produced as the default CD45 splicing product (292). These two isoforms are similar to the isoforms expressed by the majority of thymocytes, where CD45 plays a key role in T cell development. If these two isoforms interact to regulate CD45 function in a positive or negative manner, the same interactions that occur in thymocytes may occur in DCs. Notably, the expression of other CD45 isoforms does affect thymocyte development and apoptosis (343). The CD45 isoforms may be involved in distinct molecular complexes with LFA-1, CD4, CD8, and CD2, as proposed by Dianzani *et al* (314,315). All of these molecules are present on DCs, so the expectation that these molecular interactions with CD45 occur is reasonable. The recent production of DC cell lines (344-346) will now permit the study of DC CD45 molecular interactions. Since different cell lines represent a picture from different stages of differentiation, the occurrence of molecular complexes involving CD45 will require a composite view of the different phases of DC differentiation.

For the confirmation of DC CD45R0 expression, biochemical characterization of CD45R0 was performed. The expression of only two isoforms on DCs, simplified the characterization and permitted unequivocal demonstration of CD45R0 and CD45RB isoform expression on DCs. RT-PCR to determine the expression of the CD45R0 transcript in DCs was also vigorously attempted. This was not only desirable for DC CD45 characterization, but would have permitted the characterization of gene expression in DCs, including DC kinases which may

be critical in DC signal transduction. The failure of RT-PCR with DCs was likely due to the end stage differentiated nature of purified splenic DCs. Recent reports have described how DCs are primed for apoptosis, metabolically inactive as they stimulate T cells and await death (121). LCs are at a more immature phase of DC differentiation which likely explains the successful use of RT-PCR with isolated LCs. DC culture systems (72,73,134) and DC cell lines (344-346) will now permit the characterization of gene expression in DCs.

3.3.2 CD45 tyrosine phosphatase activity in DCs and macrophages

The significant PTP activity of CD45 in mϕs and DCs does clearly support a role for CD45 in these cells' signal transduction pathways. The PTP activity of CD45 in mϕs and splenic DCs appears to be comparable (Figure 20 and Table 4). These studies did not compare the PTP activity of mϕs and DCs to lymphocyte CD45, but most studies have not found a difference in CD45 PTP activity between different cell types (273), although others have (312,347). The continued analysis of DC and mϕ CD45 could assess the effect of *in vivo* and *in vitro* modulation in DC and mϕ activation and viability on PTP activity. DC viability is known to decrease after greater than 24 hours culture without GM-CSF (265). Since GM-CSF also affects other DC functions (Section 1.2.3.2), the continued characterization of DC CD45 PTP activity should analyze DCs grown with and without GM-CSF. Similarly, mϕ activation states may differentially affect CD45 activity. Thus, the continued assessment of mϕ CD45 PTP activity should assess IFN-γ activated mϕs, resident mϕs, elicited mϕs, and mϕ cell lines. Such studies may identify if CD45 PTP activity is modulated in mϕ cells such as RAW 309 Cr.1.

3.3.3 Transport of CD45

The transport of CD45 in PECs (Figure 22) was very rapid, with a $T_{1/2}$ of transport of 15 minutes. The study of CD45 transport has been very limited with only a few studies addressing this aspect of CD45 biology (348,349). In studies which are not within the scope of this thesis, the transport rate exhibited by PEC CD45 was found to be similar to CD45 in thymocytes and splenocytes (not shown) indicating no lymphocyte specific factors which facilitate CD45 transport. However, CD45 transport in non-hematopoeitic cells was significantly slower than the comparable isoform expressed in hematopoeitic cells. Transport of CD45 was particularly slowed if molecules with cytoplasmic domain deletions were analyzed. The non-hematopoietic cells also exhibited a 3 to 10 fold lower density of CD45 relative to lymphocytes (I. Haidl, W. Jefferies, D. Blew, A. Maita, P. Johnson unpublished data). A full analysis of the transport of CD45 including the effect of altered glycosylation and alterations of protein structure, could reveal molecular components of CD45 that control transport. By transfecting cells with a panel of CD45 deletion mutants, regions controlling efficient CD45 transport may be defined. A comparison of CD45 transport in non-hematopoietic CD45 transfectants with CD45 in hematopoietic cells may also reveal that specific factors in hematopoietic cells facilitate CD45 transport.

3.3.4 Physical status of CD45 in the membrane

The initial observation of CD45R0 co-immunoprecipitating with CD45RB has provided the most convincing evidence for multimers of CD45. Unfortunately, this co-immunoprecipitation was not easily repeatable with DCs CD45. The results described in

Sections 3.2.7.1.2 and 3.2.7.2 were intended to address the issue of the physical association among CD45 molecules in DCs and mϕs.

The caveats to the interpretation of the CD45 sedimentation properties are involved with the technical aspects of the procedure and the validity of assumptions that one makes in assessing the data. With class II MHC there was no observation of association of the MHC class II α or β chains or Ii with other protein components. Therefore, the sedimentation coefficient and M_r of the respective complexes could be assumed to be due to differences in only the α, β, or Ii chains in the complex. The situation for CD45 is complicated by the association of CD45 with cytoskeletal components including fodrin (338). Since fraction 12 contains the 20% sucrose cushion, the CD45 in this fraction is likely associated with high density cytoskeletal components which travel through the gradient. These complexes are not evident for I-A^d. The absence of additional proteins detected with the higher Mr CD45 complexes (fractions 7 to 11, Figure 23) suggests that CD45 multimerization is the most likely explanation for the high Mr complexes. The association of individual cytoskeletal components with CD45 could be significant enough to alter the $S_{20,w}$ and M_r of CD45. Detection of these associated proteins would be dependent on the degree of protein labeling with[^{35}S]-Met-Cys and the affinity of the protein for CD45. If the protein were to slowly dissociate during ultracentrifugation, the $S_{20,w}$ would still be affected by the initial period of association. However, when the fractions are collected and CD45 immunoprecipitated, the protein initially associated to CD45 would not be detected.

A second assumption in the calculations of $S_{20,w}$ and M_r is that the Stokes's radius obtained from (350) is valid for the CD45 for each fraction isolated. To more accurately address the Stokes' radius of different CD45 multimers, size exclusion chromatography data would have

to be correlated with the sedimentation data. Thus, the CD45 complexes with a larger $S_{20,w}$ will likely have a larger Stokes' radius which will impact on the calculation of M_r.

The ability to demonstrate CD45 multimer complexes will remain difficult since common techniques to show protein association are often viewed skeptically when CD45 is analyzed (335). The density of CD45 on lymphocytes can give false positive results with fluorescent energy transfer experiments, cell surface crosslinking, and co-immunoprecipitation data. Consistent results with a multitude of techniques to demonstrate the presence of CD45 multimers, may be more readily accepted if the association is demonstrated on mϕs where the CD45 density is lower. The Ly5.1 and Ly5.2 alleles may also provide a method to better monitor CD45 association. If CD45 is associating as multimers, immunoprecipitation with a mAb to Ly5.1 should also immunoprecipitate Ly5.2 and *vice versa* when both alleles are expressed on the same cell.

If CD45 was to assemble into dimers or multimers, the interaction may have implications for control of CD45 phosphatase activity. The dimerization of receptor Tyr kinases, such as the EGF receptor, in the induction of downstream signaling events has been well established. The dimerization of a recombinant molecule of the extracellular EGF domain and cytoplasmic CD45 domain inhibited TcR signaling which indirectly suggested that CD45 PTP activity was inhibited (330). Thus, the establishment of the existence of CD45 dimers or multimers in physiological situations could also reveal that PTPs can alter their phosphatase activity by multimerization. These possibilities have been discussed in the literature (330,335,339), but a definitive demonstration of CD45 multimerization and its functional impacts remains to be demonstrated.

3.3.5 Function of CD45 in macrophages

CD45 has clearly been implicated in signal transduction events in lymphocytes (335) and mast cells (307) and is potentially involved in signal transduction complexes involving ITAM motifs (238). In addition, specific functions for CD45's extracellular domain and the alternatively spliced regions are likely as proposed for CD45 isoforms in lymphocytes (269,314-316). With these two potential functional roles for CD45 in mind, mϕ CD45 isoform expression and PTP activity were characterized. This characterization of mϕ's restricted CD45 isoform expression, justifies the expectation that isoform specific functions in mϕ exist. Similarly, the demonstration of active CD45 PTP activity in mϕs, suggests CD45's proposed role in mϕ signal transduction is likely.

The precise role of the CD45 isoforms expressed by mϕs is difficult to assess. In lymphocytes, where CD45 isoform expression has been far more extensively studied, the ligands or other role for different isoforms are also not precisely known. The predominant expression of CD45R0 on mϕs (Figure 18 and Figure 19) may relate to the smaller molecular size of this isoform (Figure 10). The CD45R0 isoform extends nearly half as far from the membrane as the CD45RABC isoform (28nm versus 51 nm respectively). Therefore, CD45R0 should interfere less with interaction of other cell surface molecules with their extracellular ligands. Mϕs which are searching for foreign particles to phagocytose, opsonins to bind, or cells to interact with may function better with the smaller CD45R0 isoform rather than isoforms with the alternatively spliced exons.

The most likely signal transduction pathways involving CD45 in mϕs are those which trigger effector functions following the engagement of CD16(FcRγIII), CD32(FcRγII), and CD64(FcRγI). Each of these receptor complexes involves the γ chain from the FcRεRI complex which has ITAM motifs and is related to the TcR ζ chain (351). The FcR signaling pathway has been shown to involve Tyr phosphorylation and Ca^{++} fluxes, similar to the response to TcR signaling (326). Several reports

have now directly implicated CD45 in the induction of signaling following FcR engagement, although the results are not entirely congruous. Rankin *et al.* have shown that co-crosslinking of CD45 with CD32 or CD64 inhibit Tyr phosphorylation and intracellular Ca^{++} increase which normally follow the FcR crosslinking (322) and precede the biological response such as IL-1, IL-6, or TNF-α secretion, superoxide generation, and enhancement of antigen presentation (351). Corvaïa *et al.* demonstrated that the co-crosslinking of CD45 with CD32 or CD64 did affect Tyr phosphorylation and Ca^{++} flux, but did not affect the biological response of FcR crosslinking, IL-6 production (352). Furthermore, crosslinking of CD45 alone was enough to elicit an IL-6 response from monocytes. The actual biological role of CD45 in FcR signaling rather than the artificial effect of CD45 crosslinking remains to be shown. Localization of CD45 to the FcR complexes would at least indicate that CD45 can spatially exist with the FcR complexes at the initiation of FcR signaling. The analysis of CD45 negative mϕ cell lines or knockout mice for the response to FcR crosslinking, would also solidify the role of CD45 in yet another signaling pathway involving proteins with ITAM motifs.

As mentioned above, CD45 has been demonstrated to initiate mϕ cytokine secretion including IL-6 (352) independently of FcR signal transduction events. Since crosslinking of CD45 was once again used to trigger the response, it is difficult to conclude if CD45 is directly responsible for the biological effect. The co-capping of molecules associated with CD45 or the cytoskeletal reorganization following CD45 crosslinking, may initiate events independently of the CD45 PTP activity. However, if the response following CD45 crosslinking is biologically relevant, CD45 ligand engagement would serve to trigger mϕ cytokine secretion which would in turn potentiate the entire IR. Galectin-3 binding to mϕs will trigger IL-1 secretion indicating that carbohydrates of mϕ cell surface molecules, potentially including CD45, can serve as the physiological target for inducing IL-1 production (198).

3.4 Function of CD45 in DCs

The maintenance by DCs of only CD45R0 and CD45RB isoform expression, suggests that these two isoforms may be relevant to DC function. The isoforms may be positively involved in a DC function, or simply be the isoforms which least interfere with other DC functions. Since the CD45R0 is the least extended molecule from the membrane, it may interfere the least in MHC-TcR, and adhesion molecule interactions which occur between T cells and DCs (88). Positive functions of CD45 in DCs could involve CD45 participation in protein complexes within the membrane. Dianzani *et al.* have proposed that different CD45 isoforms will interact with CD4, CD8, LFA-1, or CD2 in the T cell membrane (314,315). Subsets of DCs can express all of these molecules, which could be capable of forming complexes with the DC CD45R0 and RB. In T cells the membrane complexes are thought to influence TcR signaling, so any functional effect in DCs would be mediated through other signaling complexes. The clustering of CD45 with, for example LFA-1, upon DC binding to ICAM-1 on an adjacent cell, may initiate a response within DCs which enhances DC's antigen presentation. The actual presence of molecular complexes involving CD45 in DCs can now be more thoroughly investigated with DC cell lines. Perhaps similar results to those in T cells will be observed, but the presence of other complexes, or no association of CD45 with other proteins would also provide important information about the regulation of CD45 complex formation.

The absence of an antigen receptor complex in DCs, indicates that CD45 would exert its effect through other signaling complexes. The demonstration that CD45 possesses functional PTP activity (Section 3.2.4), indicates that DC CD45 is functionally capable of mediating signal transduction events in DCs. The demonstration of phosphatase activity of DC CD45 may not be

viewed as significant by lymphocyte researchers, but this demonstration is, to my knowledge, the first isolation of an enzymatically active component of signal transduction in DCs.

As indicated in the introduction to this chapter (Section 3.1.2), the FcRεRI complex was the most likely candidate for CD45 involvement due to the ITAM motifs in its β and γ chains (353). This hypothesis has now been addressed to some degree by Bieber *et al.* (127). Using isolated, purified human LCs, crosslinking of CD45 prior to FcεRI crosslinking interfered with calcium flux normally induced upon FcεRI crosslinking. These experiments do not directly assess the requirement for CD45 involvement in FcRεI signaling. As described in the previous section, crosslinking of CD45 alone is able to induce biological responses such as IL-6 secretion in mϕs. Rather than the segregation of CD45 from the FcRεI complex as suggested by Bieber *et al.*, DCs may respond to the initial CD45 crosslinking in a manner that makes them refractory to subsequent FcRεI signaling. The demonstration of deficient responsiveness to IgE in mast cells from CD45 knockout mice is a more convincing demonstration that CD45 is indeed involved in the FcRεI signaling (307), although DCs FcRεRI has not been studied in these mice.

4. THE F4/80 PLASMA MEMBRANE ANTIGEN OF MURINE MACROPHAGES

4.1 Introduction

mAbs specific for certain cell lineages, have long provided valuable reagents for identifying and studying specific cell types. The F4/80 mAb has been widely used for mouse mϕ identification since the original description of its specificity in 1981(264). Many other mAbs produced at that time period have resulted in the characterization of the proteins recognized by these mAbs, the cloning of the cDNA for these proteins, and a detailed functional and structural analysis of the various proteins. The molecule recognized by the F4/80 mAb has remained enigmatic despite concerted effort by several labs at further characterization. Only one report (354) has superficially probed the nature of the glycoprotein recognized by the F4/80 mAb. The motivation to characterize the F4/80 molecule, was provided by curiosity about the structural characteristics of the molecule, an intense interest in the potential biological function of this molecule, and the prospect of characterizing a molecule expressed solely on mϕs and DCs.

4.1.1 Distribution of F4/80 reactive cells

The F4/80 mAb is reactive with mϕs in many anatomical locations including the red pulp of spleen, peritoneal cavity, lung, liver, gut, and brain (264,355-357). The MOMA-1 mϕ marker appears to label a distinct subset of mϕs from the F4/80 mAb (358). Therefore, the F4/80 mAb does not label all mature mϕ subsets. All bone marrow derived mϕs appear to be F4/80$^+$ (359), which indicates that the F4/80 molecule is selectively downregulated during mϕ differentiation. LCs and many other DC populations also possess medium to low expression of the F4/80 molecule (94,355). The state of cell activation is also important in modulating the expression of the F4/80 molecule. Antigen stimulated

mϕs such as mϕs from BCG infected mice generally express low levels of the F4/80 molecule, elicited mϕs express moderate F4/80 molecule levels, and resting or cultured mϕs are highly F4/80 positive (264,360). Furthermore, fresh LCs express moderate levels of the F4/80 molecule, but this expression is lost upon antigen stimulation or *in vitro* culture (89,361).

4.1.2 Prior molecular characterization of the F4/80 molecule

The molecule recognized by the F4/80 mAb is remarkably uncharacterized in comparison to other cell surface molecules. The initial characterization of the F4/80 mAb described its recognition of a 160 kDa cell surface molecule. A report by Starkey and colleagues (354) in 1987 confirmed the original data and characterized a limited number of characteristics for the F4/80 molecule. The F4/80 molecule is initially detected as a 110 kDa precursor which is processed to the 160 kDa mature form. The glycoprotein nature of the molecule was confirmed by [^{14}C] GlcNAc labeling. In addition, a protease sensitive site in the extracellular domain was demonstrated. Much of the data were not shown or were reported in such a form that left many questions to be answered.

4.1.3 Objectives and approach

The investigation of the structure and function of the F4/80 molecule, was approached from two perspectives. The first priority was to determine the F4/80 molecule amino acid sequence by cloning the cDNA for the F4/80 molecule. The cDNA cloning was first attempted by COS cell expression cloning (362), but was not successful for a number of potential reasons. Therefore, the strategy was altered to pursue protein purification from which amino acid sequence could be obtained. By constructing degenerate oligonucleotides corresponding to the amino acid sequence, a cDNA library could be screened for clones encoding the cDNA for the F4/80 molecule. The

possession of the cDNA sequence would likely provide clues of the molecule's function from homology to other proteins. In the event of no homology to other known proteins, the cDNA sequence would permit selective expression of the protein in F4/80$^-$ cells for assaying of function, the mutation of specific regions on the molecule, and the construction of recombinant molecules to probe the molecule for functional domains.

As a complimentary approach to the pursuit of a cDNA clone, characterization of the F4/80 molecule's post-translational modifications was pursued. Post-translational modification can provide structural roles relevant in protein transport, protein folding, and protein stability (153,164,166,363) Furthermore, post-translational modifications can impart specific functions to the protein. For example, molecular recognition events have been recently described which involve carbohydrates or GAGs. These post-translational modifications serve as ligands for other receptor molecules including CD22, sialoadhesin, CD44, and the selectin and galectin family of molecules (see Section 1.3). To probe the nature of the F4/80 molecule's post-translational modifications, a combination of various protein labeling methods, endoglycosidase and exoglycosidase analysis, lectin binding, and standard protein techniques were utilized to analyze the F4/80 molecule.

4.2 Results

4.2.1 Expression of the F4/80 molecule

4.2.1.1 PECs

Prior to embarking into the molecular characterization of the F4/80 molecule, the specificity of the mAb was assessed by characterizing mϕs and mϕ cell lines for their F4/80 reactivity. Although resident mϕs possessed higher levels of the F4/80 molecule (264) than elicited mϕs, only 10^6 resident mϕs can be obtained per mouse compared with 2 x 10^7 PECs per mouse. Therefore, the expression of the F4/80 molecule on thioglycollate elicited mϕs in culture was monitored to determine if the F4/80 reactivity increased. FACS analysis of PECs with mϕ and other cell surface proteins indicated that the F4/80 molecule expression was upregulated upon *in vitro* culture (Figure 25). Day zero PECs, prior to adherence, comprise a mixed population of cells with approximately 70% mϕs. The F4/80$^+$ mϕs displayed a MLF of only 7.0 units. After 24 hours of *in vitro* culture, the F4/80 molecule expression reached 32.9 MLF units. This level of F4/80 molecule expression was maintained over 48 hours, but declined again on day three of culture (not shown) to reach a MLF of 5.6 by day 4 of culture. Other cell surface proteins including FcRγII, CD11b, and ICAM-1 underwent a similar decrease in expression by day 4 of culture, although the most drastic decrease among these molecules was 2.3 fold compared to the 5.9 fold decrease in F4/80 molecule expression from day 1 to day 4. In subsequent studies of the F4/80 molecule on PECs, the cells were labeled or harvested on day 1 or 2 of *in vitro* culture to maximize the molecule's expression.

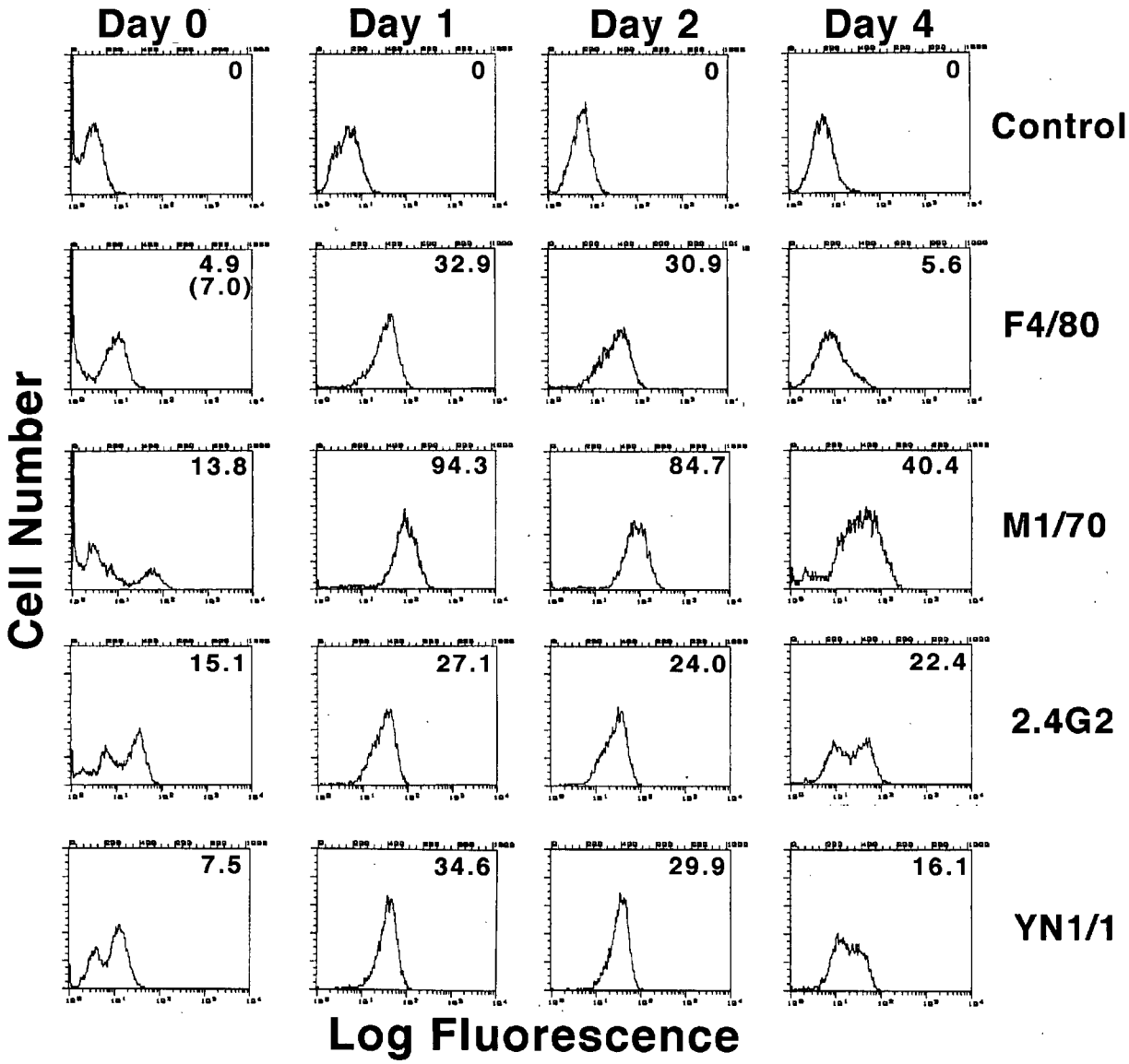

Figure 25: Expression of the F4/80 molecule on PECs

PECs were harvested by peritoneal lavage and plated in tissue culture treated dishes or analyzed immediately for Day 0 samples. FACS staining was performed as described in Section 2.1.5 with the mAbs as indicated: control (SFR8-B6), F4/80 (F4/80 molecule), M1/70 (CD11b), 2.4G2 (FcRγII), and YN1/1 (ICAM-1). Samples were fixed in paraformaldehyde and analyzed with the same fluorescence settings for all samples on a FACScan (Becton Dickinson). Live cells were selected by gating with FSC and SSC. The values shown for each mAb are the MLF values after subtraction of the control mAb MLF. The log fluorescence axes each range from 1 to 10,000 fluorescence units.

4.2.1.2 Dendritic cells

The expression of the F4/80 molecule on DCs was of central interest in pursuing its characterization. The expression of the F4/80 molecule on purified splenic DCs was assessed relative to other DC cell surface molecules. This comparison revealed that F4/80 molecule expression was significantly less than some DC molecules such as ICAM-1, MHC class II, and $CD11_C$ (Figure 26). However, the F4/80 molecule was expressed at levels comparable to the molecule recognized by the DC-specific 33D1 mAb. The level of F4/80 molecule expression was still clearly above background, due to DC analysis 16 hours after isolation to minimize the reduction in expression which follows DC isolation (94,95).

4.2.1.3 Macrophage Cell Lines

The expression of the F4/80 molecule on mϕ cell lines was also of interest since a cell line would provide a more convenient cell source for studying the protein and would be useful in the large scale purification of the molecule for amino acid sequencing. FACS analysis of a few of the mϕ cell lines tested indicated that the F4/80 molecule was variably expressed on mϕ cell lines (Figure 27). The J774A.1 cell line had no reactivity with the F4/80 mAb whereas the J774.2 cell line showed an F4/80 reactivity level of 20.4 MLF units. These two cell lines were derived from the same J774 sarcoma (364), indicating clonal variation in the F4/80 molecule expression. The $P388D_1$-mϕ cell line also had detectable expression of the F4/80 molecule. Much of the initial characterization of the F4/80 molecule utilized the J774.2 cell line, but the F4/80 molecule expression was found to vary after prolonged culture or in large scale spinner culture conditions.

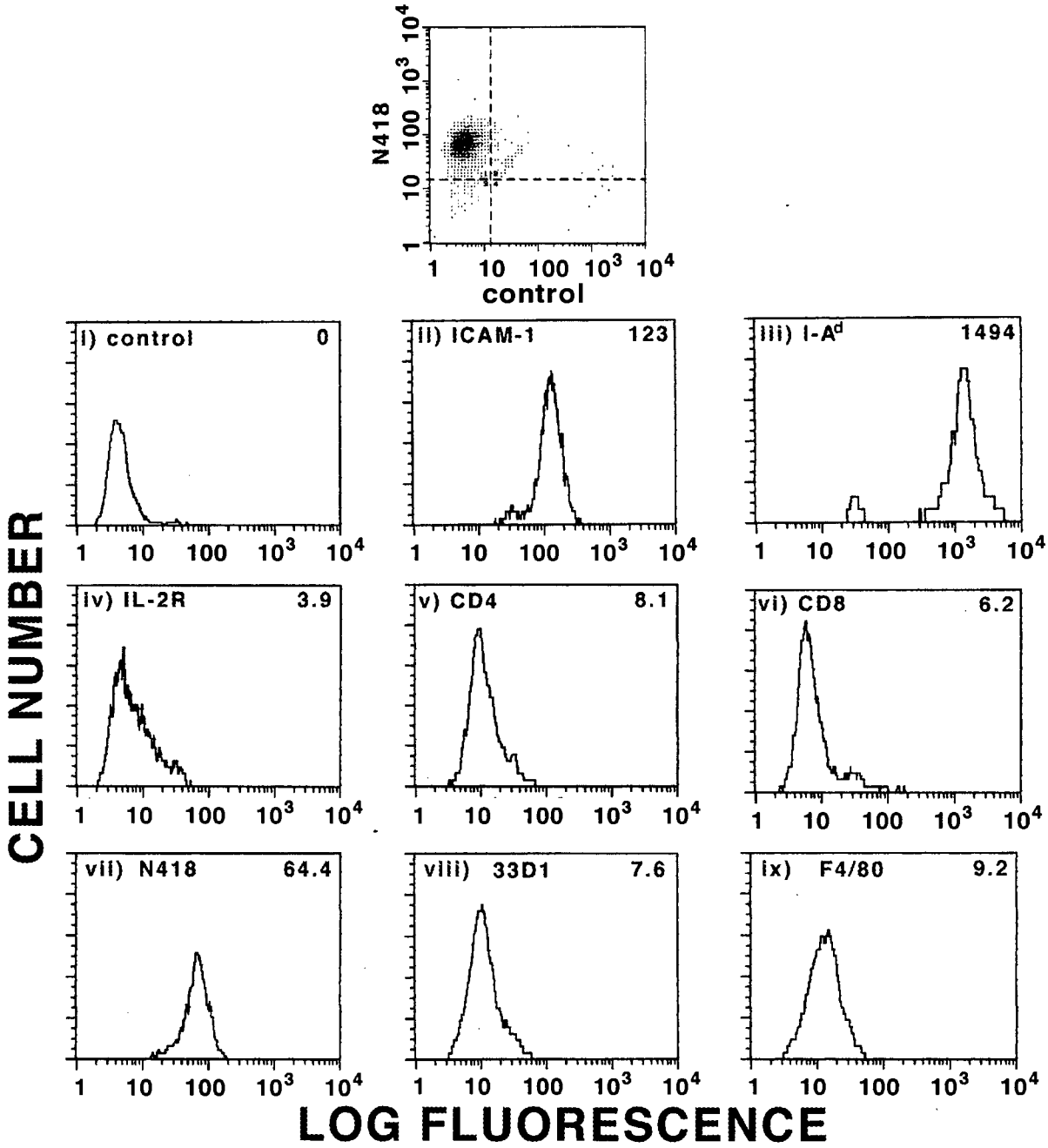

Figure 26: Dendritic cell F4/80 molecule expression

Murine splenic DCs were harvested from BALB/c mice as described in Section 2.1.3. The cells were prepared for FACS analysis by double labeling the cells with the hamster mAb N418 and the following mAbs against the molecules indicated in each panel: i) SFR8-B6, ii) YN1/1, iii) MK-D6, iv) PC61, v) GK1.5, vi) 53-6.72, vii) N418, viii) 33D1, and ix) F4/80. The N418 reactivity was detected with a goat-anti-hamster PE reagent. The other mAb reactivities were detected with a highly specific Donkey anti-rat IgG FITC reagent with the exception of MK-D6 for which a specific goat-anti-mouse IgG_{2a} FITC reagent was used. The cells were gated for N418 positive cells as indicated in the dot plot shown, and the fluorescence histograms for the other mAbs are displayed. The log fluorescence axes range from 1 to 10,000 fluorescence units.

For this reason, other cell lines including RAW 309 Cr.1 were tested for F4/80 reactivity. Expression of the F4/80 molecule was clearly greater on RAW 309 Cr.1 cells relative to other cell lines and was similar to PECs. Although the RAW 309 staining shown is from a separate experiment relative to the other 3 cell lines, the MLF are consistent with values observed when staining was performed on the same day. The results by FACS staining were confirmed by biosynthetic labeling and immunoprecipitation of the F4/80 molecule (Figure 44).

4.2.1.4 Modulation of F4/80 molecule expression by BCG infection

One trait of the F4/80 mAb is its decreased reactivity with activated mϕs, including mϕs from BCG infected mice (360). To confirm the specificity of the mAb and the reported result, FACS staining of resident, purified protein derivative (PPD) elicited, and BCG infected mϕs was performed[3] (Figure 28). These results were performed with different secondary antibodies relative to Figure 25 and Figure 27 so the MLF values are not directly comparable. However, a 70% decrease in F4/80 expression in PPD elicited mϕs relative to RPMs (Figure 28) was clearly evident. BCG activated mϕs expressed only 38% as much F4/80 molecule relative to RPMs. The level of expression of FcRγII and CD11b on the three mϕ populations were not as significantly affected as the F4/80 molecule. The expression of I-A^d by the BCG activated mϕs indicated that the mϕs were activated.

---

[3] This work was performed in collaboration with Dr. Rick Stokes and Dr. David Speert in the Dept. of Pediatrics, UBC, Vancouver, Canada.

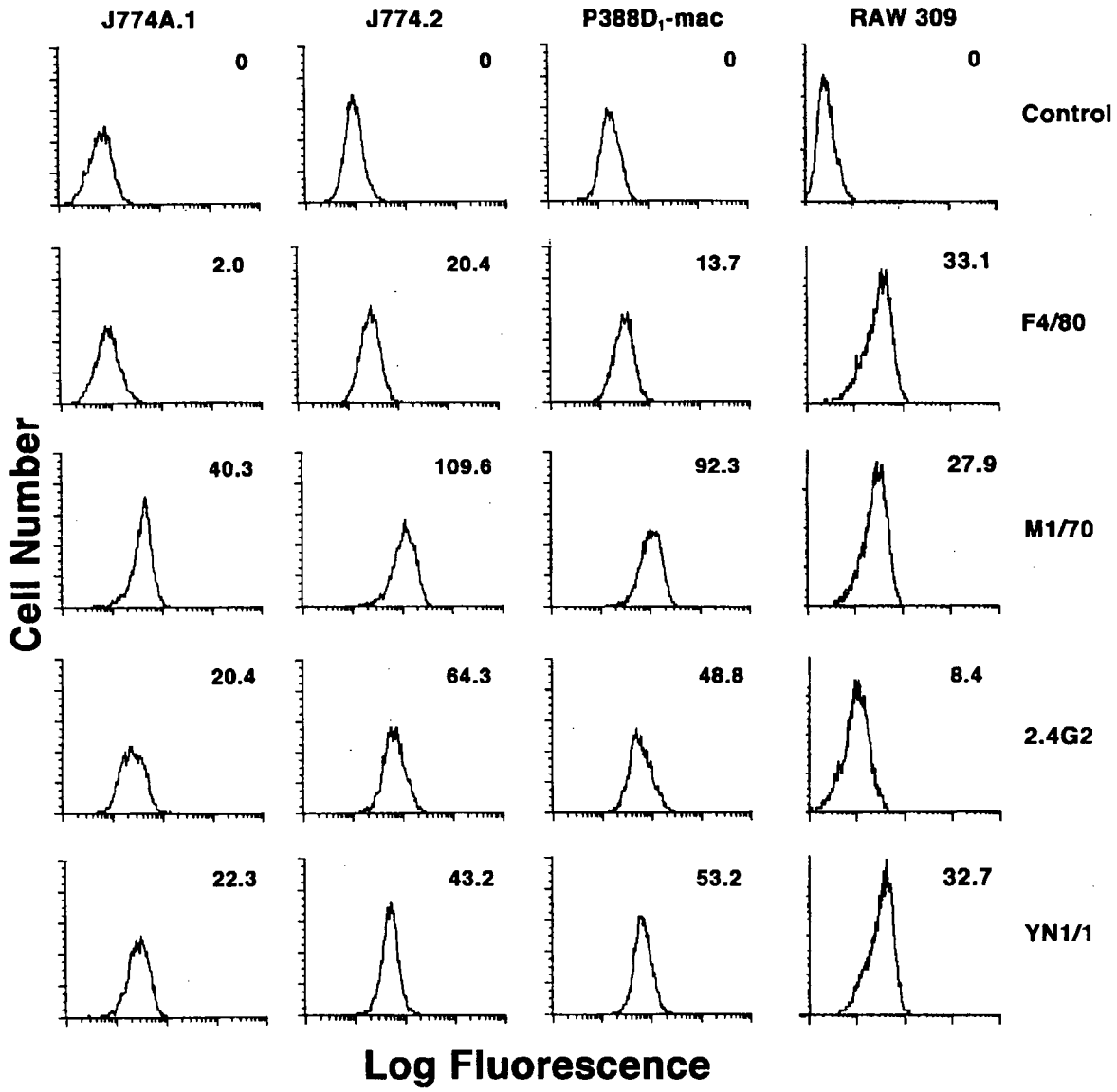

Figure 27: Expression of the F4/80 molecule on murine macrophage cell lines

The cell lines J774A.1, J774.2, P388D$_1$-mϕ, and RAW 309 Cr.1 (see), were analyzed by FACS analysis with the mAbs as indicated: control, (SFR8-B6), F4/80 (F4/80 molecule), M1/70 (CD11b), 2.4G2 (FcRγII), and YN1/1 (ICAM-1). Samples were fixed in paraformaldehyde and analyzed with the same fluorescence settings for all samples on a FACScan (Becton Dickinson). The RAW 309 Cr.1 cell line was analyzed in a separate experiment, but with the same reagents and fluorescent settings. Live cells were selected by gating with FSC and SSC. The values shown for each mAb are the MLF values after subtraction of the control mAb MLF. The log fluorescence axes each range from 1 to 10,000 fluorescence units.

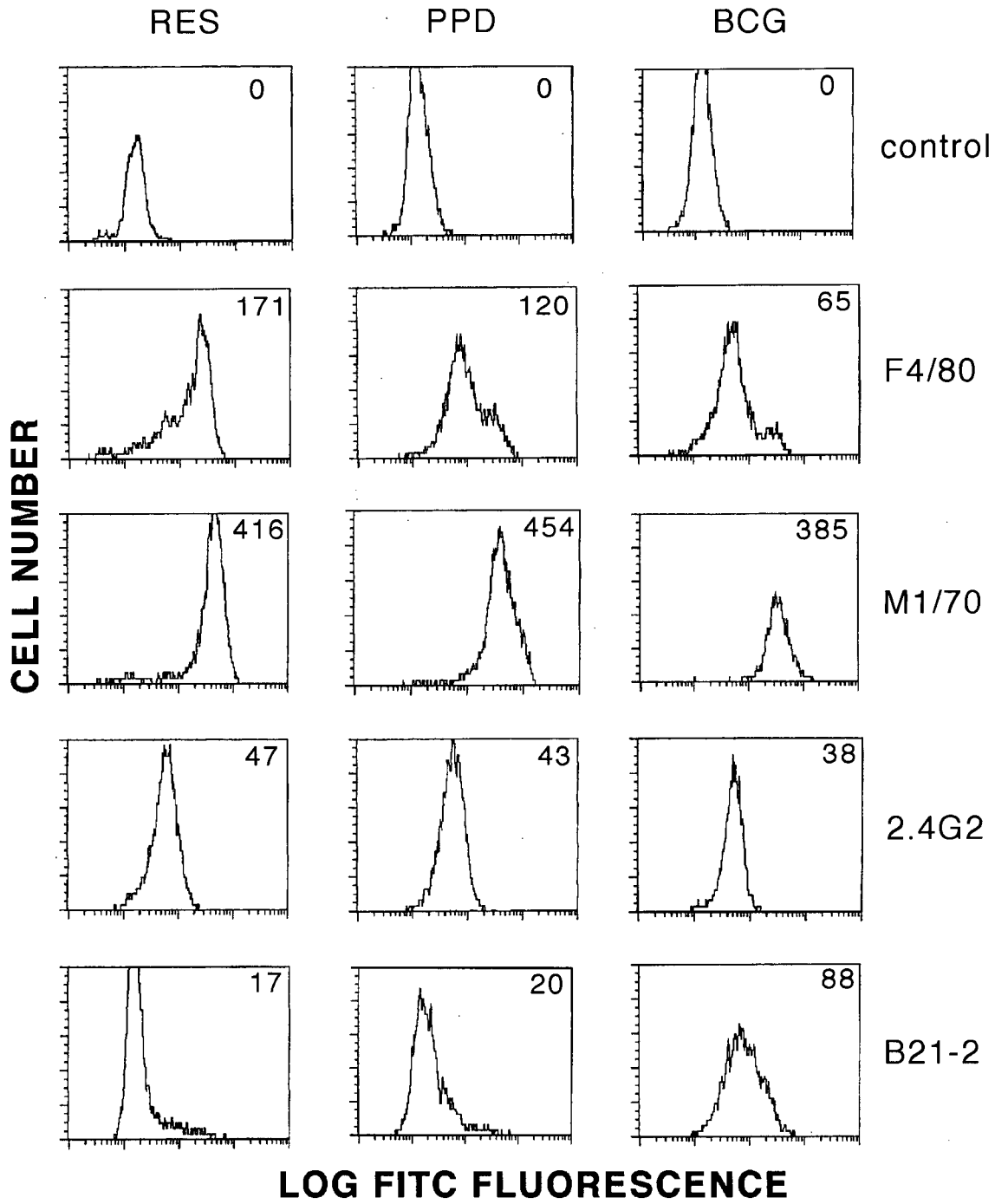

Figure 28: Expression of the F4/80 molecule on PECs following BCG infection

Resident, PPD elicited, or mϕs from BCG infected mice were prepared and harvested as described in section 2.1.4. The cells were analyzed by FACS analysis with the mAbs as indicated: control, (SFR8-B6), F4/80 (F4/80 molecule), M1/70 (CD11b), 2.4G2 (FcRγII), and YN1/1 (ICAM-1). Samples were fixed in paraformaldehyde and analyzed with the same fluorescence settings for all samples on a FACScan (Becton Dickinson). Live cells were selected by gating with FSC and SSC. The values shown for each mAb are the MLF values after subtraction of the control mAb MLF. The log fluorescence axes each range from 1 to 10,000 fluorescence units.

4.2.2 Molecular characterization of the F4/80 molecule

With clear sources of the F4/80 molecule identified, the molecule was characterized at a molecular level. The characterization of the F4/80 molecule's biochemical nature including its transport and post-translational modifications is presented in Section 4.2.2 . The purification of the F4/80 molecule and attempted peptide sequencing are presented in Section 4.2.3.

4.2.2.1 Cell surface F4/80 molecule

Our initial analysis of the F4/80 molecule by cell surface labeling and immunoprecipitations agreed with previous studies showing an Mr of 160 kDa under reducing conditions in SDS-PAGE (264). However, in contrast to previous reports (264), under non-reducing conditions cell-surface F4/80 molecule had an apparent Mr of 130 kDa which indicated the presence of extensive intramolecular disulfide bonding (Figure 29). This relatively simple and clear observation, at odds with other published data, spurred the re-investigation of certain aspects of the original F4/80 molecule characterization (264,354).

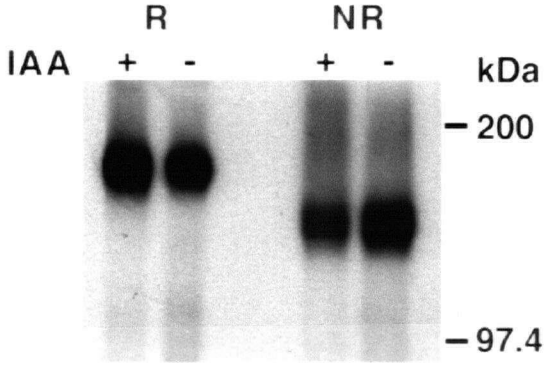

Figure 29: SDS-PAGE analysis of cell surface F4/80 molecule

PECs were cell surface biotinylated and lysed in NP-40 in the presence or absence of 5 mM IAA. The F4/80 molecule was immunoprecipitated using 2 x 10^6 cells per lane and prepared for electrophoresis with or without 30 mM DTT followed by 80 mM IAA final concentration. The samples were subsequently separated by 5-15 % SDS-PAGE and blotted to a PVDF membrane. Biotinylated proteins were detected with SA-HRPO and ECL detection.

4.2.2.2 Transport kinetics of the F4/80 molecule

4.2.2.2.1 Endo H analysis

The intracellular transport kinetics of the F4/80 molecule (Figure 30) confirmed the synthesis of a 110 kDa immature form (354), demonstrated a $T_{½}$ of 60 minutes, and in addition provided several new insights. It is known that N-linked carbohydrates initially undergo trimming of the initial glucose residues and certain core Man residues in the ER which results in a slight decrease in Mr over time before the addition of further carbohydrates (153). This process was evident for the F4/80 molecule precursor (Figure 30, minus Endo H). Treatment of the immunoprecipitated F4/80 molecule with Endo H removes the immature N-linked carbohydrates. Following Endo H treatment, the precursor F4/80 molecule increased in molecular mass during transport in contrast to the observation without Endo H treatment. This result gave the first clue that modifications in addition to N-linked carbohydrate processing were occurring. Endo H digestion reduced the precursor form of the F4/80 molecule to an apparent molecular mass of 85-90 kDa, which indicated that up to half of the mature F4/80 molecule 160 kDa molecular mass consisted of post-translational modifications.

4.2.2.2.2 Effect of Tunicamycin

The large degree of glycosylation added from the immature to the mature form of the F4/80 molecule, indicated that N-linked glycosylation plays an important role in the F4/80 molecule's overall nature. The long $T_{1/2}$ of 60 minutes for transport, also suggested that the F4/80 molecule folding occurs slowly, possibly due to the extensive disulfide bonding. Since misfolded proteins are often retained in the ER (363,365), the inhibition of N-linked glycosylation can affect protein transport (153). Tunicamycin inhibits the transfer of the core glycan from the dolichol phosphate donor to the peptide backbone, thus resulting in protein

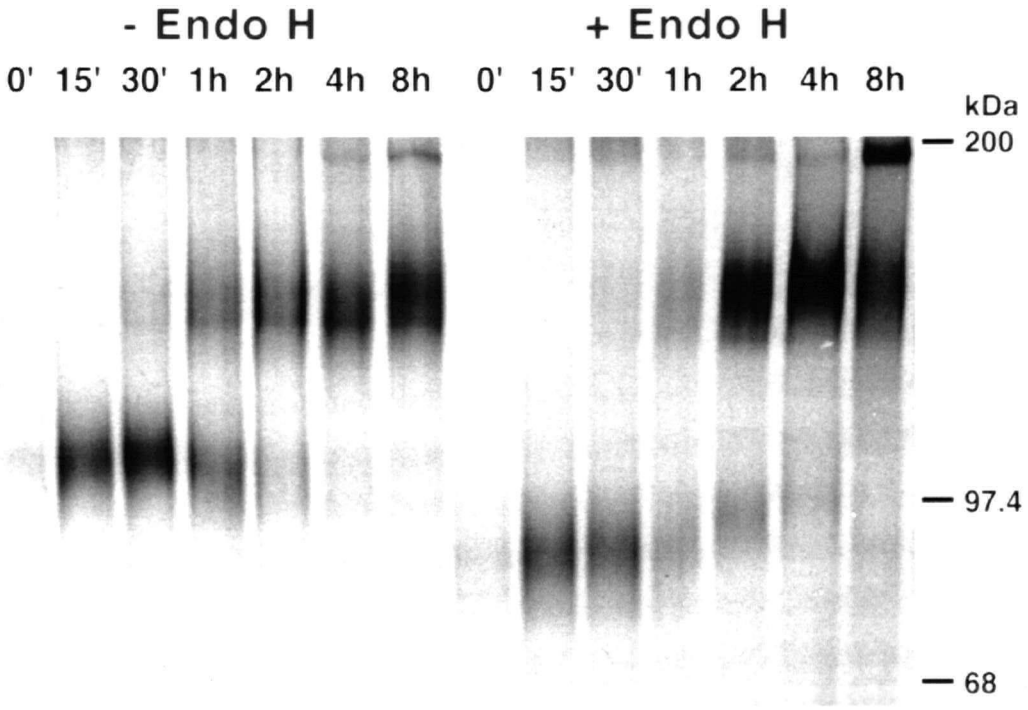

Figure 30: Transport of the F4/80 molecule

PECs were pulsed for 15 minutes with [^{35}S]-Met-Cys and chased with cold medium for the times indicated before the cells were lysed. The F4/80 molecule was immunoprecipitated from detergent lysates of 3 x 10^6 cells at each time point. The immunoprecipitated proteins were next incubated for 20 hours in the presence or absence of Endo H. The proteins were separated by 5-15% SDS-PAGE and the gel was prepared for fluorography. The film was exposed to Kodak-XAR film for 8 days.

backbones without N-linked glycans (366). The transport of the F4/80 molecule was completely inhibited in cells treated with tunicamycin (Figure 31). This supported the supposition that the N-linked carbohydrates are important for the correct folding and subsequent transport of the F4/80 molecule. The F4/80 molecule can still be immunoprecipitated from tunicamycin treated cells, although in much lower quantities than in untreated cells. The apparent molecular mass of 85-90 kDa for the F4/80 molecule from tunicamycin treated cells, parallels the apparent mass following Endo H digestion of the precursor (Figure 30). Therefore, the protein core of the F4/80 molecule is likely 85-90 kDa in molecular mass.

Figure 31: Effect of tumicamycin on the transport of the F4/80 molecule

PECs were pretreated with or without 7 μg/ml tunicamycin in complete tissue culture medium for 1 hour. The medium was then removed and medium minus Met and Cys was added to the cells with or without tunicamycin for 1 hour. PECs were next pulsed for 15 minutes with [^{35}S]-Met-Cys with or without tunicamycin and chased with complete medium with or without tunicamycin for the times indicated before the cells were lysed. The F4/80 molecule was immunoprecipitated from detergent lysates of 2 x 10^6 cells at each time point. A control mAb (SFR8-B6) was also used to indicate non-specific protein immunoprecipitation. The proteins were separated by 5-10% SDS-PAGE and the gel was prepared for fluorography. The film was exposed to Kodak-XAR film for 14 days.

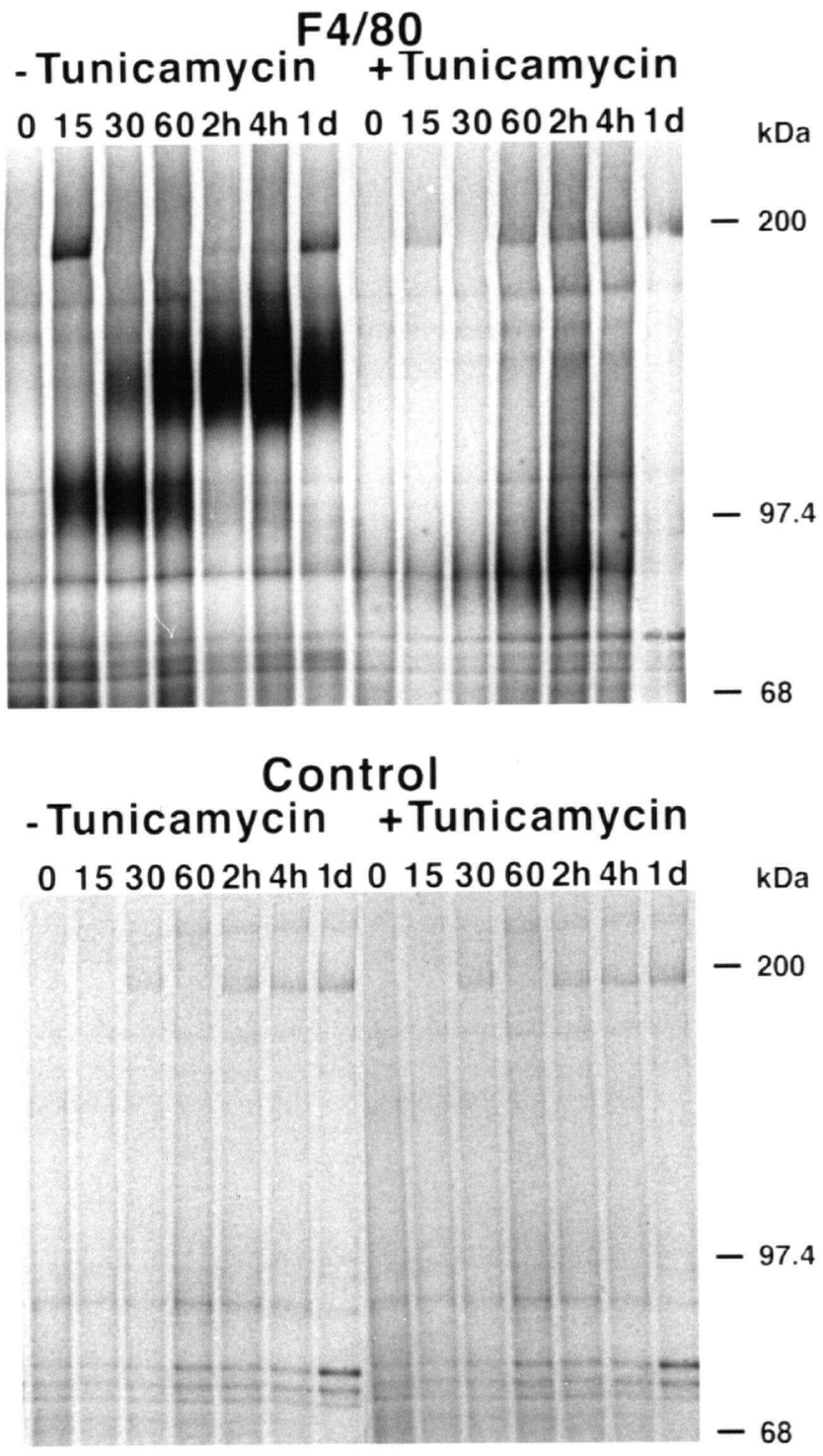
F4/80
-Tunicamycin
+Tunicamycin
0 15 30 60 2h 4h 1d 0 15 30 60 2h 4h 1d
kDa
200
97.4
68
Control
-Tunicamycin
+Tunicamycin
0 15 30 60 2h 4h 1d 0 15 30 60 2h 4h 1d
kDa
200
97.4
68

4.2.2.3 N-linked carbohydrate analysis

To further analyze the N-linked carbohydrates of the mature F4/80 molecule, the F4/80 molecule was immunoprecipitated from cell surface labeled cells and digested with PNGase F. PNGase F removes almost all forms of N-linked carbohydrates by cleaving the linkage between the asparagine residue and the first GlcNAc (367). PNGase F digestion decreased the apparent molecular mass of the F4/80 molecule by 40 kDa-50 kDa to 120 kDa under reducing SDS-PAGE conditions and 80-90 kDa in non-reducing conditions (Figure 32). Therefore, the N-linked carbohydrates of the F4/80 molecule constitute a significant component of the mature molecule, but do not entirely account for the difference in the observed mature molecular mass of 160 kDa and the protein core apparent molecular mass of 85-90 kDa.

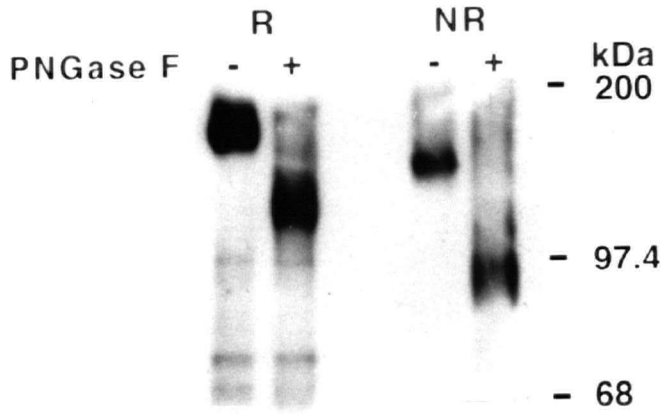

Figure 32: PNGase F digestion of the F4/80 molecule

PECs were cell surface biotinylated, lysed, and immunoprecipitated with the F4/80 mAb. The immunoprecipitates were treated with or without PNGase F for 12 hours at 37° C. The proteins were separated by 5-15% SDS-PAGE, blotted to a PVDF membrane, and detected with SA-HRPO and ECL detection. Lysate from 1 x 10^6 cells was used for each lane.

4.2.2.4 O-linked carbohydrate analysis

To examine the possibility that O-linked carbohydrate addition is one of the modifications, immunoprecipitated F4/80 molecule was analyzed with O-glycosidase. The presence of SA on the F4/80 molecule was also evaluated since O-glycosidase requires the prior removal of SAs from O-linked side chains for cleavage of the O-linked carbohydrates (368). Removal of SAs with neuraminidase treatment of the F4/80 molecule resulted in a decrease of 10-15 kDa. Treatment with O-glycosidase caused a further 5-10 kDa decrease in the molecular mass of the F4/80 molecule (Figure 33). Similar results were obtained for the F4/80 molecule immunoprecipitated from the RAW 309 Cr.1 mϕ cell line and from PECs (data not shown). These data indicate that O-linked carbohydrates constitute a portion of the post-translational modifications of the F4/80 molecule.

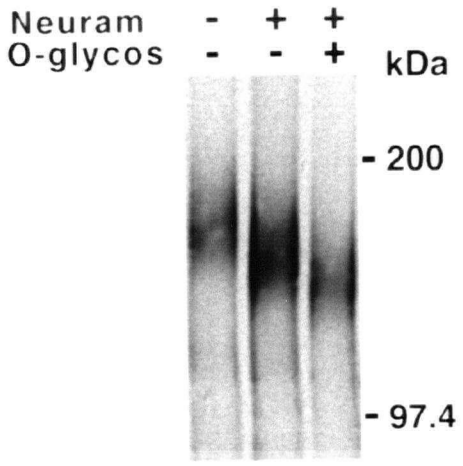

Figure 33: O-glycosidase and neuraminidase digestion of the F4/80 molecule

RAW 309 Cr.1 cells were labeled with [^{35}S] Met-Cys for 18 hours and lysed. The F4/80 molecule was immunoprecipitated from 1 x10^6 cells per lane and incubated with or without *Vibrio cholera* neuraminidase (Neuram) for 2 hours at 37°C followed by incubation with or without O-glycosidase (O-glycos) for 12 hours at 37°C. The proteins were separated by 5-10 % SDS-PAGE. The gel was prepared for fluorography and exposed to Kodak XAR film for 40 hours.

4.2.2.5 Sialic acids of the F4/80 molecule

4.2.2.5.1 Nature of the SA modification

Since α2,6 and α2,3 linkages of SA to oligosaccharides have been implicated in specific binding phenomena involving CD22 and sialoadhesin, respectively (171,172), the nature of the SA linkages of the F4/80 molecule were investigated. In order to delineate the nature of the SA linkages of the F4/80 molecule, immunoprecipitated F4/80 molecule was digested with *Vibrio cholera* or NDV neuraminidase and analyzed by Western blotting with biotinylated RCA lectin to

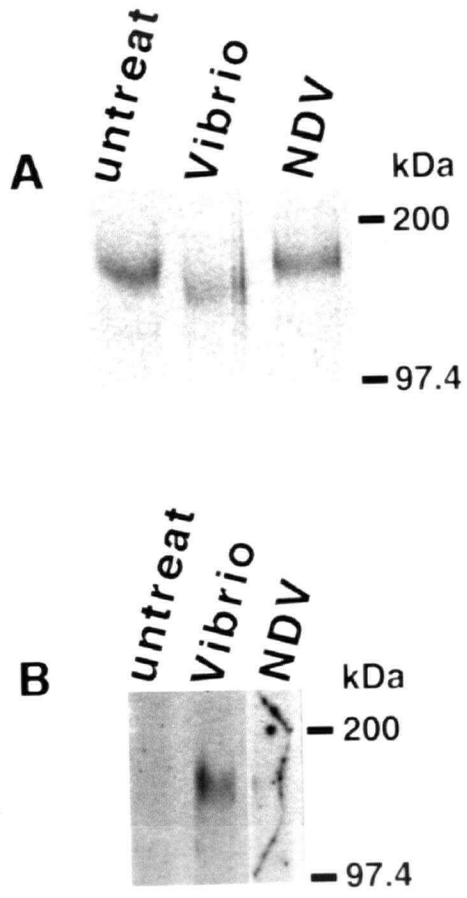

Figure 34: Determination of the nature of the sialic acid modifications on the F4/80 molecule

A) PECs were labeled with [^{35}S] Met-Cys for 18 hours and lysed. The F4/80 molecule was immunoprecipitated from 8 x 10^5 cells per lane and incubated with or without *Vibrio cholera* or NDV neuraminidases for 2 hours at 37°C. The proteins were separated by 7.5 % SDS-PAGE, blotted to a PVDF membrane, and exposed to film for 22 hours. B) To detect terminal Gal residues the PVDF membrane from A) was blotted with biotinylated RCA. Following incubation with SA-HRPO, the RCA binding was detected by incubation with SA-HRPO and ECL

detect the presence of terminal Gal residues. *Vibrio cholera* neuraminidase exhibits a broad specificity for α2-3, α2-6, and α2-8 linked SAs whereas NDV neuraminidase will cleave only α2-3 and α2,8 linked SAs (369). The *Vibrio cholera* neuraminidase was able to remove SAs from the F4/80 molecule as indicated by the decreased apparent molecular mass and the exposure of RCA binding sites. The NDV neuraminidase caused neither a decrease in the apparent mass or exposure of terminal Gal residues. This indicates that the SAs of the F4/80 molecule are not linked α2-3 or α2-8 to Gal. Therefore, the majority of SAs on the F4/80 molecule are likely α2-6 linked to Gal.

4.2.2.6 Lectin binding profile of the F4/80 molecule

4.2.2.6.1 Binding of lectins to immobilized F4/80

To obtain an indication of the specific nature of the carbohydrate structures on the F4/80 molecule, a panel of biotinylated lectins was utilized to Western blot immunoprecipitated F4/80 molecule (Figure 35). The two lectins which exhibited the strongest reactivities to the F4/80 molecule are the PHA-E lectin (lane 1) and the DS lectin (lane 10). PHA-E reactivity is determined by specificity for the sequence Galβ1-4GlcNAcβ1-2Manα1-6Man. The DS lectin recognizes β1-4 linked GlcNAc oligomers or N-acetyllactosamine units (370,371). Minor reactivity of the F4/80 molecule with the *Pisum sativum* lectin (lane 4) and the *Lens culinaris* lectin (lane 5) indicated the presence of α-linked Man residues, likely retained from the core N-linked oligosaccharide. PHA-L reactivity with the F4/80 molecule was weakly detectable (lane 2). No other lectin exhibited reactivity with the F4/80 molecule, which indicated the absence of detectable amounts of αlinked GlcNAc (lane 3), GalNAc (lanes 6 and 7), terminal Gal (lane 8), and Fuc (lane 9). Previous studies have

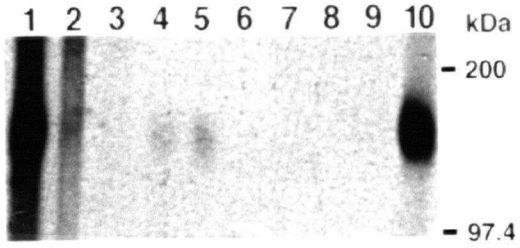

Figure 35: Lectin binding profile of the F4/80 molecule

The F4/80 molecule was immunoprecipitated from 6 x 10^5 PECs per lane, separated by 7.5 % SDS-PAGE, and blotted to a PVDF membrane. A panel of biotinylated lectins was used to blot the immobilized F4/80 molecule, followed by SA-HRPO and ECL. The lectins shown in the respective lanes are: 1) *PHA-E*, 2) *PHA-L*, 3) *Bandeirea simplificifolia* lectin I, 4) *Pisum sativum*, 5) *Lens culinaris*, 6) *Dolichus biflorus* agglutinin 7) *Vicia villosa* lectin 8) *RCA* 9) *Ulex europaeus* agglutinin I 10) DS *lectin*.

demonstrated that DS lectin reactivity in 90% of cases is associated with branched complex type N-linked carbohydrates (372). Longer exposures also detected the interaction of DS with the 110 kDa F4/80 molecule precursor (not shown). Therefore, the minimal recognition structure for DS binding is formed in the medial-Golgi before the further addition of glycans.

4.2.2.6.2 Behavior of the F4/80 molecule in *Datura stramonium* affinity chromatography

The binding of the F4/80 molecule to the DS lectin was further investigated by DS lectin chromatography. The affinity of binding of a molecule to the DS lectin is greater with a larger number of repeating β1-4 GlcNAc units and even higher if branched glycans with β1-4 linked GlcNAc are present (370). If branched glycan structures were present on the F4/80 molecule, elution of the molecule with 3'-3'-3'-3'-N-tetraacetylchititetrose would not be possible. Therefore, further details

of the structural nature of the F4/80 molecule's N-linked carbohydrates would be obtained. In all experiments attempted, the F4/80 molecule could not be competitively eluted from the DS lectin column. A representative experiment is displayed in Figure 36. The 3'-3'-3'-3'-N-tetraacetylchititetrose at 20 mM was unable to elute the F4/80 molecule bound to the DS lectin. Following the elution with 3'-3'-3'-3'-N-tetraacetylchititetrose, the DS-Sepharose beads were eluted with pH 11.5 elution buffer to demonstrate that the F4/80 molecule had remained bound. This information further supported the presence of multi-antennary N-linked carbohydrates in the F4/80 molecule since multi-antennary N-linked ligands of the DS lectin exhibit 100-1000 fold greater affinity for the DS lectin than for linear GlcNAc oligomers (370). The decrease in F4/80 molecule recovery from the mAb alone versus the mAb plus DS Sepharose column, likely represented losses during washes, since prior experiments did not detect the F4/80 molecule in the non-binding fraction following DS lectin chromatography. The apparent decrease in recovery in the pH 11.5 elutions possibly represented additional loss during washing steps and inefficient elution since only one round of the pH 11.5 elution was performed in this experiment. Often two rounds of pH 11.5 elution were necessary for the small volumes used prior to gel electrophoresis (see Figure 45 for an indication of the efficiency of one versus two pH 11.5 elutions).

Figure 36: *Datura stramonium* chromatography of the F4/80 molecule

The F4/80 molecule was immunoprecipitated from RAW 309 Cr.1 cell lysate following 18 hour labeling with [^{35}S]-Met-Cys. $5x10^5$ cell equivalents were used for each lane. The samples were immunoprecipitated with F4/80-Sepharose and eluted with 30 µl of 0.5% C_8Glc, 50 mM DEA, pH 11.5. For subsequent binding of the eluate to DS-Sepharose, the eluates were neutralized and NP-40 lysis buffer was added to 150 µl. Following binding for 2 hours at 4°C, the DS-Sepharose samples were washed as described in Section 2.2.7. The DS-Sepharose beads were eluted with two separate additions of 15 µl of 3'-3'-3'-3'-N-tetraacetylchititetrose at the indicated concentration. Following the carbohydrate elution, the beads were washed once with one ml of 10 mM Tris pH 7.5 and eluted once with 15 µl pH 11.5 buffer. The eluates at all steps were prepared for electrophoresis and proteins separated on a 5-10 % gradient SDS-PAGE gel. The gel was prepared for fluorography and exposed to Kodak XAR film for 5 days.

4.2.2.7 Labeling of the F4/80 molecule by $^{35}S\ SO_4$

4.2.2.7.1 Detection of $^{35}S\ SO_4$ incorporation into the F4/80 molecule

In addition to N- and O-linked carbohydrate modification of proteins, sulfate can be incorporated into glycoprotein components including via Tyr, O-linked and N-linked carbohydrates, and GAG addition (173,208,209,214). Labeling of both the RAW cell line (Figure 37) , and PECs (data not shown) with $^{35}S\ Na_2SO_4$ followed by immunoprecipitation with F4/80, clearly demonstrated that the F4/80 molecule incorporated radioactive sulfate. CD45 was not labeled indicating that the labeling with $[^{35}S]\ Na_2SO_4$ is not occurring via ^{35}S incorporation into Met or Cys. It was noticeable that the apparent molecular mass of the$[^{35}S]\ SO_4$ labeled F4/80 was higher than previously noted for the$[^{35}S]$ Met labeled F4/80 molecule. However, cell surface biotinylation of the cells following radioactive labeling, indicated that the alteration affects all F4/80 molecules, possibly due to modifications in subsequent processing during transport in the sulfate minus medium .

4.2.2.7.2 Pulse chase of the F4/80 molecule with $^{35}S\ SO_4$ labeling

The sulfation of protein moieties typically occurs in the medial to trans-Golgi apparatus where sulfatases are located (154,214). In order to assess if the F4/80 molecule's sulfation occurred past the cis-Golgi, a pulse chase was performed with $^{35}S\ SO_4$ in comparison to $[^{35}S]$-Met-Cys. The $[^{35}S]$-Met-Cys pulse chase labeling demonstrated the kinetics of F4/80 molecule transport with a $T_{1/2}$ of one hour. The labeling with $^{35}SO_4$ at time zero already showed labeling of the mature M_r form of the F4/80 molecule (Figure 38). The sulfation was, therefore, not occurring prior to the late medial-Golgi or trans-Golgi, where the F4/80 molecule undergoes conversion to the 160 kDa, Endo H^R form from the 110 kDa, Endo H^S precursor (Figure 30).

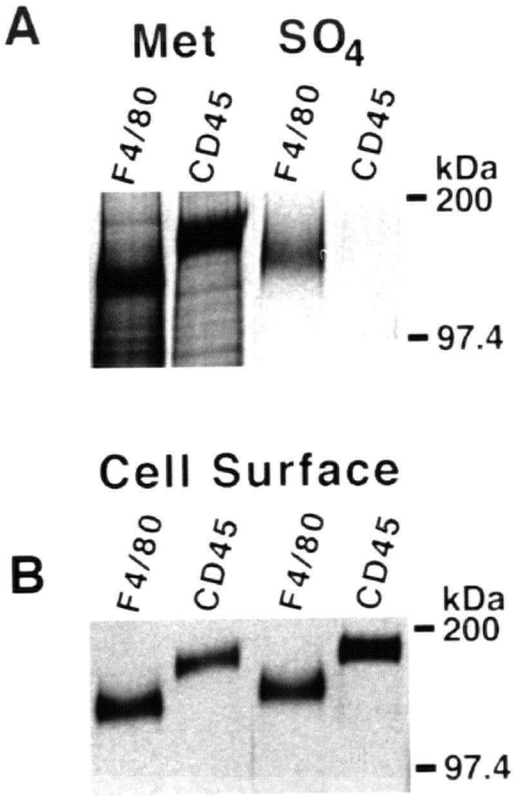

Figure 37: Labeling of the F4/80 molecule with ^{35}S SO_4

RAW 309 Cr.1 cells were labeled were labeled with $Na^{35}SO_4$ or [^{35}S] Met-Cys for 18 hours, cell surface biotinylated, and lysed. The F4/80 molecule or CD45 were immunoprecipitated from 1.5 x 10^6 cells per lane. Panel A shows the results of autoradiography following separation of the proteins by 7.5 % SDS-PAGE, blotting to a PVDF membrane, and exposure to x-ray film for 6 hours. Panel B) represents the detection cell surface labeled CD45 or F4/80 molecules after the PVDF membrane was blotted with SA-HRPO and developed with ECL.

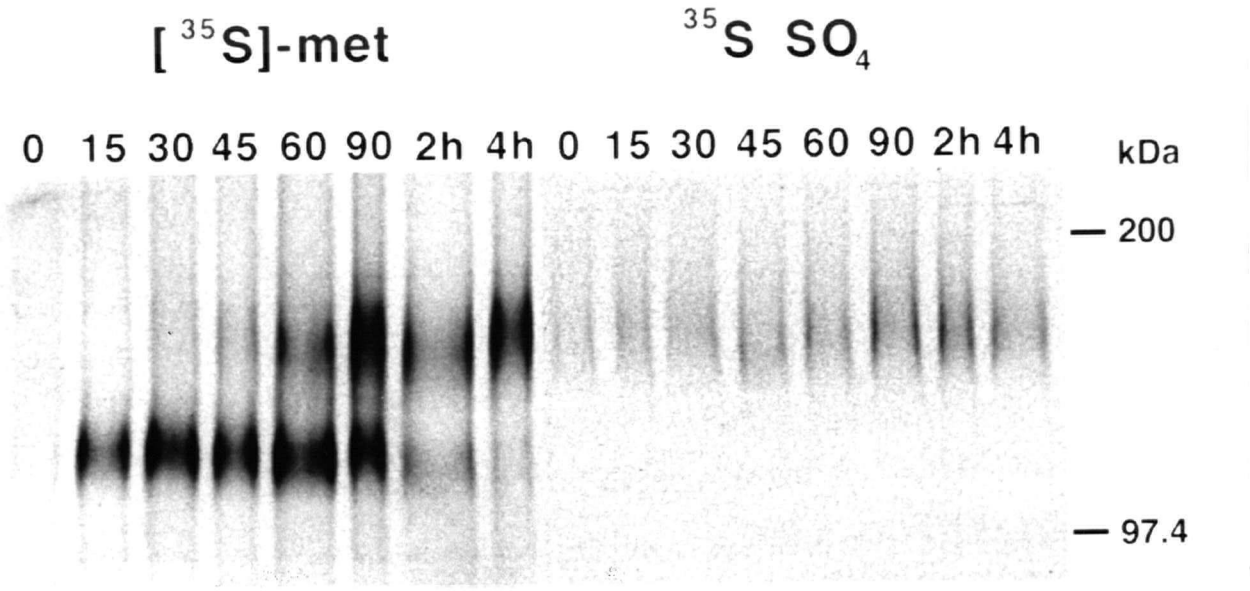

Figure 38: Pulse chase of the F4/80 molecule with ^{35}S SO_4

PECs were pulsed for 15 minutes with [^{35}S]-Met-Cys or ^{35}S Na_2SO_4 and chased with non-radioactive complete medium for the times indicated before the cells were lysed. The F4/80 molecule was immunoprecipitated from detergent lysates of 3 x 10^6 cells at each time point. The proteins were separated by 5-15% SDS-PAGE and the gels were prepared for fluorography. The gels were exposed to Kodak-XAR film for 6 days.

4.2.2.7.3 Effect of PNGase F on the ^{35}S SO_4 in the F4/80 molecule

As mentioned above, SO_4 can be added to several moieties of proteins. Since the F4/80 molecule is so highly glycosylated, it was possible that the SO_4 modification is located on the N-linked carbohydrates. To address this possibility, $^{35}SO_4$ labeled F4/80 was digested with PNGase F. The result of the PNGase F digestion showed the clear decrease in apparent molecular mass of the F4/80 molecule, but revealed no loss of the $^{35}SO_4$ label (Figure 39). Therefore, the $^{35}SO_4$ modification of the F4/80 molecule is not located in the N-linked carbohydrates.

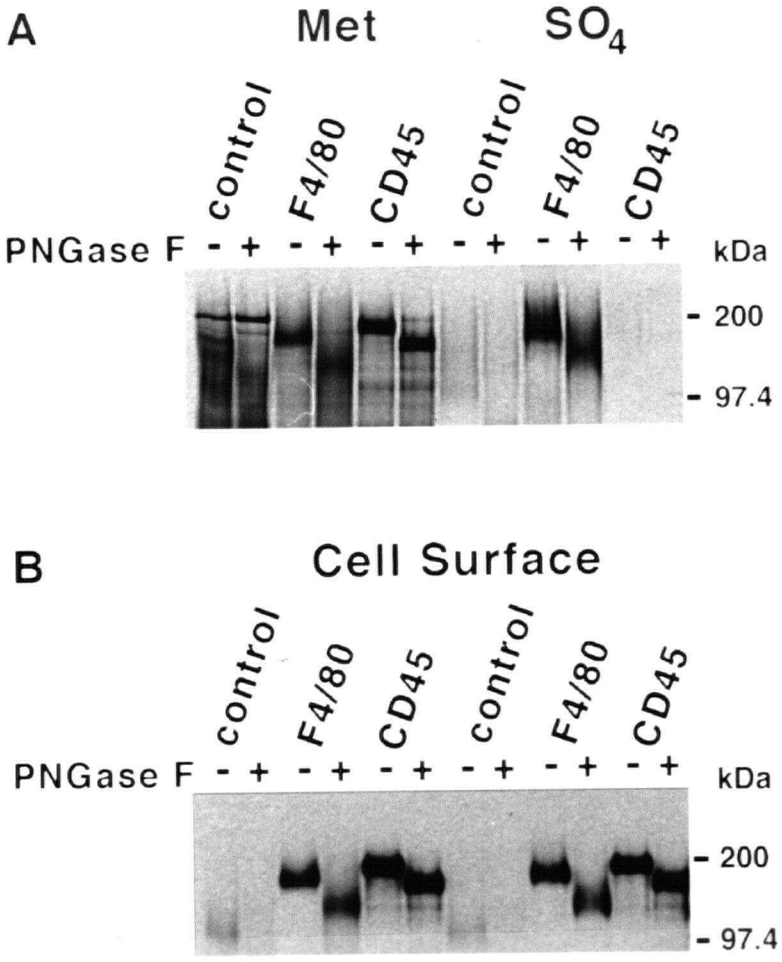

Figure 39: PNGase F digestion of ^{35}S SO_4 labeled F4/80 molecule

RAW 309 Cr.1 cells were labeled for 18 hours with $^{35}SO_4$ and subsequently cell surface labeled with biotin before lysis in NP-40 lysis buffer. $5x10^5$ cell equivalents were utilized for each immunoprecipitation with the control mAb (SFR8-B6), anti-CD45 (M1/9), or anti-F4/80 molecule (F4/80). The proteins were separated on a 7.5% SDS-PAGE, blotted to PVDF membrane, and exposed to Kodak-XAR film for 18 hours to detect $^{35}SO_4$ labeled proteins. Blotting of the membrane with SA-HRPO followed by ECL detection was utilized to localize the biotinylated proteins.

4.2.2.7.4 Effect of glycosaminoglycan lyases on ^{35}S SO_4 in the F4/80 molecule

To determine if the ^{35}S SO_4 modification of the F4/80 molecule was via GAG addition, specific hydrolases were tested for their abilities to remove the ^{35}S SO_4 modification of the F4/80 molecule. Chondroitinase ABC lyase cleaved greater than 93% of the ^{35}S SO_4 from the F4/80 molecule whereas heparitinase has no effect (Figure 40). Therefore, the GAG modification of the F4/80 molecule involves CS. The number of GAG modifications is likely minimal since the apparent molecular mass of the F4/80 molecule did not significantly change following the Chondroitinase ABC lyase treatment.

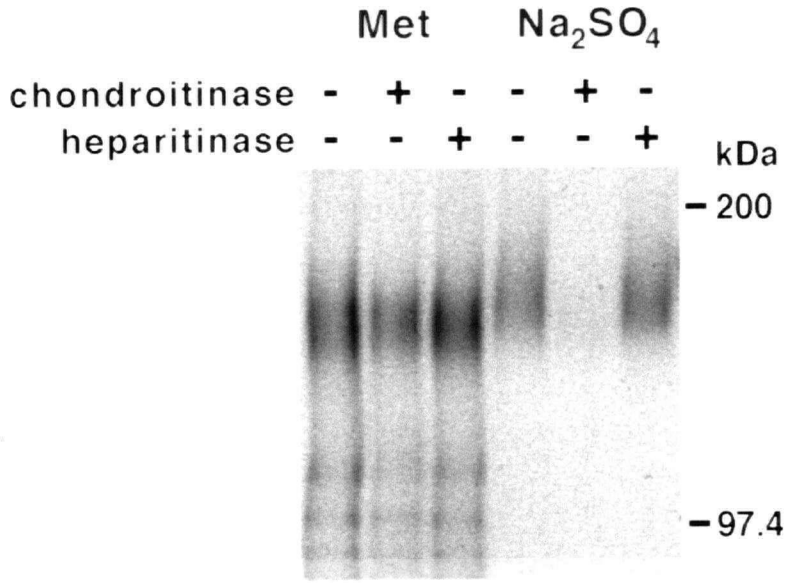

Figure 40: Digestion of the F4/80 molecule with glycosaminoglycan lyases

PECs were pulsed for 18 hours with $Na^{35}SO_4$ or [^{35}S] Met-Cys. The F4/80 molecule was immunoprecipitated from 7 x 10^5 PECs per lane and treated with Chondroitinase ABC or Heparitinase III. Following digestion the proteins were separated by 5-10 % SDS-PAGE, transferred to a PVDF membrane, and autoradiographed for 20 hours.

4.2.2.8 Isoelectric focusing analysis

Given the acidic nature of the SA and CS post-translational modifications of the F4/80 molecule, it was assumed that the molecule would have an overall negative charge. However, IEF analysis of immunoprecipitated F4/80 molecule revealed that the entire molecule has a pI of 7.5 to 8.0 (Figure 41). Thus, it appears that the F4/80 molecule is composed of a basic inner protein core surrounded by a covering of highly negatively charged SAs and GAGs.

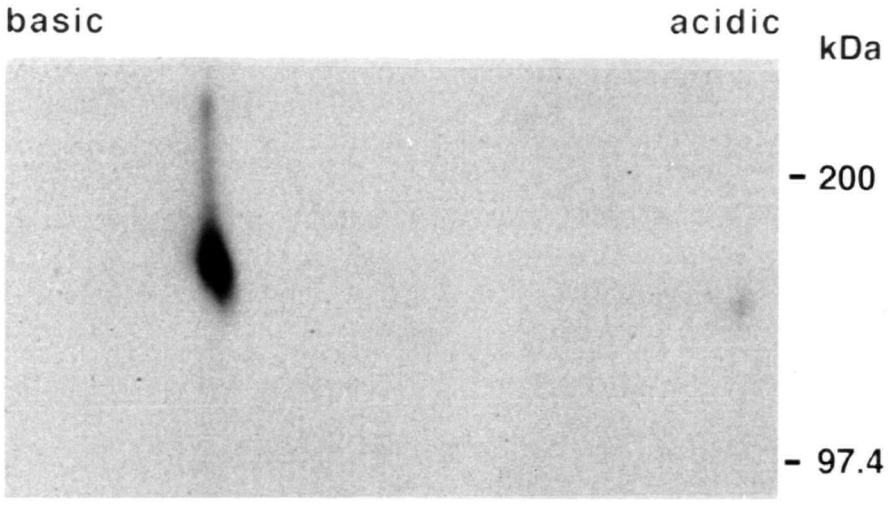

Figure 41: 2-D gel analysis of the F4/80 molecule with IEF and SDS-PAGE

PECs were labeled for 18 hours with [^{35}S] Met-Cys and lysed in NP-40 lysis buffer. The F4/80 molecule was immunoprecipitated from 2.5 x 10^5 cells and separated by IEF as described (271). The second dimension for separation was 5-10 % SDS-PAGE. The gels were prepared for fluorography and exposed to x-ray film for 14 days.

4.2.2.9 Anion exchange chromatography of the F4/80 molecule

The basic nature of the F4/80 molecule contrasts with the acidic nature of the CS and sialic acid modification. Since the IEF analysis analyzes the denatured molecule, the possibility that the native molecule's physical charge would be governed by the external negatively charged modifications was considered. PECs were labeled with [^{35}S]-Met-Cys and lysed in lysis buffer,

but with zero NaCl and at pH 9.0. This lysate was then loaded onto a Mono Q column, a quaternary amine anion exchange resin. The elution profile and distribution of the F4/80 molecule are displayed in Figure 42. The majority of the lysate clearly bound to the MonoQ column. The majority of the proteins (52%) eluted between 0.2 and 0.3 M NaCl which were fractions 13 to 19. The F4/80 molecule did not begin to elute until fraction 18 and continued until fraction 26. The most significant fraction of the F4/80 molecule did not elute until 1.0 M NaCl in fractions 52 to 58. The discrepancy in the two regions of F4/80 molecule elution may be due to heterogeneity in the molecule's post-translational modifications. Even amongst CS chains, the number of SO_4 residues can vary between an average of 0.2 and 2.3 SO_4 residues per disaccharide unit. This difference would drastically change the charge characteristic of the protein. Sialylation differences could also account for the heterogeneity. Although the IEF result (Figure 41) has been repeated several times, no significant heterogeneity has been consistently noted. A diffuse separation of the proteins throughout the IEF, would leave only the major glycoform as that detected by IEF. Attempts to remove the CS or SA moieties has produced technical difficulties with focusing of the F4/80 molecule. Regardless, the binding of the F4/80 molecule to the anionic column, underlines the fact that the F4/80 molecule is covered with acidic modifications.

4.2.2.10 Structure of the extracellular domains of the F4/80 molecule

Previous studies of the F4/80 molecule (264,354) had demonstrated the presence of a protease sensitive site in the extracellular domain. Limited protease cleavage produced a 100 kDa fragment suggesting that a minimum of 60 kDa of the F4/80 molecule is situated extracellularly. In

Figure 42: Analysis of the F4/80 molecule by anion exchange chromatography

The F4/80 molecule detergent was solublized in detergent in the absence of NaCl at pH 9.0. The cell lysate from $4x10^6$ cells was loaded onto a MonoQ column in lysis buffer (zero M NaCl, pH 9.0). The F4/80 molecule was eluted with a gradient of NaCl from zero to 1.0 M NaCl and 1.0 ml fractions were collected. A) The cpm from each fraction and NaCl concentration were calculated and plotted for each fraction. B) The F4/80 molecule was immunoprecipitated from the even numbered fractions and separated on 7.5% SDS-PAGE. The gels were prepared for fluorography and exposed to Kodak XAR film for 30 days.

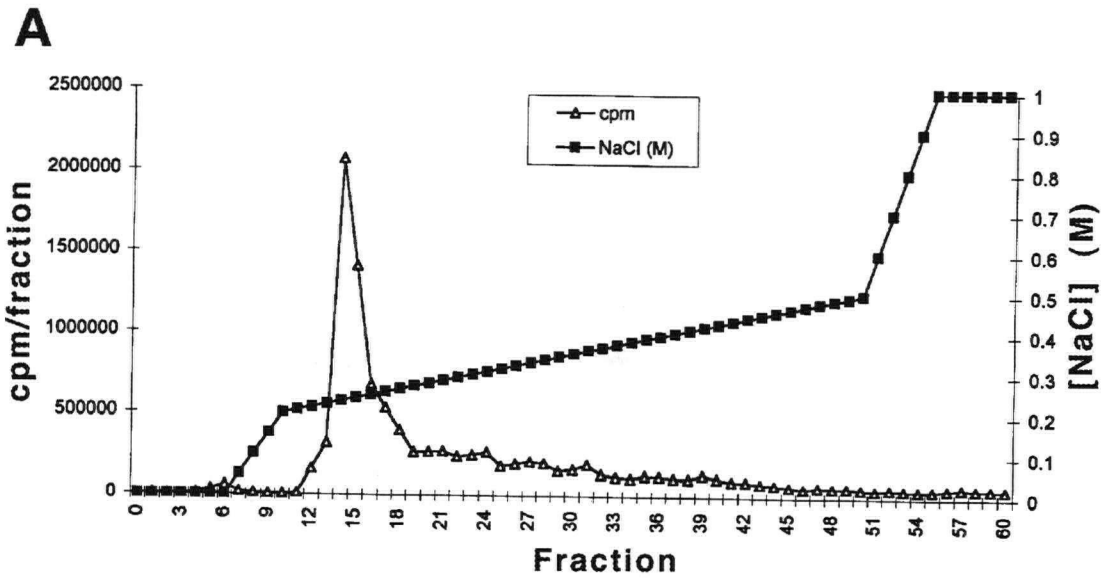
A
2500000
2000000
1500000
1000000
500000
0
cpm/fraction
cpm
NaCl (M)
1
0.9
0.8
0.7
0.6
0.5
0.4
0.3
0.2
0.1
0
[NaCl] (M)
0 3 6 9 12 15 18 21 24 27 30 33 36 39 42 45 48 51 54 57 60
Fraction

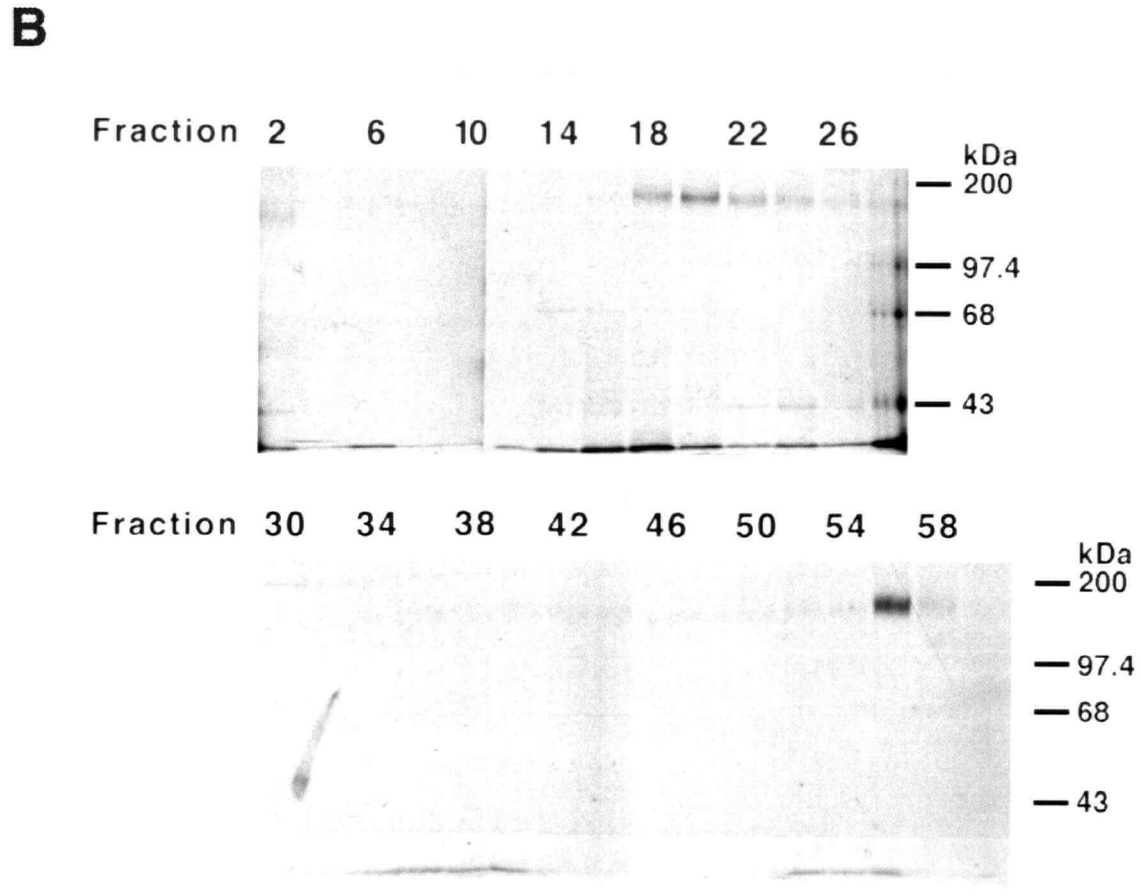
B
Fraction 2 6 10 14 18 22 26
kDa
200
97.4
68
43
Fraction 30 34 38 42 46 50 54 58
kDa
200
97.4
68
43

order to localize the CS attachment site, trypsin digestion on $^{35}SO_4$ labeled F4/80 molecule was performed. For comparative purposes cells after cell surface labeling with sNHS-biotin which labels Lys residues, and biotin hydrazide which primarily labels the SA residues under the conditions used were also trypsinized. The cleavage of the F4/80 molecule by trypsin is evident in the first 5 minutes of digestion (Figure 43). Similar results were obtained if the SDS-PAGE analysis utilized non-reducing conditions. The absence of any $^{35}SO_4$ labeled 100 kDa fragment, localizes the CS modification to the membrane distal 60 kDa region of the F4/80 molecule. The labeling of SAs and protein with biotin before trypsinization, indicates that the trypsin resistant domain retains a percentage of the glycosylation. Thus, the glycosylation of the F4/80 molecule is throughout the extracellular domain and not clustered in one region. The relative amount of glycosylation in the 100 versus 60 kDa fragments could not be determined since the 100 kDa fragment is degraded or becomes non-reactive with the F4/80 mAb with extended trypsin digestion time ((354) and Figure 43).

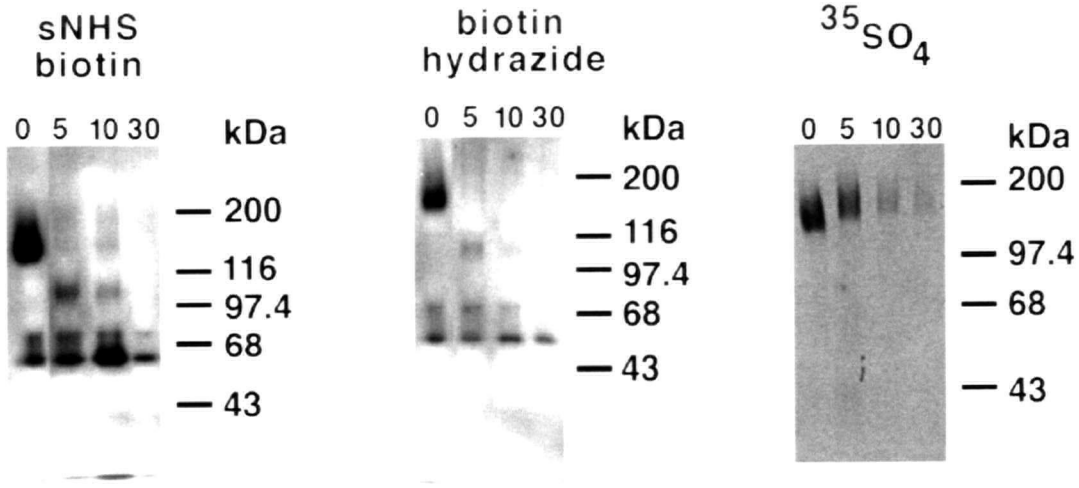

Figure 43: Trypsin digestion of the F4/80 molecule reveals the location of the molecule's post-translational modifications

RAW 309 Cr.1 cells were labeled for 18 hours with $^{35}SO_4$, sNHS biotin, or biotin hydrazide as described in Sections 2.2.4.2, 2.2.2, and 2.2.3. Following labeling, the cells were washed twice in PBS and incubated with 0.05% trypsin in 1.0 mM EDTA, for the times indicated. The trypsin was inactivated by washing twice with complete tissue culture medium at 4°C. The cells were lysed in lysis buffer plus PMSF. Lysate equivalent to $5x10^5$ cells per lane was used for immunoprecipitation of the F4/80 molecule. The samples were separated by 7.5% SDS-PAGE in reducing conditions and blotted to PVDF membranes. The $^{35}SO_4$ labeled proteins were detected by autoradiography with Kodak XAR film for 29 hours. The biotinylated proteins were detected by blotting with SA-HRPO followed by ECL detection and exposure to Kodak XAR film.

4.2.3 Purification of the F4/80 molecule

4.2.3.1 Strategy and rationale

The cloning of the cDNA for the F4/80 molecule was the initial goal after commencing work on this molecule. Given the power of expression cloning (362), cDNA cloning with the COS cell expression system and selection of clones reactive with the F4/80 mAb was initially attempted. Although other cDNAs could be cloned with expression cloning, this method was not successful for the F4/80 molecule which then prompted the molecular characterization described in Section 4.2.2. The first observations were with respect to the high degree of N-linked glycosylation (Figure 32). One limitation of the COS cell expression system is the assumption that the mAb epitope will be present in the molecule expressed in COS cells. Glycosylation can vary between different cell types which can affect epitopes dependent on the carbohydrates themselves or protein epitopes that are dependent on the carbohydrates during protein folding. In the expression cloning of human CD22, Stamenkovic and Seed noted that of the 5 epitopes recognized by a panel of mAbs, only two were maintained in COS cell expressed CD22 (373). Since there was only one mAb to the F4/80 molecule, the potential existed that COS cell expressed F4/80 molecule would not be recognized by the mAb. For this reason the strategy to pursue the purification of the F4/80 molecule was altered.

The purification of cell surface molecules and the production of peptides for sequencing has been a well characterized and efficient means of characterizing cell surface proteins (274). The design of degenerate oligonucleotides from the amino acid sequence can be used to screen cDNA libraries to isolate cDNA clones for the purified protein.

The single most important consideration in purifying a protein is to establish a reliable source of large amounts of the protein of interest. The current protein sequencing technology can normally obtain N-terminal sequence from 10 pmol of protein or peptides. In the production of internal peptides for sequencing, significantly more protein is required as starting material due to losses during peptide production and purification. Even under optimized conditions it is estimated that only 10 to 20% of the starting material is recovered for biochemical work (274). In order to obtain 100 pmol of protein, $6.02x10^{13}$ F4/80 molecules (from Avagadro's number: $6.02x10^{23}$ molecules/mol) would be required. Assuming an expression level of 25,000 molecules per cell by relating the F4/80 FACS to the expression levels of other molecules (Figure 25 and Figure 27), $2.4x10^{9}$ cells would be required if 100% recovery was attained. If the percent recovery was in the 10-20% range, $2x10^{10}$ cells would be required as starting material.

4.2.3.2 Selection of the RAW 309 Cr.1 cell line for purification

The choice of a cell source for the F4/80 molecule purification was determined by the expression level of the cell type and the potential to harvest large numbers of cells. The difficulty in using cells directly from animals was the relatively small numbers of cells that can be obtained from a mouse. At most $2x10^{7}$ PECs can be obtained from a single mouse of which 1.4×10^{7} mϕs will be recovered. Therefore, even 100 mice will produce only $1.4x10^{9}$ cells. Additional sources of mϕs would include Kuppfer cells and bone marrow mϕs. However, each of these sources will produce similar numbers of cells to PECs resulting in only $5x10^{9}$ cells from 100 mice. Therefore, a mϕ cell line was chosen for the F4/80 purification. I initially chose the J774.2 cell line which had F4/80 molecule expression of two-thirds of the PEC F4/80 expression level (Figure 25 and Figure 27). However, repeated efforts to culture the J774.2 cells in large scale

cultures, resulted in the decrease of F4/80 molecule expression to one-sixth of the PEC level, a four fold decrease (not shown). Therefore, several mϕ cell lines were retested for F4/80 expression. The RAW 309 Cr.1 cell line demonstrated similar expression of the F4/80 molecule relative to PECs by FACS analysis and [^{35}S]-Met-Cys labeling (Figure 44). The properties of the F4/80 molecule from RAW 309 Cr.1 cells appeared similar in its migration in non-reducing versus reducing SDS-PAGE and the degree of N-linked glycosylation as demonstrated by PNGase F digestion (Figure 44). In this particular experiment, the increased migration in non-reduced SDS-PAGE was not as pronounced for the untreated F4/80 molecule, but was evident for the PNGase F treated molecule. These results clearly demonstrated that the RAW 309 Cr.1 cells were suitable for large scale purification of the F4/80 molecule. Although the culture conditions required some modification for the optimization of F4/80 molecule expression, RAW 309 Cr.1 cells could be cultured in large spinner flasks without loss of F4/80 molecule expression.

4.2.3.3 F4/80 monoclonal antibody column preparation and testing

Prior to attempting a full scale purification of the F4/80 molecule, the F4/80-Sepharose column was tested for binding of the F4/80 molecule and the efficiency of elution. Previous analysis by immunoprecipitation had established that solubilization of cells in NP-40 resulted in the most efficient recovery of the F4/80 molecule relative to other detergents or conbinations of detergents (not shown). The elution of the F4/80 molecule from the mAb-Sepharose column with C_8Glc, pH 11.5 appeared to elute almost all of the F4/80 molecule (Figure 45). The proteins were eluted by boiling in SDS-PAGE loading buffer (lane 1), with two elutions of

Figure 44: Expression of the F4/80 molecule by the RAW 309 Cr.1 cell line

B) PECs and RAW 309 Cr.1 cells were labeled with [^{35}S]-Met-Cys for 18 hours and lysed in NP-40 lysis buffer. $5x10^5$ cell equivalents were used for each immunoprecipitation with the control mAb SFR8-B6 or F4/80. Following immunoprecipitation, the proteins were incubated in the presence or absence of PNGase F for 12 hours at 37°C. The proteins were prepared for reducing (R) or non-reducing (NR) conditions and separated with 5-10% SDS-PAGE. The gel was prepared for fluorography and exposed to Kodak-XAR film for 6 days.

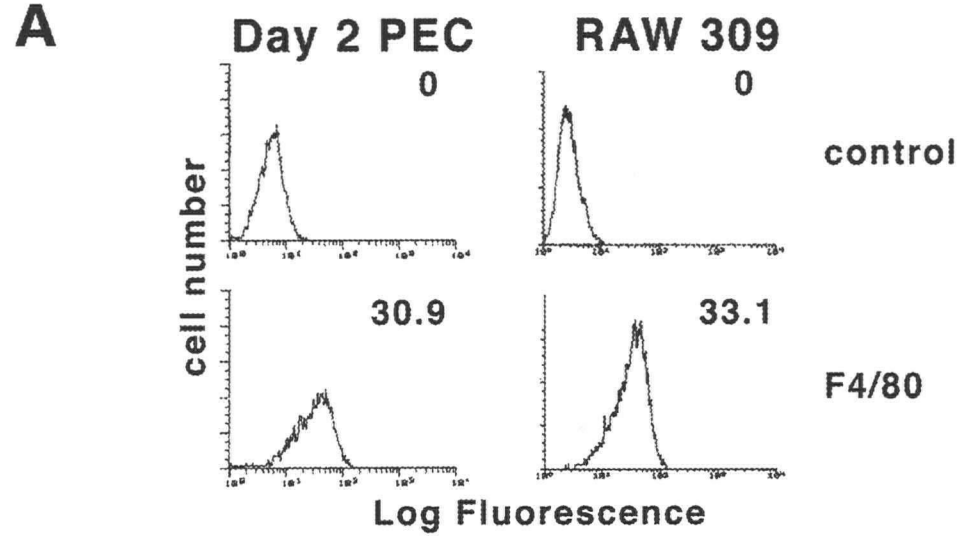
A
Day 2 PEC
RAW 309
0
0
control
cell number
30.9
33.1
F4/80
Log Fluorescence

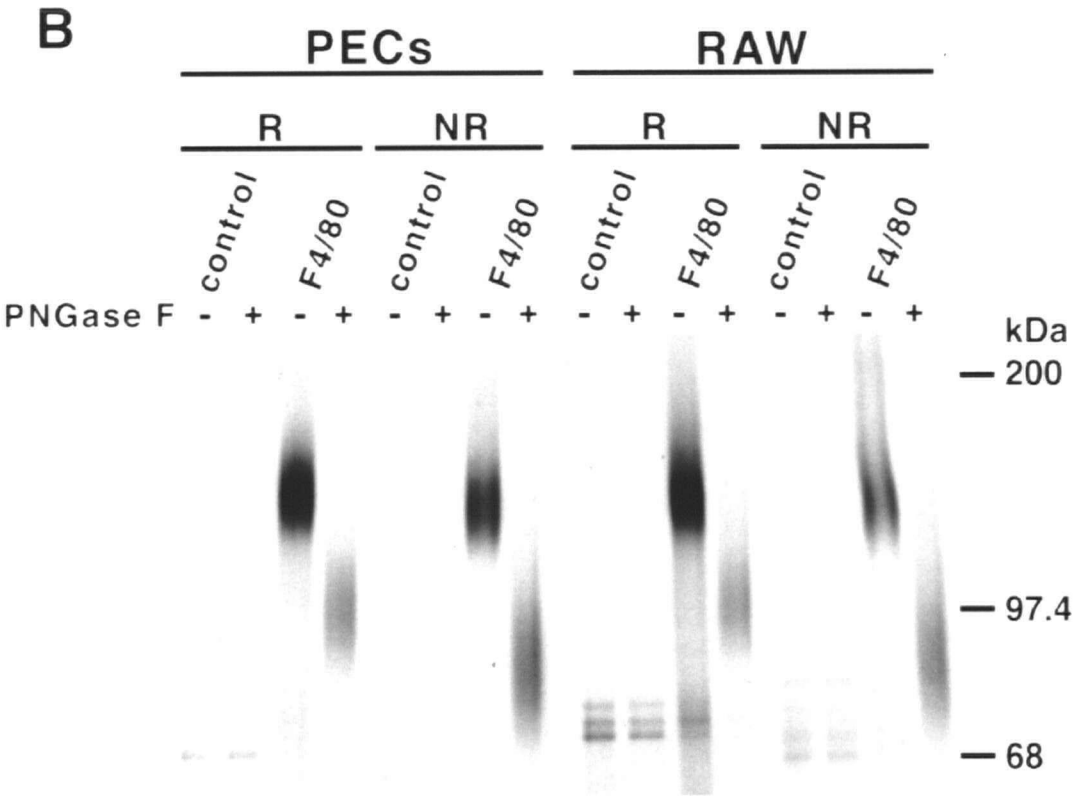
B
PECs
RAW
R
NR
R
NR
control
F4/80
control
F4/80
control
F4/80
control
F4/80
PNGase F - + - + - + - + - + - + - + - +
kDa
200
97.4
68

deoxycholate (DOC), pH 11.5 (lanes 2 and 3), or two elutions with C_8Glc, pH 11.5 (lanes 5 and 6). The pH 11.5 elutions in DOC and C_8Glc were each followed by boiling the beads with SDS-PAGE loading buffer (lanes 4 and 7 respectively). The C_8Glc elution buffer was chosen since it appeared to efficiently elute the F4/80 molecule and would interfere less than DOC with subsequent steps such as SDS-PAGE.

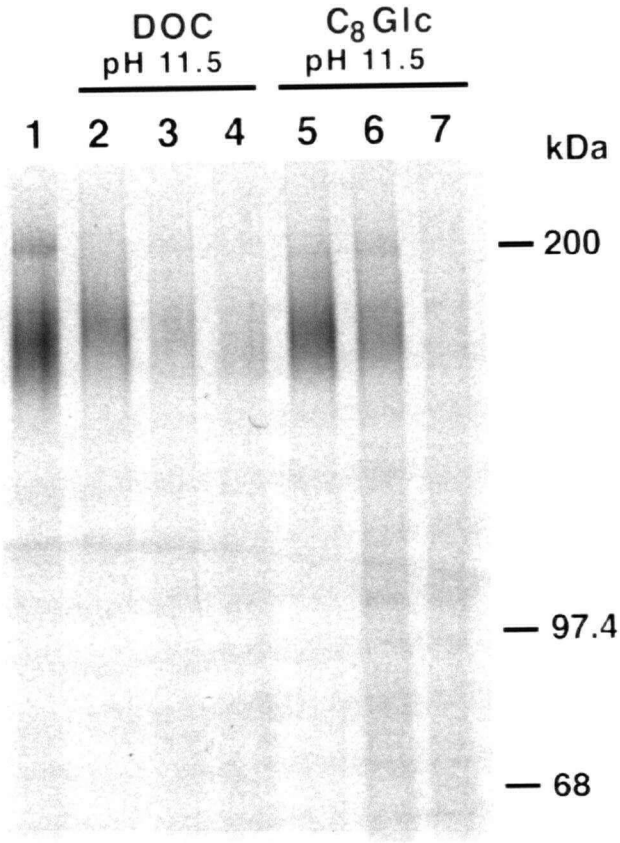

Figure 45: Testing of the F4/80 mAb column

RAW 309 Cr.1 cells were labeled 18 hours with [^{35}S]-Met-Cys and lysed in NP-40 lysis buffer. For each lane 1 x10^6 cells were used to immunoprecipitate the F4/80 molecule. The proteins were eluted by boiling in SDS-PAGE loading buffer (lane 1). Two elutions with 0.5% DOC, 50mM DEA, pH 11.5 (lanes 2 and 3) were followed by boiling the beads with SDS-PAGE loading buffer (lane 4). Similarly, two elutions with 0.5% C_8Glc, 50mM DEA, pH 11.5 (lanes 5 and 6) were followed by boiling with SDS-PAGE loading buffer. The proteins were separated with 5-10% SDS-PAGE and the gel prepared for fluorography before exposing to Kodak XAR film for 18 hours.

4.2.3.4 Peptide sequencing of the purified F4/80 molecule

The first large scale purification with the RAW 309 Cr.1 cells, utilized the F4/80 mAb column (Figure 45) and a DS-Sepharose column (Figure 36). The DS-Sepharose column appeared to eliminate many of the contaminating proteins and recover 50% of the F4/80 molecule that eluted from the F4/80 column. Therefore, the RAW 309 Cr.1 membrane lysate was passed over the F4/80 mAb column, the column washed and eluted at pH 11.5, and the eluted fractions pooled and applied to the DS-Sepharose column. The elutions from the DS column were examined by silver staining since the biotinylated DS lectin blotting was not utilized at this stage of the research project.

This purification appeared to produce significant recovery of the F4/80 molecule, as judged by the quantity of 160 kDa protein eluted from the DS-Sepharose column (Figure 46). This protein comigrates with the major [^{35}S]-Met-Cys labeled protein in fractions 2 and 3 of the DS-Sepharose elution. The differences in the [^{35}S]-Met-Cys and silver stain gels may be explained by the pooling of the [^{35}S]-Met-Cys and bulk RAW 309 Cr.1 cell lysates only prior to the F4/80 mAb column. If degradation had occurred in the bulk preparation, the [^{35}S]-Met-Cys label would not reflect this degradation. The 95 kDa and 68 kDa proteins visible by total protein staining are not detected with [^{35}S]-Met-Cys. The 95 kDa protein is similar to the F4/80 molecule fragment size after limited protease digestion (Figure 43), whereas no 68 kDa protein fragment of the F4/80 molecule was ever noted.

To test the identity of the three proteins, the 95 and 68 kDa proteins were N-terminal sequenced following separation by SDS-PAGE and blotting to PVDF membrane. The 160 kDa protein produced no signal with test N-terminal sequencing, so the remainder was prepared for O-phthalaldehyde sequencing (374). CNBr digestion of the blotted protein was carried out by

standard methods. The membrane was washed extensively with ddH_2O before sequencing by standard PITC chemistry. One third of the CNBr sample was sequenced in order to identify the first Pro residue from the mixed peptide pool. In theory, the remaining two-thirds of the sample is sequenced up to one cycle before the first Pro residue. O-phthalaldehyde will block all N-termini in the mixed peptide pool except the peptide with an N-terminal Pro. Therefore, when sequencing is restarted, only one peptide sequence will be obtained. However, the original sequencing of the 160 kDa protein CNBr digest produced only one sequence. The explanation for this result can be that very few Met residues are successfully cleaved in the protein, or that the resulting peptides were washed off during the digestion or during the subsequent washing steps. The peptide was resequenced, confirming the sequence shown in Table 6

Sample	*1*	*2*	*3*	*4*	*5*	*6*	*7*	*8*	*9*	*10*
Sequence from CNBr Digest of 160 kDa	-	R	V	D	N	I	Y	T	E	-
N-terminal sequence of 95 kDa protein	R	T	P	T	D	R	K	T	T	-
N-terminal sequence of 68 kDa protein	A	-	K	S	T	I	A	V	-	F

Table 6: Peptide sequence from F4/80 molecule purification

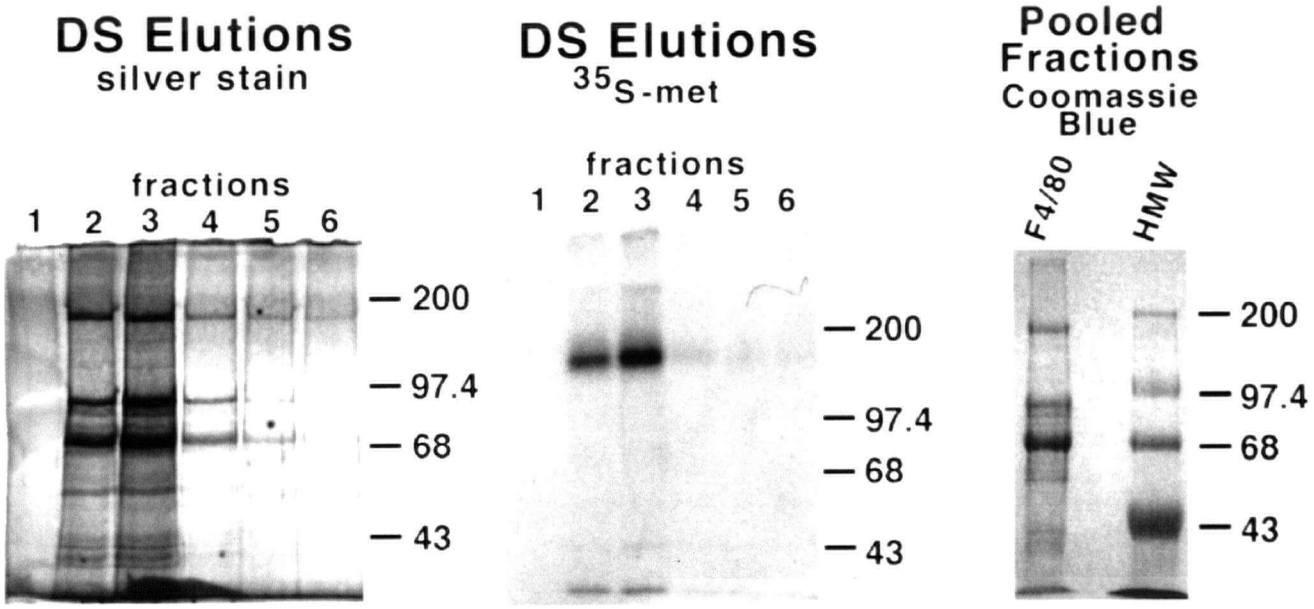

Figure 46: Peptide sequencing of the F4/80 molecule

RAW 309 Cr.1 cells ($2x10^{10}$) were grown in spinner flasks, harvested, and used to produce an NP-40 membrane lysate. The F4/80 molecule was purified with an F4/80 mAb column, elution of the bound protein, and application to a DS lectin column. The DS-Sepharose column eluates were analyzed by silver staining of fractions and SDS-PAGE and fluorography of fractions. The fractions containing protein were pooled and concentrated before separation on SDS-PAGE, blotting to PVDF membrane, and staining with Coomassie Blue. The 160 kDa protein was digested with CNBr and subjected to PITC sequencing. The sequence obtained from duplicates of this procedure is shown in Table 6.

4.2.3.5 Monitoring of the F4/80 molecule purification

Many reports of protein purification with mAbs do not utilize an assay of the protein's antigenic epitope during purification. However, monitoring of purification simply by SDS-PAGE can be misleading if a major contaminant has a similar migration compared to the protein of interest (274). The results obtained in the purification shown in Figure 46, emphasized the need to more quantitatively address the F4/80 molecule purification. Williams and Barclay have described a simple assay which measures binding of mAb to control cells. Preincubation of the mAb to with purified protein or samples from the various steps during purification, results in mAb-antigen complexes which can be pelleted by centrifugation (274). If a sample contains more of the protein of interest, more mAb will be centrifuged out of solution. This results in a decrease in the mAb binding to the control cells. Despite concerted attempts, this assay could not be adapted to monitor the F4/80 molecule purification. Therefore, the F4/80 molecule purification was initially monitored by SDS-PAGE and silver staining of fractions during the purification. A more precise quantitation of the F4/80 molecule content would have averted or detected difficulties with the F4/80 molecule purification.

Following the characterization of the DS lectin reactivity with the F4/80 molecule, this interaction was utilized to monitor F4/80 molecule purification. The protocol required immunoprecipitation of the F4/80 molecule from each step of the purification, SDS-PAGE and transfer of the proteins to PVDF membrane, and blotting of the membrane with biotinylated DS lectin and SA-HRPO. The signal obtained could be quantitated and related to the amount of F4/80 molecule from standard cells. An initial attempt to quantify the F4/80 molecule purification is shown in (Figure 47). This result displays that quantitation of the F4/80 molecule recovery is possible with this method, but also outlines some of the limitations of the system.

The requirement for immunoprecipitation of all samples except for the eluted fractions and densitometric analysis of the results, increases the labor required for each analysis. Due to this fact, only one or two dilutions of each sample could be tested. This can produce difficulties when the dilution chosen lies outside the range of the standards as is evident in Lane 4, for the NP-40 solublized membranes. To make the results more reliable, duplicate samples were immunoprecipitated in subsequent experiments. The protocol for biotinylated DS lectin blotting in the monitoring of F4/80 molecule purification is described in Section 2.2.14.

Sample	*Protein (mg)*	*F4/80 molecule (cell equivalents)*	*Dilution Analyzed*	*Cell Equivalent Recovery*	*Purification Factor*
Cells	2045	$1.5x10^{10}$			1
1k pellet	166	$1.15x10^{9}$	750	$8.63x10^{8}$	NA
1k sup	1890	$8.64x10^{6}$	7143	$6.18x10^{9}$	0.45
NP-40 lysate*	175	$2.53x10^{6}$ *	6400	$1.27x10^{9}$ *	1.3*
Eluted Fractions	0.2	$6.01x10^{6}$	200	$6.73x10^{8}$	459
post-column lysate	ND	0	6000	0	NA

ND - not determined NA - not applicable

* - The values obtained in this purification were abnormally low compared to other purifications. See text and Table 8 for details and comparison.

Table 7 : Monitoring of F4/80 purification with DS blotting

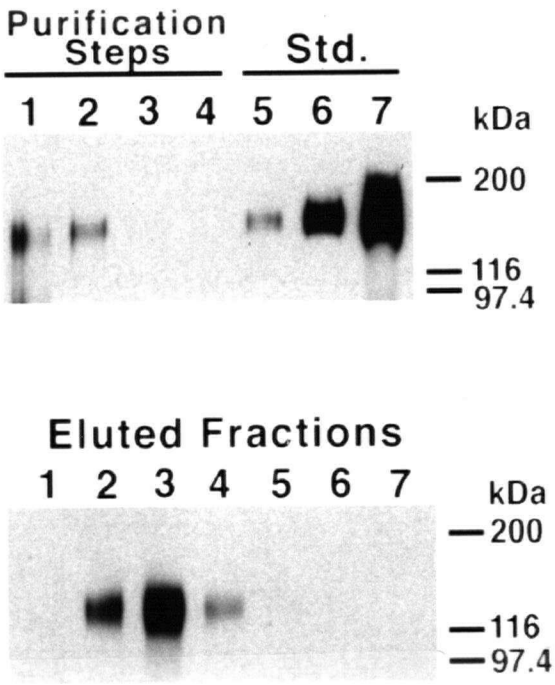

Figure 47: The use of DS lectin blotting to monitor F4/80 molecule purification

RAW 309 Cr.1 cells were grown in large scale spinner cultures. An aliquot of the cells were retained to utilize as the control cells (100% F4/80 molecule content). The remaining cells were utilized for a Tween-40 membrane preparation (Section 2.2.13), followed by solublization with NP-40, and passing of the lysate over an F4/80 mAb affinity column. The column was eluted with 0.5% C_8Glc, 50 mM DEA, pH 11.5. Samples from each stage of the purification were solublized with NP-40 and immunoprecipitated with F4/80-Sepharose. The proteins were separated on 7.5% SDS-PAGE, transferred to PVDF membranes, and blotted with biotinylated DS lectin and SA-HRPO. The membrane was finally developed with ECL reagents and exposed to Kodak XAR film.

With the source of cells determined, a culture system capable of growing $2x10^{10}$ cells, the mAb and elution scheme tested, and now a method to monitor the content of F4/80 molecule throughout the purification, the large scale purification procedures were attempted again.

4.2.3.6 Affinity purification of the F4/80 molecule

A subsequent affinity purification of the F4/80 molecule is outlined in Figure 48. The goal of this purification was to address the recoveries from of the F4/80 mAb column and to use the material for amino acid composition and N-terminal sequence analysis. Therefore, if the protein was sufficiently pure after the mAb column, the DS-Sepharose column would not be necessary. Since the proteins would be separated by SDS-PAGE prior to blotting to PVDF for sequencing and amino acid analysis, the low M_r contaminants were not a problem. The only proteins greater than 70 kDa appeared to be the F4/80 molecule precursor and mature form (Figure 48A). The reactivity with the DS lectin confirms that the F4/80 molecule was recovered in significant amounts (Figure 48C-F). The purification factor and degree of F4/80 recovery are described in Table 8. These results indicated that the recovery of the F4/80 molecule was a relatively low 6% of the starting F4/80 molecule content following elution from the mAb column. A further analysis indicated that the majority of loss occurs during the mAb step, since 77% of the antigenic content was recovered at the NP-40 solublization step. The F4/80 molecule was also not present in significant amounts in the column flowthrough. Subsequent elution attempts of varying stringency also did not release any more protein from the column. The F4/80 molecule epitope recognized by the mAb could conceivably be denatured during the extended chromatography step.

The eluted fractions 2, 3, and 4 were pooled, concentrated, separated by 7.5% SDS-PAGE, transferred to PVDF membrane, and stained with Coomassie Blue (Figure 48B). Following concentration, the 110 kDa precursor is now more easily detectable than the mature form. The mature form may be more refractory to Coomassie Blue staining due to its higher glycosylation (375) or may be aggregated or digested during the concentration step. The diffuse

Figure 48: The purification of the F4/80 molecule

RAW 309 Cr.1 cells ($2x10^{10}$) were grown in spinner flasks, harvested, and used to produce an NP-40 membrane lysate. The F4/80 molecule was purified from the lysate with an F4/80 mAb column followed by elution of the bound proteins. A) The F4/80 mAb column eluates were analyzed by SDS-PAGE of the fractions and silver staining. The proteins were also analyzed for their F4/80 content by blotting of SDS-PAGE separated samples with the DS lectin (C-F). C) The F4/80 molecule was immunoprecipitated from a range of cell number equivalents of RAW 309 Cr.1 cell NP-40 lysates as shown. The F4/80 molecule content at the following steps of purification was analyzed by solublization in NP-40, immunoprecipitation with the F4/80 mAb, separation by SDS-PAGE, transfer to PVDF membrane, and blotting with DS lectin: 1) Tween-40 membrane 1000g homogenate supernatant, 2) Tween-40 membrane homogenate 1000g pellet, 3) Tween-40 membrane 100,000g pellet, 4) Tween-40 100,000g supernatant, 5) NP-40 solublized membranes, and 6) NP-40 solublized lysate following the F4/80 mAb column. The dilution factor for each sample is indicated in Table 8. Panel E is the DS lectin blotting of the fractions eluted from the F4/80 mAb column. Panel F is the DS lectin blotting of the pooled eluted fractions following concentration. Panel B is the Coomassie Blue stained PVDF membrane following SDS-PAGE separation of the pooled, concentrated, fractions.

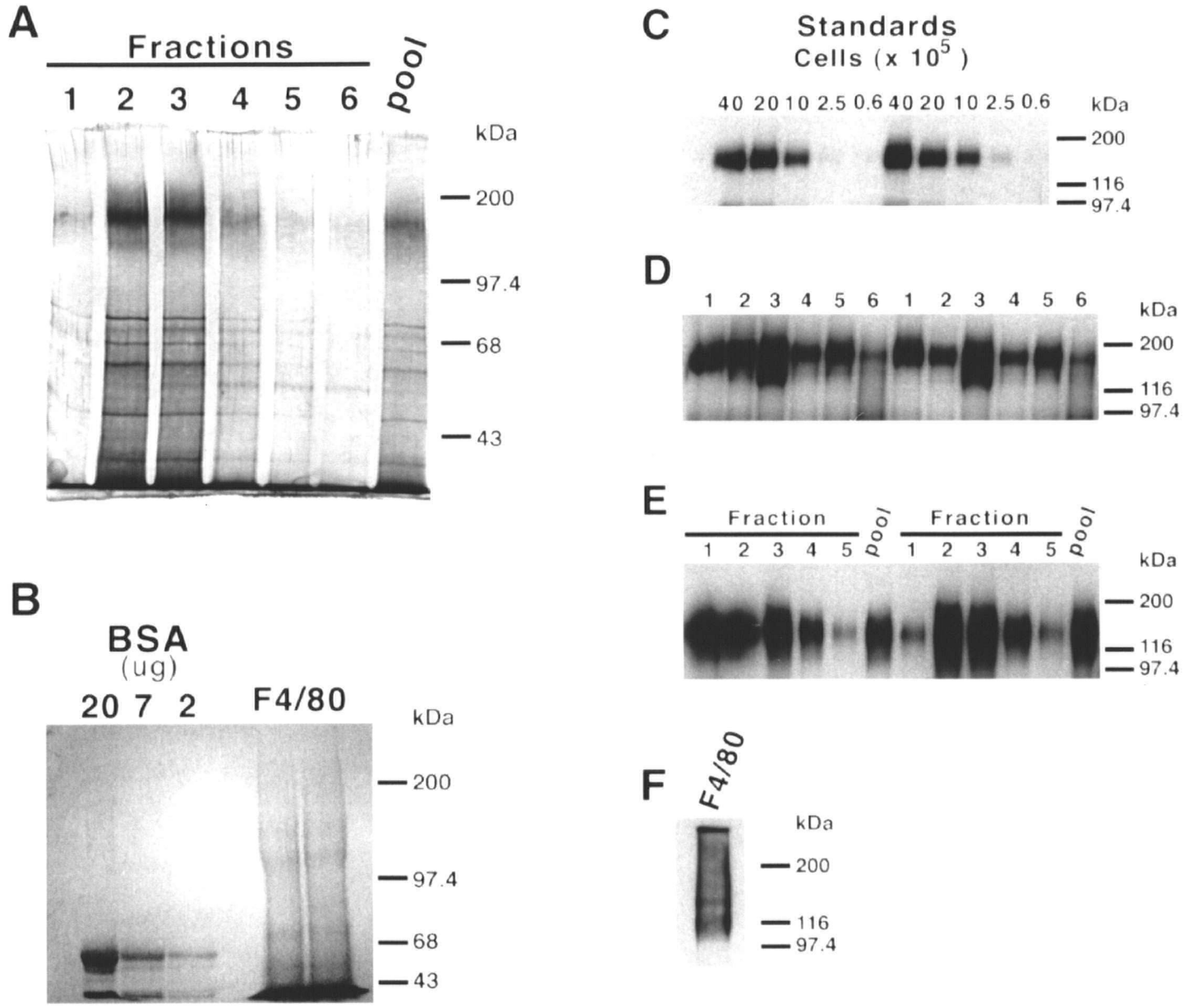
A
Fractions
1 2 3 4 5 6 pool
kDa
200
97.4
68
43
B
BSA
(ug)
20 7 2
F4/80
kDa
200
97.4
68
43
C
Standards
Cells (x 10^5)
40 20 10 2.5 0.6 40 20 10 2.5 0.6
kDa
200
116
97.4
D
1 2 3 4 5 6 1 2 3 4 5 6
kDa
200
116
97.4
E
Fraction
1 2 3 4 5 pool
Fraction
1 2 3 4 5 pool
kDa
200
116
97.4
F
F4/80
kDa
200
116
97.4

nature of the protein migration relative to that seen in Figure 46 was likely due to the denaturation of the F4/80 molecule prior to DS-Sepharose chromatography described in Figure 46. Denaturation of the F4/80 molecule in SDS prior to subsequent manipulations such as chromatography or storage at -80^{0}C produced a slightly higher M_r, more compact migration in SDS-PAGE (not shown). The 110 and 150 kDa proteins were still reactive with the DS lectin as expected (Figure 48F). The DS-reactivity confirmed the presence of more precursor F4/80 molecule than the mature form. Some of the DS reactive material was localized to the top of the separating gel (Figure 48F) which suggested that the mature F4/80 molecule may have undergone aggregation during the concentration procedure.

Sample	*Protein (mg)*	*F4/80 molecule (cell equivalents)*	*Dilution*	*Cell Equivalent Recovery*	*Purification Factor*
Cells	2518	$2x10^{10}$			1
1k sup	2250	$1.1x10^{7}$	4673	$2.5x10^{10}$	1.4
1k pellet	206	$1.7x10^{6}$	445	$2.8x10^{9}$	NA
100k sup	2218	$3.0x10^{6}$	445	$1.6x10^{9}$	NA
100k pellet	219	$8.6x10^{6}$	2273	$2.0x10^{10}$	11.6
NP-40 lysate	219	$1.4x10^{7}$	2463	$1.3x10^{10}$	7.6
Pooled Eluate	0.765	$6.8x10^{6}$	204	$1.4x10^{9}$	232
SDS-PAGE	0.050	$6.8x10^{6}$	204	$1.4x10^{9}$	3525
Flowthrough	ND	$1.8x10^{6}$	450	$8.2x10^{8}$	NA

Table 8: F4/80 molecule purification

The purification of the F4/80 molecule was monitored by DS lectin blotting to determine the efficiency of F4/80 molecule recovery throughout the purification

4.2.3.7 Amino acid analysis and N-terminal sequencing

Amino acid analysis of the protein from half of one lane in Figure 48B, indicated that 4 fold molar less of the mature form was present compared to the immature form (Table 9). The amino acid results for the mature form were less reliable due to the presence of residual Gly following transfer and rinsing of the PVDF membrane. Therefore, the molar percentages of the amino acids in the two proteins were not identical due to the skewing of the values by the Gly. However, the two proteins did show the same general pattern of amino acid composition . The more important information from this analysis, was that up to 32 pmol of the F4/80 molecule following purification could be obtained, which is sufficient for producing and recovering 5 pmol of internal peptides. In spite of this significant amount of protein, no N-terminal sequence was obtained from either protein.

	110 kDa Protein	*150-160 kDa Protein*
Total yield	**8.0 pmol**	**2.0 pmol**
Amino Acid	***Molar percentage***	***Molar percentage***
Asx	**16.11**	**12.4**
Glx	**13.69**	**12.6**
Ser	**9.08**	**7.72**
Gly	**9.81**	**17.11**
His	**0.042**	**0.06**
Arg	**2.49**	**1.86**
Thr	**7.97**	**6.51**
Ala	**5.35**	**6.28**
Pro	**4.11**	**4.87**
Tyr	**2.83**	**2.09**
Val	**5.62**	**6.05**
Met	**0.042**	**0.012**
Cys	**0.042**	**0.012**
Ile	**5.12**	**5.59**
Leu	**9.87**	**9.72**
Phe	**4.18**	**4.42**
Lys	**2.94**	**2.58**

Table 9: Amino acid analysis of the F4/80 molecule

One-half of one lane from Figure 48B was used to determine the amino acid composition of the 110 kDa and 150 kDa proteins.

4.2.3.8 Production of Internal Peptides from purified F4/80 molecule

Due to the apparent N-terminal block in the F4/80 protein, the production of internal peptides for sequencing was pursued.

4.2.3.8.1 Analytical scale

Peptide fragments of proteins can be produced by several methods including both chemical and enzymatic methods. A wide variety of enzymes with different cut site specificities have been characterized and include the following enzymes: trypsin (Lys,Arg), Lys-C (Lys), Glu-C (Glu or Glu and Asp). Among chemical cleavage methods, CNBr cleavage of proteins at met residues is by far the most commonly employed. Following protein cleavage, the peptides are most commonly separated by RP-HPLC or SDS-PAGE if the peptides are of a large enough molecular mass. To address different protocols for the production of internal peptides from the F4/80 molecule, several cleavage methods were assayed. The F4/80 molecule was analyzed prior to digestion to ensure that the protein was pure. A minor contaminant at 30 kDa remained, but this was present in far less amount relative to the F4/80 molecule (Figure 49B). Digestion of this material with the indicated digestion methods is shown in Figure 49A. Radioactive monitoring of the samples indicated near 100% recovery following digestion except for the CNBr cleavage, where only 65% is recovered. This decreased recovery was apparent in the fragment pattern on SDS-PAGE. The enzymatic digestions of the F4/80 molecule all produced a large number of fragments in the range from 1 to 30 kDa and even some higher M_r peptides. The production of these peptides from large scale preparations of the F4/80 molecule was the next goal before attempting to separate these peptide products into single peptides for sequencing.

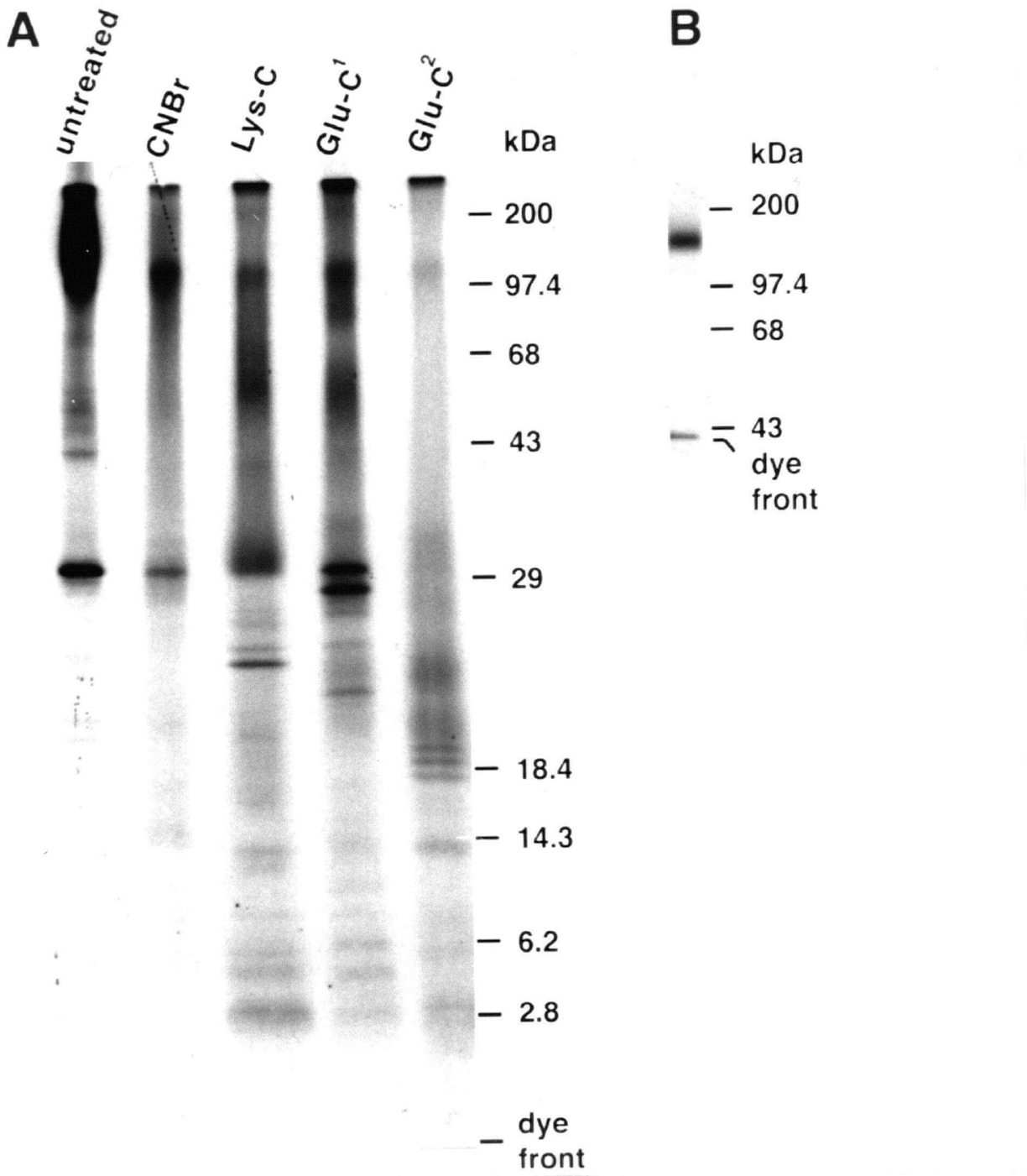

Figure 49: Test production of peptides from the F4/80 molecule

The F4/80 molecule was purified by F4/80 mAb chromatography, elution of the bound proteins, and secondary purification on a DS lectin column. A) The protocols for the digestion of the F4/80 molecule as indicated were utilized to cleave the F4/80 molecule. The digested material was analyzed by 10-17% SDS-PAGE and autoradiography with Kodak XAR film for 18 days. Panel B shows the product prior to digestion after separation by 8% SDS-PAGE and autoradiography for 2 days to Kodak XAR film.

4.2.3.8.2 Preparative scale peptide production

The large scale production of peptides from the F4/80 molecule was performed in a fashion similar to the purification described in Section 4.2.3.6. The DS lectin column step would have increased the absolute purity of the F4/80 molecule, but may have decreased the recovery below the threshold for sequencing. In attempting to replicate the analytical scale peptide production, difficulty was experienced. The increased concentration of protein in the sample was creating conditions which led to the loss of the F4/80 molecule following denaturation and concentration. An example of the silver staining profile of the column eluates before and after denaturation and concentration is shown in Figure 50. The disappearance of the 160 kDa F4/80 molecule protein was clearly evident, as was the appearance of higher molecular weight material. Attempts to dissociate this complex with higher concentration of urea, NaCl, or even SDS were not successful once the 160 kDa protein form was lost. Digestion of the material with Lys-C did not produce detectable fragments when the digest was analyzed by RP-HPLC.

To avoid the denaturation and concentration steps prior to enzyme digestion, the immediate denaturation of fractions in SDS was also attempted. SDS-PAGE and transfer of the proteins to a modified PVDF membrane provides a method for enzymatic digestion of the protein on the membrane (376). Difficulties in the elution of peptides from the membrane, reduced the final yield of peptides. Although HPLC separation of the peptides eluted from the membrane did allow the recovery of peptides for sequencing, the low amount of peptide did not allow unambiguous determination of the sequence.

During the attempts to obtain peptide sequence, we learned of the reported cloning of a candidate cDNA for the F4/80 molecule by another research group. Since other work remained

pertaining to the post-translational modifications of the F4/80 molecule, the efforts to obtain internal peptide sequence were concluded.

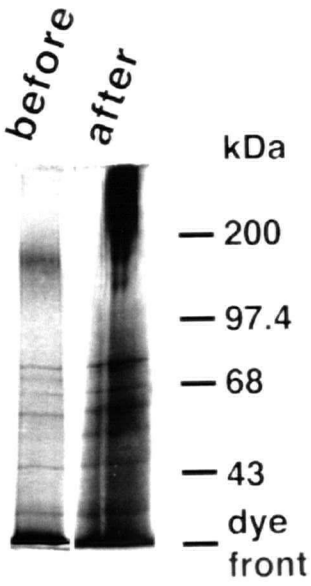

Figure 50: Attempted large scale production of peptides from the F4/80 molecule

RAW 309 Cr.1 cells ($2x10^{10}$) were grown in spinner flasks, harvested, and used to produce an NP-40 membrane lysate. The F4/80 molecule was purified from the lysate with an F4/80 mAb column followed by elution of the bound proteins. The F4/80 mAb column eluates were analyzed by SDS-PAGE of the pooled fractions and silver staining (before). The pooled fractions were concentrated as described in section 2.2.16 and analyzed by silver staining (after).

4.3 Discussion

The goal of the F4/80 molecule characterization was to determine the peptide sequence by cDNA cloning and to characterize the biochemical nature of the molecule. The pursuit of cDNA sequence did not reach a successful end. The difficulties that were encountered in this pursuit, may partially explain why the identity of this molecule has remained unknown for 15 years after the F4/80 mAb description. The results of the biochemical characterization of the F4/80 molecule have shed more light on potential functions for this molecule than a cDNA sequence alone would. That the F4/80 molecule possesses numerous post-translational modifications including disulfide bonds, extensive N-linked and moderate O-linked glycosylation, SA modifications, and CS GAGs, has been clearly demonstrated. These modifications may directly involve the F4/80 molecule in mϕ and DC recognition events. The extensive modifications may also explain the difficulty encountered with protein purification and expression cloning.

4.3.1 Transport and folding of the F4/80 molecule

The post-translational modifications of the F4/80 molecule may be implicated in multiple functions, including a role in maintaining the molecule's structural stability. For example, the glycosylation is evidently important for the molecule's efficient transport and acquisition of the F4/80 epitope since tunicamycin prevents the molecule's transport (Fig 31). Heavy glycosylation has been shown to protect glycoproteins from proteolytic degradation, which may be especially relevant for mϕ glycoproteins which can encounter the mϕ's active degradative machinery. Carbohydrates have also been demonstrated to directly participate in the stabilization of the protein backbone of human CD2 (166), thus allowing CD2 to bind CD58. A high local concentration of O-linked carbohydrates

(Figure 33) in one domain of the F4/80 molecule, could dictate a local extended structure similar to CD45 (168) or the mucin-like CD43 (169) O-glycosylated domains.

4.3.2 N- and O-linked carbohydrate modification of the F4/80 molecule

The preferential binding of the DS and PHA-E lectins to the F4/80 molecule is indicative of branched, complex type N-linked carbohydrates (371,377). The PHA-E reactivity suggests that the α1-6 Man branch has the following structure: Galβ1-4GlcNAcβ1-2Manα1-6Man. The *Datura stramonium* lectin binding characteristics of the F4/80 molecule indicate the presence of repeating β1-4 linked GlcNAc units or N-acetyllactosamine units. The binding of both PHA-E and DS lectins to their respective ligands is typically inhibited if the carbohydrate structure is sialylated (371,377). Since RCA binding detected no free Gal residues on the F4/80 molecule before neuraminidase digestion (Figure 34 and Figure 35), desialylated PHA-E and DS binding sites may represent only a minor component of the total glycosylation, but still mediate high affinity lectin binding. Alternatively, the glycan chains may be terminated with residues which do not affect the lectin binding. The DS binding to the F4/80 molecule precursor, indicates that the glycans required for DS binding are added in the medial -Golgi. This indicates that the α1-3 linked Man branch is likely substituted with β1-4 linked N-acetylglucosamines. Other studies have described the Endo H sensitive nature of these hybrid structures, with a high Man branch on the α1-6 linked Man and complex glycans on the remaining branch or branches (378). After the trimming of the α1-6 linked Man residues, the glycan will be further modified to form the final mature molecule.

Serial lectin chromatography and studies into the structural nature of the F4/80 molecule carbohydrates should resolve the precise nature of the extensive glycosylation described in this thesis.

4.3.3 Glycosaminoglycan addition to the F4/80 molecule

Molecular interactions mediated by GAGs have also acquired recent prominence. HS is important in the process of binding of bFGF to its receptor (220). This interaction of negatively charged GAGs with receptor ligands has been proposed to be relevant for other receptor-ligand interactions (179). Cell surface receptors with GAG specificity include CD44 which has a high affinity for HA and also interacts with CS (216,218). The presence of CS modifications on the F4/80 molecule (Figure 40) indicates it could function as a receptor for CD44 since even a single CS modification can mediate functional interactions with CD44 (216). Since multiple cell types can express CD44, the interaction of the F4/80 molecule could be functionally relevant for many functions including T cell stimulation, hematopoesis, recirculation, and localization of mϕs and LCs (203).

GAGs also interact with the ECM, most notably with fibronectin. Fibronectin contains a heparin-binding domain that bind heparin, HS, and CS (217). Therefore, the CS of the F4/80 molecule could mediate macrophage and DC binding to fibronectin.

4.3.4 Purification of the F4/80 molecule

The purification of the F4/80 molecule reported in this thesis, did succeed in isolating significant quantities of the F4/80 molecule, in sufficient purity to permit amino acid analysis and N-terminal sequencing (Figure 48). Although the N-terminal of the F4/80 molecule is blocked, the preparation of the protein for o-phthalaldehyde sequencing, fortuitously produced one peptide sequence (Table 6). This peptide was recovered in low amounts (2-4 pmol for sequencing), but produced similar sequence in two separate sequencing runs. The sequence

shows no homology to other known proteins. The 95 kDa protein from this purification also showed no homology to known proteins. However, the identity of the 68 kDa protein was BSA, indicating the retention or introduction of non-specific proteins at some stage in the purification. To more thoroughly identify and quantitate the F4/80 molecule content throughout the purification, monitoring by mAb immunoprecipitation and DS lectin blotting was instituted The low yield of the F4/80 molecule from the mAb column is apparently due to the loss of the F4/80 epitope during the affinity chromatography step (Table 8). The preparation of a mAb to a separate, more stable epitope, or the use of a specific antisera would provide an alternative tool to purify the molecule with greater efficiency. Other antibodies could also prove useful in attempts to clone the F4/80 molecule cDNA by expression. The N-terminal of the F4/80 molecule is blocked since two attempts to sequence of 20 pmol did not produce a sequence whereas other molecules in the same gel or from the same cells did not have blocked N-termini. Therefore, N-terminal blockage does not generally occur during the purification protocol employed. The controlled tryptic digestion of the F4/80 molecule on harvested cells (Figure 43), could potentially be utilized to overcome the natural N-terminal blockage. The 100 kDa fragment retained by the cell is recognized by the F4/80 mAb and should have a free N-terminus. However, the decreased yield of the 100 kDa fragment could limit the utility of this approach.

The difficulty in working with the F4/80 molecule primarily surfaced during attempts to concentrate or denature large quantities of the molecule in the absence of SDS (Figure 50), a standard component of protocols for the enzymatic digestion of proteins (Section 2.2.16). The analytical scale protocol did not produce extensive protein aggregation (Figure 49, and data not shown). To permit denaturation in SDS, utilization of protocols for digestion of proteins on membranes following SDS-PAGE and transfer to special, cationic PVDF membranes (376) was

attempted. The transfer was efficiently accomplished, but peptides could not be eluted in high yield from the membrane in acidic conditions with standard methods.

Other potential adjustments to the purification protocol are now apparent, but the information was not all available at the time the purification was being performed. The identification of CS modification was not definitively completed until after the purification attempts were stopped. If the purification of the F4/80 molecule was continued, the elimination of the CS modifications by digestion with chondroitin ABC lyase (Figure 40) would be incorporated into the protocol. CS moieties can impart a large negative charge of 2 to 3 negative charges per disaccharide unit (214). The negative charges of the SA residues also contribute to the negative nature of the post-translational modifications which appear to cover the protein (Figure 42). The entire molecule retains a basic nature in denatured form (Figure 41), which indicates that positive and negative charges may be juxtaposed when the protein is denatured. When higher concentrations of protein are present, the molecules may have formed the aggregates observed (Figure 50). Unfortunately, the F4/80 molecule purification has not been revisited in order to address these questions.

4.3.5 Comparison of the F4/80 molecule to known molecules

The extent and diversity of the post-translational modifications contained in the F4/80 molecule are not commonly found in proteins. The molecules of the mucin family including CD66, CD43, and CD34 are extensively glycosylated, but primarily contain O-linked carbohydrates (379) which contrasts these proteins with the F4/80 molecule. Another class of extensively glycosylated molecules includes the CD24 protein. CD24 and its related proteins have extremely small protein cores (35 amino acids in CD24) with extensive O-linked glycosylation (380), which is again unlike the F4/80 molecule. Certain members of the Ig superfamily share some properties with the F4/80

molecule. For example, CD22 contains 10-11 potential N-linked sites, and numerous potential O-linked sites which collectively contribute half of the mature CD22 apparent molecular mass as carbohydrates. CD22 also exhibits marked reduction in apparent molecular mass in non-reducing SDS-PAGE, but lacks GAG modification (381). CD45 also shares certain qualities with the F4/80 molecule. CD45 contains 11-16 N-linked glycosylation sites and numerous O-linked sites depending on the inclusion of the alternatively spliced exons (see Chapter 3). The CD45 extracellular domain also contains 16 Cys residues, some of which are involved in disulfide bonding. CD45 has also been reported to be sulfated in a T cell leukemia line and activated peripheral blood leukocytes (382), although results with PEC CD45 did not detect any sulfated CD45 (Figure 37). Two proteins which do contain the plethora of modifications in the F4/80 molecule are the Ii (CD74) and CD44 (203,383) which have N- and O-linked glycosylation and GAG modifications. However, both of these proteins have expression patterns which vary significantly from the F4/80 molecule's distribution. In addition, the protein core of CD74 is substantially smaller than the F4/80 protein core, whereas CD44 has an acidic protein core. Together these data indicate that the F4/80 molecule is distinct from CD74 and CD44. However, the F4/80 molecule joins this select group of proteoglycans which also includes the TfR, thrombomodulin, and the 114/10 molecule as transmembrane proteins with large protein cores that have been characterized as GAGs (214,384).

4.3.6 The structure of the F4/80 molecule

The work described in this thesis, describes the extensive modification of the F4/80 molecule by N- and O-linked glycosylation and CS (Figure 32, Figure 33, and Figure 40). The other information on the molecule has come from analyzing its behavior in IEF (Figure 41) and anion exchange chromatography (Figure 42) and from the tryptic digestion of the extracellular domain (Figure 43).

The F4/80 molecule's extensive glycosylation is obviously a major determinant of the proteins extracellular region. In addition, previous studies of the F4/80 molecule had demonstrated the presence of a protease sensitive site in the extracellular domain (264,354). Limited protease cleavage produced a 100 kDa fragment suggesting that a minimum of 60 kDa of the F4/80 molecule is situated extracellularly. The characterization reported here (Figure 43) further defines the structural nature of the F4/80 molecule by localizing the CS modification in the 60 kDa fragment digested by trypsin. At least a portion of the carbohydrate and protein labeling are retained in the 100 kDa fragment following trypsin digestion. The presence of highly negative SA and CS moieties was also documented. Since the F4/80 molecule retains an overall basic characteristic, it is likely that the protein core of the F4/80 molecule is basic which contrasts the negatively charged SA and CS modifications. The amino acid composition does not show an unusual excess of basic amino acids, but the amounts of Glu versus Gln and Asp versus Asn could not be determined (Table 9). Therefore, the IEF migration characteristic of the F4/80 molecule may be anomalous for as yet unknown reasons. The location of the various carbohydrates was also not tested. Therefore, the O-linked carbohydrates may be clustered in a mucin like domain or dispersed throughout the entire extracellular domain.

The large difference between reducing and non-reducing SDS-PAGE migration of the F4/80 molecule, suggests a multiple domain structure for the F4/80 molecule. The most common superfamily (SF) domains found in extracellular regions of proteins are of the IgSF (385). Other potential SF domains include fibronectin type II, nerve growth factor receptor, EGF, C-type lectin, and the cytokine receptor family (129). These superfamilies all possess conserved Cys residues, important for protein folding. The F4/80 molecule could contain multiple repeats of a single SF domain, a mixture of different SF domains, or conceivably a novel structure. The precise domain

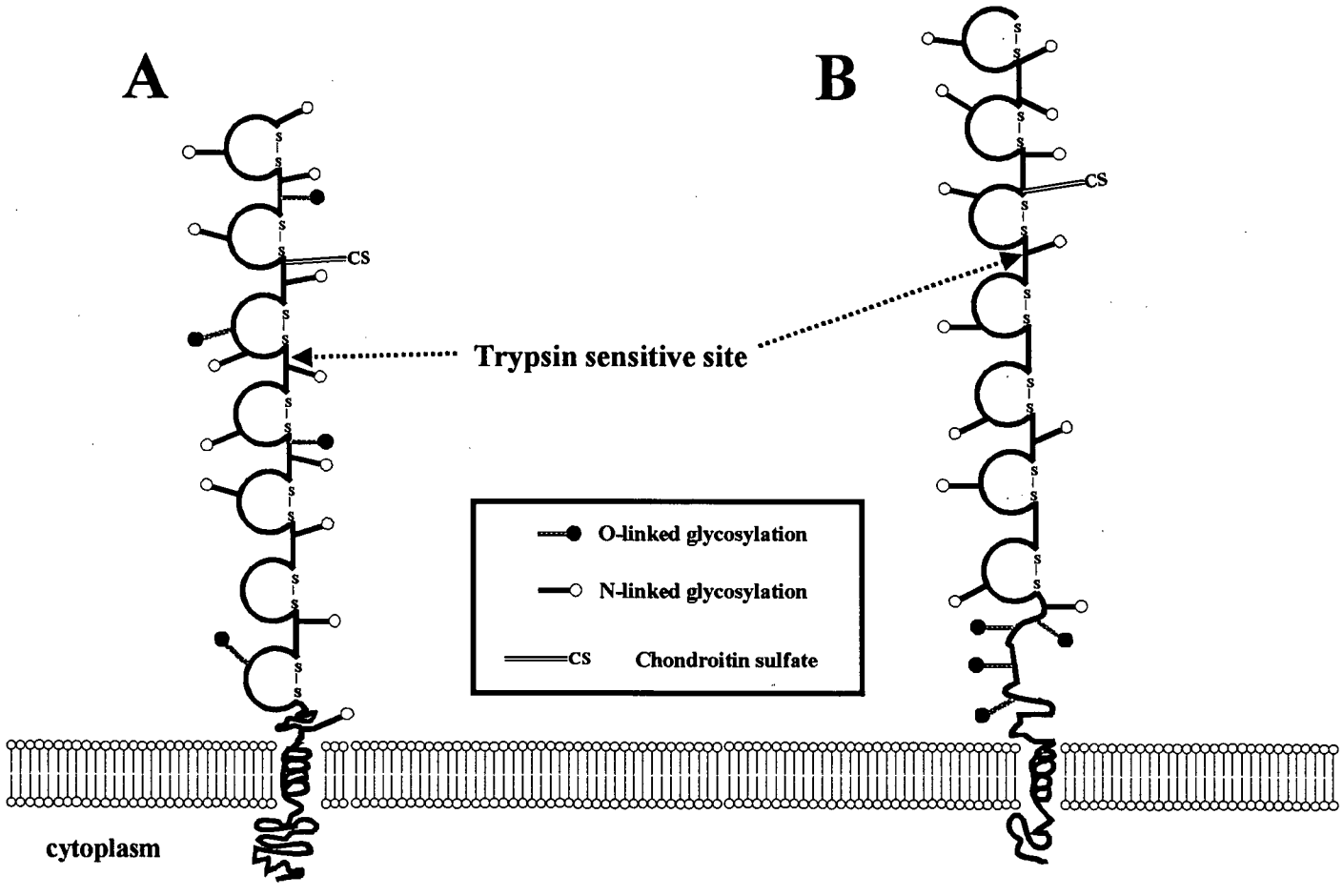

Figure 51: Structure of the F4/80 molecule

Panels A and B depict representations of the potential structure of the F4/80 molecule. A and B are identical except that the structure in B has the O-linked glycosylation sites clustered into a single domain rather than disseminated over the entire protein as in A. The Ig constant domain was chosen to represent the domain structures predicted from the numerous disulfide bonds in the F4/80 molecule. As stated in the text, other SF domains such as EGFSF and LDL receptor SF domains would also satisfy the disulfide bonded domain structure. The location of the CS residue distal to the trypsin sensitive site is indicated. Finally, the high degree of N-linked glycosylation and less prevalent O-linked glycosylation are depicted.

identity cannot currently be determined, so the structure is modeled based on IgSF domains. An IgSF domain of the constant-2 (C2) set is typically 80-100 amino acids (385). The model includes 7 Ig C2 domains in the structure to account for the observed protein core of 80-85 kDa (Figure 30 and Figure 31) and the existence of several disulfide bonds (Figure 29). These approximately 630 amino acids involved in the Ig C2 domains would leave 100-150 amino acids for the remainder of the extracellular domain, the transmembrane segment, and the cytoplasmic domain. No further information on the cytoplasmic domain has been obtained. Based on these assumptions, the structure of the F4/80 molecule would resemble the depictions in Figure 51. If the other SF domains are also involved in the structure, more amino acids may contribute to the transmembrane and intracellular domains. For example, EGFSF and LDL receptor SF domains are 40-50 amino acids and each contain 6 Cys residues. The smaller size of each domain would allow for a more substantial cytoplasmic domain than depicted in Figure 51 while still accounting for the extensive disulfide bonding.

4.3.7 Potential functions of the F4/80 molecule

Carbohydrates are now also recognized as participants in specific molecular interactions. The characterization of carbohydrate binding proteins has focused much research into identifying ligands for these proteins. Selectin ligands are extremely variable although most contain SA, sulfate and/or Fuc residues in the recognition sequence (173). These carbohydrate sequences can be found on N- and O-linked carbohydrates. Since the F4/80 molecule possesses large amounts of N-linked glycosylation and clearly detectable O-linked glycosylation, the F4/80 molecule could function as a ligand for the selectin family of molecules. Considering the absence of detectable Fuc residues on the F4/80 molecule (Figure 35), the nature of any selectin ligand on the F4/80 molecule could be a non-fucosylated selectin ligand structure.

Other proteins with requirements for carbohydrate in their recognition structures are CD22 and sialoadhesin which bind to ligands containing SA. The absence of α2-3 linked SAs indicates that the F4/80 molecule would not be a ligand for sialoadhesin (202). Conversely, the presence of α2-6 linked SAs on the F4/80 molecule (Figure 34) make it a candidate counterreceptor for CD22 (171). CD22 mediated adhesion to monocytes has been previously demonstrated in human systems (373,386) and would also likely occur with mouse monocytes. Thus, cell-cell adhesion event may be strengthened by a human F4/80 molecule homologue binding to CD22.

Galectin ligands also appear to mediate important biological processes such as thymocyte apoptosis (195), FcεRI signaling in mast cells and DCs (196,197), and IL-1 production in monocytes (198). The F4/80 molecule's carbohydrates contain the galectin ligands Gal and N-acetyllactosamine, as defined by the DS and PHA-E reactivity (Figure 35 and Figure 36). Therefore, crosslinking of the F4/80 molecule by the naturally dimeric galectins, could mediate signal transduction events that initiate mϕ physiological responses such as IL-1 production.

As already mentioned in Section 4.3.3, CS can serve as a ligand for the heparin binding domain of fibronectin. The CS modifications of CD44 have been proposed to mediate ECM interactions of lymphocytes in tissues following extravasation (217). The F4/80 molecule could likely to serve a similar role in directing macrophage and DC tissue localization. Leukocyte circulation and localization is likely to be a complicated process (179), with the F4/80 molecule perhaps tailoring the system to suit the requirements of macrophages and DCs.

Studies of CD44 have also demonstrated an additional role for carbohydrates and GAGs on glycoproteins. CD44 exists in three activation states with respect to its HA binding: inactive, inducible, or constitutively active (203). Two recent reports demonstrated that removal of the N-linked carbohydrates, removal of the SAs, and removal of the CS moieties could each convert CD44

from a non-binding state to a constitutively active HA binding phenotype (204,205). Although no differences in the post-translational modifications of the F4/80 molecule between PECs and mϕ cell lines were observed, modulation could potentially occur *in vivo* depending on the site of localization or the state of mϕ or DC activation (387,388).

The general molecular considerations of F4/80 molecule function also have functional meaning for DCs and mϕs. The migration and tissue localization of DCs and mϕs in response to certain biological responses was outlined in sections 1.2.3.2 and 1.3.1.2. Perhaps the F4/80 molecule assists in directing cell migration and helps establish the location of resident mϕs and LCs via cell-cell or cell-ECM interactions. The down-regulation of the F4/80 molecule following activation, could permit other cell membrane proteins to dictate cell-cell interactions and subsequent migration and localization. The involvement of numerous cytokines, including those of the chemokine family, in DC and mϕ functions is also clear (389). If the F4/80 molecule fulfills a receptor function, it could mediate cytokine responsiveness in resting DCs and mϕs and which is no longer required following activation.

The function of the protein component of the F4/80 molecule has not yet been resolved, but it is intriguing to consider that the molecule's post-translational modifications may determine and alter the molecule's function. The functions suggested by the post-translational modifications that are demonstrated here will now provide a direction in the search for the function of the F4/80 molecule. Ultimately, the biology of mϕs and DCs will also be further clarified as the role of F4/80 in cell-cell adhesion, cell migration, cytokine responsiveness, or other functions is discovered.

5. GENERAL CONCLUSIONS AND PERSPECTIVES

5.1 CD45

The isoform expression and function of CD45 in non-lymphocytes is an area of research open to much exploration. The work described in this thesis was designed to begin the investigation into CD45 expression and function in DCs and mϕs. The most significant findings from this research were the expression of only the CD45R0 and CD45RB isoforms by murine DCs (Figure 12 to Figure 14) and the demonstration of functional PTP activity of CD45 isolated from DCs (Figure 17) .The comparison of DC and mϕ CD45 revealed that mϕs also primarily express CD45R0, but can express isoforms with exons A and B depending on the mϕ source (Figure 18 and Figure 19). Mϕ CD45 is also a functional PTP, similar to the activity obtained for DC CD45 Figure 20).

The specific functions of DC and mϕ CD45 remain to be elucidated, but the current level of knowledge is not unlike that for CD45 in lymphocytes a few years ago. As is often the case, the work in this thesis demonstrating PTP activity of DC and mϕ CD45 is being complemented by other research. Several groups have utilized crosslinking of CD45 alone or co-crosslinking with other molecules, to implicate CD45 in certain cellular function including FcγRII signaling (322), FcεRI signaling (127,307), and IL-6 production (352). The Fc receptor signaling is not an unexpected pathway for CD45 involvement since proteins with ITAM motifs are involved in these receptor complexes (351). The induction of IL-6 secretion is perhaps the first of many new roles to be discovered for CD45 in non-lymphoid cells.

Whereas T cell and B cell kinases are well characterized, the kinases expressed by DCs in particular are not identified. An enumeration of the candidate kinases in DCs will be a

significant goal in pursuing the understanding of DC signal transduction. The approach to this goal is now feasible that DCs can be cultured *in vitro* to produce pure populations of DCs, DC cell lines have been produced, and purification methods for isolation of DCs have been improved (72,110,134,344,345). PCR with oligos to the unique regions of src family kinases and other known kinases should be able to systematically identify kinases expressed in DCs. The use of degenerate oligos to conserved regions of kinases could also PCR amplify kinases which are specifically expressed in DCs (390). Of course, the importance of kinase identification will extend beyond determining potential substrates for CD45. Kinases may also be involved in the signals governing DC maturation, DC migration, and the phenotypic change following antigen encounter. Since all of these processes are controlled by cytokines (see Section 1.2.3.2), the downstream involvement of kinases in signaling is quite likely (391). If DC-specific kinases are identified, these could be targets for DC-mediated immunotherapy. For example, if kinases control constitutive macropinocytosis, interfering with kinase activity could prevent the acquisition of autoantigens in clinical conditions such as arthritis.

The most likely involvement for CD45 in DCs *in vivo*, appears to be via FcεRI. The *in vitro* PTP activity demonstrated in our hands (Figure 17), may be involved in FcRεRI signaling in intact DCs (127,307). If DCs are truly involved in the allergic response, interfering with DC activity could be of critical importance. Although FcγR receptors are also expressed on DCs, the lower expression level and downregulation of FcγRs indicate a less important role for FcγRs in DCs. Mϕs are more dependent on their FcγRs for engulfing bacteria, endocytosing proteins, and destroying infected cells. The evidence to support a role for CD45 in FcγR signaling is mounting, raising the prospect of modulating mϕ function by interfering with CD45 function.

The other major focus of DC and mϕs CD45 research will be the identification of ligands for the CD45 extracellular domain. The restricted CD45 isoform expression of mϕs and DCs primarily to CD45R0 with some CD45RB and RA could suggest that these isoforms are integrally involved in CD45 function. CD45R0 on thymocytes has been suggested to be a galectin-1 ligand whereas CD45RB is not (194). Since galectins recognize carbohydrate, the CD45R0 specificity may be through isoform specific glycosylation. Other lectin-like molecules such as the selectins may also have specificity for CD45 glycoforms. CD22 will clearly bind to CD45, but this is not isoform specific and depends on the α2,6 linked SA on CD45 (171). In order to address the nature of CD45 glycoforms from cells varying from T cells to DCs and mϕs, a systematic assessment of CD45 glycosylation must be undertaken. The use of sequential lectin chromatography, enzymatic digestion with glycosidases, and NMR studies may reveal the structural requirements for recognition by carbohydrate binding proteins. Differences in glycosylation between cell types and cell location may also permit the selective modulation of specific cell types by utilizing soluble carbohydrates to disrupt interactions. The identification of isoform specific ligands which will recognize the CD45 protein core, is still a possibility. The use of recombinant CD45 to identify these ligands will still need to consider the effect of glycosylation on protein structure. Therefore, the host cell for recombinant protein production will need to be carefully considered.

The limited expression of CD45RA and RB on mϕs and CD45RB on DCs, suggests that these isoforms may also be of importance. As discussed in Section 3.3.1, the isoforms may be involved in molecular interactions within the cell membrane rather than between cells. A direct assessment of this hypothesis in mϕs and DCs is now warranted and feasible. If interactions between the CD45 isoforms and molecules such as LFA-1 and CD4 or 8 (314,315) also exist in

mϕs and DCs, this will provide new information on the function of these interactions in the absence of a TcR/CD3 complex. Conversely, if CD45 does not associate with other molecules in DCs and mϕs, the role of the TcR/CD3 complex in nucleating these interactions may be even more intriguing.

The identification of CD45 isoforms on DCs is also important for researchers modulating the IR with anti-CD45 mAbs. Different reports have described the use of various anti-CD45 mAbs, including anti-CD45RB, to affect IRs such as transplant rejection (392-394). The key role that DCs play in the IR, indicates that the observed effects may be due to DC modulation rather than only memory T cell modulation. The work reported in this thesis should therefore alert other researchers to assess the use of anti-CD45 mAbs in affecting T cell responses with DCs and T cells in mind.

The use of gene knockout mice has provided an invaluable tool in assessing the physiological role of specific proteins. The CD45 knockout mice (306) would be a valuable tool for the continued investigation into the role of CD45 in DCs and mϕs. If myeloid development from hematopoietic precursors is dependent on CD45 (341), $CD45^-$ mice should exhibit deficiencies in DC and mϕ populations. If CD45 is important for DC or mϕ migration, this should be evident by monitoring DC migration following skin painting with antigen (395) or mϕ migration into the peritoneum after injection of eliciting agents (174). If DCs are present in the CD45 knockout mice, the effectiveness of DCs in stimulating T cells could be addressed by comparing a primary MLR with stimulator DCs from $CD45^-$ or $CD45^+$ mice.

5.2 The F4/80 molecule

The enigmatic nature of the molecule recognized by the F4/80 mAb is clarified substantially by the molecular characterization described in Chapter 4 of this thesis. The eventual cloning of the cDNA for this molecule, will provide a complete picture of the molecule's molecular nature.

Regardless of the nature of the F4/80 molecule's protein core, the extensive post-translational modifications provide important structural information and imply several potential functions for the F4/80 molecule as discussed in Section 4.3.7. The extensive N- and O-linked glycans of the F4/80 molecule may act as ligands for any of the recently described carbohydrate binding proteins including galectins, selectins, and CD22. The CS modification could also serve as a ligand for CD44. Another potential implication of the CS moiety, is the role of the F4/80 molecule as a cytokine receptor, with the CS moiety serving to concentrate the ligand prior to specific binding (222). With these potential functions in mind, there are numerous future experiments to test these hypotheses.

If the post-translational modifications of the F4/80 molecule do control function, the modifications may change depending on the mϕ/DC location, state of maturation, or state of activation. At present, variation in F4/80 molecule modifications not been detect, but the methods typically addressed the qualities of the entire F4/80 molecule pool. An approach such as sequential lectin chromatography would differentiate between subpopulations of molecules that differ in their glycosylation. This approach was successful in identifying 8 glycoforms of Thy-1 in rat thymocytes (157). Isolation of glycoforms of the F4/80 molecule would permit their structural characterization and comparison between different tissues as was done for Thy-1.

Variation of the F4/80 molecule glycosylation could modulate the ligand structures involved in galectin, selectin, or CD22 binding. For example, galectin-CD45 interactions appear important for cell-cell binding between thymocytes and epithelial cells (194). Thymocytes appear to modulate the expression of core 2 β1,6 GlcNAc transferase which is instrumental in forming the galectin-1 ligand structure. The glycosylation could also affect the protein's function as demonstrated for CD44. By removing SA, N-linked carbohydrates, or CS chains, the CD44 affinity for HA is activated to constitutive from a non-binding phenotype (204,205). If the F4/80 molecule serves as a growth factor receptor, the CS chain may be critical for concentrating the ligand (222). Control of receptor activity could be modulated by not adding the CS moiety to the F4/80 molecule to reduce affinity for the growth factor. The CS does not appear to be added to all F4/80 molecules (Figure 42), although this point requires further investigation. Therefore, even the molecules on the same cell may display different functional capabilities with and without a CS modification

Another aspect of interest could be the residual SO_4 labeling following chondroitinase ABC digestion (Figure 40). Although 93% is removed by this enzyme, the remaining 7% may be sulfation via Tyr or O-linked carbohydrates, or simply incomplete chondroitinase ABC digestion. However, testing for Tyr sulfation is worthwhile given its importance in adherence (183,184) and proteolytic processing (213).

In the absence of a cDNA for the F4/80 molecule, the most reliable approach to ligand identification will be to utilize recombinant proteins of the potential carbohydrate binding proteins, the galectins, selectins, and CD22, in addition to CD44. Fusion proteins of these potential F4/80 binding proteins can be produced in large quantities and coupled to Sepharose at high concentration. This will allow the detection of lower affinity interactions which are

common when attempting to detect monomeric interactions as opposed to the observed affinity if the ligand can cap in a cell membrane (175). The binding of CD44 to CS appears to require only one CS chain (216) which suggests that the F4/80 molecule is a good candidate for a CD44 ligand. To address this possibility, a fusion protein of the extracellular CD44 domain linked to the IgG_1 Fc region was made. The recombinant CD44-Ig construct has been sequenced and expressed. The CD44-Ig appears to be properly expressed and will be evaluated for binding to F4/80 following the completion of this thesis. We are also attempting to obtain or construct recombinant CD22 to test for binding to the α2,6 SA of the F4/80 molecule (Figure 34), recombinant galectins to determine if galectins bind to the N-acetyllactosamine structures of the F4/80 molecule (Figure 35 and Figure 36), and recombinant E and P- selectin molecules to determine if the F4/80 molecule's extensive glycosylation serve as selectin ligands (Figure 32 and Figure 33).

If a cDNA sequence for the F4/80 molecule is obtained, new avenues for investigation will become available. A recombinant F4/80 molecule could be used to positively select for ligands by affinity chromatography or COS cell expression systems. These approaches do not require the preselection of potential ligands and therefore may identify ligands not predicted by the F4/80 molecule carbohydrate additions. The production of a recombinant F4/80 molecule should be carried out in a mϕ cell line to preserve the natural glycosylation and GAG addition.

The cDNA for the murine F4/80 molecule will also provide an immediate tool to evaluate the existence of F4/80 homologues in other species. In particular, the identification of a human F4/80 molecule could provide a mϕ/DC-specific tool for drug delivery or mϕ/DC-mediated modulation of the IR. In addition, the cDNA will allow for the isolation and characterization of the gene's promoter element. This will provide insights into the control of

gene expression in mϕs and DCs. The long term goal for these promoter/enhancer elements is to utilize them to drive expression of heterologous DNA segments *in vitro* or *in vivo* in transgenic mice. The genes to be expressed could include the diphtheria toxin A gene to produce mice ablated of DCs and mϕs lineages (396). Depletion of DCs would provide an invaluable system for assessing the *in vivo* effect of continual DC depletion on T cell tolerance, transplantation rejection or acceptance, anti-viral response, and anti-tumor response. The only DC depletion model system described to date, does not appear to be entirely DC-specific and results in a short time span (ca. one week) for phenotypic evaluation of the mice (397). Other constructs could contain antisense constructs (such as MHC class I) to evaluate a specific protein's function in DCs and mϕs, or potentially, cytokine genes to further modulate IR. These are relatively long term goals which are now attainable in the present context of knowledge and technology.

5.3 Final Comments

The unique functions of DCs and the critical controlling role that DCs exert over the immune system, has driven the research described in this thesis and the research of many scientists around the world. The description of DCs in Section 1.2.3.2 is largely a product of the past 5 years of research. The technical challenges of limited DC number have been overcome by sensitive techniques and the development of DC culture systems and cell lines to provide an emerging picture of DCs at a molecular level. By identifying molecular mechanisms that control DC development and function, methods for DC-based immunotherapy are now a reality. The areas for intervention are extremely diverse, but include inducing an anti-tumor or anti-viral IR, improved methods for vaccination, reduction of transplant rejection, reduction of allergic responses, and the control of autoimmunity. The characterization of DC and mϕ CD45 and the F4/80 molecule will provide yet another two

aspects of DC and mϕ biology which can advance our understanding of these cells' basic functions. These molecules could also potentially serve as therapeutic or experimental targets for DC modulation as described in the previous sections.

The characterization of both CD45 and the F4/80 molecule has also emphasized the importance of carbohydrates in assessing a molecule's function. The further characterization of these proteins' carbohydrates will almost certainly be involved in the characterization of their physiological ligands. Further challenges such as optimization of delivery and carbohydrate presentation will be involved in applying the new knowledge of carbohydrate ligands to clinical situations, but carbohydrate-based drug development is already well into clinical trials (398).

It is clear that scientific endeavors have been distanced from the realm of demonology, but there will never be a time when we can rest and declare that all is done. The challenge of scientists in the next years is to raise the level of knowledge of the entire biological system to finally permit the utilization of the new found molecular and biological data to assist at a clinical level. In this context, it is perhaps worth emphasizing that these clinical applications will only be attained if research and enthusiasm for discovering the basic mechanisms of biology are retained.

6. ABBREVIATIONS

β_2m	β_2-microglobulin
2-ME	2-mercaptoethanol
ADCC	antibody dependent cellular cytotoxicity
APC	antigen presenting cell
ATCC	American Type Culture Collection
ATP	adenosine triphosphate
BCG	bacillus Calmette Guérin
bFGF	basic fibroblast growth factor
BSA	bovine serum albumin
C-type lectins	Ca^{++} dependent carbohydrate binding lectin
C_8Glc	octylglucoside
cLCs	cultured Langerhans cells
CLIP	class II Ii peptide
CS	chondroitin sulfate
CTL	cytotoxic T lymphocyte
DC	dendritic cell
dCTP	cytosine triphosphate
DEA	diethylamine
DNA	deoxyribonucleic acid
DOC	deoxycholate
DS	*Datura stramonium* lectin
DTSSP	dithiobis(succinimidylpropionate)
DTT	dithiothreitol
ECL	enhanced chemiluminescence
ECM	extracellular matrix
EDTA	ethylenediaminetetraacetic acid
EGF	epidermal growth factor
Endo H	Endoglycosidase H
ER	endoplasmic reticulum
FACS	fluorescence activated cell sorter
FBS	fetal bovine serum
FITC	fluorescein isothiocyanate
fLCs	freshly isolated Langerhan cells
FUC	fucose
GAG	glycosaminoglycan
Gal	galactose
GalNAc	galactosamine
GITC	guanidinium isothiocyanate
Glc	glucose
GlcNAc	glucosamine
GM-CSF	granulocyte-macrophage colony stimulating factor
GPI	glycosylphosphatidylinositol
HA	hyaluronic acid
HEPES	4-(2-hydroxyethyl)-1-piperazineethanesulfonic acid

HEV	high endothelial venule
IEF	isoelectric focusing
IFN	interferon
Ig	immunoglobulin
Ii	invariant chain
IL	interleukin
IR	immune response
ITAM	immunoreceptor family tyrosine-based activation motif
kDa	kilodalton
LC	Langerhans cell
LDL	low density lipoprotein
LMP	low molecular weight protein
LPS	lipopolysaccharide
mAb	monoclonal antibody
Mϕ	macrophage
Man	mannose
MAP kinases	mitogen activated protein kinase
MHC	major histocompatibility complex
MIIC	major histocompatibility complex class II containing compartment
MLF	mean linear fluorescence values
MLR	mixed lymphocyte reaction
NDV	Newcastle's Disease Virus
PAGE	polyacrylamide gel electrophoresis
PBS	phosphate buffered saline
PCR	polymerase chain reaction
PECs	peritoneal exudate cells
PHA-E	*Phaseolus vulgaris* erythroagglutinin
PHA-L	*Phaseolus vulgaris* leukoagglutinin
PITC	phenylisothiocyanate
PKA	protein kinase A
PKC	protein kinase C
PMSF	phenylmethylsulfonylfluoride
PNGase F	peptide-N-glycosidase F
PPD	purified protein derivative of *Mycobacteria*
PTP	protein tyrosine phosphatase
PVDF	polyvinylidene difluoride
RCA	*Ricin communis* agglutinin
RNA	ribonucleic acid
RPMs	resident peritoneal macrophages
RT-PCR	reverse transcriptase-polymerase chain reaction
SA	sialic acids
SA-HRPO	streptavidin-horseradish peroxidase
SDS	sodium dodecyl sulfate
SF	superfamily
sIg	surface Ig
sNHS-biotin	sulfo-N-hydroxy succinimide biotin
TAP	transporter associated with antigen presentation

TCA	trichloroacetic acid
TcR	T cell receptor
TdT	terminal deoxynucleotide transferase
TFA	trifluoroacetic acid
T_h	T helper
TNF-α	tumor necrosis factor-α
Tris	Tris(hydroxymethyl)aminomethane
Xyl	xylose

7. REFERENCES

1. **Thucydides**. 1972. *History of the pelopennesian war*. Penguin, London, p. 151.

2. **Jenner, E.** 1798. *An inquiry into the causes and effects of the Variolae vaccinae*, a disease discovered in some of the western counties of England, particularly in Glouchestershire, and known by the name of The Cow Pox. London, UK.

3. **Brock, T. D.** 1961. *Milestones in microbiology*. Prentice-Hall, Inc. Englewood Cliffs, USA.

4. **Dobell, C.** 1958. *Anton van Leeuwenhoek and his "little animals."*. Russel and Russel, New York, USA.

5. **Metchnikoff, E.** 1887. Sur la lutte des cellules de l'organisme contre l'invasion des microbes. *Ann. Inst. Pasteur 7*:321.

6. **Heidelberger, M. and F. E. Kendall**. 1935. *J. Exp. Med. 62*:697.

7. **Tiselius, A. and E. A. Kabat**. 1938. Electrophoresis of immune serum. *Science 87*:416.

8. **Gorer, P. A., S. Lyman, and G. D. Snell**. 1948. Studies on the genetic and antigenic basis of tumor transplantation. Linkage between a histocompatibility gene and 'fused' in mice. *Proc. Roy. Soc. Lond. Ser. B 135*:499.

9. **Snell, G. D.** 1948. Methods for the study of histocompatibility genes. *J. Genetics 49*:87.

10. **Sachs, D. H.** 1984. The Major Histocompatibility Complex. In *Fundamental Immunology*. W.E. Paul, ed. Raven Press, NY, USA, p. 303.

11. **Zinkernagel, R. M. and Doherty, P.C.** 1974. Immunological surveillance against altered-self components by sensitized T lymphocytes in lymphocytic choriomeningitis. *Nature. 251:*547.

12. **Burnet, F. M.** 1959. *The clonal selection theory of acquired immunity*. Cambridge University Press, London, UK.

13. **Kronenberg, M., G. Siu, L. E. Hood, and N. Shastri**. 1986. The molecular genetics of the T-cell antigen receptor and T-cell antigen recognition. [Review]. *Annu. Rev. Immunol. 4*:529.

14. **Nossal, G. J. V.** 1994. Negative selection of lymphocytes. *Cell 76*:229.

15. **Davis, M. M. and P. J. Bjorkman**. 1988. T-cell Receptor Genes and T-cell Recognition. *Nature 334*:395.

16. **Unanue, E. R.** 1984. Antigen-presenting function of the macrophage. *Annu. Rev. Immunol. 2*:395.

17. **Ziegler, H. K. and E. R. Unanue**. 1982. Decrease in macrophage antigen catabolism caused by ammonia and chloroquine is associated with inhibition of antigen presentation to T cells. *Proc. Natl. Acad. Sci. USA 79*:175.

18. **Chesnut, R. S., S. Colon, and H. M. Grey**. 1982. Requirements for the processing of antigen by antigen-presenting B cells. I. Functional comparison of B cell tumors and macrophages. *J. Immunol. 129*:2382.

19. **Allen, P. M. and E. R. Unanue**. 1984. Differential requirements for antigen processing by macrophages for lysozyme-specific T cell hybridomas. *J. Immunol. 132*:1077.

20. **Allen, P. M., D. J. Strydom, and E. R. Unanue**. 1984. Processing of lysozyme by macrophages: identification of the determinant recognized by two T cell hybridomas. *Proc. Natl. Acad. Sci. USA* 81(8): 2489.

21. **Townsend, A., J. Rothbard, F. M. Gotch, G. Bahadur, D. Wraith, and A. J. McMichael**. 1986. The epitopes of Influenza nucleoprotein recognized by cytotoxic T lymphocytes can be defined with short synthetic peptides. *Cell 44*:959.

22. **Bohm, W., R. Schirmbeck, A. Elbe, K. Melber, D. Diminky, G. Kraal, N. van Rooijen, Y. Barenholz, and J. Reimann**. 1995. Exogenous hepatitis B surface antigen particles processed by dendritic cells of macrophages prime murine MHC class I-restricted cytotoxic T lymphocytes in vivo. *J. Immunol. 155*:3313.

23. **Rock, K. L., S. Gamble, and L. Rothstein**. 1990. Presentation of exogenous antigen with class I major histocompatibility complex molecules. *Science 249*:918.

24. **Springer, T. A.** 1990. Adhesion receptors of the immune system. *Nature 346*:425.

25. **Janeway, C. A.** 1992. The T cell receptor as a multicomponent signaling machine: CD4/CD8 coreceptors and CD45 in T cell activation. *Annu. Rev. Immunol. 10*:645.

26. **June, C. H., J. A. Bluestone, L. M. Nadler, and C. B. Thompson**. 1994. The B7 and CD28 receptor families. *Immunol. Today 15*:321.

27. **Steinmetz, M. and L. Hood**. 1983. Genes of the major histocompatibility complex in mouse and man. *Science 222*:727.

28. **Wolfel, T., M. Hauer, J. Schneider, M. Serrano, C. Wolfel, E. Klehmann-Hieb, E. De Plaen, T. Hankein, K. M. zum Buschenfelde, and D. Beach**. 1995. A p16INK4a-insensitive CDK4 mutant targeted by cytolytic T lymphcytes in a human melanoma. *Science 269*:1281.

29. **Mandelboim, O., G. Berke, M. Fridkin, M. Feldman, M. Eisenstein, and L. Eisenbach**. 1995. CTL induction by a tumour-associated antigen octapeptide derived from a murine lung carcinoma. *Nature 369*:67.

30. **Germain, R. N. and D. H. Margulies**. 1993. The biochemistry and cell biology of antigen processing and presentation. *Annu. Rev. Immunol. 11*:403.

31. **Surh, C. D., E. Gao, H. Kosaka, D. Lo, C. Ahn, D. B. Murphy, L. Karlsson, P. A. Peterson, and J. Sprent**. 1992. Two subsets of epithelial cells in the thymic medulla. *J. Exp. Med. 176*:495.

32. **Pichler, W. J. and T. Wyss-Coray**. 1994. T cells as antigen presenting cells. *Immunol. Today 15*:312.

33. **Paul, W. E. and R. A. Seder**. 1994. Lymphocyte responses and cytokines. *Cell 76*:241.

34. **Bjorkman, P. J., M. A. Saper, B. Samraoui, W. S. Bennett, J. L. Strominger, and D. C. Wiley**. 1987. Structure of the human class I histocompatibility antigen, HLA-A2. *Nature 329*:506.

35. **Fremont, D. H., M. Matsumura, E. A. Stura, P. A. Peterson, and I. A. Wilson**. 1992. Crystal structures of two viral peptides in complex with murine MHC class I H-2K^b. *Science 257*:919.

36. **Matsumura, M., D. H. Fremont, P. A. Peterson, and I. A. Wilson**. 1992. Emerging principles for the recognition of peptide antigens by MHC class I molecules. *Science 257*:927.

37. **Falk, K., O. Rötzschke, S. Stevanovic, G. Jung, and H. G. Rammensee**. 1991. Allele-specific motifs revealed by sequencing of self-peptides eluted from MHC molecules. *Nature 351*:290.

38. **Brown, J. H., T. S. Jardetzky, J. C. Gorga, L. J. Stern, R. G. Urban, J. L. Strominger, and D. C. Wiley**. 1993. Three-dimensional structure of the human class II histocompatibility antigen HLA-DR1. *Nature 364*:33.

39. **Janeway, C. A. and P. Travers**. 1994. *Immunobiology: The Immune System in Health and Disease*. Current Biology Ltd. London, UK.

40. **Goldberg, A. L. and K. L. Rock**. 1992. Proteolysis, proteasomes and antigen presentation. *Nature 357*:375.

41. **Löwe, J., D. Stock, B. Jap, P. Zwickl, W. Baumeister, and R. Huber**. 1995. Crystal structure of the 20S proteasome from the archaeon T. acidophilum at 3.4 Å resolution. *Science 268*:533.

42. **Gabathuler, R., G. Reid, G. Kolaitis, J. Driscoll, and W. A. Jefferies**. 1994. Comparison of cell lines deficient in antigen presentation reveals a functional role for TAP-1 alone in antigen processing. *J. Exp. Med. 180*:1415.

43. **Degen, E., M. F. Cohen-Doyle, and D. B. Williams**. 1992. Efficient dissociation of the p88 chaperone from major histocompatibility complex class I molecules requires both β2-microglobulin and peptide. *J. Exp. Med. 175*:1653.

44. **Koller, B. H., P. Marrack, J. H. Kappler, and O. Smithies**. 1990. Normal development of mice deficient in β_2M, MHC Class I proteins, and $CD8^+$ T cells. *Science 248*:1227.

45. **Van Kaer, L., P. G. Ashton-Rickardt, H. L. Ploegh, and S. Tonegawa**. 1992. TAP1 mutant mice are deficient in antigen presentation, surface class I molecules, and $CD4^-8^+$ T cells. *Cell 71*:1205.

46. **Xu, X. and S. K. Pierce**. 1995. The Novelty of Antigen-Processing Compartments. *J. Immunol. 155*:1652.

47. **Peters, P. J., J. J. Neefjes, V. Oorschot, H. L. Ploegh, and H. J. Geuze**. 1991. Segregation of MHC class II molecules from MHC class I molecules in the Golgi complex for transport to lysosomal compartments. *Nature 349*:669.

48. **Cresswell, P.** 1994. Assembly, transport, and function of MHC class II molecules. *Annu. Rev. Immunol. 12*:259.

49. **Roche, P. A., M. S. Marks, and P. Cresswell**. 1991. Formation of a Nine-subunit Complex by HLA Class II Glycoproteins and the Invariant Chain. *Nature 354*:392.

50. **Kropshofer, H., A. B. Vogt, and G. J. Hammerling**. 1995. Structural features of the invariant chain fragment CLIP controlling rapid release from HLA-DR molecules and inhibition of peptide binding. *Proc. Natl. Acad. Sci. USA 92*:8313.

51. **Bakke, O. and B. Dobberstein**. 1990. MHC class II-associated invariant chain contains a sorting signal for endosomal compartments. *Cell 63*:707.

52. **Sloan, V. S., P. Cameron, G. Porter, M. Gammon, M. Amaya, E. Mellins, and D. M. Zaller**. 1995. Mediation by HLA-DM of dissociation of peptides from HLA-DR. *Nature 375*:802.

53. **Marrack, P., L. Ignatowicz, J. W. Kappler, J. Boymel, and J. H. Freed**. 1993. Comparison of peptides bound to spleen and thymus class II. *J. Exp. Med. 178*:2173.

54. **Lanzavecchia, A.** 1987. Antigen uptake and accumulation in antigen-specific B cells. *Immunol. Rev. 99*:39.

55. **Metlay, J. P., E. Pure, and R. M. Steinman**. 1989. Distinct features of dendritic cells and anti-Ig activated B cells as stimulators of the primary mixed leukocyte reaction. *J. Exp. Med. 169*:239.

56. **Metlay, J. P., E. Pure, and R. M. Steinman**. 1989. Control of the immune response at the level of antigen-presenting cells: a comparison of the function of dendritic cells and B lymphocytes. *Adv. Immunol. 47*:45.

57. **Cassell, D. J. and R. H. Schwartz**. 1994. A quantitative analysis of antigen-presenting cell function: activated B cells stimulate naive CD4 T cells, but are inferior to dendritic cells in providing costimulation. *J. Exp. Med. 180*:1829.

58. **Unkeless, J. C., E. Scigliano, and V. H. Freedman**. 1988. Structure and function of human and murine receptors for IgG. *Annu. Rev. Immunol. 6*:251.

59. **Taylor, M. E., J. T. Conary, M. R. Lennartz, P. D. Stahl, and K. Drickamer**. 1990. Primary structure of the mannose receptor contains multiple motifs resembling carbohydrate-recognition domains. *J. Biol. Chem. 265*:12156.

60. **Elomaa, O., M. Kangas, C. Sahlberg, J. Tuukanen, R. Sormunen, A. Liakka, I. Thesieff, G. Kraal, and K. Tryggvason**. 1995. Cloning of a Novel Bacteria-binding Receptor Structurally Related to Scavenger Receptors and Expressed in a Subset of Macrophages. *Cell 80*:603.

61. **Green, S. J., L. F. Scheller, M. A. Marletta, M. C. Seguin, F. W. Klotz, M. Slayter, B. J. Nelson, and C. A. Nacy**. 1994. Nitric oxide: cytokine regulation in host resistance to intracellular pathogens. *Immunol. Lett. 43*:87.

62. **Nacy, C. A. and M. S. Meltzer**. 1991. T-cell mediated activation of macrophages. *Curr. Opin. Immunol. 3*:330.

63. **Finlay, B. B. and S. Falkow**. 1990. Common themes in microbial pathogenicity. *Microbiol. Rev. 53*:210.

64. **Crowley, M., K. Inaba, and R. M. Steinman**. 1990. Dendritic cells are the principal cells in mouse spleen bearing immunogenic fragments of foreign proteins. *J. Exp. Med. 172*:383.

65. **Steinman, R. M. and Z. A. Cohn**. 1973. Identification of a Novel Cell Type in Peripheral Lymphoid Organs of Mice I. Morphology, Quantitation, and Tissue Distribution. *J. Exp. Med. 137*:1142.

66. **Steinman, R. M. and Z. A. Cohn**. 1974. Identification of a Novel Cell Type in Peripheral Lymphoid Organs of Mice II. Functional Properties In Vitro. *J. Exp. Med. 139*:380.

67. **Steinman, R. M., G. Kaplan, M. D. Witmer, and Z. A. Cohn**. 1979. Identification of a novel cell type in peripheral lymphoid organs of mice. V. Purification of spleen dendritic cells, new surface markers, and maintenance in vitro. *J. Exp. Med. 149*:1.

68. **Steinman, R. M. and M. D. Witmer**. 1978. Lymphoid dendritic cells are potent stimulators of the primary mixed leukocyte reaction in mice. *Proc. Natl. Acad. Sci. USA 75*:5132.

69. **Steinman, R. M.** 1991. The Dendritic Cell System and Its Role in Immunogenicity. *Annu. Rev. Immunol. 9*:271.

70. **Grabbe, S., S. Beissert, T. Schwarz, and R. D. Granstein**. 1995. Dendritic cells as initiators of tumor immune responses: a possible strategy for tumor immunotherapy?. [Review]. *Immunol. Today 16*:117.

71. **Ibrahim, M. A., B. M. Chain, and D. R. Katz**. 1995. The injured cell: the role of the dendritic cell system as a sentinel receptor pathway. [Review]. *Immunol. Today 16*:181.

72. **Inaba, K., M. Inaba, N. Romani, H. Aya, M. Deguchi, S. Ikehara, S. Muramatsu, and R. M. Steinman**. 1992. Generation of Large Numbers of Dendritic Cells from Mouse Bone Marrow Cultures Supplemented with Granulocyte/Macrophage Colony Stimulating Factor. *J. Exp. Med. 176*:1693.

73. **Inaba, K., R. M. Steinman, M. Witmer-Pack, H. Aya, M. Inaba, T. Sudo, S. Wolpe, and G. Schuler**. 1992. Identification of Proliferating Dendritic Cell Precursors in Mouse Blood. *J. Exp. Med. 175*:1157.

74. **Inaba, K., M. Inaba, M. Deguchi, K. Hagi, R. Yasumizu, S. Ikehara, S. Muramatsu, and R. M. Steinman**. 1993. Granulocytes, macrophages, and dendritic cells arise from a common major histocompatibility complex class II-negative progenitor in mouse bone marrow. *Proc. Natl. Acad. Sci. USA 90*:3038.

75. **Caux, C., C. Dezutter-Dambuyant, D. Schmitt, and J. Banchereau**. 1992. GM-CSF and TNF-α Cooperate in the Generation of Dendritic Langerhans Cells. *Nature 360*:258.

76. **Kämpgen, E., F. Koch, C. Heufler, A. Eggert, L. L. Gill, S. Gillis, S. K. Dower, N. Romani, and G. Schuler**. 1994. Understanding the Dendritic Cell Lineage through a Study of Cytokine Receptors. *J. Exp. Med. 179*:1767.

77. **Santiago-Schwarz, F., N. Divaris, C. Kay, and S. E. Carsons**. 1993. Mechanisms of Tumor Necrosis Factor Granulocyte-Macrophage Colony Stimulating Factor Induced Dendritic Cell Development. *Blood 82*:3019.

78. **Ardavin, C., L. Wu, C. L. Li, and K. Shortman**. 1993. Thymic dendritic cells and T cells develop simultaneously in the thymus from a common precursor population. *Nature 362*:761.

79. **Bhardwaj, N., J. W. Young, A. J. Nisanian, J. Baggers, and R. M. Steinman**. 1993. Small amounts of superantigen, when presented on dendritic cells, are sufficient to initiate T cell responses. *J. Exp. Med. 178*:633.

80. **Nussenzweig, M. C., R. M. Steinman, B. Gutchinov, and Z. A. Cohn**. 1980. Dendritic cells are accessory cells for the development of anti-trinitrophenyl cytotoxic T lymphocytes. *J. Exp. Med. 152*:1070.

81. **Macatonia, S. E., P. M. Taylor, S. C. Knight, and B. A. Askonas**. 1989. Primary stimulation by dendritic cells induces antiviral proliferative and cytotoxic T cell responses in vitro. *J. Exp. Med. 169*:1255.

82. **Inaba, K., M. D. Witmer, and R. M. Steinman**. 1984. Clustering of dendritic cells, helper T lymphocytes, and histocompatible B cells during primary antibody responses in vitro. *J. Exp. Med. 160*:858.

83. **von Boehmer, H.** 1992. Thymic selection: a matter of life and death. *Immunol. Today 13*:454.

84. **Matzinger, P. and S. Guerder**. 1989. Does T-cell Tolerance Require a Dedicated Antigen-Presenting Cell? *Nature 338*:74.

85. **Gao, E., D. Lo, and J. Sprent**. 1990. Strong T cell Tolerance in Parent to F1 Bone Marrow Chimaeras Prepared with Supralethal Irradiation. *J. Exp. Med. 171(4)*:1101.

86. **Mazda, O., Y. Watanabe, J. Gyotoku, and Y. Katsura**. 1991. Requirement of Dendritic Cells and B cells in the Clonal Deletion of Mls-reactive T cells in the Thymus. *J. Exp. Med. 173(3)*:539.

87. **Inaba, M., K. Inaba, M. Hosono, T. Kumamoto, T. Ishida, S. Muramatsu, T. Masuda, and S. Ikehara**. 1991. Distinct mechanisms of neonatal tolerance induced by dendritic cells and thymic B cells. *J. Exp. Med. 173*:549.

88. **Carlow, D. A., N. S. C. van Oers, S. Teh, and H. Teh**. 1992. Deletion of Antigen-Specific Immature Thymocytes by Dendritic Cells Requires LFA-1/ICAM-1 Interactions. *J. Immunol. 148*:1595.

89. **Schuler, G. and R. M. Steinman**. 1985. Murine epidermal Langerhans cells mature into potent immunostimulatory dendritic cells in vitro. *J. Exp. Med. 161*:526.

90. **Pugh, C. W., G. G. MacPherson, and H. W. Steer**. 1983. Characterization of nonlymphoid cells derived from rat peripheral lymph. *J. Exp. Med. 157*:1758.

91. **Pancholi, P., A. Mirza, V. Schauf, R. M. Steinman, and N. Bhardwaj**. 1993. Presentation of mycobacterial antigens by human dendritic cells: lack of transfer from infected macrophages. *Infect. Immun. 61*:5326.

92. **Stössel, H., F. Koch, E. Kämpgen, P. Stöger, A. Lenz, C. Heufler, N. Romani, and G. Schuler**. 1990. Disappearance of certain acidic organelles (endosomes and Langerhans cell granules) accompanies loss of antigen processing capacity upon culture of epidermal Langerhans cells. *J. Exp. Med. 172*:1471.

93. **Romani, N., S. Koide, M. Crowley, M. Witmer-Pack, A. M. Livingstone, C. G. Fathman, K. Inaba, and R. M. Steinman**. 1989. Presentation of exogenous protein antigens

by dendritic cells to T cell clones. Intact protein is presented best by immature, epidermal Langerhans cells. *J. Exp. Med. 169*:1169.

94. **Crowley, M. T., K. Inaba, M. D. Witmer-Pack, S. Gezelter, and R. M. Steinman**. 1990. Use of the fluorescence activated cell sorter to enrich dendritic cells from mouse spleen. *J. Immunol. Methods 133*:55.

95. **Girolomoni, G., J. C. Simon, P. R. Bergstresser, and P. R. Cruz**. 1990. Freshly Isolated Spleen Dendritic Cells and Epidermal Langerhans Cells Undergo Similar Phenotypic and Functional Changes During Short Term Culture. *J. Immunol. 145*:2820.

96. **Reise Sousa, C., P. D. Stahl, and J. M. Austyn**. 1993. Phagocytosis of antigens by Langerhans cells *in vivo*. *J. Exp. Med. 178*:509.

97. **Inaba, K., M. Inaba, M. Naito, and R. M. Steinman**. 1993. Dendritic cell progenitors phagocytose particulates, including bacillus Calmette-Guerin organisms, and sensitize mice to mycobacterial antigens in vivo. *J. Exp. Med. 178*:479.

98. **Levine, T. P. and B. M. Chain**. 1992. Endocytosis by antigen presenting cells: dendritic cells are as endocytically active as other antigen presentting cells. *Proc. Natl. Acad. Sci. USA 89*:8342.

99. **Sallusto, F., M. Cella, C. Danieli, and A. Lanzavecchia**. 1995. Dendritic cells use macropinocytosis and the mannose receptor to concentrate macromolecules in the major histocompatibility complex class II compartment: downregulation by cytokines and bacterial products. *J. Exp. Med. 182*:389.

100. **Sallusto, F. and A. Lanzavecchia**. 1994. Efficient Presentation of Soluble Antigen by Cultured Human Dendritic Cells is Maintained by Granulocyte/Macrophage Colony Stimulating Factor Plus Interleukin 4 and Downregulated by Tumor Necrosis Factor α. *J. Exp. Med. 179*:1109.

101. **Nijman, H. W., M. J. Kleijmeer, M. A. Ossevoort, V. M. Oorschot, M. P. Vierboom, M. van de Keur, P. Kenemans, W. M. Kast, H. J. Geuze, and C. J. Melief**. 1995. Antigen capture and major histocompatibility class II compartments of freshly isolated and cultured human blood dendritic cells. *J. Exp. Med. 182*:163.

102. **Zaghouani, H., R. M. Steinman, R. Nonacs, H. Shah, W. Gerhard, and C. Bona**. 1993. Efficient presentation of a viral T helper epitope expressed in the CDR3 region of a self immunoglobulin molecule. *Science 259*:224.

103. **Jiang, W., W. J. Swiggard, C. Heufler, M. Peng, A. Mirza, R. M. Steinman, and M. C. Nussenzweig**. 1995. The Receptor DEC-205 Expressed by Dendritic Cells and Thymic Epithelial Cells is Involved in Antigen Processing. *Nature 375*:151.

104. **Puré, E., K. Inaba, M. T. Crowley, L. Tardelli, M. D. Witmer-Pack, G. Ruberti, G. Fathman, and R. M. Steinman**. 1990. Antigen processing by epidermal Langerhans cells

correlates with the level of biosynthesis of major histocompatibility complex class II molecules and expression of invariant chain. *J. Exp. Med. 172*:1459.

105. **Kämpgen, E., N. Koch, F. Koch, P. Stoger, C. Heufler, G. Schuler, and N. Romani**. 1991. Class II MHC Molecules of Murine Dendritic Cells: Synthesis, Sialylation of Invariant Chain, and Antigen Processing Capacity are Down-regulated upon Culture. *Proc. Natl. Acad. Sci. USA 88*:3014.

106. **Cumberbatch, M. and I. Kimber**. 1992. Dermal tumour necrosis factor-alpha induces dendritic cell migration to draining lymph nodes, and possibly provides one stimulus for Langerhans' cell migration. *Immunology 75*:257.

107. **Romani, N., G. Stingl, E. Tschachler, M. D. Witmer, R. M. Steinman, E. M. Shevach, and G. Schuler**. 1985. The Thy-1-bearing cell of murine epidermis. A distinctive leukocyte perhaps related to natural killer cells. *J. Exp. Med. 161*:1368.

108. **Knight, S. C., P. Fryer, S. Griffiths, and B. Harding**. 1987. Class II histocompatibility antigens on human dendritic cells. *Immunology 61*:21.

109. **Hart, D. N., G. C. Starling, V. L. Calder, and N. S. Fernando**. 1993. B7/BB-1 is a leucocyte differentiation antigen on human dendritic cells induced by activation. *Immunology 79*:616.

110. **Vremec, D., M. Zorbas, R. Scollay, D. J. Saunders, C. J. Ardavin, L. Wu, and K. Shortman**. 1992. The surface phenotype of dendritic cells purified from mouse thymus and spleen: investigation of the CD8 expression by a subpopulation of dendritic cells. *J. Exp. Med. 176*:47.

111. **Starling, G. C., A. D. McLellan, W. Egner, R. V. Sorg, J. Fawcett, D. L. Simmons, and D. N. J. Hart**. 1995. Intercellular adhesion protein-3 is the predominant co-stimulatory ligand for the leukocyte function antigen-1 on human blood dendritic cells. *Eur. J. Immunol. 25*:2528.

112. **Inaba, K. and R. M. Steinman**. 1987. Monoclonal antibodies to LFA-1 and to CD4 inhibit the mixed leukocyte reaction after the antigen-dependent clustering of dendritic cells and T lymphocytes. *J. Exp. Med. 165*:1403.

113. **Inaba, K. and R. M. Steinman**. 1986. Accessory cell-T lymphocyte interactions. Antigen-dependent and independent clustering. *J. Exp. Med. 163*:247.

114. **Young, J. W., L. Koulova, S. A. Soergel, E. A. Clark, R. M. Steinman, and B. Dupont**. 1992. The B7/BB1 antigen provides one of several costimulatory signals for the activation of CD4+ T lymphocytes by human blood dendritic cells in vitro [published erratum appears in J Clin Invest 1993 Apr;91(4):1853]. *J. Clin. Invest. 90*:229.

115. **Inaba, K., M. Witmer-Pack, M. Inaba, K. S. Hathcock, H. Sakuta, M. Azuma, H. Yagita, K. Okumura, P. S. Linsley, and S. Ikehara**. 1994. The tissue distribution of the B7-2

costimulator in mice: abundant expression on dendritic cells in situ and during maturation in vitro. *J. Exp. Med. 180*:1849.

116. **Larsen, C. P., S. C. Ritchie, R. Hendrix, P. S. Linsley, K. S. Hathcock, R. J. Hodes, R. P. Lowry, and T. C. Pearson**. 1994. Regulation of immunostimulatory function and costimulatory molecule (B7-1 and B7-2) expression on murine dendritic cells. *J. Immunol. 152*:5208.

117. **Caux, C., B. Vanbervliet, C. Massacrier, M. Azuma, K. Okumura, L. L. Lanier, and J. Banchereau**. 1994. B70/B7-2 is identical to CD86 and is the major functional ligand for CD28 expressed on human dendritic cells. *J. Exp. Med. 180*:1841.

118. **Caux, C., N. Burdin, L. Galibert, P. Hermann, N. Renard, C. Servet-Delprat, J. Banchereau**. 1994. Functional CD40 on B lymphocytes and dendritic cells. *Res. Immunol. 145*:235.

119. **Noelle, R. J., J. A. Ledbetter, and A. Aruffo**. 1992. CD40 and its ligand, an essential ligand-receptor pair for thymus-dependent B cell activation. *Immunol. Today 13*:431.

120. **Caux, C., C. Massacrier, B. Vanbervliet, B. Dubois, C. Van Kooten, I. Durand, and J. Banchereau**. 1994. Activation of human dendritic cells through CD40 cross-linking. *J. Exp. Med. 180*:1263.

121. **Ludewig, B., D. Graf, H. R. Gelderblom, Y. Becker, R. A. Kroczek, and G. Pauli**. 1995. Spontaneous apoptosis of dendritic cells is efficiently inhibited by TRAP (CD40-ligand) and TNF-alpha, but strongly enhanced by interleukin-10. *Eur. J. Immunol. 25*:1943.

122. **O'Doherty, U., R. M. Steinman, M. Peng, P. U. Cameron, S. Gezelter, I. Kopeloff, W. J. Swiggard, M. Pope, and N. Bhardwaj**. 1993. Dendritic Cells Freshly Isolated from Human Blood Express CD4 and Mature into Typical Immunostimulatory Dendritic Cells after Culture in Monocyte-conditioned Medium. *J. Exp. Med. 178*:1067.

123. **Bieber, T. A., A. Rieger, C. Neuchrist, J. C. Prinz, E. P. Rieber, G. Boltz-Nitulescu, O. Scheiner, D. Kraft, J. Ring, and G. Stingl**. 1989. Induction of FcεR2/CD23 on human epidermal Langerhans cells by human recombinant IL-4 and gamma interferon. *J. Exp. Med. 170*:309.

124. **Bieber, T., H. de la Salle, A. Wollenberg, J. Hakimi, R. Chizzonite, J. Ring, D. Hanau, and C. de la Salle**. 1992. Human epidermal Langerhans cells express the high affinity receptor for immunoglobulin E (FcεRI). *J. Exp. Med. 175*:1285.

125. **Preesman, A. H., J. G. Van de Winkel, C. G. Magnusson, J. Toonstra, S. C. van der Putte, and W. A. van Vloten**. 1991. Cell-bound IgE and increased expression of Fc epsilon-receptors on dendritic cells in cutaneous infiltrates of mycosis fungoides. *Clin. Exp. Immunol. 86*:246.

126. **Bieber, T.** 1994. Fc epsilon RI on human Langerhans cells: a receptor in search of new functions. [Review]. *Immunol. Today 15*:52.

127. **Bieber, T., M. Jurgens, A. Wollenberg, E. Sander, D. Hanau, and H. de la Salle**. 1995. Characterization of the Protein Tyrosine Phosphatase CD45 on Human Epidermal Langerhans cells. *Eur. J. Immunol. 25*:317.

128. **Steinman, R. M., M. Witmer-Pack, and K. Inaba**. 1993. Dendritic cells: antigen presentation, accessory function and clinical relevance. [Review]. *Adv. Exp. Med. Biol. 329*:1.

129. **Barclay, A. N., M. L. Birkeland, M. H. Brown**, et al. 1993. *The leukocyte antigen facts book*. Academic Press, London.

130. **Nair, S., F. Zhou, R. Reddy, L. Huang, and B. T. Rouse**. 1992. Soluble proteins delivered to dendritic cells via pH-sensitive liposomes induce primary cytotoxic T lymphocyte responses in vitro. *J. Exp. Med. 175*:609.

131. **Boog, C., J. Boes, and C. J. M. Melief**. 1988. Role of Dendritic Cells in the Regulation of Class I Restricted Cytotoxic T Lymphocyte Responses. *J. Immunol. 140*:3331.

132. **Cohen, P. J., P. A. Cohen, S. A. Rosenberg, S. I. Katz, and J. J. Mule**. 1994. Murine epidermal Langerhans cells and splenic dendritic cells present tumor-associated antigens to primed T cells. *Eur. J. Immunol. 24*:315.

133. **Flamand, V., T. Sornasse, K. Thielemans, C. Demanet, M. Bakkus, H. Bazin, F. Tielemans, O. Leo, J. Urbain, and M. Moser**. 1994. Murine dendritic cells pulsed in vitro with tumor antigen induce tumor resistance in vivo. *Eur. J. Immunol. 24*:605.

134. **Romani, N., S. Gruner, D. Brang, E. Kämpgen, A. Lenz, B. Trockenbacher, G. Konwalinka, P. O. Fritsch, R. M. Steinman, and G. Schuler**. 1994. Proliferating Dendritic Cell Progenitors in Human Blood. *J. Exp. Med. 180*:83.

135. **Nonacs, R., C. Humborg, J. P. Tam, and R. M. Steinman**. 1992. Mechanisms of mouse spleen dendritic cell function in the generation of influenza-specific, cytolytic T lymphocytes. *J. Exp. Med. 176*:519.

136. **Steinman, R. M.** 1989. Dendritic cells: clinical aspects. *Res. Immunol. 140*:911.

137. **Knight, S. C., J. Farrant, J. Chan, A. Bryant, P. A. Bedford, and C. Bateman**. 1988. Induction of autoimmunity with dendritic cells: studies on thyroiditis in mice. *Clin. Immunol. Immunopathol. 48*:277.

138. **Stagg, A., B. Harding, R. A. Hughes, A. Keat, and S. C. Knight**. 1991. The Distribution and Functional Properties of Dendritic Cells in Patients with Seronegative Arthritis. *Clin. Exp. Immunol. 84(1)*:66.

139. **Austyn, J. M.** 1993. Dendritic cells in transplantation. [Review]. *Adv. Exp. Med. Biol. 329*:489.

140. **Larsen, C. P., R. M. Steinman, M. Witmer-Pack, D. F. Hankins, P. J. Morris, and J. M. Austyn**. 1990. Migration and maturation of Langerhans cells in skin transplants and explants. *J. Exp. Med. 172*:1483.

141. **Larsen, C. P. and J. M. Austyn**. 1991. Langerhans cells migrate out of skin grafts and cultured skin: a model in which to study the mediators of dendritic leukocyte migration. *Transplant. Proc. 23*:117.

142. **Austyn, J. M., D. F. Hankins, C. P. Larsen, P. J. Morris, A. S. Rao, and J. A. Roake**. 1994. Isolation and characterization of dendritic cells from mouse heart and kidney. *J. Immunol. 152*:2401.

143. **Iwai, H., S. Kuma, M. Inaba, R. A. Good, T. Yamashita, T. Kumazawa, and S. Ikehara**. 1989. Acceptance of Murine Thyroid Allografts by Pretreatment of Anti-Ia Antibody or Anti-Dendritic Cell Antibody In Vitro. *Transplantation 47*:45.

144. **Faustman, D. L., R. M. Steinman, H. M. Gebel, V. Hauptfeld, J. M. Davie, and P. E. Lacy**. 1984. Prevention of rejection of murine islet allografts by pretreatment with anti-dendritic cell antibody. *Proc. Natl. Acad. Sci. USA 81*:3864.

145. **Meltzer, M. S., D. R. Skillman, P. J. Gomatos, C. Kalter, and H. E. Gendelman**. 1990. Role of mononuclear phagocytes in the pathogenesis of HIV infection. *Annu. Rev. Immunol. 8*:169.

146. **Cameron, P. U., M. G. Lowe, S. M. Crowe, U. O'Doherty, M. Pope, S. Gezelter, and R. M. Steinman**. 1994. Susceptibility of dendritic cells to HIV-1 infection in vitro. [Review]. *J. Leuk. Biol. 56*:257.

147. **Patterson, S. and S. C. Knight**. 1987. Susceptibility of human peripheral blood dendritic cells to infection by human immunodeficiency virus. *J. Gen. Virol. 68*:1177.

148. **Langhoff, E., E. F. Terwilliger, H. J. Bos, K. H. Kalland, M. C. Poznansky, O. M. Bacon, and W. A. Haseltine**. 1991. Replication of human immunodeficiency virus type 1 in primary dendritic cell cultures. *Proc. Natl. Acad. Sci. USA 88*:7998.

149. **Pope, M., M. G. Betjes, N. Romani, H. Hirmand, P. U. Cameron, L. Hoffman, S. Gezelter, G. Schuler, and R. M. Steinman**. 1994. Conjugates of dendritic cells and memory T lymphocytes from skin facilitate productive infection with HIV-1. *Cell 78*:389.

150. **Cameron, P. U., P. S. Freudenthal, J. M. Barker, S. Gezelter, K. Inaba, and R. M. Steinman**. 1992. Dendritic cells exposed to human immunodeficiency virus type-1 transmit a vigorous cytopathic infection to CD4+ T cells [published erratum appears in Science 1992 Sep;257(5078):1848]. *Science 257*:383.

151. **Nunnari, J. and P. Walker**. 1992. Protein targeting to and translocation across the membrane of the endoplasmic reticulum. *Curr. Opin. Cell Biol. 4*:573.

152. **Noiva, R. and W. J. Lennarz**. 1992. Protein disulfide isomerase. A multifunctional protein resident in the lumen of the endoplasmic reticulum. *J. Biol. Chem. 267*:3553.

153. **Kornfeld, R. and S. Kornfeld**. 1985. Assembly of asparagine-linked oligosaccharides. *Annu. Rev. Biochem. 54*:631.

154. **Hirschberg, C. B. and M. D. Snider**. 1987. Topography of glycosylation in the rough endoplasmic reticulum and golgi apparatus. *Annu. Rev. Biochem. 56*:63.

155. **Goldberg, D. E., C. A. Gabel, and S. Kornfeld**. 1983. Studies of the biosynthesis of the mannose 6-phosphate receptor in receptor-positive and -deficient cell lines. *J. Cell Biol. 97*:1700.

156. **Gabel, C. A., D. E. Goldberg, and S. Kornfeld**. 1982. Lysosomal enzyme oligosaccharide phosphorylation in mouse lymphoma cells: specificity and kinetics of binding to the mannose 6-phosphate receptor in vivo. *J. Cell Biol. 95*:536.

157. **Parekh, R. B., A. G. Tse, R. A. Dwek, A. F. Williams, and T. W. Rademacher**. 1987. Tissue-specific N-glycosylation, site-specific oligosaccharide patterns and lentil lectin recognition of rat Thy-1. *EMBO J. 6*:1233.

158. **Rademacher, T. W., R. B. Parekh, and R. A. Dwek**. 1988. Glycobiology. [Review]. *Annu. Rev. Biochem. 57*:785.

159. **Sadler, J. E.** 1984. *Biosynthesis of glycoproteins: formation of O-linked oligosaccharides*. p. 199.

160. **Trombetta, S. E. and A. J. Parodi**. 1992. Purification to apparent homogeneity of rat liver UDP-Glc:glycoprotein glucosyltransferase. *J. Biol. Chem. 267*:9236.

161. **Sousa, M. and A. J. Parodi**. 1995. The molecular basis for the recognition of misfolded glycoproteins by the UDP-Glc:glycoprotein glucotransferase. *EMBO J. 14*:4196.

162. **Hammond, C., I. Braakman, and A. Helenius**. 1994. Role of N-linked oligosaccharide recognition, glucose trimming, and calnexin in glycoprotein folding and quality control. *Proc. Natl. Acad. Sci. USA 91*:913.

163. **Helenius, A.** 1994. How N-linked oligosaccharides affect glycoprotein folding in the endoplasmic reticulum. *Mol. Biol. Cell. 5*:253.

164. **Scheiffele, P., J. Peränen, and K. Simons**. 1995. N-glycans as apical sorting signals in epithelial cells. *Nature 378*:96.

165. **Parekh, R. B., R. A. Dwek, B. J. Sutton, D. L. Fernandes, A. Leung, D. Stanworth, T. W. Rademacher, T. Mizuochi, T. Taniguchi, and K. Matsuta**. 1985. Association of

rheumatoid arthritis and primary osteoarthritis with changes in the glycosylation pattern of total serum IgG. *Nature 316*:452.

166. **Wyss, D. F., J. S. Choi, J. Li, M. H. Knoppers, K. J. Willis, A. R. N. Arulanandam, A. Smolyar, E. L. Reinherz, and G. Wagner**. 1995. Conformation and function of the N-linked glycan in the adhesion domain of human CD2. *Science 269*:1273.

167. **Driscoll, P. C., J. G. Cyster, I. D. Campbell, and A. F. Williams**. 1991. Structure of domain 1 of rat T lymphocyte CD2 antigen. *Nature 353*:762.

168. **Woollett, G. R., A. F. Williams, and D. M. Shotton**. 1985. Visualisation by low-angle shadowing of the leukocyte-common antigen. A major cell surface glycoprotein of lymphocytes. *EMBO J. 4*:2827.

169. **Cyster, J. G., D. M. Shotton, and A. F. Williams**. 1991. The dimensions of the T lymphocyte glycoprotein leukosialin and identification of linear protein epitopes that can be modified by glycosylation. *EMBO J. 10*:893.

170. **Drickamer, K. and M. E. Taylor**. 1993. Biology of Animal Lectins. *Annu. Rev. Cell Biol. 9*:237.

171. **Powell, L. D., D. Sgroi, E. R. Sjoberg, I. Stamenkovic, and A. Varki**. 1993. Natural ligands of the B cell adhesion molecule CD22b carry N-linked oligosaccharides with a2-6 linked sialic acids that are required for recognition. *J. Biol. Chem. 268*:7019.

172. **Crocker, P. R., S. Mucklow, V. Bouckson, A. McWilliam, A. C. Willis, S. Gordon, G. Milon, S. Kelm, and P. Bradfield**. 1994. Sialoadhesin, a Macrophage Sialic Acid Binding Receptor for Haemopoietic Cells with 17 Immunoglobulin-like Domains. *EMBO J. 13*:4490.

173. **Varki, A.** 1994. Selectin Ligands. *Proc. Natl. Acad. Sci. USA 91*:7390.

174. **Ley, K. and T. F. Tedder**. 1995. Leukocyte interactions with vascular endothelium: new insights into selectin-mediated attachment and rolling. *J. Immunol. 155*:525.

175. **Rosen, S. D. and C. R. Bertozzi**. 1994. The selectins and their ligands. *Curr. Opin. Cell Biol. 6*:663.

176. **Hattori, R., K. K. Hamilton, R. D. Fugate, R. P. McEver, and P. J. Sims**. 1989. Stimulated secretion of endothelial von Willebrand factor is accompanied by rapid redistribution to the cell surface of the intracellular granule membrane protein GMP-140. *J. Biol. Chem. 264*:7768.

177. **Larsen, E., A. Celi, G. E. Gilbert, B. C. Furie, J. K. Erban, R. Bonfanti, D. D. Wagner, and B. Furie**. 1989. PADGEM protein: a receptor that mediates the interaction of activated platelets with neutrophils and monocytes. *Cell 59*:305.

178. **Lawrence, M. B. and T. A. Springer**. 1991. Leukocytes roll on selectin at physiologic flow rates: distinction from and prerequisite for adhesion through integrins. *Cell 65*:857.

179. **Springer, T. A.** 1994. Traffic Signals for Lymphocyte Recirculation and Leukocyte Emigration: The MultiStep Paradigm. *Cell 76*:301.

180. **Mayadas, T. N., H. R. Johnson, R. O. Hynes, and D. D. Wagner**. 1993. Leukocyte rolling and extravasation are severely compromised in P selectin-deficient mice. *Cell 74*:541.

181. **Lasky, L. A., M. S. Singer, T. A. Yednock, D. Dowbenko, C. Fennie, H. Rodriguez, T. Nguyen, S. Stachel, and S. D. Rosen**. 1989. Cloning of a lymphocyte homing receptor reveals a lectin domain. *Cell 56*:1045.

182. **Bowen, B., C. Fennie, and L. A. Lasky**. 1990. The MEL-14 antibody binds to the lectin domain of the murine peripheral lymph node homing receptor. *J. Biol. Chem. 110*:147.

183. **Pouyani, T. and B. Seed**. 1995. PSGL-1 recognition of P-selectin is controlled by a tyrosine sulfation consensus at the PSGL-1 amino terminus. *J. Immunol. 83*:333.

184. **Sako, D., K. M. Comess, K. Barone, R. T. Camphausen, D. A. Cumming, and G. D. Shaw**. 1995. A sulfated peptide segment at the amino terminus of PSGL-1 is critical for P-selectin binding. *Cell 83*:323.

185. **Vercelli, D., B. Helm, P. Marsh, E. Padlan, R. S. Geha, and H. Gould**. 1989. The B cell binding site on human immunoglobulin E. *Nature 338*:649.

186. **Aubry, J., S. Pochon, P. Graber, K. U. Jansen, and J. Bonnefoy**. 1992. CD21 is a ligand for CD23 and regulates IgE production. *Nature 358*:505.

187. **Pochon, S., P. Graber, M. Yeager, K. Jansen, A. R. Bernard, J. Aubry, and J. Bonnefoy**. 1992. Demonstration of a second ligand for the low affinity receptor for IgE (CD23) using recombinant CD23 reconstituted into fluorescent liposomes. *J. Exp. Med. 176*:389.

188. **Spiess, M.** 1990. The asialoglycoprotein receptor: a model for endocytic transport receptors. [Review]. *Biochemistry 29*:10009.

189. **Holmskov, U., R. Malhotra, R. B. Sim, and J. C. Jensenius**. 1994. Collectins: collagenous C-type lectins of the innate immune defense system. *Immunol. Today 15*:67.

190. **Ezekowitz, R. A. B., K. Sastry, P. Baily, and A. Warner**. 1990. Molecular characterization of the human macrophage mannose receptor: demonstration of multiple carbohydrate recognition-like domains and phagocytosis of yeasts in COS-1 cells. *J. Exp. Med. 172*:1785.

191. **Kuhlman, M., K. Joiner, and R. A. Ezekowitz**. 1989. The human mannose-binding protein functions as an opsonin. *J. Exp. Med. 169*:1733.

192. **Lu, J., A. C. Willis, and K. B. Reid**. 1992. Purification, characterization and cDNA cloning of human lung surfactant protein D. *Biochem. J. 284*:795.

193. **Barondes, S. H., V. Castronovo, D. N. W. Cooper, R. D. Cummings, K. Drickamer, T. Feinzi, M. A. Gitt, J. Hirabayashi, C. Hughes, K. Kasai, H. Leffler, F. Liu, R. Lotan, A. M. Mercurio, M. Monsigny, S. Pillai, F. Poirer, A. Raz, P. W. J. Rigby, J. M. Rini, and J. L. Wang**. 1994. Galectins: a family of animal β-galactoside binding lectins. *Cell 76*:597.

194. **Baum, L. G., M. Pang, N. L. Perillo, T. Wu, A. Delegeane, C. H. Uittenbogaart, M. Fukuda, and J. J. Seilhamer**. 1995. Human Thymic Epithelial Cells Express an Endogenous Lectin, Galectin-1, which Binds to Core 2 O-Glycans on Thymocytes and T Lymphoblastoid Cells. *J. Exp. Med. 181*:877.

195. **Perillo, N. L., K. E. Pace, J. J. Seilhamer, and L. G. Baum**. 1995. Apoptosis of T cells mediated by galectin-1. *Nature 378*:736.

196. **Frigeri, L. G., R. I. Zuberi, and F. T. Liu**. 1993. εBP, a beta-galactoside-binding animal lectin, recognizes IgE receptor (FcεRI) and activates mast cells. *Biochemistry 32*:7644.

197. **Wollenberg, A., H. de la Salle, D. Hanau, F. T. Liu, and T. Bieber**. 1993. Human keratinocytes release the endogenous beta-galactoside-binding soluble lectin immunoglobulin E (IgE-binding protein) which binds to Langerhans cells where it modulates their binding capacity for IgE glycoforms. *J. Exp. Med. 178*:777.

198. **Jeng, K. C., L. G. Frigeri, and F. T. Liu**. 1994. An endogenous lectin, galectin-3 (epsilon BP/Mac-2), potentiates IL-1 production by human monocytes. *Immunol. Lett. 42*:113.

199. **Woo, H. J., L. M. Shaw, J. M. Messier, and A. M. Mercurio**. 1990. The major non-integrin laminin binding protein of macrophages is identical to carbohydrate binding protein 35 (Mac-2). *J. Biol. Chem. 265*:7097.

200. **Ahmed, H. and G. R. Vasta**. 1994. Galectins: conservation of functionally and structurally relevant amino acid residues defines two types of carbohydrate recognition domains. *Glycobiology 4*:545.

201. **Sgroi, D., A. Varki, S. Braesch-Anderson, and I. Stamenkovic**. 1993. CD22, a B Cell-specific Immunoglobulin Superfamily Member, Is a Sialic Acid-binding Lectin. *J. Biol. Chem. 268*:7011.

202. **Crocker, P. R., S. Kelm, C. Dubois, B. Martin, A. S. McWilliam, D. M. Shotton, J. C. Paulson, and S. Gordon**. 1991. Purification and Properties of Sialoadhesin, a Sialic Acid-binding Receptor of Murine Tissue Macrophages. *EMBO J. 10*:1661.

203. **Lesley, J., R. Hyman, and P. W. Kincade**. 1993. CD44 and Its Interaction with Extracellular Matrix. *Adv. Immunol. 54*:271.

204. **Katoh, S., Z. Zheng, K. Oritani, T. Shimozato, and P. W. Kincade**. 1995. Glycosylation of CD44 Negatively Regulates Its Recognition of Hyaluronan. *J. Exp. Med. 182*:419.

205. **Lesley, J., N. English, A. Perschl, J. Gregoroff, and R. Hyman**. 1995. Variant Cell Lines Selected for Alterations in the Function of the Hyaluronan Receptor CD44 Show Differences in Glycosylation. *J. Exp. Med. 182*:431.

206. **Green, E. D. and J. U. Baenziger**. 1988. Asparagine-linked oligosaccharides on lutropin follitropin and thyrotropin: I. Structural elucidation of the sulfated and sialylated oligosaccharides on bovine, ovine, and human pituitary glycoprotein hormones. *J. Biol. Chem. 263*:25.

207. **Smith, P. L. and J. U. Baenziger**. 1992. Molecular basis of recognition by the glycoprotein hormone-specific N-acetylgalactosamine-transferase. *Proc. Natl. Acad. Sci. USA 89*:329.

208. **Fiete, D., V. Srivastava, O. Hindsgaul, and J. U. Baenziger**. 1991. A Hepatic Reticuloendothelial Cell Receptor Specific for SO_4-4GalNAcb1,4GlcNAcb1,2Mana That Mediates Rapid Clearance of Lutropin. *Cell 67*:1103.

209. **Huttner, W. B.** 1982. Sulphation of tyrosine residues- a widespread modification of proteins. *Nature 299*:273.

210. **Hortin, G. L., T. C. Farries, J. P. Graham, and J. P. Atkinson**. 1989. Sulfation of tyrosine residues increases activity of the fourth component of complement. *Proc. Natl. Acad. Sci. USA 86*:1338.

211. **Leyte, A., H. B. van Schijndel, C. Niehrs, W. B. huttner, M. P. Verbeet, K. Mertens, and J. A. van Mourik**. 1990. Sulfation of tyr1680 of human blood coagulation factor VIII is essential for the interaction of factor VIII with von Willebrand factor. *J. Biol. Chem. 266*:740.

212. **Hofsteenge, J., S. R. Stone, A. Donella-Deana, and L. A. Pinna**. 1990. The effect of the substitution of phosphotyrosine for sulphotyrosine on the activity of hirudin. *Eur. J. Biochem. 188*:55.

213. **Bundgaard, J. R., J. Vuunst, and J. F. Rehfeld**. 1995. Tyrosine 0-sulfation promotes proteolytic processing of progastrin. *EMBO J. 14*:3073.

214. **Kjellén, L. and U. Lindahl**. 1991. Proteoglycans: Structures and Interactions. *Annu. Rev. Biochem. 60*:443.

215. **Bame, K. J., R. V. Reddy, and J. D. Esko**. 1991. Coupling of N-deacetylation and N-sulfation in a Chinese hamster ovary cell mutant defective in heparan sulfate N-sulfotransferase. *J. Biol. Chem. 266*:12461.

216. **Naujokas, M. F., M. Morin, M. S. Anderson, M. Peterson, and J. Miller**. 1993. The Chondroitin Sulfate Form of Invariant Chain Can Enhance Stimulation of T Cell Responses through Interaction with CD44. *Cell 74*:257.

217. **Jalkanen, S. and M. Jalkanen**. 1992. Lymphocyte CD44 Binds the COOH-terminal Heparin-binding Domain of Fibronectin. *J. Cell Biol. 116*:817.

218. **Aruffo, A., I. Stamenkovic, M. Melnick, C. B. Underhill, and B. Seed**. 1990. CD44 Is the Principal Cell Surface Receptor for Hyaluronate. *Cell 61*:1303.

219. **Arch, R., K. Wirth, M. Hofmann, H. Ponta, S. Matzku, P. Herrlich, and M. Zöller**. 1992. Participation in normal immune responses of a metastasis-inducing splice variant of CD44. *Science 257*:682.

220. **Rapraeger, A. C., A. Krufka, and B. B. Olwin**. 1991. Requirement of Heparan Sulfate for bFGF-Mediated Fibroblast Growth and Myoblast Differentiation. *Science 252*:1705.

221. **Ornitz, D. M., A. B. Herr, M. Nilsson, J. Westman, C. Svahn, and G. Waksman**. 1995. FGF Binding and FGF Receptor Activation by Synthetic Heparan-Derived Di- and Trisaccharides. *Science 268*:432.

222. **Tanaka, Y., D. H. Adams, S. Hubscher, H. Hirano, U. Siebenlist, and S. Shaw**. 1993. T-cell adhesion induced by proteoglycan-immobilized cytokine MIP-1β. *Nature 361*:79.

223. **Ullrich, A. and J. Schlessinger**. 1990. Signal transduction by receptors with tyrosine kinase activity. *Cell 61*:203.

224. **Heldin, C.** 1995. Dimerization of cell surface receptors in signal transduction. *Cell 80*:213.

225. **App, H., R. Hazan, A. Zilberstein, J. Schlessinger, and U. R. Rapp**. 1991. EGF stimulates association and kinase activity of RAF-1 with the EGF receptor. *Mol. Cell. Biol. 11*:913.

226. **Kyriakis, J. M., H. App, X. Zhang, P. Banerjee, D. L. Brautigan, U. R. Rapp, and J. Avruch**. 1992. Raf-1 activates MAP kinase-kinase. *Nature 358*:417.

227. **Howe, L. R., S. J. Leevers, N. Gomez, S. Nakielny, P. Cohen, and C. J. Marshall**. 1992. Activation of the MAP kinase pathway by the protein kinase raf. *Cell 71*:335.

228. **Dent, P., T. A. Haystead, W. Haser, L. A. Vincent, T. M. Roberts, and T. W. Sturgill**. 1992. v-Raf protein kinase activates MAP kinase-kinase in NIH3T3 cells and *in vitro*. *Science 257*:1404.

229. **Mochly-Rosen, D.** 1995. Localization of protein kinases by anchoring proteins: a theme in signal transduction. *Science 268*:247.

230. **Pawson, T.** 1995. Protein modules and signalling networks. *Nature* 373:573.

231. **Chan, A. C., D. M. Desai, and A. Weiss**. 1994. The role of protein tyrosine kinases and protein tyrosine phosphatases in T cell antigen receptor signal transduction. *Annu. Rev. Immunol. 12*:555.

232. **Sefton, B. M. and M. Campbell**. 1991. The Role of Tyrosine Protein Phosphorylation in Lymphocyte Activation. *Annu. Rev. Cell Biol. 7*:257.

233. **Koretzky, G. A., M. Kohnmetscher, and S. Ross**. 1993. CD45-associated kinase activity requires lck but not T cell receptor expression in the Jurkat T cell line. *J. Biol. Chem. 268*:8958.

234. **Caron, L., N. Abraham, T. Pawson, and A. Veillette**. 1992. Structural requirements for enhancement of T cell responsiveness by the lymphocyte-specific tyrosine protein kinase $p56^{lck}$. *Mol. Cell. Biol. 12*:2720.

235. **Veillette, A., M. A. Bookman, E. M. Horak, and J. B. Bolen**. 1988. The CD4 and CD8 T cell surface antigens are associated with the internal membrane tyrosine kinase $p56^{lck}$. *Cell 55*:301.

236. **Hatakeyama, M., T. Kono, N. Kobayashi, A. Kawahara, S. D. Levin, R. M. Perlmutter, and T. Tanaguchi**. 1991. Interaction of the IL-2 receptor with the *src* family kinase $p56^{lck}$: identification of a novel intermolecular interaction. *Science 252*:1523.

237. **Ng, D. H. W., J. D. Watts, R. Aebersold, and P. Johnson**. 1996. Demonstration of a direct interaction between $p56^{lck}$ and the cytoplasmic domain of CD45 *in vitro*. *J. Biol. Chem. 271*:1295.

238. **Cambier, J. C.** 1995. Antigen and Fc receptor signaling: the awesome power of the immunoreceptor tyrosine-based activation motif (ITAM). *J. Immunol. 155*:3281.

239. **Crabtree, G. R. and N. A. Clipstone**. 1994. Signal transmission between the plasma membrane and nucleus of T lymphocytes. *Annu. Rev. Biochem. 63*:1045.

240. **Sieh, M., J. B. Bolen, and A. Weiss**. 1993. CD45 specifically modulates binding of Lck to a phosphopeptide encompassing the negative regulatory tyrosine of Lck. *EMBO J. 12*:315.

241. **Rapp, U. R., M. D. Goldsborough, G. E. Mark, T. I. Bonner, J. Groffen, F. H. Reynolds, and J. R. Stephenson**. 1983. Structure and biological activity of v-raf, a unique oncogene transduced by a retrovirus. *Proc. Natl. Acad. Sci. USA 80*:4218.

242. **Siegel, J. N., R. D. Klausner, U. R. Rapp, and L. E. Samelson**. 1990. T cell antigen receptor engagement stimulates c-raf phosphorylation and induces c-raf kinase activity via a protein kinase C-dependent pathway. *J. Biol. Chem. 265*:18472.

243. **Peter, M., A. Gartner, J. Horecka, G. Ammerer, and I. Herskowitz**. 1993. FAR1 links the signal transduction pathway to the cell cycle machinery in yeast. *Cell 73*:747.

244. **Pulverer, B. J., J. M. Kyriakis, J. Avruch, E. Nikolakaki, and J. R. Woodgett**. 1991. Phosphorylation of c-jun mediated by MAP kinases. *Nature 353*:670.

245. **Sweeney Crovello, C., B. C. Furie, and B. Furie**. 1995. Histidine Phosphorylation of P-Selectin upon Stimulation of Human Platelets: A Novel Pathway for Activation-Dependent Signal Transduction. *Cell 82*:279.

246. **Sefton, B. M. and J. E. Buss**. 1987. The covalent modification of eukaryotic proteins with lipid. *J. Cell Biol. 104*:1449.

247. **Willumsen, B. M., K. Norris, A. G. Papageorge, N. L. Hubbert, and D. R. Lowry**. 1984. Harvey murine sarcoma virus p21 ras protein: biological and biochemical significance of the cysteine nearest the carboxy terminus. *EMBO J. 3*:2581.

248. **Schmidt, B., T. Selmer, A. Ingendoh, and K. von Figura**. 1995. A Novel Amino Acid Modification in Sulfatases That is Defective in Multiple Sulfatase Deficiency. *Cell 82*:271.

249. **Kolodny, E. H. and A. L. Fluharty**. 1995. Metachromatic leukodystrophy and multiple sulfatase deficiency: sulfatide lipidosis. In *The Metabolic and Molecular Bases of Inherited Disease*. C.R. Scriver, A.L. Beaudet, W.S. Sly and D. Valle, eds. McGraw-Hill, NY, USA, p. 2693.

250. **Ciechanover, A.** 1994. The ubiquitin-proteasome proteolytic pathway. *Cell 79*:13.

251. **Doering, T. L.** 1993. Glycosyl Phosphatidylinositol-linked membrane proteins: structure, function, biosynthesis, and function. In *Cell surface and extracellular glycoconjugates*. D.D. Roberts and R.P. Mecham, eds. Academic Press Ltd. NY, NY, USA, p. 83.

252. **Ferguson, M. A. J. and A. F. Williams**. 1988. Cell-Surface Anchoring Of Proteins Via Glycosyl-Phosphatidylinositol Structures. *Annu. Rev. Biochem. 57*:285.

253. **Moran, P., H. Raab, W. J. Kohr, and I. W. Caras**. 1991. Glycophospholipid membrane anchor attachment: molecular analysis of the cleavage/attachment site. *J. Biol. Chem. 266*:1250.

254. **Zhang, F., B. Crise, B. Su, Y. Hou, J. K. Rose, A. Bothwell, and K. Jacobson**. 1991. Lateral diffusion of membrane-spanning and GPI-linked proteins: toward establishing rules governing the lateral mobility of membrane proteins. *J. Cell Biol. 115*:75.

255. **Rothberg, K. G., Y. Ying, J. F. Kolhouse, B. A. Kamen, and R. G. W. Anderson**. 1990. The Glycophospholipid-linked Folate Receptor Internalizes Folate Without Entering the Clathrin-coated Pit Endocytic Pathway. *J. Cell Biol. 110*:637.

256. **Rothberg, K. G., J. E. Heuser, W. C. Donzell, Y. S. Ying, J. R. Glenney, and R. G. W. Anderson**. 1992. Caveolin, a Protein Component of Caveolae Membrane Coats. *Cell 68*:673.

257. **O'Doherty, U., W. J. Swiggard, K. Inaba, Y. Yamaguchi, I. Kopeloff, N. Bhardwaj, and R. M. Steinman**. 1993. Tolerizing mice to human leukocytes: a step toward the production of monoclonal antibodies specific for human dendritic cells. *Adv. Exp. Med. Biol. 329*:165.

258. **Nussenzweig, M. C., R. M. Steinman, M. D. Witmer, and B. Gutchinov**. 1982. A monoclonal antibody specific for mouse dendritic cells. *Proc. Natl. Acad. Sci. USA 79*:161.

259. **Metlay, J. P., M. D. Witmer-Pack, R. Agger, M. T. Crowley, D. Lawless, and R. M. Steinman**. 1990. The distinct leukocyte integrins of mouse spleen dendritic cells as identified with new hamster monoclonal antibodies. *J. Exp. Med. 171*:1753.

260. **Breel, M., R. Mebius, and G. Kraal**. 1987. Dendritic Cells of the Mouse Recognized by Two Monoclonal Antibodies. *Eur. J. Immunol. 17*:1555.

261. **Kraal, G., M. Breel, M. Janse, and G. Bruin**. 1986. Langerhans' Cells, Veiled Cells, and Interdigitating Cells in the Mouse Recognized by a Monoclonal Antibody. *J. Exp. Med. 163*:981.

262. **Inaba, K., W. J. Swiggard, M. Inaba, J. Meltzer, A. Mirza, T. Sasagawa, M. C. Nussenzweig, and R. M. Steinman**. 1995. Tissue distribution of the DEC-205 protein that is detected by the monoclonal antibody NLDC-145. I. Expression on dendritic cells and other subsets of mouse leukocytes. *Cell Immunol. 163*:148.

263. **Crowley, M., K. Inaba, M. Witmer-Pack, and R. M. Steinman**. 1989. The cell surface of mouse dendritic cells: FACS analyses of dendritic cells from different tissues including thymus. *Cell Immunol. 118*:108.

264. **Austyn, J. M. and S. Gordon**. 1981. F4/80, a Monoclonal Antibody Directed Specifically Against the Mouse Macrophage. *Eur. J. Immunol. 11*:805.

265. **Witmer-Pack, M. D., W. Olivier, J. Valinsky, G. Schuler, and R. M. Steinman**. 1987. Granulocyte/Macrophage Colony-Stimulating Factor is Essential for the Viability and Function of Cultured Murine Epidermal Langerhans Cells. *J. Exp. Med. 166*:1484.

266. **Johnson, P., A. Maiti, and D. H. W. Ng**. 1995. CD45: A Family of Leukocyte Specific Cell Surface Proteins. In *Handbook of Experimental Immunology*. 5th ed. D.M. Weir, L.A. Herzenberg and L.A. Herzenberg, eds. Blackwell Scientific Publications, Oxford, England.

267. **Stokes, R. W., I. D. Haidl, W. A. Jefferies, and D. P. Speert**. 1993. Mycobacteria-Macrophage Interactions: macrophages phenotype determines the nonopsonic binding of *Mycobacterium tuberculosis* to murine macrophages. *J. Immunol. 12*:7067.

268. **Radka, S. F., D. D. Kostyu, and D. B. Amos**. 1982. A Monoclonal Antibody Directed Against the HLA-Bw6 Epitope. *J. Immunol. 128(6)*:2804.

269. **Chui, D., C. J. Ong, P. J. Johnson, H. Teh, and J. Marth**. 1994. Specific CD45 Isoforms Differentially Regulate T cell Receptor Signaling. *EMBO J. 13*:798.

270. **Laemmli, U. K.** 1970. Cleavage of Structural Proteins During the Assembly of the Head of Bacteriophage T4. *Nature 227*:680.

271. **Celis, J. E., B. Gesser, H. Holm Rasmussen, P. Madsen, H. Lefers, K. Dejgaard, B. Honore, E. Olsen, G. Ratz, J. B. Jette, B. Basse, S. Mouritzen, M. Hellerup, A. Anderson, E. Walbum, A. Celis, G. Bauw, M. Puype, J. Van Damme, and J. Vandekerckhove**. 1990. Comprehensive 2-D gel protein databases offer a global approach to the analysis of human cells: The transformed amnion cells (AMA) master database and its link to genome DNA sequence data. *Electrophoresis 11*:989.

272. **Towbin, H., T. Staehelin, and J. Gordon**. 1979. Electrophoretic Transfer of Proteins from Polyacrylamide Gels to Nitrocellulose Sheets: Procedure and some Applications. *Proc. Natl. Acad. Sci. USA 76*:4350.

273. **Ng, D., K. W. Harder, I. Clark-Lewis, F. Jirik, and P. Johnson**. 1995. Non-radioactive Method to Measure CD45 Protein Tyrosine Phosphatase Activity Isolated Directly from Cells. *J. Immunol. Methods 179*:177.

274. **Williams, A. F. and A. N. Barclay**. 1986. Glycoprotein antigens of the lymphocyte cell surface and their purification by antibody affinity chromatography. In *Handbook of experimental immunology*. 4th ed. D.M. Weir, ed. Blackwell Scientific Publications, Oxford, Great Britain, p. 22.1.

275. **Martin, R. G. and B. N. Ames**. 1961. A method for determining the sedimentation behavior of enzymes: application to protein mixtures. *J. Biol. Chem. 236*:1372.

276. **Luqman, M., P. Johnson, I. S. Trowbridge, and K. Bottomly**. 1991. Differential expression of the alternatively spliced exons of murine CD45 in TH_1 and TH_2 cell clones. *Eur. J. Immunol. 21*:17.

277. **Sambrook, J., E. F. Fritsch, and T. Maniatis**. 1989. *Molecular Cloning: A Laboratory Manual*. Cold Spring Harbor Laboratory Press, Cold Spring Harbor, NY.

278. **Thomas, M. L.** 1989. The Leukocyte Common Antigen Family. *Annu. Rev. Immunol. 7*:339.

279. **Thomas, M. L., P. J. Reynolds, A. Chain, Y. Ben-Neriah, and I. S. Trowbridge**. 1987. B-cell Variant of Mouse T200 (Ly-5): Evidence for Alternative mRNA Splicing. *Proc. Natl. Acad. Sci. USA 84*:5360.

280. **Saga, Y., J. Tung, F. Shen, and E. A. Boyse**. 1987. Alternative Use of 5' Exons in the Specification of Ly-5 Isoforms Distinguishing Hematopoietic Cell Lineages. *Proc. Natl. Acad. Sci. USA 84*:5364.

281. **Barclay, A. N., D. I. Jackson, A. C. Willis, and A. F. Williams**. 1987. Lymphocyte Specific Heterogeneity in the Rat Leukocyte Common Antigen (T200) is Due to Differences in the Polypeptide Sequences near the NH2-terminus. *EMBO J. 6(5)*:1259.

282. **Ralph, S. J., M. L. Thomas, C. C. Morton, and I. S. Trowbridge**. 1987. Structural Variants of Human T200 Glycoprotein (Leukocyte-Common) Antigen. *EMBO J. 6(5)*:1251.

283. **Streuli, M., L. R. Hall, Y. Saga, S. F. Schlossman, and H. Saito**. 1987. Differential Usage of Three Exons Generates at Least Five Different mRNAs Encoding Human Leukocyte Common Antigens. *J. Exp. Med. 166*:1548.

284. **Chang, H., L. Lefrancois, M. H. Zaroukian, and W. J. Esselman**. 1991. Developmental Expression of CD45 Alternative Exons in Murine T cells. *J. Immunol. 147*:1687.

285. **Birkeland, M. L., P. Johnson, I. S. Trowbridge, and E. Puré**. 1989. Changes in CD45 Isoform Expression Accompany Antigen-induced Murine T-cell Activation. *Proc. Natl. Acad. Sci. USA 86*:6734.

286. **Plebanski, M., M. Saunders, S. S. Burtles, S. Crowe, and D. C. Hooper**. 1992. Primary and Secondary Human in vitro T-cell Response to Soluble Antigens are Mediated by Subsets Bearing Different CD45 Isoforms. *Immunology 75*:86.

287. **Akbar, A. N., L. Terry, A. Timms, P. C. Beverley, and G. Janossy**. 1988. Loss of CD45R and gain of UCHL1 reactivity is a feature of primed T cells. *J. Immunol. 140*:2171.

288. **Rothstein, D. M., A. Yamada, S. F. Schlossman, and C. Morimoto**. 1991. Cyclic regulation of CD45 isoform expression in a long term human $CD4^+$ $CD45R4^+$ T cell line. *J. Immunol. 146*:1175.

289. **Warren, H. and L. Skipsey**. 1991. Loss of activation induced CD45R0 with maintenance of CD45RA expression during prolonged culture of T cells and NK cells. *Immunology 74*:78.

290. **Bell, E. R. and S. M. Sparshott**. 1990. Interconversion of CD45R subsets of CD4 T cells *in vivo*. *Nature 348*:163.

291. **Deans, J. P., A. W. Boyd, and L. M. Pilarski**. 1991. Transition from high to low molecular weight isoforms of CD45 (T200) involve rapid activation of alternative mRNA splicing and slow turnover of surface CD45R. *Immunology 143*:1233.

292. **Saga, Y., J. S. Lee, C. Saraiya, and E. A. Boyse**. 1990. Regulation of alternative splicing in the generation of isoforms of the mouse Ly-5 (CD45) glycoprotein. *Proc. Natl. Acad. Sci. USA 87*:3728.

293. **Rothstein, D. M., H. Saito, M. Streuli, S. F. Schlossman, and C. Morimoto**. 1992. The alternative splicing of the CD45 tyrosine phosphatase is controlled by negative regulatory trans-acting splicing factors. *J. Biol. Chem. 267*:7139.

294. **Streuli, M. and H. Saito**. 1989. Regulation of tissue-specific alternative splicing: exon-specific cis-elements govern the splicing of leukocyte common antigen pre-mRNA. *EMBO J. 8*:787.

295. **Charbonneau, H., N. K. Tonks, K. A. Walsh, and E. H. Fischer**. 1988. The leukocyte common antigen (CD45): a putative receptor-linked protein tyrosine phosphatase. *Proc. Natl. Acad. Sci. USA 85*:7182.

296. **Tonks, N. K., H. Charbonneau, C. D. Diltz, E. H. Fischer, and K. A. Walsh**. 1988. Demonstration that the leukocyte common antigen CD45 is a protein tyrosine phosphatase. *Biochemistry 27*:8695.

297. **Pingel, J. T. and M. L. Thomas**. 1989. Evidence that the Leukocyte-Common Antigen is Required for Antigen-Induced T Lymphocyte Proliferation. *Cell 58*:1055.

298. **Koretzky, G. A., J. Picus, M. L. Thomas, and A. Weiss**. 1990. Tyrosine phosphatase CD45 is essential for coupling T-cell antigen receptor to the phosphatidyl inositol pathway. *Nature 346*:66.

299. **Justement, L. B., K. S. Campbell, N. C. Chien, and J. C. Cambier**. 1991. Regulation of B Cell Antigen Receptor Signal Transduction and Phosphorylation by CD45. *Science 252*:1839.

300. **Koretzky, G. A., J. Picus, T. Schultz, and A. Weiss**. 1991. Tyrosine Phosphatase CD45 is Required for T Cell Antigen Receptor and CD2-mediated Activation of a Protein Tyrosine Kinase and Interleukin-2 Production. *Proc. Natl. Acad. Sci. USA 88*:2037.

301. **Desai, D. M., J. Sap, O. Silvennoinen, J. Schlessinger, and A. Weiss**. 1994. The Catalytic Activity of the CD45 Membrane-proximal Phosphatase Domain is Required for TCR Signaling and Regulation. *EMBO J. 13*:4002.

302. **Ostergaard, H. L., D. A. Schackelford, T. R. Hurley, P. Johnson, R. Hyman, B. M. Sefton, and I. S. Trowbridge**. 1989. Expression of CD45 Alters Phosphorylation of the *lck*-encoded Tyrosine Protein Kinase in Murine Lymphoma Cell Lines. *Proc. Natl. Acad. Sci. USA 86*:8959.

303. **Mustelin, T., T. Pessa-Morikawa, M. Autero, M. Gassmann, L. Andersson, C. G. Gahmberg, and P. Burn**. 1992. Regulation of the p59fyn Protein Tyrosine Kinase by the CD45 Phosphotyrosine Phosphatase. *Eur. J. Immunol. 22*:1173.

304. **Yamanashi, Y., T. Kakiuchi, J. Mizuguchi, T. Yamamota, and K. Toyoshima**. 1991. Association of B Cell Antigen Receptor with Protein Tyrosine Kinase Lyn. *Science 251*:192.

305. **Burkhardt, A. L., M. Brunswick, J. B. Bolen, and J. J. Mond**. 1991. Anti-immunoglobulin Stimulation of B Lymphocytes Activates Src-related Protein-tyrosine Kinases. *Proc. Natl. Acad. Sci. USA 88*:7410.

306. **Kishihara, K., J. Penninger, V. A. Wallace, T. M. Kündig, K. Kawai, A. Wakeham, E. Timms, K. Pfeffer, P. S. Ohashi, M. L. Thomas, C. Furlonger, C. J. Paige, and T. W. Mak**. 1993. Normal B Lymphocyte Development but Impaired T cell Maturation in CD45-Exon 6 Protein Tyrosine Phosphatase-Deficient Mice. *Cell 74*:143.

307. **Berger, S. A., T. W. Mak, and C. J. Paige**. 1994. Leukocyte Common Antigen (CD45) is Required for Immunoglobulin E-mediated Degranulation of Mast Cells. *J. Exp. Med. 180*:471.

308. **Streuli, M., N. X. Krueger, T. Thai, M. Tang, and H. Saito**. 1990. Distinct functional roles of the two intracellular phosphatase like domains of the receptor-linked protein tyrosine phosphatases LCA and LAR. *EMBO J. 9*:2399.

309. **Johnson, P., H. L. Ostergaard, C. Wasden, and I. S. Trowbridge**. 1992. Mutational analysis of CD45. A leukocyte-specific protein tyrosine phosphatase. *J. Biol. Chem. 267*:8035.

310. **Ng, D. H. W., A. Maiti, and P. Johnson**. 1995. Point mutation in the second phosphatase domain of CD45 abrogates tyrosine phosphatase activity. *Biochem. Biophys. Res. Commun. 206*:302.

311. **Tan, X. H., D. R. Stover, and K. A. Walsh**. 1993. Demonstration of protein tyrosine phosphatase activity in the second of two homologous domains of CD45. *J. Biol. Chem. 268*:6835.

312. **Ostergaard, H. L. and I. S. Trowbridge**. 1991. Negative regulation of CD45 protein tyrosine phosphatase activity by ionomycin in T cells. *Science 253*:1423.

313. **Stover, D. R., H. Charbonneau, N. K. Tonks, and K. A. Walsh**. 1991. Protein tyrosine phosphatase CD45 is phosphorylated transiently on tyrosine upon activation of Jurkat T cells. *Proc. Natl. Acad. Sci. USA 88*:7704.

314. **Dianzani, U., M. Luqman, J. Rojo, J. Yagi, J. L. Baron, A. Woods, C. A. J. Janeway, and K. Bottomly**. 1990. Molecular associations on the T cell surface correlate with immunological memory. *Eur. J. Immunol. 20*:2249.

315. **Dianzani, U., V. Redoglia, M. Bragardo, A. Pileri, C. A. J. Janeway, and K. Bottomly**. 1992. Isoform-specific associations of CD45 with accessory molecules in human T lymphocytes. *Eur. J. Immunol. 22*:365.

316. **Novak, T. J., D. Farber, D. Leitenberg, S. Hong, P. Johnson, and K. Bottomly**. 1994. Isoforms of the Transmembrane Tyrosine Phosphatase CD45 Differentially Affect T cell Recognition. *Immunity 1*:109.

317. **Mittler, R. S., B. M. Rankin, and P. A. Kiener**. 1991. Physical associations between CD45 and CD4 or CD8 occur as late activation events in antigen receptor-stimulated human T cells. *J. Immunol. 147*:3434.

318. **Stamenkovic, I., D. Sgroi, A. Aruffo, M. S. Sy, and T. Anderson**. 1991. The B Lymphocyte Adhesion Molecule CD22 Interacts with Leukocyte Common Antigen CD45R0 on T cells and alpha 2-6 Sialyltransferase, CD75, on B Cells. *Cell 66*:1133.

319. **Prickett, T. C. R. and D. N. J. Hart**. 1990. Anti-Leukocyte Common (CD45) Antibodies Inhibit Dendritic Cell Stimulation of CD4 and CD8 T-Lymphocyte Proliferation. *Immunology 69*:250.

320. **Wood, G. S., P. S. Freudenthal, A. Edinger, R. M. Steinman, and R. A. Warnke**. 1991. CD45 Epitope Mapping of Human CD1A Positive Dendritic Cells and Peripheral Blood Dendritic Cells. *Am. J. Pathol. 138*:1451.

321. **Schwinzer, R., R. Siefken, R. A. Franklin, J. Saloga, K. Wonigeit, and E. W. Gelfand**. 1994. Human CD45RA+ and CD45R0+ T cells exhibit similar CD3/T cell receptor-mediated transmembrane signaling capacities but differ in response to co-stimulatory signals. *Eur. J. Immunol. 24*:1391.

322. **Rankin, B. M., S. A. Yocum, R. S. Mittler, and P. A. Kienser**. 1993. Stimulation of tyrosine phosphorylation and calcium mobilization by Fc-gamma receptor cross-linking. *J. Immunol. 150*:605.

323. **Weinstein, S. L., M. R. Gold, and A. L. DeFranco**. 1991. Bacterial LPS stimulates protein tyrosine phosphorylation in macrophages. *Proc. Natl. Acad. Sci. USA 88*:4148.

324. **Letari, O., S. Nicosia, C. Chiavarolli, P. Vacher, and W. Schlegel**. 1991. Activation by bacterial LPS causes changes in the cytosolic free calcium concentration in single peritoneal macrophages. *J. Biol. Chem. 147*:980.

325. **Ziegler, S. F., J. D. Marth, D. B. Lewis, and R. M. Perlmutter**. 1987. Novel protein-tyrosine kinase gene (hck) preferentially expressed in cells of hematopoietic origin. *Mol. Cell. Biol. 7*:2276.

326. **Masuda, M. and D. Roos**. 1993. Association of all three types of Fc gamma R (CD64, CD32, and CD16) with a gamma-chain homodimer in cultured human monocytes. *J. Immunol. 151*:7188.

327. **Ashwell, J. D. and R. D. Klausner**. 1990. Genetic and mutational analysis of the T-cell antigen receptor. *Annu. Rev. Immunol. 8*:139.

328. **Irving, B. A. and A. Weiss**. 1991. The cytoplasmic domain of the T cell receptor chain is sufficient to couple receptor-associated signal transduction pathways. *Cell 64*:891.

329. **Romeo, C., M. Amiot, and B. Seed**. 1992. Sequence requirements for induction of cytolysis by the T cell antigen/Fc receptor zeta chain. *Cell 68*:889.

330. **Desai, D. M., J. Sap, J. Schlessinger, and A. Weiss**. 1993. Ligand-mediated negative regulation of a chimeric transmembrane receptor tyrosine phosphatase. *Cell 73*:541.

331. **Brown, W. R. A. and A. F. Williams**. 1982. Lymphocyte cell surface glycoproteins which bind to soybean and peanut lectins. *Immunology 46*:713.

332. **Cook, R. G., N. F. Landolfi, V. Mehta, J. Leone, and D. Hoyland**. 1987. Interleukin 2 mediates an alteration in the T200-antigen expressed on activated B cells. *J. Immunol. 139*:991.

333. **Ardavin, C. and K. Shortman**. 1992. Cell Surface Marker Analysis of Mouse Thymic Dendritic Cells. *Eur. J. Immunol. 22*:859.

334. **Ardavin, C., L. Wu, I. Ferrero, and K. Shortman**. 1993. Mouse Thymic Dendritic Cell Subpopulations. *Immunol. Lett. 38*:19.

335. **Trowbridge, I. S. and M. L. Thomas**. 1994. CD45: An Emerging Role as a Protein Tyrosine Phosphatase Required for Lymphocyte Activation and Development. *Annu. Rev. Immunol. 12*:85.

336. **Neefjes, J. J. and H. L. Ploegh**. 1992. Inhibition of endosomal proteolytic activity by leupeptin blocks surface expression of MHC Class II molecules and their conversion to SDS resistant ab heterodimers in endosomes. *EMBO J. 11*:411.

337. Anonymous1966. *The Handbook of Biochemistry and Biophysics*. Cleveland World Publishing, Cleveland.

338. **Bourguignon, L., S. Suchard, M. Nagpal, and J. Glenny**. 1985. A T-lymphoma transmembrane glycoprotein (gp180) is linked to the cytoskeletal protein, fodrin. *J. Cell Biol. 101*:477.

339. **Takeda, A., J. J. Wu, and A. L. Maizel**. 1992. Evidence for momomeric and dimeric forms of CD45 associated with a 30-kDa phosphorylated protein. *J. Biol. Chem. 267*:16651.

340. **Schraven, B., M. Roux, B. Hutmacher, and S. C. Meuer**. 1989. Triggering of the alternative pathway of human T cell activation involves members of the T 200 family of glycoproteins. *Eur. J. Immunol. 19*:397.

341. **Broxmeyer, H. E., L. Lu, G. Hangoc, S. Cooper, P. C. Hendrie, J. A. Ledbetter, M. Xiao, D. E. Williams, and F. W. Shen**. 1991. CD45 cell surface antigens are linked to stimulation of early human myeloid progenitor cells by interleukin 3 (IL-3), granulocyte/macrophage colony-stimulating factor (GM-CSF), a GM-CSF/IL-3 fusion protein, and mast cell growth factor (a c-kit ligand). *J. Exp. Med. 174*:447.

342. **Schwinzer, R., B. Schraven, U. Kyas, S. C. Meuer, and K. Wonigeit**. 1992. Phenotypical and biochemical characterization of a variant CD45R expression pattern in human leukocytes. *Eur. J. Immunol. 22*:1095.

343. **Ong, C. J., D. Chui, H. S. Teh, and J. D. Marth**. 1994. Thymic CD45 tyrosine phosphatase regulates apoptosis and MHC-restricted negative selection. *J. Immunol. 152*:3793.

344. **Paglia, P., G. Girolomoni, F. Robbiati, F. Granucci, and P. Ricciardi-Castagnoli**. 1993. Immortalized dendritic cell line fully competent in antigen presentation initiates primary T cell responses in vivo. *J. Exp. Med. 178*:1893.

345. **Boehmelt, G., J. Madrugs, P. Dörfler, K. Briegel, H. Schwarz, P. J. Enrietto, and M. Zenke**. 1995. Dendritic cell progenitor is transformed by a conditional v-rel estrogen receptor fusion protein v-RelER. *Cell 80*:341.

346. **Xu, S., K. Arizumi, D. Edelbaum, P. R. Bergstresser, and A. Takashima**. 1995. Cytokine dependent regulation of growth and maturation in murine epidermal dendritic cell lines. *Eur. J. Immunol. 25*:1018.

347. **Goldman, S. J., S. Uniyal, L. M. Ferguson, D. E. Golan, S. J. Burakoff, and P. A. Kiener**. 1992. Differential activation of phosphotyrosine protein phosphatase activity in a murine T-cell hybridoma by monoclonal antibodies to CD45. *J. Biol. Chem. 267*:6197.

348. **Pulido, R. and F. Sanchez-Madrid**. 1992. Glycosylation of CD45: carbohydrate processing through Golgi apparatus is required for cell surface expression and protein stability. *Eur. J. Immunol. 22*:463.

349. **Pulido, R. and F. Sanchez-Madrid**. 1990. Glycosylation of CD45: carbohydrate composition and its role in acquisition of CD45R0 and CD45RB T cell maturation-related antigen specificities during biosynthesis. *Eur. J. Immunol. 20*:2667.

350. **Fabre, J. W. and A. F. Williams**. 1977. Quantitative serological analysis of a rabbit anti-rat lymphocyte serum and preliminary biochemical characterization of the major antigen recognized. *Transplantation 23*:349.

351. **Van der Winkel, J. G. J. and P. J. A. Capel**. 1993. Human IgG Fc receptor heterogeneity: molecular aspects and clinical implications. *Immunol. Today 14*:215.

352. **Corvaïa, N., I. G. Reischl, E. Kroemer, and G. C. Mudde**. 1995. Modulation of Fc-gamma receptor-mediated early events by the tyrosine phosphatase CD45 in primary human monocytes. Consequences for IL-6 production. *Eur. J. Immunol. 25*:738.

353. **Beaven, M. A. and H. Metzger**. 1993. Signal transduction by Fc receptors: the Fc epsilon RI case. [Review]. *Immunol. Today 14*:222.

354. **Starkey, P. M., L. Turley, and S. Gordon**. 1987. The Mouse Macrophage-specific Glycoprotein Defined by Monoclonal Antibody F4/80: Characterization, Biosynthesis and Demonstration of a Rat Analogue. *Immunology 66*:117.

355. **Hume, D. A., A. P. Robinson, G. G. MacPherson, and S. Gordon**. 1983. The mononuclear phagocyte system of the mouse defined by immunohistochemical localization of the antigen F4/80. *J. Exp. Med. 158*:1522.

356. **Hume, D. A. and S. Gordon**. 1983. Mononuclear phagocyte system of the mouse defined by immunohistochemical localization of antigen F4/80: Identification of resident macrophages in renal medullary and cortical interstitium and the juxtaglomerular complex. *J. Exp. Med. 157*:1704.

357. **Lawson, L. J., V. H. Perry, P. Dri, and S. Gordon**. 1990. Heterogeneity in the distribution and morphology of microglia in the normal adult mouse brain. *Neuroscience 39*:151.

358. **Kraal, G., M. Rep, and M. Janse**. 1987. Macrophages in T and B cell compartments and other tissue macrophages recognized by monoclonal antibody MOMA-2. *Scand. J. Immunol. 26*:653.

359. **Hirsch, S., J. M. Austyn, and S. Gordon**. 1981. Expression of the macrophage-specific antigen F4/80 during differentiation of mouse bone marrow in culture. *J. Exp. Med. 154*:713.

360. **Ezekowitz, R. A. B., J. M. Austyn, P. D. Stahl, and S. Gordon**. 1981. Surface properties of bacillus Calmette-Guerin-activated macrophages. Reduced expression of mannose-specific endocytosis, Fc receptors, and antigen F4/80 accompanies induction of Ia. *J. Exp. Med. 154*:60.

361. **Witmer-Pack, M. D., J. Valinsky, W. Olivier, and R. M. Steinman**. 1988. Quantitation of surface antigens on cultured murine epidermal Langerhans cells: rapid and selective increase in the level of surface MHC products [published erratum appears in J Invest Dermatol 1988 Sep;91(3):286]. *J. Invest. Dermatol. 90*:387.

362. **Seed, B. and A. Aruffo**. 1987. Molecular Cloning of the CD2 antigen, the T-cell Erythrocyte Receptor, by a Rapid Immunoselection Procedure. *Proc. Natl. Acad. Sci. USA 87*:3365.

363. **Ou, W. J., P. H. Cameron, D. Y. Thomas, and J. J. Bergeron**. 1993. Association of folding intermediates of glycoproteins with calnexin during protein maturation. *Nature 364*:771.

364. **Diamond, B., B. R. Bloom, and M. D. Scharff**. 1978. The Fc receptors of primary and cultured phagocytic cells studied with homogeneous antibodies. *J. Immunol. 121*:1329.

365. **Munro, S. and H. R. B. Pelham**. 1986. An Hsp70-like protein in the ER:identity with the 78 kd glucose-regulated protein and immunoglobulin heavy chain binding protein. *Cell 46*:291.

366. **Elbein, A. D.** 1987. Inhibitors of the biosynthesis and processing of N-linked oligosaccharide chains. *Annu. Rev. Biochem. 56*:497.

367. **Tarentino, A. L., C. M. Gómez, and T. H. Plummer**. 1985. Deglycosylation of asparagine-linked glycans by peptide:N-glycosidase F. *Biochemistry 24*:4665.

368. **Umemoto, J., V. P. Bhavanandan, and E. A. Davidson**. 1977. Purification and properties of an endo-alpha-N-acetyl-D-galactosaminidase from Diplococcus pneumoniae. *J. Biol. Chem. 252*:8609.

369. **Paulson, J. C., J. Weinstein, L. Dorland, H. van Halbeek, and J. F. Vliegenthart**. 1982. Newcastle disease virus contains a linkage-specific glycoprotein sialidase. Application to the localization of sialic acid residues in N-linked oligosaccharides of alpha 1-acid glycoprotein. *J. Biol. Chem. 257*:12734.

370. **Crowley, J. F., I. J. Goldstein, J. Arnarp, and J. Lönngren**. 1984. Carbohydrate binding studies on the lectin from *Datura stramonium* seeds. *Arch. Bioch. Bioph. 231*:524.

371. **Cummings, R. D. and S. Kornfeld**. 1982. Characterization of the structural determinants required for the high affinity interaction of N-linked oligosaccharides with immobilized *Phaseolus vulgaris* leukoagglutinating and erythroagglutinating lectins. *J. Biol. Chem. 257*:11230.

372. **Cummings, R. D. and S. Kornfeld**. 1984. The distribution of repeating [Galβ1,4GlcNAcβ1,3] sequences in asparagine-linked oligosaccharides of the mouse lymphoma cel line BW5147 and PHA^R 2.1. *J. Biol. Chem. 259*:6253.

373. **Stamenkovic, I. and B. Seed**. 1990. The B-cell antigen CD22 mediates monocyte and erythrocyte adhesion. *Nature 345*:74.

374. **Brauer, A. W., C. L. Oman, and M. N. Margolies**. 1984. The use of o-phthalaldehyde to reduce background during automated Edman degradation. *Anal. Biochem. 137*:134.

375. **Lasky, L. A., M. S. Singer, D. Dowbenko, Y. Imai, W. J. Henzel, C. Grimley, C. Fennie, N. Gillett, S. R. Watson, and S. D. Rosen**. 1992. An Endothelial Ligand for L-Selectin Is a Novel Mucin-like Molecule. *Cell 69*:927.

376. **Patterson, S. D., D. Hess, T. Yungwirth, and R. Aebersold**. 1992. High-yield recovery of electroblotted proteins and cleavage fragments from a cationic polyvinylidene fluoride-based membrane. *Anal. Biochem. 202*:193.

377. **Yamashita, K., A. Hitoi, and A. Kobata**. 1983. Structural determinants of *Phaseolus vulgaris* erythroagglutinating lectin for oligosaccharides. *J. Biol. Chem. 258*:14753.

378. **Geyer, R., H. Geyer, H. Egge, H. H. Schott, and S. Stirm**. 1984. Structure of the oligosaccharides sensitive to endo-β-n-acetylglucosaminidase H. *Eur. J. Biochem. 143*:531.

379. **Hikens, J., M. J. L. Ligtenberg, H. L. Vos, and S. V. Litvinov**. 1992. Cell Membrane-associated Mucins and Their Adhesion-modulating Property. *Trends Biochem. Sci. 17*:359.

380. **Kay, R., P. M. Rosten, and R. K. Humphries**. 1991. CD24, a signal transducer modulating B cell activation responses, is a very short peptide with a glycosyl phosphatidylinositol membrane anchor. *J. Immunol. 147*:1412.

381. **Law, C. L., S. P. Sidorenko, and E. A. Clark**. 1994. Regulation of lymphocyte activation by the cell-surface molecule CD22. [Review]. *Immunol. Today 15*:442.

382. **Giordanengo, V., M. Limouse, J. Peyron, and J. Lefebre**. 1995. Lymphocytic CD43 and CD45 Bear Sulfate Residues Potentially Implicated in Cell to Cell Interactions. *Eur. J. Immunol. 25*:274.

383. **Sant, A. J. and J. Miller**. 1994. MHC class II antigen processing: biology of invariant chain. *Curr. Opin. Immunol. 6*:57.

384. **Dougherty, G. J., R. J. Kayt, and K. Humphries**. 1989. Molecular cloning of 114/A10, a cell surface antigen containing highly conserved repeated elements, which is expressed by murine hemopoietic progenitor cells and interleukin-3-dependent cell lines. *J. Biol. Chem. 264*:6509.

385. **Williams, A. F. and A. N. Barclay**. 1988. The immunoglobulin superfamily - domains for cell surface recognition. *Annu. Rev. Immunol. 6*:381.

386. **Engel, P., Y. Nojima, D. Rothstein, L. J. Zhou, G. L. Wilson, J. H. Kehrl, and T. F. Tedder**. 1993. The same epitope on CD22 of B lymphocytes mediates the adhesion of erythrocytes, T and B lymphocytes, neutrophils, and monocytes. *J. Immunol. 150*:4719.

387. **Mercurio, A. M. and P. W. Robbins**. 1985. Activation of mouse peritoneal macrophages alters the structure and surface expression of protein-bound lactosaminoglycans. *J. Immunol. 135*:1305.

388. **Petryniuak, J., T. K. Huard, G. D. Nordblom, and I. J. Goldstein**. 1986. Lectin binding studies on murine peritioneal cells: physicochemical characterization of the binding of lectins *Datura stramonium, Evonymus europaea,* and *Griffonia simplicifolia* to murine peritoneal cells. *Arch. Bioch. Bioph. 244*:57.

389. **Schall, T. J. and K. B. Bacon**. 1994. Chemokines, leukocyte trafficking, and inflammation. *Curr. Opin. Immunol. 6*:865.

390. **Marcelle, C. and A. Eichmann**. 1992. Molecular cloning of a family of protein kinase genes expressed in avian embryo. *Oncogene 7*:2479.

391. **Miyajima, A., T. Kitamura, N. Harada, T. Yokota, and K. Arai**. 1992. Cytokine receptors and signal transduction. *Annu. Rev. Immunol. 10*:295.

392. **Lazarovits, A. I., S. Poppema, M. J. White, and J. Karsh**. 1992. Inhibition of alloreactivity *in vitro* by monoclonal antibodies directed against restricted isoforms of the leukocyte-common antigen. *Transplantation 54*:724.

393. **Zhang, Z., R. Zhong, D. Grant, B. Garcia, M. White, C. Stiller, and A. I. Lazarovits**. 1995. Prevention and reversal of renal allograft rejection by a monoclonal antibody to CD45RB in the mouse model. *Transplant. Proc. 27*:389.

394. **Kraft, N., A. Stein-Oakley, J. Bal, R. C. Atkins, and N. M. Thomson**. 1989. Effect of anti-common leucocyte (CD45R, CD45) monoclonal antibodies on human lymphocyte activation: their potential for modifying kidney dendritic cells. *Transplant. Proc. 21*:1023.

395. **Hill, S., A. J. Edwards, I. Kimber, and S. C. Knight**. 1990. Systemic migration of dendritic cells during contact sensitization. *Immunology 71*:277.

396. **Breitman, M. L., H. Rombola, I. H. Maxwell, G. K. Klintworth, and A. Bernstein**. 1990. Genetic ablation in transgenic mice with an attenuated diphtheria toxin A gene. *Mol. Cell. Biol. 10*:474.

397. **Salomon, B., P. Lores, C. Pioche, P. Racz, J. Jami, and D. Klatzmann**. 1994. Conditional ablation of dendritic cells in transgenic mice. *J. Immunol. 152*:537.

398. **Glaser, V.** 1994. Carbohydrate biotechnology enters the domain of rational drug design. *Genetic Engineering News* 6.